CLINICAL APPLICATIONS OF DIXON CHEMICAL SHIFT MR IMAGING

Morbus Hansen

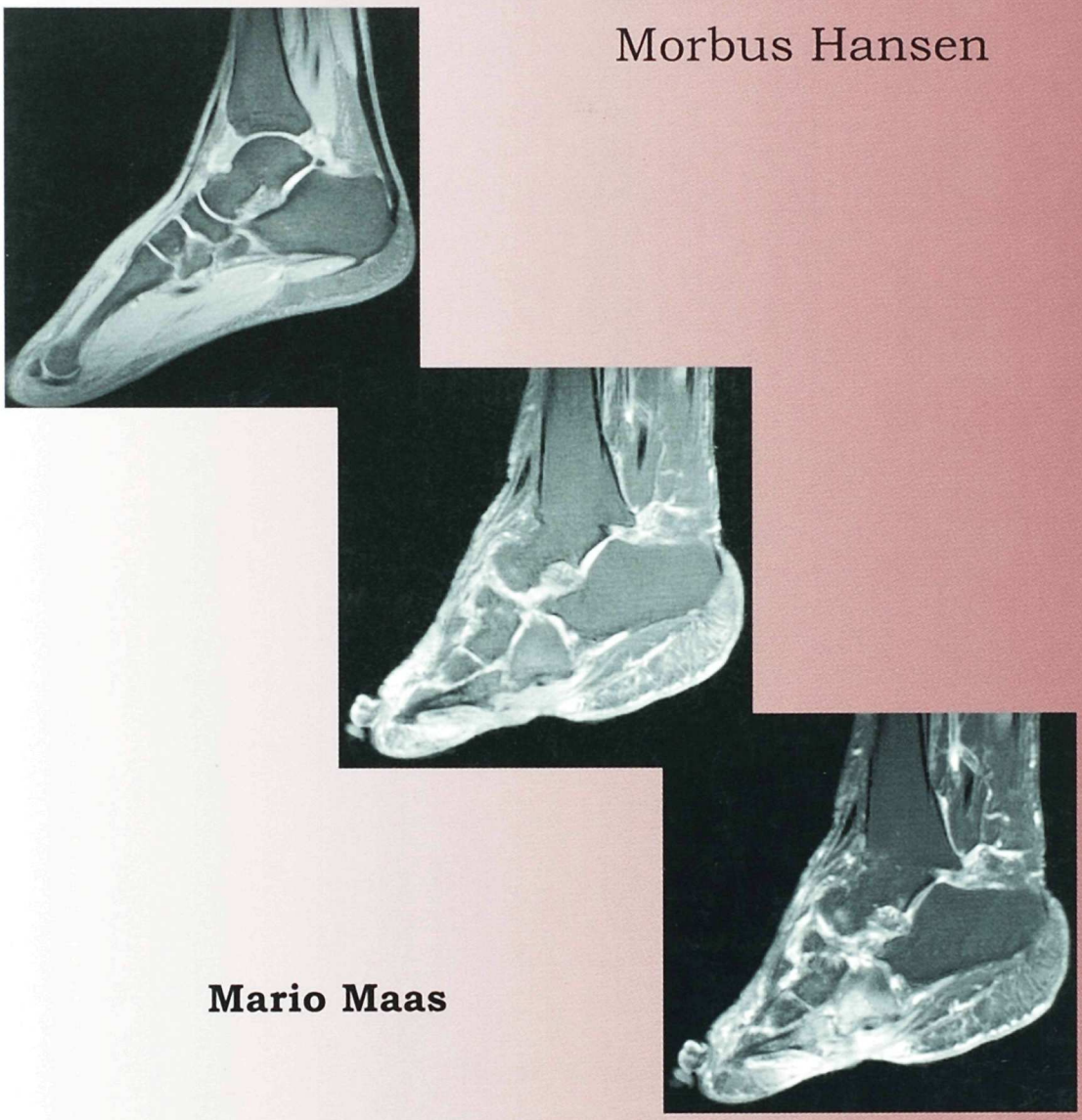

Mario Maas

Clinical applications of Dixon chemical shift MR Imaging

Morbus Gaucher

Mario Maas

CLINICAL APPLICATIONS OF DIXON CHEMICAL SHIFT MR IMAGING

ACADEMISCH PROEFSCHRIFT

ter verkrijging van de graad van doctor

aan de Universiteit van Amsterdam

op gezag van de Rector Magnificus

Prof. mr. P.F. van der Heijden

ten overstaan van een door het college voor promoties ingestelde

commissie, in het openbaar te verdedigen in de Aula der Universiteit

op woensdag 19 juni 2002, te 12.00 uur

door Mario Maas

geboren te Amsterdam

Promotiecommissie

Promotores
Prof.dr. G.J. den Heeten
Prof.dr. W.R. Faber

Co-promotores
dr. E.M. Akkerman
dr. J. Stoker

Overige Leden
Prof.dr. J.S. Laméris
Prof.dr. J.L. Bloem
Prof.dr. J.M.F.G. Aerts
Prof.dr. R. Goudsmit
Prof.dr. A. Huson
dr. B. Naafs

Faculteit Geneeskunde

ISBN 90-9015888-X
© Mario Maas 2002
Printed by Ridderprint B.V. Ridderkerk

The financial support of the following companies is gratefully acknowledged:
Gaucher Stichting, Huidstichting Chanfleury van IJsselsteijn, QM Gastmann Wicher Stichting

Coloplast B.V., Genzyme Nederland B.V., Merck Sharp & Dohme B.V., Novo Nordisk Farma B.V., Oxford Glyco Sciences, Schering Nederland B.V.

Contents

Clinical applications of Dixon chemical shift MR Imaging

Morbus Gaucher

Chapter 1	Introduction	7
Chapter 2	Dixon quantitative chemical shift MRI for bone marrow evaluation in the lumbar spine: A reproducibility study in healthy volunteers *JCAT 2001; 25(5):691-697*	21
Chapter 3	Imaging and quantifying skeletal involvement in Gaucher disease *Br J Radiology 2002,*75 (Suppl. 1): A13-A24.	39
Chapter 4	Quantification of skeletal involvement in adults with type 1 Gaucher disease: fat fraction measured by dixon quantitative chemical shift imaging (DQCSI) is a valid parameter *accepted in AJR*	59
Chapter 5	Dixon quantitative chemical shift imaging is a sensitive tool for the evaluation of bone marrow responses to individualized doses of enzyme supplementation therapy in type 1 Gaucher disease *Blood Cells Mol Dis 2001; 27(6): 1005-1012*	75
Chapter 6	Response of Gaucher bone disease to enzyme replacement therapy *Br J Radiology 2002,*75 (Suppl. 1):A25-A36.	89
Chapter 7	The vertebra-disc ratio as a parameter for bone marrow involvement and its application in Gaucher disease *submitted*	113

Chapter 8	Quantification of bone disease in Gaucher disease: MRI bone marrow burden score as an alternative for Dixon quantitative chemical shift imaging (QCSI) *submitted*	129
Chapter 9	Summary, general discussion and future research	145
Chapter 10	Samenvatting	155
	Dankwoord	165

CHAPTER 1

Introduction

* *What is Gaucher disease?*
* *Bone marrow - a short introduction*
* *Bone marrow - MRI*
* *Bone marrow - Gaucher disease - MRI*
* *Dixon quantitative chemical shift imaging*
* *Aim and outline of the conducted studies*

WHAT IS GAUCHER DISEASE?

Gaucher disease is the most prevalent of the lysosomal storage disorders. The French pathologist Philippe C. E. Gaucher described this disease for the first time in 1882 as a splenic epithelioma [1]. Later it was noted that the splenic enlargement was caused by storage of lipid material that was identified as a cerebroside in 1924 and as a glucocerebroside (glucosylceramide), a glycolipid, ten years later. The accumulation of the glucocerebroside was found to be due to a deficient activity of a lysosomal enzyme, glucocerebrosidase (glucosylceramidase). The deficient activity of the enzyme results in accumulation of glucocerebroside in macrophages. These lipid-loaden macrophages, so-called Gaucher cells, accumulate mainly in the spleen, liver, and bone marrow [2].

Three phenotypes are recognized on basis of the clinical features of the disease; type 1, non-neuronopathic, type 2, acute neuronopathic, and type 3, subacute neuronopathic [2].

This thesis only involves patients with type 1 Gaucher disease; the most prevalent form. The birth prevalence of Gaucher disease in the Netherlands was calculated for Gaucher disease type 1 as 0.9 per 100.000 and as 1.16 per 100.000 for all types combined [3].

Of the clinical symptoms splenomegaly is the most striking feature, leading to hypersplenism with gradual pancytopenia [2,4-6]. Hepatomegaly is often less dramatic, however, gross enlargement is mostly found in splenectomized patients. The active red bone marrow often is infiltrated with Gaucher cells. As the demand for marrow function increases, so does reconversion of the dormant yellow marrow in the limbs to active red marrow. Eventually these new areas also become packed by Gaucher cells. This may lead to deformities, as the classical Erlenmeyer flask appearance of the distal femurs, representing bone marrow packing, however, not exclusively seen in Gaucher disease [7].

Bone pain and acute bone crisis, or aseptic osteomyelitis that resemble those seen in sickle cell disease may be seen [5,8]. Bone infarcts and avascular necrosis may develop. Eventually in some patients severe progressive and destructive bone disease necessitating joint replacement will occur. It should be noted that the degree of hematological problems and the scale of organomegaly do not always correlate with the severity of bone disease [9]. This necessitates separate evaluation of each compartment for disease activity using a sensitive modality [4,8,10].
The availability of enzyme supplementation therapy (Ceredase ® alglucerase, placentally derived glucocerebrosidase; Cerezyme ® imiglucerase, recombinant glucocerebrosidase; both manufactured by Genzyme Co., MA, USA) has had a great impact on the symptoms of the disease [11]. Intravenous administration of the enzyme results in the breakdown of accumulated glycolipids and, subsequently, in reversal of the manifestations of the disease [12]. Cytopenia improves, and spleen and liver size decrease. Bone disease tends to respond much more slowly, and it is much more difficult to assess skeletal involvement [13]. Whereas there is no doubt about clinical efficacy of enzyme supplementation, several issues remain unclear, such as the criteria for initiating treatment and the best way to monitor effects, especially in the bone marrow compartment. The variability in clinical responses to treatment and the extremely high costs (about $200.000 to $500.000 per patient per year) are important in these respects [11].

BONE MARROW- A SHORT INTRODUCTION[14]

Bone marrow is one of the largest organs of the body by weight, approaching 3000 g in adult men and approximately 2600 g in women. Its function is to provide a continual supply of red cells, platelets, and white cells to meet the body's demands for oxygenation, coagulation, and immunity. The basic structure of bone marrow consists of a trabecular framework housing fat cells, covered with hematopoietic cells, supported by a system of reticulum cells, nerves and vascular sinusoids. Cellular marrow constituents include all stages of erythrocytic and leucocytic development, as well as fat cells and reticulum cells. Fat cells are a major component of bone marrow. The size of these cells appears to be responsive to hematopietic activity.

During periods of decreased hematopoiesis, the fat cells increase in volume and number, wheras in increased hematopoiesis fat cells atrophy. Reticulum cells can be divided in two major groups - the phagocytic cell, and the undifferentiated non-phagocytic cell. The phagocytic group consists of macrophages, found predominantly in regions that are hematopoietically active.

Figure 1. Bone marrow samples, with haematoxylin and eosin stain, from red cellular marrow (left), yellow marrow (center) and bone marrow infiltrated with Gaucher cells (right).

"Yellow marrow" is composed predominantly of fat cells (15% water, 80% fat and 5% protein). "Red marrow" is considered hematopoietically active marrow. It contains approximately 40% water, 40% fat and 20% protein (Fig. 1). Virtually the entire fetal marrow space is dedicated to red marrow at birth. In the immediate postnatal period, conversion from red to yellow marrow begins in a predictable and orderly pattern. This conversion begins in the terminal phalanges and progresses from peripheral (appendicular) towards central (axial). In an individual long bone it progresses from diaphysis to metaphysis. The cartilaginous epiphysis and apophysis can be characterized as yellow marrow. By the time a person is 25 years old, marrow conversion is considered complete and the adult pattern is achieved. Red marrow predominantly is concentrated in the axial skeleton and proximal parts of the appendicular skeleton. However, there is a great variation possible, i.e. hematopoietic marrow may occupy up to two-thirds of the femoral shaft. Ultimately, a balanced distribution of red and yellow marrow is achieved. Alterations in the body's demand for hematopoiesis will disturb this balance. With increasing demand for red cells, a reconversion of yellow to red marrow takes place, from axial to appendicular skeleton, in reverse to the conversion pattern.

BONE MARROW- MRI

In adult long bones, fat is the predominant contributor to the bone marrow signal pattern on MR images [14,15]. Both on T1-weighted spin echo sequences as well as fastspin echo T2-weighted sequences the signal from fatty marrow is optimized. Especially on T1-weighted images the contrast between fatty marrow and red marrow as well as most pathological processes is enhanced. When general marrow screening is performed, the primary anatomic sites for evaluation are the spine, particularly the lumbar spine due to the larger vertebral bodies, and the pelvis and proximal femurs. Since these areas contain a large percentage of red marrow throughout life it is logical to focus on these areas.

Typical signal patterns on T1-weighted images of yellow marrow roughly is similar to the subcutaneous fat [14,16,17]. Normal red cellular marrow is hypo-intense to yellow marrow on T1-weighted images. On fast spin echo T2-weighted sequences both fat and water will show high signal intensity [14,16,17].

BONE MARROW- GAUCHER DISEASE- MRI

In Gaucher disease the normal marrow contains is replaced by glucocerebroside-loaded macrophages, Gaucher cells, leading to a lowering of signal intensities both on T1- and T2-weighted images [18-21]. The marked shortening of the T2 relaxation time appears to be the principal cause. This effect differs from most other diseases in bone marrow, in which a high signal intensity on T2-weighted sequences is encountered [22]. The bright signal that arises from normal bone marrow fat on T1-weighted images contrasts strongly with weak signal from Gaucher tissue and thus the T1-weighted sequences are most useful in assessing the extent of disease. In Gaucher disease both homogeneous and heterogeneous patterns of involvement are encountered [23]. Marrow involvement generally follows the distribution of red cellular marrow in Gaucher disease, progressing from axial to peripheral and in a long bone from proximal to distal with a tendency to spare epiphysis and apophysis [19,24,25].

In order to quantify bone marrow changes in Gaucher disease Quantitative Chemical Shift Imaging (QCSI) was explored [26].

This technique, described in more detail in one of the next paragraphs of the introduction of this thesis, was evaluated in hematological bone marrow disorders by the group from Massachusetts General Hospital [27]. They investigated the use of QCSI in healthy volunteers, patients with leukemia or aplastic anemia. It was shown that the fat-fraction, measured by this QCSI technique, was the single best discriminator between the groups. The change in fat-fraction was found to represent the underlying reason for many of the changes observed in conventional MRI. The same research group also explored the use of this technique to quantify longitudinal changes in bone marrow that occur during induction chemotherapy in patients with acute leukemia [28]. Results were correlated with bone marrow biopsy results. QCSI data showed sequential increase in fat-fractions among responding patients, consistent with biopsy-confirmed clinical remission. It was concluded that QCSI proved useful in assessing treatment response in acute leukemia during early bone marrow regeneration and later in ascertaining remission or relapse. Furthermore, an additional described benefit of QCSI was the ability to sample a large portion of bone marrow.

The same group tested the QCSI technique in vertebral bone marrow in patients with Gaucher disease [26]. The measured fat-fractions were correlated with quantitative analysis of marrow triglycerides and glucocerebrosides. An MR spectroscopy performed in these surgical marrow specimens showed a single fat and water peak, thus validating use of QCSI. Glucocerebroside concentrations were higher in Gaucher marrow and inversely correlated with triglyceride concentrations. It was concluded that QCSI is a sensitive non-invasive technique for evaluating bone marrow infiltration in Gaucher disease, showing great promise as a non-invasive method to monitor bone marrow response to treatment. In order to validate bone marrow response data acquired by QCSI an analysis of the lipids of normal and Gaucher bone marrow is performed [29]. In normal marrow triglycerides were by far the most abundant lipid (278 ± 70 mg/gm wet weight); the concentration of glucocerebroside in normal marrow was 0.061 ± 0.06 mg/gm wet weight. Gaucher marrow had dramatically lower triglyceride levels of 82% (51 ± 53 mg/gm wet weight) and as expected marked elevation of glucocerebroside (7.1 ± 3.4 mg/gm wet weight) [29]. It was concluded that these data support a model of bone marrow alteration in Gaucher disease in which triglyceride-rich adipocytes are progressively replaced by Gaucher cells, leading to an overall reduction in total lipid content.

This phenomenon is concluded to provide an explanation for the changes found in QCSI measurements in Gaucher patients [29].

DIXON QUANTITATIVE CHEMICAL SHIFT IMAGING

The MR-signal for a normal MR-image originates from two types of hydrogen nuclei: nuclei in water molecules and nuclei in fat molecules [30]. The two types of nuclei have a slightly different MR frequency,

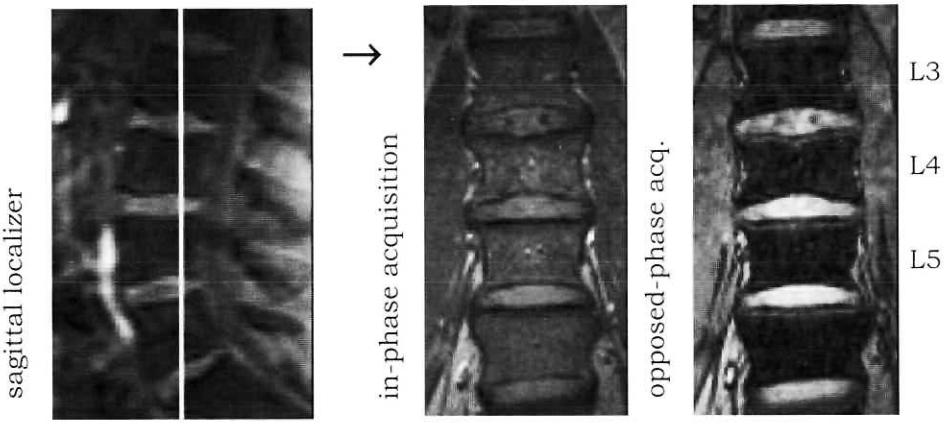

Figure 2. Localizer and Dixon acquisitions of the lumbar vertebrae L3, L4, and L5

due to the so-called "chemical shift" effect. The Dixon method uses this frequency difference to separate the signals from water and fat, which makes it possible to quantify the fat signal fraction, *Ff*. Hence: Dixon quantitative chemical shift imaging (Dixon QCSI).

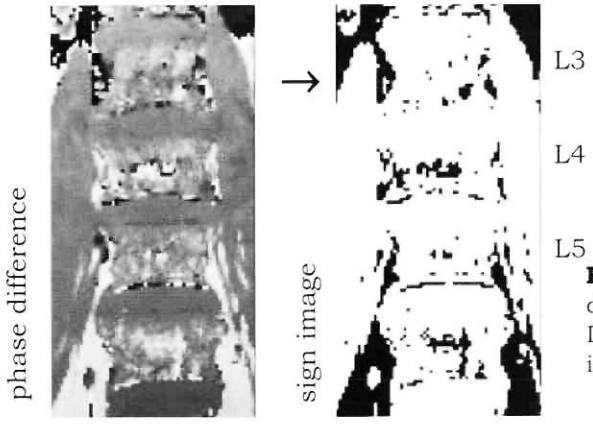

Figure 3. From the phase difference between the Dixon acquisitions the sign image is deduced.

We apply this method to measure *Ff* in the lumbar vertebrae (L3, L4, and L5). As shown in Fig. 2, a coronal measurement slice (if necessary slightly tilted to transversal) is set out on a sagittal localizer image, such that the posterior part of the vertebrae of interest are optimally visualized (Fig. 2).
In the original Two-Point Dixon technique, which we use, two sets of acquisitions are performed [30]. One in which the water signal (W) and the fat signal (F) are "in-phase" (I), which means that at any moment in time, the fat and water spins point in the same direction, and their signals add up in the image: I = W + F. In the second acquisition fat and water have opposed-phases (O): fat and water spins point in opposite directions, and the resulting image shows the magnitude of the difference of the fat and water signals: O = |W - F|. (See Fig. 2).

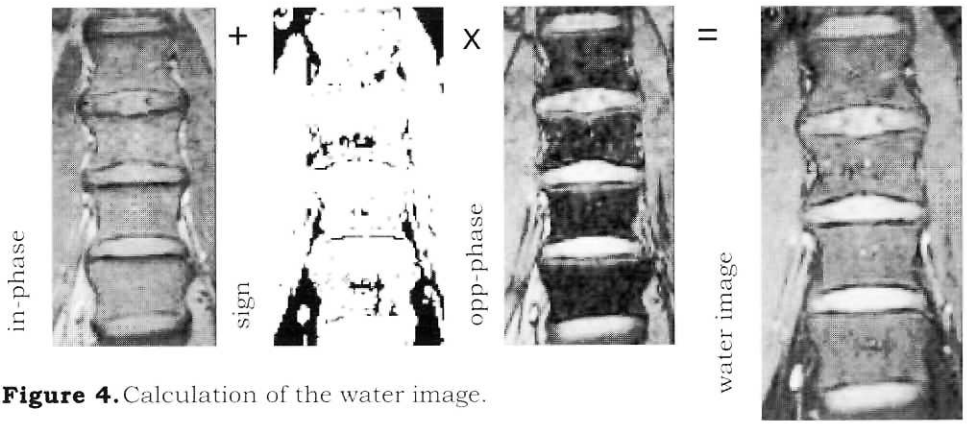

Figure 4. Calculation of the water image.

In order to separate the water and fat signals we need to know in every pixel which signal is stronger. The phase-difference between the two acquisitions helps us to sort out regions with water dominant signal and regions with fat dominant signal. In the example of Figure 3, water dominant regions are grey in the phase-difference image, fat dominant regions are either white or black. A complication may be formed by inhomgeneities in the main magnetic field, which cause grey scale intensity variations across the phase-difference image. We developed an algorithm [31] that takes care of all these effects, and is able to produce from the phase-difference a sign image (S) (Fig. 3), which tells water dominant regions (white, S = +1) from fat dominant regions (black, S = -1).
With help of the sign image, water and fat images are obtained by simple

algebraic manipulations. For the water image (W) we have: W = I + S • O (Fig. 4), and for the fat image (F) we have: F = I - S • O (Fig. 5).

The last step is to compute *Ff*, again by elementary algebra, as shown in Figure 6: *Ff* = F / (F + W). In order to easily read the *Ff* values from the image, we display the *Ff* image with a color scale: the color strip next to the image tells which color corresponds to which *Ff* value from 0 (black) to 1 (white).

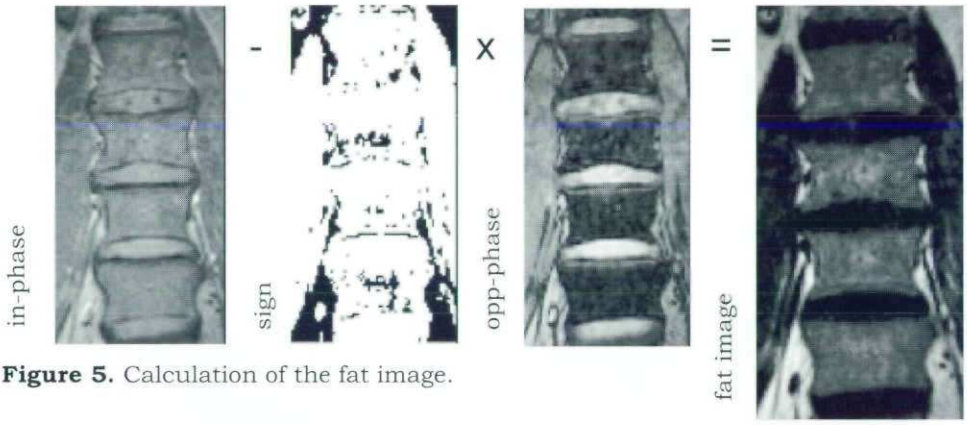

Figure 5. Calculation of the fat image.

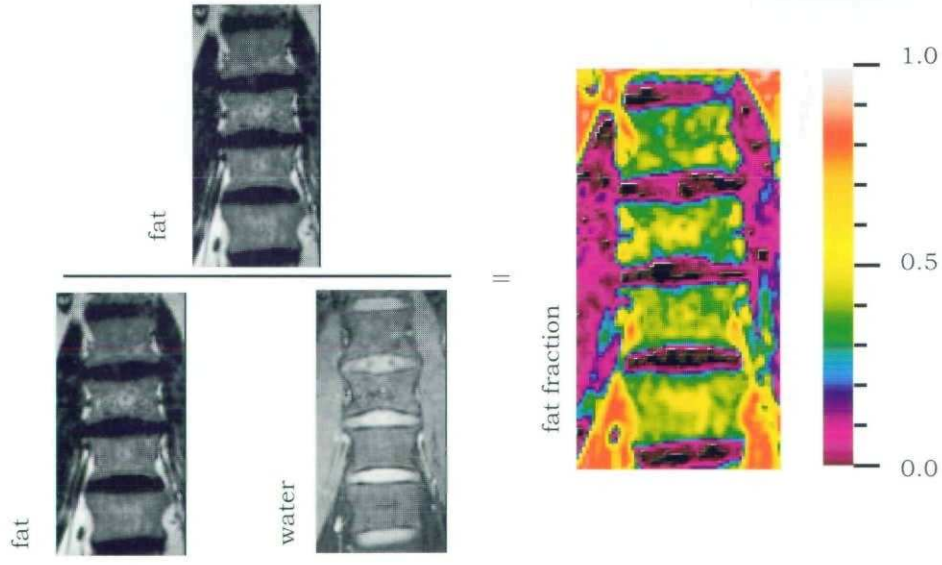

Figure 6. Calculation of the fat-fraction and display of the fat-fraction with a color scale.

AIM AND OUTLINE OF THE CONDUCTED STUDIES

To evaluate the applicability and feasibility of Dixon QCSI as a technique to assess bone marrow invasion in our Dutch population of patients with Gaucher disease at first the technique was tested in healthy volunteers. In **Chapter 2** the reproducibility of the Dixon QCSI technique in healthy volunteers as well as various operator dependent variables are tested. Furthermore, the results are compared to literature data. The differences are discussed.

In **Chapter 3** an overview is given of the available imaging modalities at hand for the evaluation of skeletal involvement in Gaucher disease, both qualitative and quantitative. Various perspectives from different radiological groups in the world on this subject as well as an overview of the available literature is presented. In **Chapter 4** the Dixon QCSI results are presented of the Dutch adult Gaucher disease population at baseline, without therapy. These fat-fraction data are related to clinical bone disease parameters such as presence of infarction, bone pain, bone crisis, avascular necrosis and joint replacement. The clinical relevance of the obtained fat-fraction number is illustrated.

In **Chapter 5** the results of a study concerning Dixon QCSI as follow-up parameter for bone marrow response to enzyme supplementation therapy (EST) are described. Both treated and untreated patients are longitudinally evaluated. In **Chapter 6** an overview is presented on the data available from various Gaucher treatment centers in Europe and one center in the USA as well as the Gaucher Registry Database concerning response of bone marrow to EST. A variety of modalities are used at the different centers to evaluate bone marrow response.

The need for widely available easy to use alternatives to Dixon QCSI for centers in which this technique is not present is obvious. In the next two chapters alternatives are tested against Dixon QCSI. In **Chapter 7** a parameter is studied based on the ratio between signal intensity in a vertebral body and an intervertebral disc. This vertebral-disk ratio (VDR) is measured in patients without bone marrow disease and Gaucher disease. Furthermore, the VDR as parameter to detect response of bone marrow to EST is tested. **Chapter 8** describes the study of another alternative for Dixon QCSI, namely the bone marrow burden score (BMB).

Two observers test this score in patients with Gaucher disease without treatment against Dixon QCSI. Also the strength of BMB as response parameter is evaluated.
In **Chapter 9** an overview of the results of these studies is given and the conclusions are discussed. Some areas for future research are described.

REFERENCES

1. Gaucher PCE. De l'epithelioma primitif de la rate, hypertrophie idiopathique de la rate sans leukemie. Thesis 1882; Paris.
2. Beutler E, Grabowski GA. Glucosylceramide lipidoses: Gaucher disease. In: Scriver CR, Beaudet AL, Sly WS, Valle D, editors. The Metabolic and Molecular Basis of Inherited Diseases, New York: McGraw-Hill, 1995:2641-2670.
3. Poorthuis BJHM, Wevers RA, Kleijer WJ, Groener JEM, de Jong JGN, van Weely S, Niezen-Koning KE, van Diggelen OP. The frequency of lysosomal storage diseases in The Netherlands. Human Genetics 1999; 105:151-156.
4. Beutler E, Kuhl W, Vaughan LM. Failure of alglucerase infused into Gaucher disease patients to localize in marrow macrophages. Mol Med 1995; 1(3):320-324.
5. Charrow J, Esplin JA, Gribble TJ, et al. Gaucher disease: recommendations on diagnosis, evaluation, and monitoring. Arch Intern Med 1998; 158:1754-1760.
6. Cox TM, Schofeld JP. Gaucher disease: clinical features and natural history. Baillieres Clin Haematol 1997; 10:657-689.
7. Mankin HJ, Doppelt SH, Rosenber AE, Barranger JA. Metabolic bone disease in patients with Gaucher's disease. In: Metabolic bone disease and clinically related disorders (eds. Avioli LV, Krane SM). W.B. Saunders Company, 1990; 735-752.
8. Charrow J, Andersson HC, Kaplan P, et al. The Gaucher Registry. Demographics and disease characteristics of 1698 patients with Gaucher disease. Arch Intern Med 2000; 160:2835-2843.
9. Pastores G, Wallenstein S, Desnick RJ, Luckey MM. Bone density in Type 1 Gaucher disease. J Bone Min Res 1996; 11:1801-1807.
10. Rademakers RP. Radiologic evaluation of Gaucher bone disease. Semin Hemtol 1995; 32(suppl. 1):14-19
11. Hollak CEM, Maas M, Aerts JM. Clinically relevant therapeutic endpoints in type 1 gaucher disease. J Inherit Metab Dis 2001; 24(suppl. 2):97-105.
12. Hollak CE, Aerts JM, Goudsmit R, et al. Individualised low-dose alglucerase therapy for type 1 Gaucher's disease. Lancet 1995; 345:1474-1478.

13. Grabowski GA, Leslie N, Wenstrup R. Enzyme therapy for Gaucher disease: the first 5 years. Blood Rev 1998; 12:115-133.
14. Vogler JB III, Murphy WA. Bone marrow imaging. Radiology 1988; 168:679-693.
15. Dooms GC, Fisher MR, Hricak H, Richardson M, Crooks LE, Genant HK. Bone marrow imaging: magnetic resonance studies related to age and sex. Radiology 1985; 155:429-432.
16. Steiner RM, Mitchell DG, Rao VM, et al. Magnetic resonance imaging of bone marrow: diagnostic value in diffuse hematologic disorders. Magnetic Resonance Quarterly 1990; 6:17-34.
17. Steiner RM, Mitchell DG, Rao VM, Schweitzer ME. Magnetic resonance imaging in diffuse bone marrow disease. Rad Clin North Am 1993; 31:383-409.
18. Hermann G, Shapiro RS, Abdelwahab IF, Grabowski G. MR imaging in adults with Gaucher disease type I: evaluation of marrow involvement and disease activity. Skeletal Radiol 1993; 22:247-251.
19. Rosenthal DI, Scott JA, Barranger J, et al. Evaluation of Gaucher disease using magnetic resonance imaging. J Bone Joint Surg Am 1986; 68:802-808.
20. Terk MR, Esplin J, Lee K, Magre G, Colletti PM. MR imaging of patients with type 1 Gaucher's disease: relationschip between bone and visceral changes. AJR 1995; 165: 599-604.
21. O'Keefe D, Rosenthal DI. Computed tomography and magnetic resonance imaging in Gaucher's disease. In: Bloem JL, Sartoris DJ, and Eds. MRI and CT of the musculoskeletal system: a text-atlas. Baltimore: William & Wilkins, 1992; 130-138.
22. Moulopoulos LA, Dimpoulos MA. Magnetic resonance imaging of the bone marrow in hematoloigic malignancies. Blood 1997; 90:2127-2147.
23. Cremin BJ, Davey H, Goldblatt J. Skeletal complications of type I Gaucher disease: the magnetic resonance features. Clin Radiol 1990; 41:244-247.
24. Hermann G, Goldblatt J, Levy RN, Goldsmith SJ, Desnick RJ, Grabowski GA. Gaucher's disease type 1: assessment of bone involvement by CT and scintigraphy. Am J Roentgenol 1986; 147:943-948.
25. Rosenthal DI, Barton NW, McKusick KA, et al. Quantitative imaging of Gaucher disease. Radiology 1992; 185:841-845.
26. Johnson LA, Hoppel BE, Gerard EL, et al. Quantitative chemical shift imaging of vertebral bone marrow in patients with Gaucher disease. Radiology 1992; 182:451-455.
27. Rosen BR, Fleming DM, Kushner DC, et al. Hematologic bone marrow disorders: quantitative chemical shift MR imaging. Radiology 1988; 169:799-804.

28. Gerard EL, Ferry JA, Amrein PC, et al. Compositional changes in vertebral bone marrow during treatment for acute leukemia: assessment with quantitative chemical shift imaging. Radiology 1992; 183:39-46.
29. Miller SPF, Zirzow GC, Doppelt SH, et al. Analysis of the lipids of normal and Gaucher bone marrow. J Lab Clin Med 1996; 127:353-358.
30. Dixon WT. Simple proton spectroscopic imaging. Radiology 1984; 153:189-194.
31. Akkerman EM, Maas M. A region-growing algorithm to simultaneously remove dephasing influences and separate fat and water in two-point Dixon imaging. In: Proceedings of the Society for Magnetic Resonance in Medicine and the European Society for Magnetic Resonance in Medicine and Biology 1995; 649.

CHAPTER 2

Dixon quantitative chemical shift MRI for bone marrow evaluation in the lumbar spine: A reproducibility study in healthy volunteers

Mario Maas, Erik M. Akkerman, Henk W. Venema,
Jaap Stoker, Gerard J. den Heeten

Department of Diagnostic Radiology, Academic Medical Center,
Amsterdam, the Netherlands

J Comput Assist Tomogr 2001; 25(5):691-697

ABSTRACT

Purpose:

The purpose of this work was to explore the reproducibility of fat-fraction measurements using Dixon quantitative chemical shift imaging (QCSI) in the lumbar spine (L3, L4, and L5) of healthy volunteers.

Method:

Sixteen healthy volunteers were examined at 1.5 T two times to obtain a repeated measurement in the same slice and a third time in three parallel slices. Single slice, two point Dixon spin echo (TR/TE 2,500/22.3) sequences were used, from which fat-fraction images were calculated. The fat-fraction results are presented as averages over regions of interest, which were derived from the contours of the vertebrae. Reproducibility measures related to repeated measurements on different days, slice position, and contour drawing were calculated.

Results:

The mean fat-fraction was 0.37 (SD 0.08). The SD due to repeated measurement was small (σ_R = 0.013 to 0.032), almost all of which can be explained by slice-(re)-positioning errors.

Conclusion:

When used to evaluate the same person longitudinally in time, Dixon QCSI fat-fraction measurement has an excellent reproducibility. It is a powerful non-invasive tool in the evaluation of bone marrow composition.

INTRODUCTION

The three major constituents of bone marrow in healthy individuals are mineralized osseous matrix, red cellular hematopoietic marrow, and yellow fatty marrow [1]. Red and yellow marrow are interconvertible [2], and normally they are in a dynamic balance that is age and gender dependent [3,4]. Disorders in this balance may occur following a number of pathophysiologic mechanisms: reconversion of yellow into red marrow (e.g., anemia, myeloproliferative diseases), marrow infiltration or replacement (e.g., neoplasm, infection, myelofibrosis, Gaucher disease), and myeloid depletion of red marrow (aplastic anemia, radiation therapy, chemotherapy) [1,5,6].

MRI is sensitive to both the water and the fatty components in bone marrow. Conventional qualitative MR images represent the sum of the signals from water and fat. In case of a disturbed balance of red and yellow marrow, the relative contribution of the fat signal to the total signal, known as "fat-fraction", may be a useful diagnostic quantitative parameter [7]. In Dixon quantitative chemical shift imaging (QCSI), based on the phase contrast technique described by Dixon [8], the MR signal is separated into the individual contributions of fat and water [9], from which the Dixon QCSI fat-fraction (F_f) is calculated. F_f has been demonstrated to be an excellent discriminator between healthy subjects, subjects with aplastic anemia, and subjects with leukemia [9]; furthermore, it has been shown to be useful in monitoring the extent of disease, disease progression, and response to therapy in acute leukemia [10,11] and Gaucher disease [12,13].

Although Dixon's principal idea was published back in 1984 [8], interest in the method has never ceased. Among the more recent publications are application of gradient echo instead of spin echo in the imaging of bone marrow [14], quantitative assessment of water fraction and T2 in bone marrow [15], and the use of Dixon imaging as a fat-suppression method in hands and feet [16] and in children [17].

Relatively little, however, has been published about the reproducibility of Dixon QCSI in vivo. Buxton et al. [18] described the influence of some technical parameters at 0.6 T. Gückel et al. [19] conducted a serial measurement of gluteal muscle at 1.5 T. Rosen et al. [9] elaborated on the overall reproducibility of serial measurements as measured in three healthy volunteers at 0.6 T.

We conducted the current study to explore the reproducibility issue for the measurement of F_f in the vertebrae L3, L4, and L5 at 1.5 T in a group of healthy volunteers in a clinical setting, that is, using exactly the same procedures as used in patients. Our main research question was: What is the reproducibility of F_f when repeating the measurement on a different day? We also investigated the influence on the reproducibility of two operator-dependent aspects of the method: (re-)positioning of the measurement slice and determination of contours from which the regions of interest (ROIS) were calculated. Furthermore, we evaluated the available Dixon QCSI data in literature, compared these with our results, and evaluated the differences.

MATERIAL & METHODS

Subjects

For the measurements, we used a group of 16 healthy volunteers (8 men: mean age 39 years, range 24-60 years; 8 women: mean age 38 years, range 26-55 years). There was no history of bone marrow pathology in this group. Approval of the local medical ethics committee was obtained, and all volunteers gave their written informed consent.

Experimental Procedures

Every volunteer was examined on 3 different days. In two of the examinations, a fat-fraction measurement was performed in the same single slice, referred to as measurements a and b; together they are called the repeated measurement. The average interval of the two examinations was 43 days (range 7-155 days, median 28 days). During a third examination, fat-fraction measurements were performed in three parallel slices, referred to as measurements c1, c2, and c3; together they are called the threefold measurement. All procedures took place at our institution, and the MR examinations were performed on a 1.5 T Magnetom 63SP/4000 later upgraded to a 1.5 T Magnetom Vision (Siemens, Erlangen, Germany). Volunteers were examined either entirely on the Magnetom SP (n = 9) or entirely on the Magnetom Vision (n = 7).

A Dixon fat-fraction measurement sequence consisted of two spin echo sequences. The first one was a conventional spin echo sequence, in which the signals from fat and water are in-phase. The second sequence was identical to the first one, except that the 180° inverting radio-frequency

pulse was shifted by a time τ, such that in the center of the readout gradient (k_x = 0), the signals of water and fat had opposed-phases [8,20,16]. The value of τ depends on the field strength and on the frequency difference between fat ($-CH_2-$) and water (H_2O), which is approximately 3.4 ppm [21]. At 1.5 T, this corresponds with a value of τ = 1.15 ms.

In-phase and opposed-phase proton density-weighted Dixon spin echo sequences were performed with the following parameters: TR 2,500 ms, TE 22.3 ms, slice thickness 4 mm, matrix 256 x 256, NEX 1, FOV 350 x 350 mm, resulting in a pixel size of 1.37 x 1.37 mm. The sequences had a bandwidth of 130 Hz/pixel. The acquisition time for one spin echo sequence was 10 min 40 s and for a Dixon measurement sequence (in-phase and opposed-phase) 21 min 20 s. Only single slice acquisition was performed, with no presaturation slabs, to avoid errors due to cross-talk and off-resonance effects [9]. Since presaturation slabs could not be used, both the RF coil and the direction of the measurement slice had to be selected with care to avoid motion artifacts.

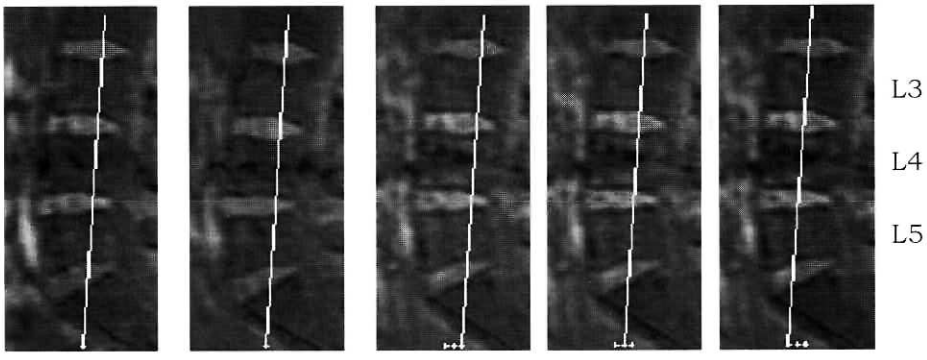

Figure 1. Mid-sagittal localizer images of volunteer v03. Measurement slices a and b (repeated measurement) and c1, c2, and c3 (threefold measurement) are indicated on the images, and each slice is perpendicular to the localizer images. Measurement slices should pass through the junction of the anterior three-fourths with the posterior one-fourth of vertebral body L4. Slight angulation from coronal toward transversal is allowed to also make the slices pass, as best one can, through the posterior parts of L3 and L5. To improve the reproducibility of the slice positioning, previous localizer images always were consulted for subsequent slice positioning in the same volunteer.

We used (para)-coronal slices, which were positioned on a mid-sagittal localizer image, passing through the middle of the posterior parts of L3, L4, and L5, as illustrated in Fig. 1. The distance between the slices of the threefold measurement was 3 or 4 mm, depending on the size of the vertebrae.

On the Magnetom SP, the body Helmholtz coil was used; on the Magnetom Vision, we used the small flex coil, flattened out and placed underneath the body along the spine. In this way, the intensity distribution in the images as well as the signal-to-noise ratio of both coil-scanner combinations were similar. We did not use a phased array coil because our sequences could not provide useful phase images for phased array coils.

Postprocessing

Postprocessing was performed on a Sun Sparc 20-51 workstation (Sun Microsystems, Mountain View, CA, U.S.A.). The postprocessing steps necessary to obtain a fat-fraction image from the Dixon acquisitions are illustrated in Fig. 2. In the in-phase image, the signals from water and fat are added together (Fig. 2a). The information about the difference of the signals is contained in the opposed-phase image (Fig. 2b) and the phase angle of the acquired signals (Fig. 2c). Using an algorithm earlier described [16,22] a pixel-to-pixel, region-growing version of a method by Brix et al. [23] we obtained water-only (Fig. 2e) and fat-only (Fig. 2f) images. Due to the chemical shift displacement effect, there is a fat-water shift of 1.7 pixels in the readout (head-feet) direction. We corrected for this by shifting back the water-only image relative to the fat-only image by 2 pixels. This correction removed almost all of the displacement artifacts in the fat-fraction image (Fig. 2g), which would have been present otherwise. The fat-fraction image was calculated using the following formula:

$$F_f = \frac{M_f}{M_f + M_w}$$

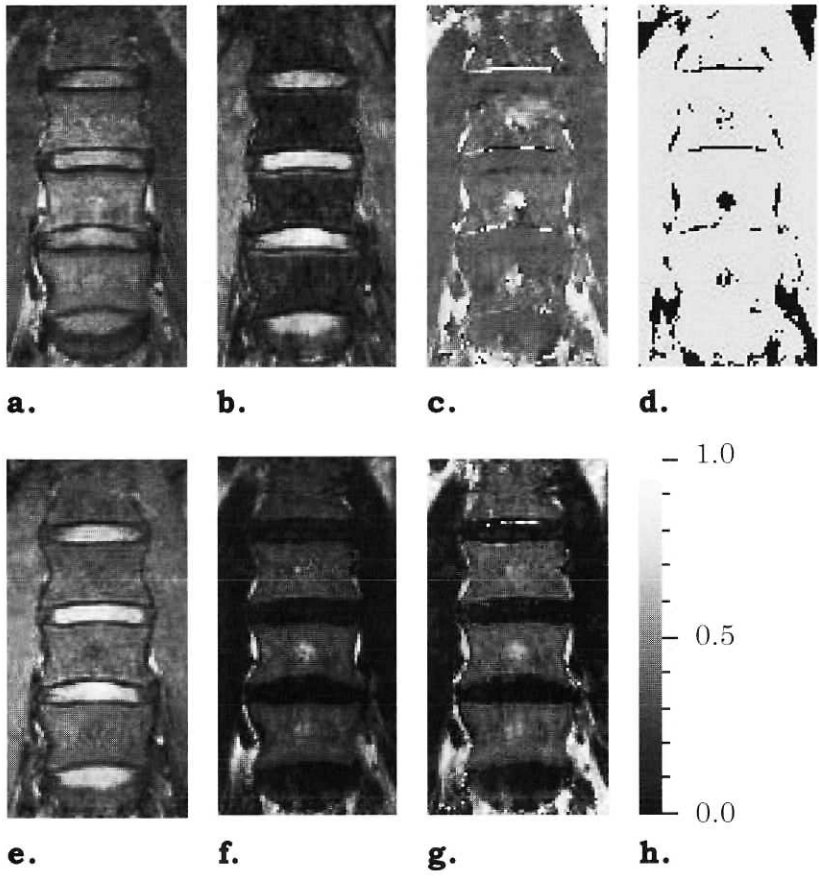

Figure 2. Postprocessing of a Dixon sequence. Shown are the in-phase magnitude image (**a**), opposed-phase magnitude image (**b**), and image of the phase difference between in-phase and opposed-phase sequences (**c**). From (c), the sign information (**d**) is obtained: In the lighter parts, water signal > fat signal; in the darker parts water signal < fat signal. Combining (a), (b) and (d), the water image (**e**) and the fat image (**f**) are obtained. Parts (e) and (f) have been shifted two pixels in the vertical direction with respect to each other, so as to correct for the chemical shift displacement. From (e) and (f), we calculate the fat-fraction image (**g**). Also shown is the scale relating gray values in (g) to fat-fraction numbers (**h**). Note: Postprocessing is done with rectangles of 64 x 128 pixels, as displayed here, containing L3, L4, and L5, which have been cut out of the original 256 x 256 images.

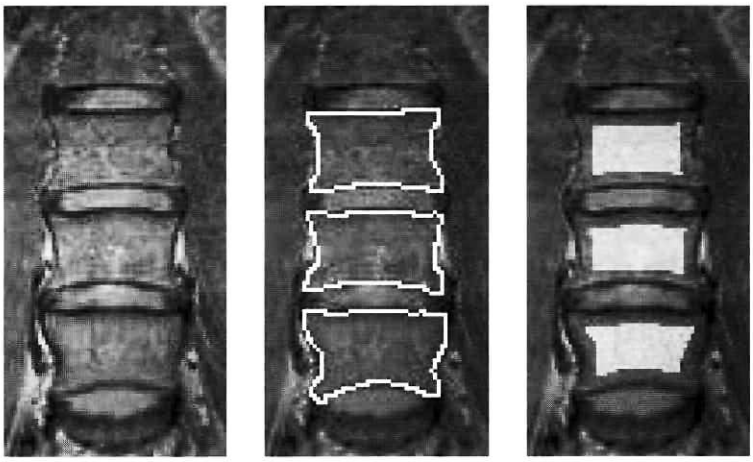

Figure 3. Determination of regions of interest. In the in-phase magnitude image (**a**), the vertebrae are clearly distinguishable from their surroundings. Interactively, with the help of a mouse, the contours of the vertebrae L3, L4, and L5 are drawn (**b**). By applying three erosion operations to the interior region of the contours, the regions of interest (**c**) are obtained.

in which F_f denotes the pixel values in the fat-fraction image, M_f the pixel values in the fat-only image, and M_w the pixel values in the water-only image. In this way, for every pixel, an F_f value was obtained, between 0 (no fat) and 1 (only fat, no water).

To obtain one fat-fraction value for each vertebra, we averaged the pixel values in an ROI. Figure 3 shows how these ROIS were obtained. In the in-phase image, the contours of the vertebrae L3, L4, and L5 were manually drawn, using a mouse. ROIs were calculated by applying three erosions to the region enclosed by the contours (Fig. 3c). "Erosion" is an image-processing procedure in which the edge pixels of a region are removed [24]. In this way, the outer parts of the vertebrae were excluded, which was done to avoid partial volume effects and sequelae of secondary bony change in degenerative disc disease [9,25]. ROIs with <100 pixels were considered non-representative and were discarded. To assess the influence of contour drawing on F_f, a second observer independently drew contours in the images of measurement a.

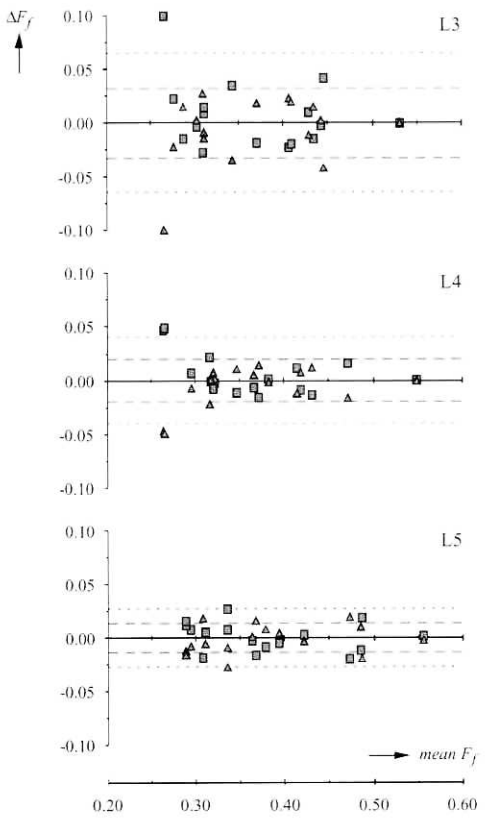

Figure 4. Data plot of the threefold measurement. x axis: mean F_f; y axis: differences of measurement data with the individual means (ΔF_f). Squares: measurement a; triangles: measurement b; dashed lines at $\pm \sigma_R$; SD of all points; dotted lines at $\pm 2\sigma_R$: 95% confidence intervals.

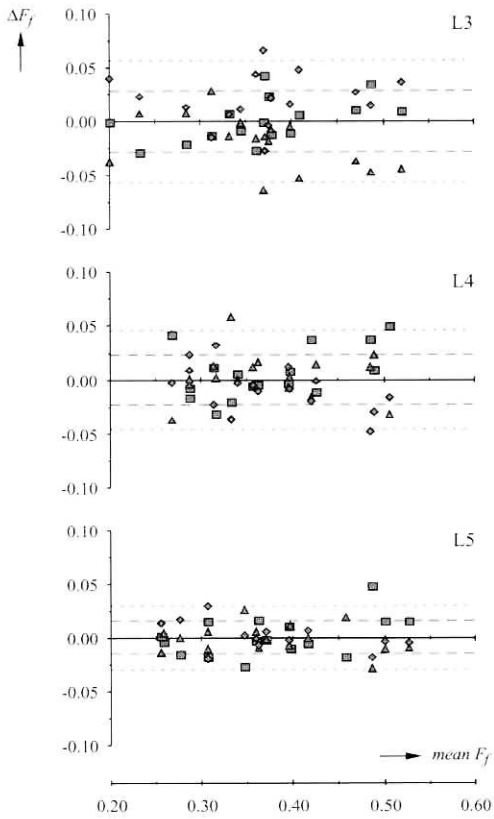

Figure 5. Data plot of the threefold measurement. x axis: mean F_f; y axis: differences of measurement data with the individual means (ΔF_f). Squares: measurement c1; triangles: measurement c2; diamonds: measurement c3; dashed lines at $\pm \sigma_f$; dotted lines at $\pm 2\sigma_R$: 95% confidence interval

In the analysis of the repeated measurement, we assumed that a specific measured F_f value was drawn from a normal distribution N(μ_i,σ_R), where the average value μ_i is the true F_f value for that volunteer and the SD σ_R is the error associated with repeating the measurement on a different day. σ_R was taken as our measure for the reproducibility and was derived by

plotting the data as described in Results (Fig. 4) similar to that previously described [26,27]. In the same way, we derived σ_T, the SD associated with the slice-repositioning error from the threefold measurement (Fig. 5), and σ_C, the SD associated with interoperator contour drawing variability, from the results of the two contours. All calculations were performed for the three vertebrae separately. The significance of differences was tested with a two sided paired t test. Results were considered significant if $p < 0.05$.

RESULTS

All volunteers underwent the procedures without problems. Every examination was adequate. In one volunteer, there was a significant scoliosis of the spine, which made it somewhat difficult to obtain a mid-sagittal localizer slice for accurate positioning of the measurement plane. Three volunteers had a relatively large lordosis, causing the ROI of L5 in the most anterior slice of the threefold measurement to be smaller than 100 pixels. Therefore, these data were discarded. The remaining ROIs had an average (range) of 254 (153-343) pixels in the repeated measurement and 242 (128-341) pixels in the threefold measurement. We observed no consistent differences between the results from the two coil-scanner combinations.

In Fig. 4, we show the results of the repeated measurement: on the x axis, the individual mean F_f values of measurements a and b are plotted (as an estimate of the "true" individual value μ_i) and on the γ axis, the differences of the F_f values with these means (ΔF_f). The SD in the γ direction is σ_R = 0.032 in L3, 0.020 in L4, and 0.013 in L5. We found no significant differences between the F_f values of measurements a and b. The group averaged F_f (SD) values were 0.37 (0.08) in L3 and L4, and 0.38 (0.08) in L5.

In the same manner, the results of the threefold measurement are shown in Fig 5. For the SDs, we find σ_T = 0.028 in L3, 0.023 in L4 and 0.015 in L5. We found no significant differences between the F_f values of measurements c1, c2, and c3.

There were no significant differences between the results from the contours from two operators, as performed in measurement a.

The associated reproducibility measure, σ_C, was 0.003 in L3, 0.002 in L4, and 0.002 in L5.

DISCUSSION

Dixon QCSI is an established method for the characterization of various bone marrow disorders [18,19,25]. It has been reported as a powerful non-invasive tool for the quantitative analysis of bone marrow invasion [9-12,28], and it is stated to be the most sensitive technique to evaluate bone marrow response to the expensive enzyme supplementation therapy in Gaucher disease [29]. In view of the small number of evaluation studies of this method, we performed the present measurements to assess a number of reproducibility aspects in a group of healthy volunteers. We also compare our results with the available literature data.

Reproducibility

The σ_R, the reproducibility of F_f, when the measurement is repeated on a different day, comprises many sources of error, among which are physiological variabilities, machine instabilities, slice-positioning errors, and contour drawing (ROI) variations. The two latter variables are operator dependent and therefore were analyzed in detail.

The contribution of contour drawing to σ_R is very small. Since the σ values are SDs, they add quadratically, and therefore the contribution of σ_C to σ_R is negligible. Apparently, the procedure for obtaining ROIs is very reproducible. Slice positioning was performed on an (interpolated) localizer image with an anteroposterior resolution of about 4 mm, and we do not expect the positioning accuracy in the repeated measurement to be much smaller. In the threefold measurement, we deliberately varied the slice position by 3-4 mm, which is comparable with the estimated positioning variance. From the fact that σ_T and σ_R are of the same magnitude, we conclude that the contribution of the error due to slice (re)-positioning to σ_R is considerable. Paying attention to accurately repositioning the measurement slice is of crucial importance to the reproducibility; a localizer image with a higher resolution is likely to give improvement.

We did not analyze in detail the physiological variability, instabilities in the equipment, and other causes for error and variations that may contribute to σ_R. However, σ_R is the upper limit; whatever the effect of the physiological variability on this measurement, it could never have been larger than σ_R. Since we have seen already, that slice positioning can

explain the larger part of σ_R, these other influences can be of only minor importance.

An interesting observation from the σ values and Figs. 4 and 5 is that both in the repeated measurement (σ_R) as well as in the threefold measurement (σ_T), L3 has the worst reproducibility. When reviewing the images, there appeared to be more artifacts in L3, probably owing to respiration or blood flow in vessels, causing artifacts in the phase direction (left-right).

Comparison with literature data on healthy volunteers

We found only one study in the literature that included repeated measurements with Dixon QCSI in the lumbar vertebrae: Rosen et al. [9] report fat-fraction measurements at 0.6 T in three volunteers, repeated two or three times, giving a total of only seven measurements. Recalculation of their data using our analysis method yields σ_R = 0.023, which is comparable to the results of our study: σ_R = 0.013 to 0.032.

Dixon QCSI fat-fractions of healthy volunteers without repetition of measurements are reported more frequently: Table 1 lists our data together with data from the literature with F_f values ranging from 0.29 to 0.48. To understand the apparent differences between the various studies, the methodological and physiological factors that might affect the measured F_f values should be considered.

The most important methodological factors that vary in these studies are TR, the field strength, and whether relaxation correction is applied. Water T1 is considerably longer than fat T1, so T1-weighting causes a stronger reduction of the water signal than of the fat signal, and therefore a shorter TR will lead to a higher measured F_f. This might explain the high F_f values found previously [19,25,28], for these authors used the shortest TR (1,200 ms); their mutual differences are small compared with the reported SDs. At a lower field strength, T1 relaxation is faster, and hence the measured F_f will be lower. By explicitly applying relaxation correction, which implies performing T1-, T2- and proton density-weighted Dixon sequences, one is insensitive to TR, TE and B_0.

TABLE 1. Average fat-fraction values of healthy volunteers, measurement parameters, age and gender

Ref.	B_0 (T)	RC*	TR/TE (ms)	n	Gender	Age (yrs)	Vertebrae	F_f	SD
This study	1.5	No	2,500/ 22.3	16	8M, 8F	24-60	L3-5	0.37	0.09
21	1.5	No	2,000/22	3	1M, 2F	18-21	L4-5	0.33	0.04
19	1.5	No	1,200/22	9	?	19-49	L4-5	0.48	0.10
25	1.5	No	1,200/22	10	?	12-49	L3-5	0.41	0.13
28	1.5	No	1,200/22	17	?	18-52	L3-5	0.44	?
12 (9)	0.6	Yes		6	?	21-47	L2-5	0.29	0.06

*RC = relaxation corretion

In fact, this corresponds to a proton density-weighted sequence with TR $\rightarrow \infty$ and TE $\rightarrow$ 0, and the resulting F_f will be lower than without relaxation correction. This explains the low F_f value at 0.6 T reported in Table 1. Disadvantages of relaxation correction, however, are increasing imaging time and performing additional calculations, which often cause problems [9,10].

Important physiological factors known to influence F_f are age and gender. Ishijima et al. [4] reported fat-fractions in females slowly increasing with age from 5 to 44 years and rapidly increasing in women older than 45 years; for males, a rapid increase of fat-fraction in the age group of 5-25 years with virtually no increase above 25 years was reported. The low F_f values reported previously [18] might be explained by their very young volunteers. The relations we find (Fig. 6) are in accordance with those reported by Ishijima et al. [4], with no correlation of F_f with age in the male group (ages 24-60 years) and a strong correlation in the female group (ages 26-55 years).

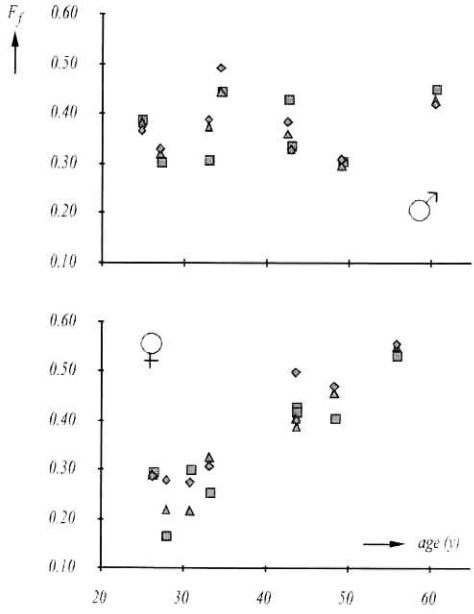

Figure 6. F_f in relation to age and gender: data from measurement a. Squares: L3; triangles: L4; diamonds: L5. Correlation coefficients for L3, L4, and L5 in men: r= 0.32, 0.09, and 0.04; in women: r= 0.91, 0.95, and 0.96.

Clinical Implications

The σ_R (0.013-0.032) we found is quite small compared with the influence of pathology on F_f as found in the literature. The reported changes in F_f values due to various hematologic pathologies as well as Gaucher disease range from 0.19 to 0.35 [10,12,25,28]. Furthermore, σ_R is three to four times as small as the SD of F_f in our population: 0.08.

Our results support the use of this technique as a non-invasive parameter in various hematologic or other bone marrow pathologies as a parameter of response to therapy or as a detector of relapse of disease. The use of fast or turbo spin echo may shorten the imaging time [30]. This has been explored, however, only for fat-suppression purposes; there is no experience yet with its use in QCSI.

One must remain careful in comparing results between studies and centers. It seems necessary to set up a database of normal population with age/gender values specific for the MR parameters used and the properties of the sequences used in every institution that wishes to implement this technology. Furthermore, every patient who will be studied repeatedly in time should be scanned with all technical parameters kept constant.

CONCLUSIONS

Dixon QCSI fat-fraction measurement, when repeated on different days, has a very good reproducibility: σ_R = 0.013 (in L5) to 0.032 (in L3). σ_R is quite small compared with the changes due to pathology as found in literature. Differences in the fat-fraction between various vertebrae in the same volunteer are very small.

The contribution of contour drawing variations to the reproducibility is negligible. The slice- repositioning error, however, is of some importance. The use of a high resolution localizer image seems to be advisable.

Taking into account the influence of age, gender, and technical factors on the fat-fraction, our fat-fractions are in accordance with the literature, as are the age and gender dependencies we found. However, one must be careful when comparing fat-fraction values between centers.

The most valuable application of Dixon QCSI fat-fraction measurements in the lumbar vertebrae is in following the same person longitudinally in time, keeping all technical parameters constant. In that case, one profits most from the good reproducibility; pathologic variations as well as the effects of treatment are most likely to show. The inclusion of this method in research protocols concerning red bone marrow involvement or marrow characterization is therefore highly recommended. Its potential in the clinical evaluation of bone marrow pathology is a subject of ongoing study.

ACKNOWLEDGEMENT

The authors thank Carla E.M. Hollak M.D., Ph.D., and Johannes M.F.G. Aerts, Ph.D., for their support in executing this study.

REFERENCES

1. Vogler JB III, Murphy WA. Bone marrow imaging. Radiology 1988; 168:679-693.
2. Weiss L. Cell and Tissue Biology. 6th Ed. Baltimore: Urban & Schwarzenberg, 1988; 469-478.
3. Cristy M. Active bone marrow distribution as a function of age in humans. Phys Med Biol 1981; 26:389-400.
4. Ishijima H, Ishizaka H, Horikoshi H, Sakurai M. Water fraction of lumbar vertebral bone marrow estimated from chemical shift misregistration on MR imaging: normal variations with age and sex. AJR 1996; 167:355-358.

5. Lecouvet FE, Vande Berg BC, Michaux L, et al. Stage III multiple myeloma: clinical and prognostic value of spinal bone marrow MR imaging. Radiology 1998; 209:653-660.
6. Steiner RM, Mitchell DG, Rao VM, et al. Magnetic resonance imaging of bone marrow: diagnostic value in diffuse hematologic disorders. Magnetic Resonance Quarterly 1990; 6:17-34.
7. Smith SR, Williams CE, Davies JM, Edwards RHT. Bone marrow disorders: characterization with quantitative MR imaging. Radiology 1989; 172:805-810.
8. Dixon WT. Simple proton spectroscopic imaging. Radiology 1984; 153:189-194.
9. Rosen BR, Fleming DM, Kushner DC, et al. Hematologic bone marrow disorders: quantitative chemical shift MR imaging. Radiology 1988; 169:799-804.
10. Gerard EL, Ferry JA, Amrein PC, et al. Compositional changes in vertebral bone marrow during treatment of acute leukemia: assessment with quantitative chemical shift imaging. Radiology 1992; 183:39-46.
11. Gückel F, Brix G, Semmler W, et al. Proton chemical shift imaging of bone marrow for monitoring therapy in leukemia. J Comput Assist Tomogr 1990; 14:945-959.
12. Johnson LA, Hoppel BE, Gerard EL, et al. Quantitative chemical shift imaging of vertebral bone marrow in patients with Gaucher disease. Radiology 1992; 182:451-455.
13. Maas M, Akkerman EM, Hollak CEM, Rademakers RP. Evaluation of skeletal involvement in M. Gaucher: Use of quantitative chemical shift imaging (QCSI). Eur Radiol 1997; 7 Supplement:206.
14. Disler DG, McCauley TR, Ratner LM, Kesack CD, Cooper JA. In-phase and out-of-phase MR imaging of bone marrow: prediction of neoplasia based on the detection of coexistent fat and water. AJR 1997; 169:1439-1447.
15. Ballon D, Jakubowski AA, Tulipano PK, et al. Quantitative assessment of bone marrow hematopoiesis using parametric magnetic resonance imaging. Magn Reson Med 1998; 39:789-800.
16. Maas M, Dijkstra PF, Akkerman EM. Uniform fat-suppression in hands and feet through the use of two point Dixon chemical shift imaging. Radiology 1999; 210:189-193.
17. Sargent MA, Poskitt KJ, Xiang QS, An L. Application of a three-point method for water-fat MR imaging in children. Pediatr Radiol 1999; 29:444-448.
18. Buxton RB, Wismer GL, Brady TJ, Rosen BR. Quantitative proton chemical shift imaging. Magn Reson Med 1986; 3:881-900.

19. Gückel F, Brix G, Semmler W, et al. Systemic bone marrow disorders: characterisation with proton chemical shift imaging. J Comput Assist Tomogr 1990; 14:633-642.
20. Lee JKT, Dixon WT, Ling D, Levitt RG, Murphy jr. WA. Fatty infiltration of the liver: demonstration by proton spectroscopic imaging. Radiology 1984; 153:195-201.
21. Brix G, Heiland S, Belleman ME, Koch T, Lorenz WJ. MR imaging of fat-containing tissues: validation of two quantitative imaging techniques in comparison with localized proton spectroscopy. Magn Reson Imaging 1993; 11:977-991.
22. Akkerman EM, Maas M. A region-growing algorithm to simultaneously remove dephasing influences and separate fat and water in two-point Dixon imaging. In: Proceedings of the Society for Magnetic Resonance in Medicine and the European Society for Magnetic Resonance in Medicine and Biology 1995; 649.
23. Brix G, Schad LR, Lorenz WJ. ^{1}H-spectroscopic imaging using a modified Dixon method. Magn Reson Imaging 1988; 6:617-622.
24. Gonzalez RC, Woods RE. Digital Image Processing. Addison Wesley, 1992; 518-524.
25. Kauczor HU, Brix G, Dietl B, Jarosch K, Knopp MV, van Kaick G. Bone marrow after autologous blood stem cell transplantation and total body irradiation: magnetic resonance and chemical shift imaging. Magn Reson Imaging 1993; 11:965-975.
26. Altman DG. Practical Statistics for Medical Research. 1st ed. London UK, Chapman & Hall 1991, reprint 1997.
27. Bland JM, Altman DG. Statistical methods for assessing agreement between two methods of clinical measurement. Lancet 1986; Feb:307-310.
28. Kauczor HU, Dietl B, Brix G, Jarosch K, Knopp MV, van Kaick G. Fatty replacement of bone marrow after radiation therapy for Hodgkin disease: quantification with chemical shift imaging. JMRI 1993; 3:575-580.
29. Rosenthal DI, Doppelt SH, Mankin HJ, et al. Enzyme replacement therapy for Gaucher disease: skeletal responses to macrophage-targeted glucocerebrosidase. Pediatrics 1995; 96:629-637.
30. Hardy PA, Hinks RS, Tkach JA. Separation of fat and water in fast spin-echo MRI imaging with the three-point Dixon technique. JMRI 1995; 5:181-185.

CHAPTER 3

Imaging and Quantifying Skeletal Involvement in Gaucher Disease

M. Maas [1], L.W. Poll [2], and M.R.Terk [3]

Department of Radiology [1], Academic Medical Center,
Amsterdam, The Netherlands;
Institute of Diagnostic Radiology [2], Heinrich Heine University,
Düsseldorf, Germany; and
Keck School of Medicine [3], University of Southern California, USA

Br J Radiology 2002; 75(Suppl. 1):A13-A24

ABSTRACT

Radiological imaging is used in patients with Gaucher disease to estimate the disease burden, to evaluate the presence of specific skeletal complications, and to track response to therapy. MRI is currently the best technique for assessing bone marrow involvement in Gaucher disease. Gaucher cell infiltrated bone marrow is characterized by an abnormal low signal intensity on conventional T1- and T2-weighted spin echo sequences, owing to a reduction in fat marrow, which gives a high signal intensity. Enzyme replacement therapy results in a degradation of Gaucher cell deposits with a reconversion of marrow fat and consequently an increased signal on T1-weighted images. Conventional MRI also detects other skeletal complications in Gaucher disease, including oedema resulting from acute bone infarction, infection and trauma, avascular necrosis, pathological fractures, and vertebral compression. The main drawback of conventional MRI is that it is not quantitative. Quantitative chemical shift imaging is the most sensitive quantitative method for evaluating bone marrow but is not widely available. Alternative MRI-based methods include calculation of the T1 relaxation constant and proton spectroscopy. Scoring of imaging changes detected on conventional MRI may be useful in estimating disease burden and risk of complications. Dual-energy X-ray absorptiometry (DXA) is sensitive to generalized osteopenia and changes in bone mineral density with extended enzyme replacement therapy. However, DXA is insensitive to local changes and cannot yet be used to predict fracture risk in these patients. Until the ideal quantitative technique is developed, conventional MRI will remain the best diagnostic modality for assessing skeletal complications in Gaucher disease and monitoring response to enzyme replacement therapy.

INTRODUCTION

In Gaucher disease, accumulation of Gaucher cells in the bone marrow triggers a series of events that lead to skeletal pathology. Skeletal involvement is seen on radiography in nearly all patients [1,2] but is not always associated with symptoms. When skeletal symptoms occur they can be totally debilitating [3].

The severity of bone involvement and the rate of progression vary considerably in Gaucher disease [3-9], but the disease is generally more aggressive in patients who present with symptoms during childhood. Osteopenia, osteonecrosis, osteosclerosis, bone crisis, chronic bone pain, pathological fracture and vertebral collapse can all be associated with Gaucher disease [3,10,11]. Although progression of many of these complications can be halted or reversed by enzyme replacement therapy (ERT), osteonecrosis, osteosclerosis and vertebral compression cannot be reversed. It is therefore imperative that skeletal involvement is assessed early and monitored routinely.

The main goals of imaging bone and bone marrow in Gaucher disease are to estimate the disease burden, to evaluate the presence of specific skeletal complications and to track response to therapy. A variety of techniques have been used including plain radiography, CT, MRI and radionuclide imaging. Newer quantitative technologies and quantitative applications of older technologies are now being tested in Gaucher disease, such as dual-energy X-ray absorptiometry (DXA), quantitative CT and quantitative MRI techniques such as quantitative chemical shift imaging (QCSI) and bone marrow spectroscopy.

We will describe these modalities and their use in imaging and quantifying skeletal complications in Gaucher disease.

QUALITATIVE METHODS

Plain radiography

Plain radiography is almost universally available and is relatively inexpensive, but its sensitivity for defining the pattern of skeletal disease is only 30-40% [12]. Plain radiography is therefore not useful for diagnosing Gaucher disease or monitoring the response of the skeleton to therapy. Instead, plain radiography should be used for detecting complications such as fractures and for monitoring arthroplasty. Arthroplasty failure may be more frequent in patients with Gaucher

disease because of poor bone stock. Plain radiography can also be used to detect modelling disorders such as Erlenmeyer flask deformity of the distal femur and focal lesions such as avascular necrosis. Focal lesions can occur almost anywhere in the skeleton, which necessitates a broad-ranging X-ray screen, which is undesirable, especially in children.

Computed tomography

In patients with Gaucher disease, the main use of helical CT is to measure spleen and liver volumes [13,14]. In general, there is no role for CT in assessing bone disease. Applications for CT are generally limited to unusual circumstances, such as when conventional radiographs leave doubt, MRI is unavailable or patients are not MRI-compatible, and sectional images are desired.

Magnetic resonance imaging

MRI is the best technique for assessing skeletal involvement in Gaucher disease [15]. It is extremely sensitive to the skeletal pathologies found in Gaucher disease including acute bone infarction, infection, trauma, marrow infiltration with Gaucher cells and avascular necrosis [15-18].
With MRI (T1-weighted spin echo and turbo spin echo sequences, short tau inversion recovery (STIR) sequences, and T2-weighted spin echo, turbo spin echo, or T2* or gradient echo sequences), yellow bone marrow generates a hyperintense signal on T1- and an intermediate to hyperintense signal on T2- and T2*-weighted images in healthy adults (Figure 1A). On STIR sequences, fat marrow appears hypointense. In Gaucher disease, the fat marrow is replaced by the infiltration of Gaucher cells, which dramatically changes the signal to hypointense on T1-, T2- and T2*-weighted images (Figure 1B). In some patients with Gaucher disease, the T1-weighted signal is hypointense and the T2-weighted fat-suppressed or STIR images show hyperintense inclusions (Figure 1C, 1D). This may indicate an active or 'complicated' bone marrow process, such as acute bone crisis, occult fracture, infection or bone infarction. In extreme examples, these inclusions appear in over 50% of the femur marrow and are clearly visible on T1- and T2-weighted images (Figure 1E).

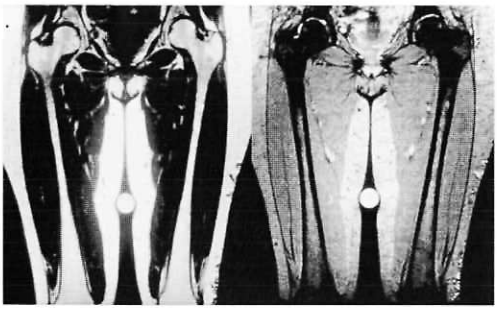

A

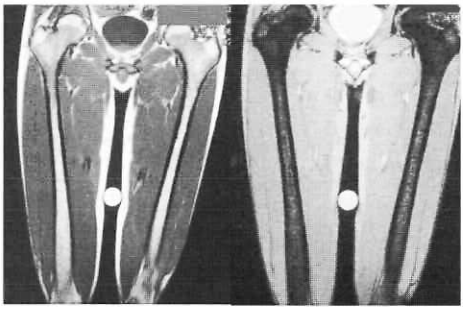

B

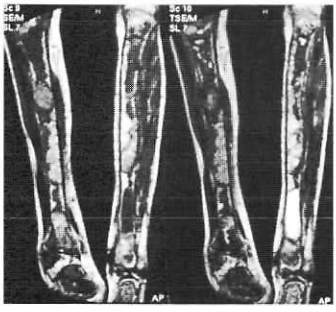

C

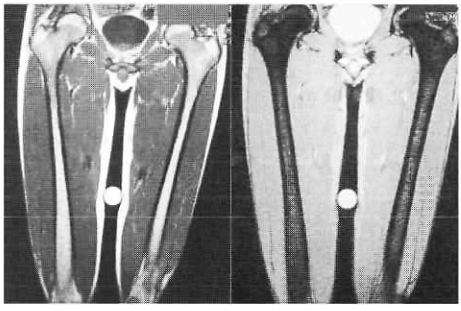

D

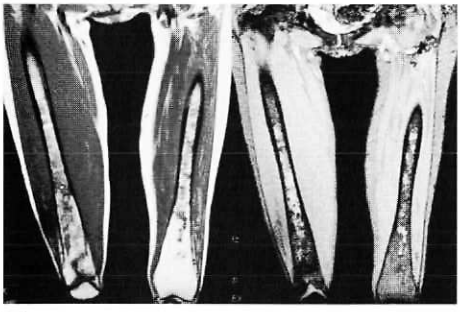

E

Figure 1. Patterns of bone marrow involvement on magnetic resonance images of the lower limbs. Coronal T1-weighted (TR/TE, 650/17) and T2*-weighted images of the femurs (**1A** and **1B**), T1-weighted spin echo and T2-weighted turbo spin echo images of the tibiae (**1C**), and fat-suppressed STIR images of the femurs (**1D** and **1E**) (TR/TE, 550/15).
(**A**) Normal healthy volunteer; (**B**), (**C**), (**D**) and (**E**) four different patients with type 1 Gaucher disease. T1-weighted images on the left and T2-weighted images on the right.

Bone marrow changes were evident in the spine of all examined patients with Gaucher disease, even when the involvement of the extremities was variable: this suggests that Gaucher disease is present initially in the lumbar spine, but with progression of disease the extremities become more affected [15]. The Gaucher cell infiltration subsequently extends to

the periphery of the extremities. The epiphysis and apophysis remain relatively unaffected except in the most severe cases. A variety of MRI protocols, all of which include T1-weighted sequences, have been used for imaging bone marrow changes in Gaucher disease [19,20]. A practical approach for MRI of Gaucher bone disease is to evaluate the lumbar spine and/or the lower extremity with conventional T1- and T2- or T2*-weighted spin echo sequences. However, a fat-suppressed sequence, for example STIR or fat-suppressed T2-/T2*-weighted, is mandatory for the detection of complications.

At birth, bone marrow is principally red (40% water, 40% fat, 20% protein) but with maturation the lipid content increases and red bone marrow is converted to yellow bone marrow (15% water, 80% fat, 5% protein), in a centripetal direction, with the epiphysis containing inactive yellow marrow from birth [21,22]. These natural changes in childhood and adolescence can be difficult to distinguish from Gaucher cell infiltration, which consequently makes the assessment of marrow changes in children with Gaucher disease by MRI more difficult. As the conversion from red to yellow marrow has a centripetal spread, the best way to establish severe disease in children may be the imaging of the lower part of the lower extremities, i.e. the tibia and ankle.

Radionuclide imaging

Nuclear scans with technetium-99m methylene-diphosponate (^{99m}Tc-MDP) show osteoblastic activity, which could potentially be useful for assessing bone turnover in Gaucher disease. In addition, marrow infiltration and response to therapy in Gaucher disease has been assessed using ^{99m}Tc-MDP, ^{99m}Tc-sestamibi and technetium-99m hexamethylpropylene amine oxime (^{99m}Tc-HMPAO) [23]. These nuclear techniques are very sensitive, but have a lower specificity - the main disadvantage is the poor spatial resolution compared with MRI [8,24]. Radionuclide imaging may help to distinguish between bone crisis and osteomyelitis in Gaucher disease.

QUANTITATIVE METHODS

To provide the clinician with a quantitative measurement of bone marrow infiltration, a number of quantitative imaging modalities are being tested in Gaucher disease.

Quantitative chemical shift imaging

Quantification of bone marrow changes in patients with Gaucher disease will help to assess disease status and response to therapy. QCSI may be the best method currently available for this.

QCSI, which is a modification of the Dixon technique [25], quantifies the fat content in bone marrow using the differences in the resonant frequencies of fat and water in bone marrow (3.3 ppm). It can therefore detect the reduction in the fat fraction of bone marrow that occurs in Gaucher disease [24,26]. Results obtained with QCSI correlate well with Gaucher disease activity [26] and response to ERT has been detected with this method [27].

Studies using QCSI in Gaucher disease have focused on vertebral bone marrow because abnormalities in vertebral bone marrow are homogenous and located in a fixed region, and because the spine contains active red marrow, which has been shown to change with disease in Gaucher disease and other hematological pathologies [26,28]. Coronal MRI of the lumbar spine is used and the fat content can be represented using a colour scale (Figure 2).

As with all MRI-based quantitative methods, the advantages of QCSI include its non-invasive nature and its ability to measure axial bone marrow. In addition, results with this method are highly reproducible [29]. In 16 healthy adults, the fat content in the lumbar bone marrow was measured twice in the same slice by QCSI and on a third visit the same slice was assessed as well as two parallel slices, 3 mm anterior and 3 mm posterior. The mean fat fraction in this group was 37% and standard deviation of triplicate measurements was only 1.3-3.2%, which could be explained by errors in the slice positioning. In comparison, the marrow fat content measured by QCSI was lower in most of the 31 patients with Gaucher disease tested (Figure 3).

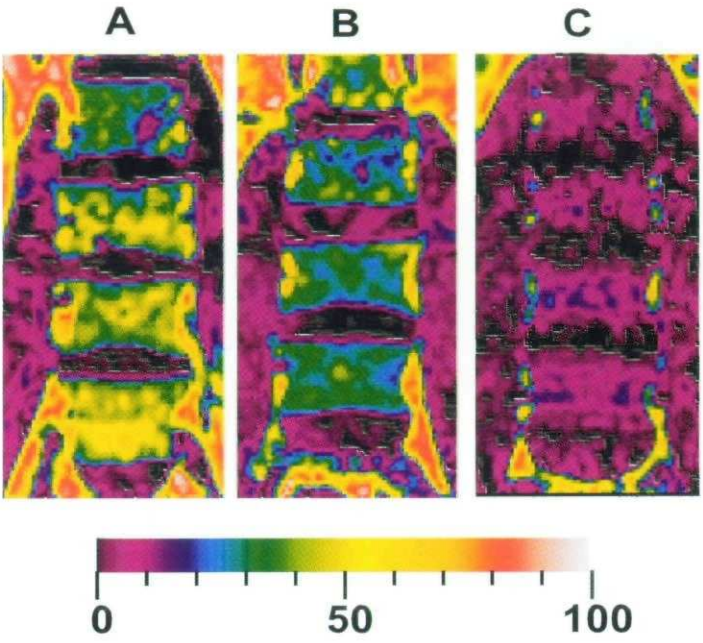

Figure 2. Colour representation of the fat content of lumbar spine measured by QCSI. (**A**) healthy individual; (**B**) patient with Gaucher disease with mild bone marrow involvement; and (**C**) patient with Gaucher disease with severe bone marrow involvement.

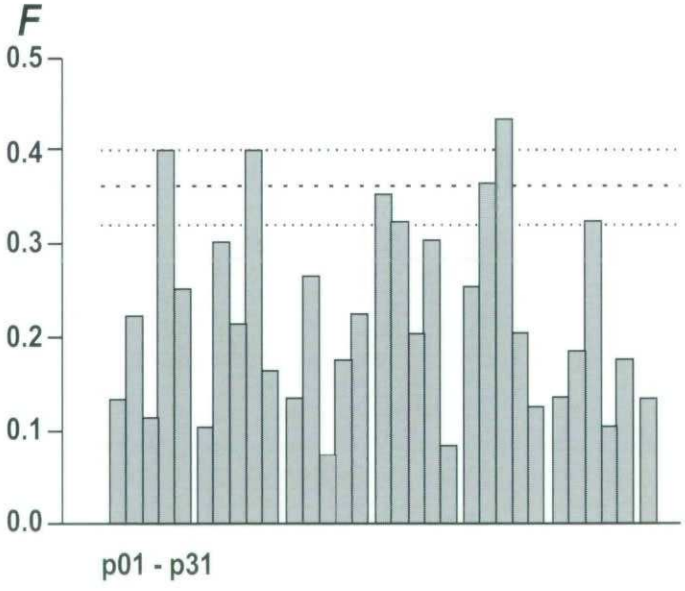

Figure 3. Percentage fat content in lumbar spine marrow, measured by QCSI in 31 patients with Gaucher disease before therapy (Academic Medical Center).

QCSI shows great promise as a quantitative measure of bone involvement in Gaucher disease. It is now a standard modality at the Academic Medical Center in Amsterdam for assessment of bone marrow burden, and all patients receiving treatment are evaluated annually. The limitations of QCSI are that the technology is not widely available, it does not use a standard MRI sequence (although the sequences are easy to implement) and a dedicated physicist and radiologist are mandatory to gain reliable results.

Bone marrow H1 spectroscopy

An experimental quantitative method for detecting relative differences in the fat concentration in bone marrow using H1 spectroscopy has been developed at the Keck School of Medicine of the University of Southern California, USA. The first step in this method is to determine the ratio of fat to water content for both the metaphysis and epiphysis, taking advantage of the 3.3 ppm difference in proton resonant frequencies between fat and water. The ratio of these values is then calculated. This method requires careful placement of the voxel so as to avoid areas of irreversible pathology, which yield unrepresentative fat:water ratios because they contain fluid cavities, fibrous tissue, or calcifications.

In a small study, the metaphyseal/epiphyseal fat:water ratio was significantly lower for patients with Gaucher disease than for normal subjects (0.70 and 1.41, respectively; $p<0.001$) [30]. However, until further studies are published the value of this technique for the assessment of clinically relevant bone disease in Gaucher disease is unknown.

Dual-energy X-ray absorptiometry

DXA quantifies bone mineral density by measuring the attenuation of the X-ray beam, with correction for soft tissue attenuation. This technique is widely used for assessing bone mineral density in patients with osteoporosis and is also useful for measuring bone mineral density in Gaucher disease [2]. Generalized osteopenia in the patient can be measured by comparing bone mineral densities with healthy age-matched and sex-matched adult controls [2].

The Z scores in patients with Gaucher disease are generally lower than those in healthy individuals, a finding that applies to many parts of the

skeleton (Figure 4) [2]. Furthermore, the severity of osteopenia in patients with Gaucher disease correlates with other indicators of disease severity, such as splenomegaly and hepatomegaly [2]. However, correlation between low bone mineral density and the risk of fractures in post-menopausal osteoporosis [31] cannot be extrapolated to the Gaucher disease population until further research is carried out.

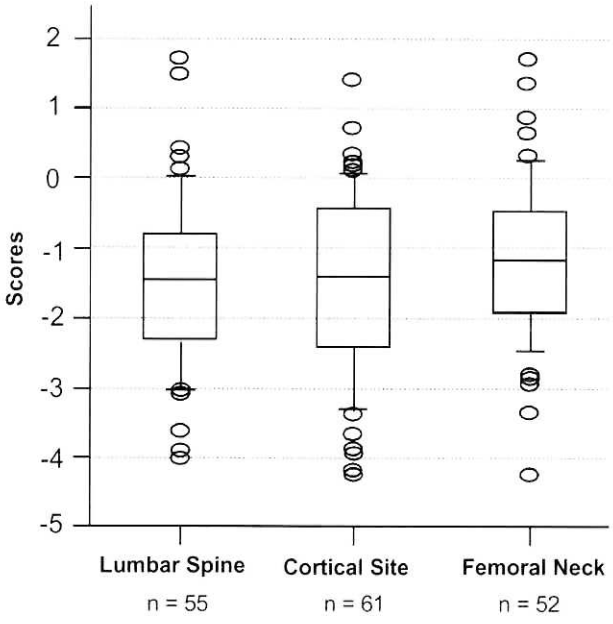

Figure 4. Mean bone mineral density at different anatomical sites in patients with Gaucher disease, measured by dual-energy X-ray absorp-tiometry. Reproduced from *J Bone Miner Res 1996;11:1801-1807 [2]* with permission of the American Society for Bone and Mineral Research.

DXA is insensitive to local changes in bone mineral density, but it is a good measure of generalized osteopenia. As such, DXA may be used to monitor the response of bone mineral density to therapy, although it takes several years of ERT before changes in bone mineral density are detectable [37]. The use of DXA in the patient with Gaucher disease is limited because areas of avascular necrosis, infarction or vertebral body collapse may cause erroneously high bone mineral density readings.

Quantitative CT

Dual-energy quantitative CT (DEQCT) is another method for measuring bone mineral density. As with DXA, values obtained using DEQCT are compared with standard values for healthy individuals. Trabecular bone loss may be a better indicator of osteopenia than general bone loss and the biggest advantage of DEQCT compared with DXA is its ability to differentiate between trabecular and cortical bone [24,32,33]. However, DEQCT is not recommended as it exposes the patient to much higher levels of radiation than single-energy quantitative CT (SEQCT) [34].

SEQCT is widely available, is less costly than DEQCT and involves lower radiation exposure than DEQCT. But the use of a single energy makes SEQCT less accurate than DEQCT, because fat marrow influences the measurements.

SEMI-QUANTITATIVE METHODS

Vertebra-disc ratio

The clinical utility of the vertebra-disc ratio (VDR), defined as the ratio of the T1-weighted MRI signal intensities of the L3 vertebra and a healthy L3/L4 disc, is being investigated at the Academic Medical Center in Amsterdam [35,36]. Data from 46 healthy adults without bone marrow disorders, degenerative disc disorders, or other pathological conditions of the spinal column showed that the mean VDR was about 1.68, taking into account an age-related increase in VDR. In contrast, the VDR for a patient undergoing radiotherapy, which is associated with an elevated yellow marrow fat content, was 2.6 and the VDRs for two patients with Gaucher disease were 1.00 and 1.23.

Rosenthal staging system

A semi-quantitative staging system was developed by Rosenthal et al [15,27], in which 11 sites of Gaucher cell infiltration in the lower extremities are numbered. This is based on the centrifugal spread of disease with infiltration of epiphysis and apophysis in severe disease. The score is the highest numbered site at which MRI demonstrates involvement. This scoring system demonstrated improvement in bone marrow during ERT [27] but was less sensitive than other measures that assess lumbar spine bone marrow. Furthermore, scores using this system are not yet correlated with QCSI results.

Düsseldorf bone marrow disease score

A similar approach has been taken at the Institute of Diagnostic Radiology, Heinrich-Heine-University, Düsseldorf, Germany. Sites of altered marrow (based on MRI) are given a score and the highest numbered site of involvement is taken as a measure of disease severity (Figure 5). In 63 patients with Gaucher disease, an abnormal low MRI signal intensity was observed in areas 1 and 2 of the femur in 98% of patients, in area 3 of the femur in 88%, in areas 4 and 5 of the tibia in 74%, in areas 6 and 7 (the epiphyses of the knees) in 39%, and in area 8 of the tibia in 36% [20]. This finding confirms previous studies showing that the epiphyses of the knees are spared in most patients with Gaucher disease. This scoring system suffers the same problems with sensitivity as the Rosenthal system, but did correlate with other symptoms of severe disease. The score in 13 patients with femoral head necrosis was 7.8 whereas in 49 patients without femoral head necrosis the score was 5.6 ($p < 0.0001$; unpublished results).

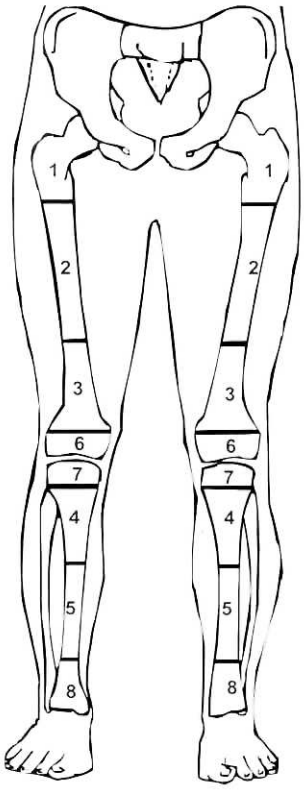

Figure 5. The Düsseldorf Gaucher score (modified "Rosenthal-score" [15]); anatomical score of the lower extremities for quantification and localization of bone marrow abnormalities.

Bone marrow burden score

At the Academic Medical Center in Amsterdam, a bone marrow burden scoring system has been developed that takes into account the progressive pattern of infiltration in the lumbar spine and the femur. Its use in the assessment of treatment response compared with QCSI is being evaluated in ongoing studies.

Classification and indirect measures

At the Keck School of Medicine, a system of classifying the severity of bone marrow infiltration in patients with Gaucher disease has been developed based on the changes in MRI signal intensities shown in Figure 1 (Table 1). Bone marrow involvement is further subclassified based on the absence or presence of avascular necrosis. One finding at the Keck School of Medicine was that avascular necrosis was much more prevalent in classes 2 and 3 than in classes 0 and 1, suggesting that this system of classification may have some prognostic value.

Table 1. Bone marrow classification based on T1- and T2-weighted signal intensity and avascular necrosis

Class	T1-weighted signal	T2-weighted signal	Avascular necrosis
0a	normal	normal	absent
0b	normal	normal	present
1a	decreased	decreased	absent
1b	decreased	decreased	present
2a	decreased	increased	absent
2b	decreased	increased	present
3a	decreased	increased >50%, heterogenous	absent
3b	decreased	increased >50%, heterogenous	present

Preliminary data from the Keck School of Medicine suggest that the degree of visceral response to ERT may be correlated with the response of bone marrow. In 14 patients who responded to ERT, there was a significant correlation between a bone marrow response (from the T1-weighted image) and the reduction in the volume of the liver ($p<0.005$) or spleen ($p<0.005$) [19].

Another Gaucher disease bone marrow classification system based on the pattern of T1- and T2-weighted images has been used at the Institute of Diagnostic Radiology, Düsseldorf [20]. In this system, a homogenous pattern of bone marrow is classified as type A morphology and a heterogenous or patchy pattern is classified as type B morphology (Figure 6). The rationale behind this classification was the assumption that a heterogenous pattern of bone marrow signal intensity represents a higher incidence of irreversible bone changes. In 63 adults with non-neuronopathic Gaucher disease, type B bone marrow morphology correlated with more severe skeletal disease (p<0.0001) and the presence of bone infarcts (p=0.0021).

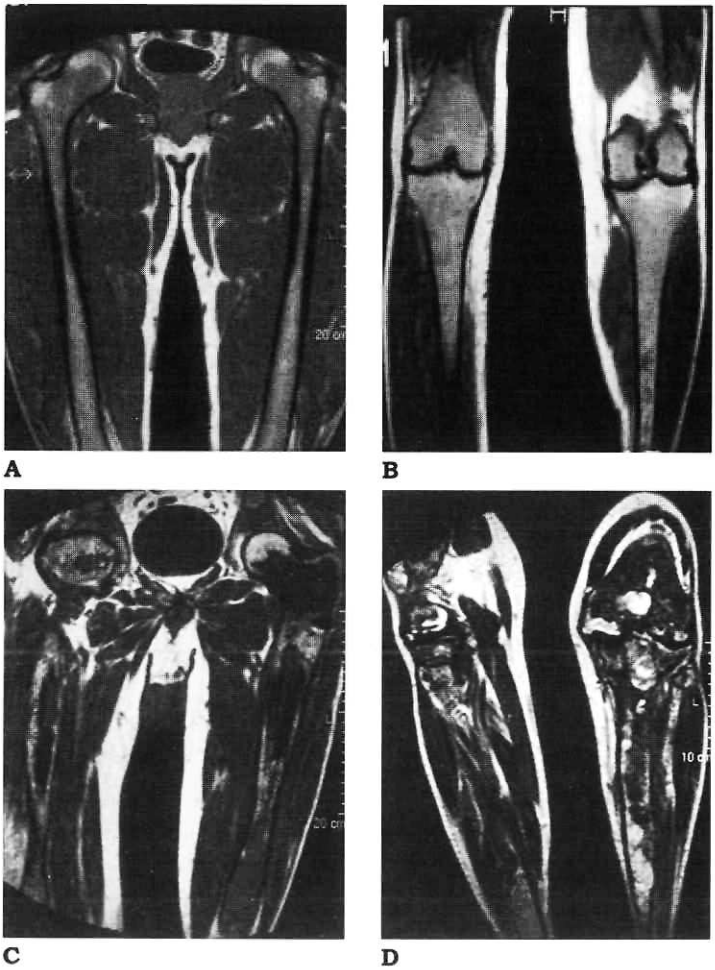

Figure 6. Coronal T1-weighted spin echo images of the lower extremities showing morphology type A (**6A** and **6B**) and B (**6C** and **6D**).

DISCUSSION

The skeletal complications of Gaucher disease are generally progressive but have an unpredictable course, and the response to therapy must be monitored in order to make decisions regarding dosage. The use of radiological imaging for patients with Gaucher disease should therefore not be restricted to differential diagnosis of skeletal complications, but should be performed at regular intervals.

Although the choice of radiological imaging techniques used to examine these patients is influenced by practical considerations such as availability and cost, this discussion will concentrate on the applicability of the technique to Gaucher disease.

MRI is the most widely applicable imaging technique for the skeletal complications of Gaucher disease, as it can used to detect infarction, infection, focal lesions, fractures, red marrow expansion, and bone marrow infiltration. This method is widely available in many western countries. It is the best technique for evaluating bone marrow infiltration in Gaucher disease. The main disadvantage of conventional MRI for evaluating bone marrow is that it is not quantitative.

Several MRI-based quantitative methods for measuring bone marrow infiltration in patients with Gaucher disease are being investigated, including Dixon QCSI, T1-relaxation calculations, and NMR spectroscopy. Dixon QCSI may become the standard quantitative method but protocols for this technique are not yet standardized. Furthermore, it is only available at a few centres worldwide. The majority of Gaucher patients therefore cannot currently benefit from this technique. Semi-quantitative scoring systems based on MRI and indirect methods for assessing bone marrow infiltration are also being researched. The advantage of the MRI scoring systems is that they are no more difficult or expensive than MRI and could become as widely available as conventional MRI, but the clinical relevance of these techniques for monitoring response to ERT is unknown. The ideal quantitative method for measuring skeletal complications and response to ERT in patients with Gaucher disease would be easy to perform, inexpensive, widely available, non-invasive, and the results would be consistent with skeletal outcome data. At present, no method for measuring skeletal involvement in Gaucher disease meets all these criteria.

A consensus on the optimum site of measurement must be reached before any quantitative or semi-quantitative technique for measuring bone marrow infiltration becomes widely accepted. Evaluation of the bone marrow of the lumbar vertebra and femur both have clinical advantages and disadvantages. In addition, a better understanding of the pathophysiology of changes in bone marrow morphology on MRI. For example, if a region that previously showed a homogenous signal of normal intensity on T2*-images later shows a heterogenous pattern, this may indicate an active disease state that may be irreversible. However, if a region of homogenous hypointense signal intensity on T1- and T2-weighted images shows a heterogenous pattern after ERT, this could indicate areas of bone marrow responding to treatment adjacent to areas of irreversible change.

A number of disease staging systems have been developed. These systems are less sensitive than QCSI for detecting response to ERT, and the absence of a standardized system may reflect our limited understanding of the natural history of Gaucher disease.

Plain radiography may be used for imaging orthopedic complications such as fractures and arthroplasty failure and for detecting focal lesions such as avascular necrosis. This technique has the advantages of being widely available and inexpensive. However, because of the low sensitivity of plain radiography, lesions initially detected with plain radiography may not show a response to therapy on follow-up plain radiography investigations. Plain radiography should therefore not play a major role in tracking or monitoring the skeletal response to therapy in Gaucher disease.

DXA and quantitative CT can provide quantitative data for assessing generalized osteopenia and measuring bone mineral density. Measurements with both of these techniques are compared with those of healthy, age- and sex-matched subjects. DXA may be used to measure response to ERT but quantitative CT currently plays a more scientific than practical role. In the absence of collapsed vertebrae, the lumbar spine may be the best site to use when measuring changes in bone mineral density with therapy, and the same site should be used during each assessment. More research is required to determine the long-term value of bone mineral density measurements in patients with Gaucher disease, for example to investigate the relationship between bone mineral density and fracture risk in these patients.

In conclusion, MRI is the most appropriate technique for assessing many of the skeletal manifestations, particularly bone marrow complications, of Gaucher disease. DXA is the most useful method for measuring bone mineral density. More research is needed to develop and optimize quantitative methods for measuring bone marrow infiltration and to understand the pathophysiology of skeletal complications of Gaucher disease so that the risk of complications may be predicted and the response to ERT optimized.

ACKNOWLEDGEMENTS

We would like to thank and acknowledge the invaluable input by J.-A. Koch (Germany), S. vom Dahl (Germany), E.M. Akkerman (The Netherlands), C.E.M. Hollak (The Netherlands) and J.F.M.G Aerts (The Netherlands).

REFERENCES

1. Rademakers RP. Radiologic evaluation of Gaucher bone disease. Semin Hematol 1995;32 (Suppl. 1):14-9.
2. Pastores G, Wallenstein S, Desnick RJ, Luckey MM. Bone density in Type 1 Gaucher disease. J Bone Min Res 1996;11:1801-7.
3. Stowens DW, Teitelbaum SL, Kahn AJ, Barranger JA. Skeletal complications of Gaucher disease. Medicine (Baltimore) 1985;64:310-22.
4. Beutler E, Demina A, Laubscher K, et al. The clinical course of treated and untreated Gaucher disease. A study of 45 patients. Blood Cells Mol Dis 1995;21:86-108.
5. Giraldo P, Perez-Calvo JI, Giralt M, Pocovi M. Clinical characteristics of type I Gaucher's disease in Spain. Preliminary results of national survey. Spanish Group on Gaucher's Disease. Med Clin (Barc) 1997;109:619-22.
6. Goldblatt J, Beighton P. Gaucher disease in the Afrikaner population of South Africa. S Afr Med J 1979;55:209-10.
7. Maaswinkel-Mooij P, Hollak C, van Eysden-Plaisier M, Prins M, Aerts H, Poll R. The natural course of Gaucher disease in The Netherlands: implications for monitoring of disease manifestations. J Inherit Metab Dis 2000;23:77-82.
8. Hermann G, Goldblatt J, Levy RN, Goldsmith SJ, Desnick RJ, Grabowski GA. Gaucher's disease type 1: assessment of bone involvement by CT and scintigraphy. Am J Roentgenol 1986;147:943-8.
9. Cremin BJ, Davey H, Goldblatt J. Skeletal complications of type I Gaucher disease: the magnetic resonance features. Clin Radiol 1990;41:244-7.

10. Pastores GM, Einhorn TA. Skeletal complications of Gaucher disease: pathophysiology, evaluation and treatment. Semin Hematol 1995;32 (Suppl. 1):20-7.
11. Mankin HJ, Doppelt SH, Rosenberg AE, et al. Metabolic bone disease in patients with Gaucher disease. In: Avioli LV, Krane SM, editors. Metabolic Bone Disease, Philadelphia: W B Saunders, 1990:730-52.
12. Colbert C. The osseous system. An overview. Invest Radiol 1972;7:223-39.
13. Glass RB, Poznanski AK, Young S, Urban MA. Gaucher disease of the liver: CT appearance. Pediatr Radiol 1987;17:417-8.
14. Charrow J, Esplin JA, Gribble TJ, et al. Gaucher disease: recommendations on diagnosis, evaluation, and monitoring. Arch Intern Med 1998;158:1754-60.
15. Rosenthal DI, Scott JA, Barranger J, et al. Evaluation of Gaucher disease using magnetic resonance imaging. J Bone Joint Surg Am 1986;68:802-8.
16. Sziklas JJ, Negrin JA, Rosshirt W, Rosenberg RJ, Spencer RP. Diagnosing osteomyelitis in Gaucher's disease. Observations on two cases. Clin Nucl Med 1991;16:487-9.
17. Hermann G, Shapiro RS, Abdelwahab IF, Grabowski G. MR imaging in adults with Gaucher disease type I: evaluation of marrow involvement and disease activity. Skeletal Radiol 1993;22:247-51.
18. Farahati J, Trenn G, John-Mikolajewski V, et al. Use of various diagnostic methods in a patient with Gaucher disease type I. Clin Nucl Med 1996;21:619-25.
19. Terk MR, Dardashti S, Liebman HA. Bone marrow response in treated patients with Gaucher disease: evaluation by T1-weighted magnetic resonance images and correlation with reduction in liver and spleen volume. Skeletal Radiol 2000;29:563-71.
20. Poll LW, Koch J-A, vom Dahl S, et al. Magnetic resonance imaging of bone marrow changes in Gaucher disease during enzyme replacement therapy: first German long-term results. Skeletal Radiol 2001;30:496-503.
21. Vogler JB, 3rd, Murphy WA. Bone marrow imaging. Radiology 1988;168:679-93.
22. Cristy M. Active bone marrow distribution as a function of age in humans. Phyl Med Biol 1982; 26(3):389-400.
23. Mariani G, Molea N, La Civita L, Porciello G, Lazzeri E, Ferri C. Scintigraphic findings on 99mTc-MDP, 99mTc-sestamibi and 99mTc-HMPAO images in Gaucher's disease. Eur J Nucl Med 1996;23:466-70.
24. Rosenthal DI, Barton NW, McKusick KA, et al. Quantitative imaging of Gaucher disease. Radiology 1992;185:841-5.
25. Dixon WT. Simple proton spectroscopic imaging. Radiology 1984;153:189-94.

26. Johnson LA, Hoppel BE, Gerard EL, et al. Quantitative chemical shift imaging of vertebral bone marrow in patients with Gaucher disease. Radiology 1992;182:451-5.
27. Rosenthal DI, Doppelt SH, Mankin HJ, et al. Enzyme replacement therapy for Gaucher disease: skeletal responses to macrophage-targeted glucocerebrosidase. Pediatrics 1995;96:629-37.
28. Rosen BR, Fleming DM, Kushner DC, Zaner KS, Buxton RR, Bennet WP, Wismer GL, Brady TJ. Hematologic bone marrow disorders: Quantitative Chemical Shift MR Imaging Radiology 1988; 169:799-804.
29. Maas M, Akkerman EM, Venema HW, Stoker J, Den Heeten GJ. Dixon quantitative chemical shift MRI for bone marrow evaluation in the lumbar spine: a reproducibility study in healthy volunteers. J Comput Assist Tomogr 2001;25:691-7.
30. Tran SD, Terk MR, Colletti PM. MR spectroscopy of bone marrow: precision and reliability. American Roentgen Ray Society 100th Annual Meeting 2000; 174:60.
31. Council of the National Osteoporosis Foundation. Guidelines for the early detection of osteoporosis and prediction of fracture risk. S Afr Med J 1996;86:1113-6.
32. Goodsitt MM, Rosenthal DI. Quantitative computed tomography scanning for measurement of bone and bone marrow fat content. A comparison of single- and dual-energy techniques using a solid synthetic phantom. Invest Radiol 1987;22:799-810.
33. Rosenthal DI, Mayo-Smith W, Goodsitt MM, Doppelt S, Mankin HJ. Bone and bone marrow changes in Gaucher disease: evaluation with quantitative CT. Radiology 1989;170:143-6.
34. Johnston CC, Jr., Slemenda CW, Melton LJ, 3rd. Clinical use of bone densitometry. N Engl J Med 1991;324:1105-9.
35. Maas M, Vlieger EJP, Akkerman EM, Hollak CEM, den Heeten GJ, Aerts JFMG. T1-W intensity ratio of vertebra and disc (V/D Ratio) in bone marrow evaluation: preliminary results in bone marrow. International Society for Magnetic Resonance in Medicine 1999:1043.
36. Vlieger EJP, Maas M, Akkerman EM, Hollak CEM, Aerts JFMG, den Heeten GJ. The application of the Vertebra-Disc Ratio in a population of patients with Gaucher's disease. International Society for Magnetic Resonance in Medicine 2000:2131.
37. Poll LW, Maas M, Terk MR, Roca M, Bembi B, Ciana G, Weinreb NJ. Response of Gaucher bone disease to enzyme replacement therapy. Br J Radiol 2002; 75(Suppl. 1):

CHAPTER 4

Quantification of skeletal involvement in adults with type 1 Gaucher disease: fat fraction measured by Dixon quantitative chemical shift imaging (Dixon QCSI) is a valid parameter

Mario Maas [1], Carla E.M. Hollak [2], Erik M. Akkerman [1], Johannes M.F.G. Aerts [3], Jaap Stoker [1], Gerard J. den Heeten [1]

Departments of Radiology[1], Hematology [2] and Biochemistry [3], Academic Medical Center, Amsterdam, the Netherlands

Accepted in AJR

ABSTRACT

Objective:

The objective of this study is to determine the merit of the fat fraction F_f of axial bone marrow measured by Dixon quantitative chemical shift imaging (Dixon QCSI) as a clinical parameter to quantitatively assess the extent of skeletal involvement in type 1 Gaucher disease.

Materials and Methods:

Dixon QCSI was performed in 30 untreated adult patients (mean age 39 years (range 18-69 years)) with type 1 Gaucher disease. The relation between the mean value of F_f in the vertebrae L3, L4 and L5 and the presence, absence and the severity of clinical bone complications (chronic bone pain, bone crisis, fracture, avascular necrosis and joint replacement) as well as the conventional MR imaging evaluation of bone marrow involvement were studied. Also the relation of F_f with gender, age and other disease parameters (history of splenectomy, liver and spleen volume, plasma chititriosidase, hemoglobin level and platelet count) was evaluated. Our results were compared to the F_f of healthy volunteers.

Results:

The F_f measured in patients with Gaucher disease ranged from 0.08-0.40 (mean 0.20). Bone complications occurred primarily in patients with F_f less than 0.23. Univariate logistic regression analysis indicated that for every decrease of F_f of 0.1 the risk of bone complications increased with 85% ($p<0.05$). F_f was correlated to liver size, but no correlation to other disease parameters was found. In the patient population F_f was significantly lower than in the healthy population (0.27-0.55, mean 0.37) ($p<0.001$).

Conclusion:

The fat fraction of the lumbar spine when measured with Dixon QCSI is associated with the occurrence of bone complications. It may therefore be a clinically useful parameter.

INTRODUCTION

Gaucher disease is the most prevalent lysosomal storage disorder, first described in 1882 by the French pathologist Philippe C. E. Gaucher [1]. The non-neuronopathic type 1 variant of the disease is the most common phenotype. The decreased activity of the lysosomal hydrolase, glucocerebrosidase, results in the accumulation of glucosylceramide (glucocerebroside) laden macrophages (Gaucher cells) in liver, spleen and in bone marrow. Bone disease is the most debilitating feature of type 1 Gaucher disease: in almost all patients there is skeletal involvement, ranging from mild osteopenia with minimal symptoms to major bone disease such as bone infarcts, osteonecrosis or fractures [2-7].

MR imaging is the imaging modality of choice for the evaluation of the extent of bone marrow disease due to its excellent soft tissue contrast and its sensitivity for the detection of both focal and diffuse disease [8-13]. The striking features of Gaucher disease infiltration on MR imaging are the focal or diffuse low signal intensity both on T1- and T2-weighted sequences in the bone marrow of the axial and peripheral skeleton [9-11]. The epiphyses of the long bones are relatively spared in mild disease and their infiltration is thought to represent severe Gaucher disease [9-11]. Areas in the bone marrow with high signal intensity on T2-weighed images are considered to represent acute disease [10].

Quantification of bone marrow involvement has become increasingly important in clinical management, both for the purpose of determining eligibility for therapy and for therapy monitoring, as the currently used enzyme supplementation therapy is very costly. For this purpose Dixon quantitative chemical shift imaging (Dixon QCSI) of the lumbar spine has been investigated [4,10-12,14]. This non-invasive technique is based on the phase contrast technique described by Dixon [15], in which the MR imaging signal is separated into the individual contributions of fat signal and water signal [12]. In this way the amount of fat can be quantified, and is represented as a fat-fraction F_f [4,10-12,14]. Evidence has been presented that infiltration of bone marrow in Gaucher disease causes a decrease of F_f since the total mass of lipid is less than normal because of displacement of triglyceride-rich adipocytes by Gaucher cells [3,4,13,14]. These data support a model of a dynamic process of bone marrow alterations in which F_f is inversely correlated with the amount of Gaucher

cells in the bone marrow, thus reflecting severity of bone marrow involvement [4,11,12,14].

The use of F_f as a parameter for Gaucher disease invasion is recognized among researchers and clinicians. Also the excellent reproducibility of this technique has recently been addressed [16]. Since F_f is a bone marrow parameter it may be useful as parameter of bone disease. This would be very convenient since a validated dynamic bone disease parameter is currently not available in the management of Gaucher disease.

The goal of this study is to validate lumbar F_f as a quantitative overall bone disease parameter. Therefore the relation of lumbar F_f with the presence and the clinical extent of skeletal disease is analyzed. Also the value of F_f as a prognostic parameter for bone disease is studied by calculating the relative risk. Furthermore F_f in healthy volunteers is compared to the data from the Gaucher population. In addition the correlation of F_f with the degree of organomegaly and cytopenia, as a measure of visceral and hematological involvement of Gaucher disease, is studied.

MATERIALS & METHODS

Patients & Volunteers

This study was performed in a University Hospital setting, a national referral center for Gaucher disease [17], between July 1993 and June 1998. We consecutively included untreated adult patients with type 1 Gaucher disease, who were referred for evaluation of eligibility for treatment. All patients underwent Dixon QCSI analysis as part of the diagnostic work-up that also includes MR imaging of the lumbar spine and the femur [18]. The measurement of glucocerebrosidase activity in leukocytes and genotyping was used to confirm the diagnosis of Gaucher disease in all patients [19-21]. The data from healthy volunteers were reported in a previous study in which the reproducibility of Dixon QCSI as a technique of measuring the F_f of bone marrow was evaluated [16].

Dixon QCSI fat-fraction of the axial skeleton

In-phase and opposed-phase proton density weighted spin echo sequences were performed on a 1.5 T magnet (Magnetom SP4000 and Vision, Siemens, Erlangen, Germany) with the following parameters: TR

2500 ms, TE 22.3 ms, slice thickness 4 mm, matrix 256x256, number of excitations 1, field of view 350x350 mm^2. The coronal measurement acquisition slices were positioned on a mid-sagittal localizer image, passing through the middle of the posterior parts of L3, L4 and L5, as illustrated in Figure 1 [16]. The direction of the measurement slice was selected with care to avoid motion artifacts.

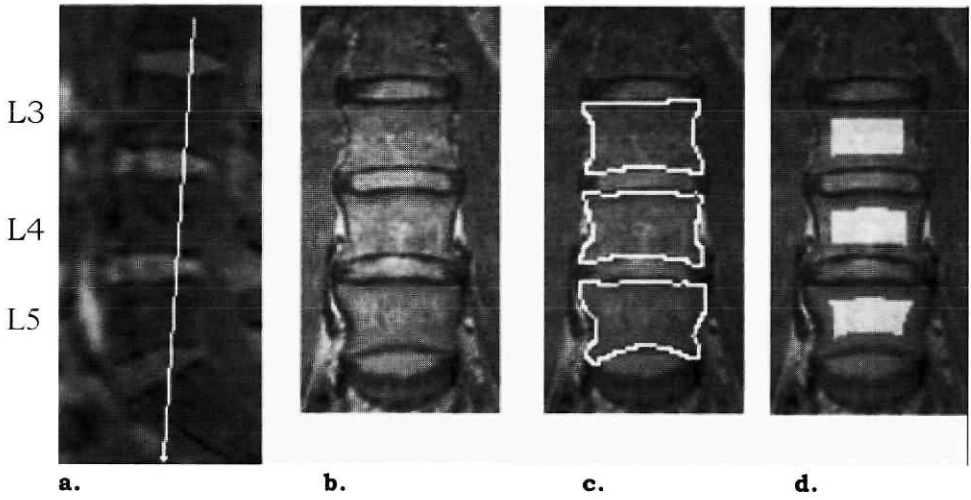

Figure 1. 35-year old healthy male volunteer in whom placement of measurement slice and determination of region of interest (ROI) is illustrated. **a**. Measurement slice is indicated on a mid-sagittal localizer image; it is perpendicular to localizer image and it passes through junction of the anterior three-quarter with the posterior one-quarter of vertebral body L4. Angulation from coronal towards transversal is applied to make slice pass optimally through the posterior parts of L3 and L5. **b**. In coronal in-phase magnitude image the vertebrae are clearly distinguishable from their surroundings. **c**. Interactively, with help of a mouse, the contours of vertebrae L3, L4 and L5 are drawn. **d**. By applying four erosion operations to the interior region of the contours, the ROI's are obtained in coronal plane.

Post-processing and data analysis were performed on a Sun Sparc 20-51 workstation (Sun Microsystems, Mountain View, CA), using a previously described algorithm [22,23]. To obtain one fat-fraction value for each vertebra, we averaged the pixel values over a user-defined region of interest (ROI). This ROI covered all but the peripheral edges of the vertebral bodies, thus avoiding inclusion of reactive changes due to

degenerative disc disease and avoiding partial volume averaging (Fig. 1). The mean F_f of the three vertebrae L3, L4 and L5 was used as overall *Ff*.

Clinical assessment of bone disease

The clinical signs related to severity of skeletal disease in Gaucher disease were assessed as follows: the presence of a history of bone complications was recorded for each patient. To analyze the relation between the severity of skeletal disease and F_f we clinically subdivided bone complications in the presence or absence of either of the following: chronic bone pain, bone crisis, fracture, avascular necrosis and joint replacement. If a fracture, avascular necrosis or a joint replacement was present the complications were considered to be severe. If only bone pain or a history of a bone crisis was present, then the complications were considered to be mild. Also the gender of the patients was analyzed, since male gender is described as a risk factor for osteonecrosis [7].

Radiological assessment of bone disease by conventional MR imaging

The radiological involvement of bone marrow was assessed using conventional MR imaging of the peripheral skeleton as described previously [5,11]. The scoring system is based on the fact that Gaucher disease spreads centrifugally starting from the diaphysis. The infiltration of the femoral diaphysis was scored as 1 point, the infiltration of the proximal epiphysis/apophysis was scored as 2 points and the infiltration of the distal epiphysis of the femurs was scored as 3 points.

Other clinical and laboratory parameters

The history of splenectomy was recorded. The exact volumes of liver and spleen were measured with the use of helical-CT with a method described earlier [17]. Plasma chitotriosidase levels served as a marker for total visceral Gaucher cell burden [24]. As hematological parameters the hemoglobin levels and platelet counts were determined.

Data analysis and statistics

Data were analyzed using SPSS 10.0 software (SPSS, Chicago, Illinois). Differences between groups were tested using the non-parametric Mann-Whitney test. A p-value of less than 0.05 was considered to represent significance. Correlation was calculated using the two-tailed non-parametric rank correlation (Spearman's ρ).

Furthermore a univariate logistic regression analysis was performed in order to analyze F_f as a bone disease parameter for the prediction of the relative risk. For this purpose the F_f was subdivided in categories of 10% fat-fraction.

RESULTS

Patients & Volunteers

A total number of 30 consecutive adult type 1 Gaucher disease patients were included. One patient was diagnosed with an additional bone marrow disorder; multiple myeloma and therefore was excluded from this study. This leads to 29 patients for further analysis, 16 men, 13 women, with a mean age 40 years (range 18-69 years).

Table 1. List of the 9 patients with their fat-fractions and bone complications.

	Age (years)	Gender	Fat fraction	Chronic bone pain	Bone crisis	Pathological fracture	Avascular necrosis	Joint replacement
1	37	M	0.11	-	+	+	+	-
2	39	F	0.11	+	+	-	+	-
3	71	F	0.19	-	+	-	-	-
4	29	M	0.10	-	+	+	+	+
5	65	M	0.12	+	+	-	+	+
6	44	F	0.16	-	-	-	+	+
7	57	M	0.34	-	+	+	+	+
8	36	M	0.22	+	+	-	-	-
9	36	F	0.08	+	-	-	-	-

Nine patients had a clinical history of bone disease of which six had severe bone disease (Table 1). Of these nine patients seven patients were splenectomized. The total number of patients with a splenectomy was nine.

The healthy volunteers group consisted of eight men and eight women: mean age 39 years (range 24-60 years).

Fat fraction, Ff

The fat-fractions measured in Gaucher disease patient's vertebral marrow ranged from 0.08-0.40 (mean 0.20). The value of F_f in the healthy population ranged from 0.27-0.55 (mean 0.37). The difference between the groups was statistically significant ($p<0.001$) (Fig. 2). In Figure 3 the distribution of F_f amongst the various subgroups is shown. No significant relation was found between fat-fraction and age ($p=0,12$). No statistical significant difference between men and women was found ($p=0.88$).

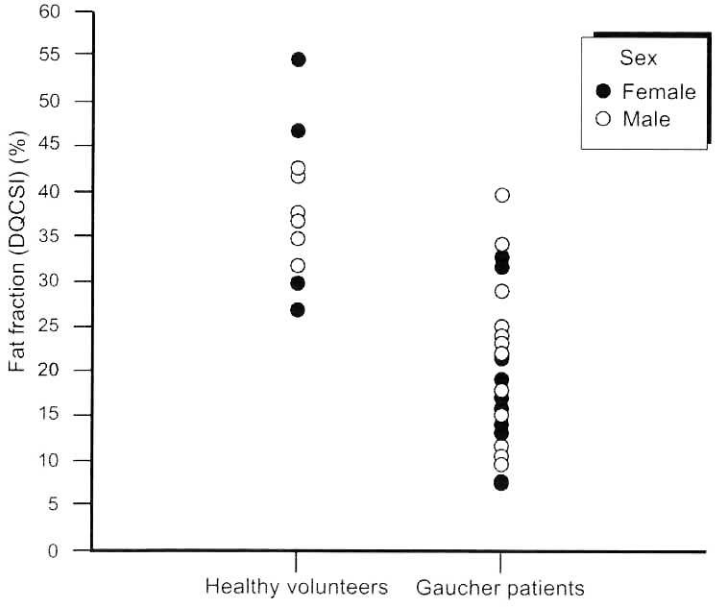

Figure 2. Plot of fat-fraction F_f for healthy volunteers and Gaucher disease patients.

Skeletal disease and F_f

When analyzing the relation between clinical bone complications and fat-fraction it is noted that eight out of nine patients with bone complications had an F_f less than 0.23. In order to analyze the relation between F_f and bone complications a univariate analysis was performed. (The outlier was excluded in this analysis.)

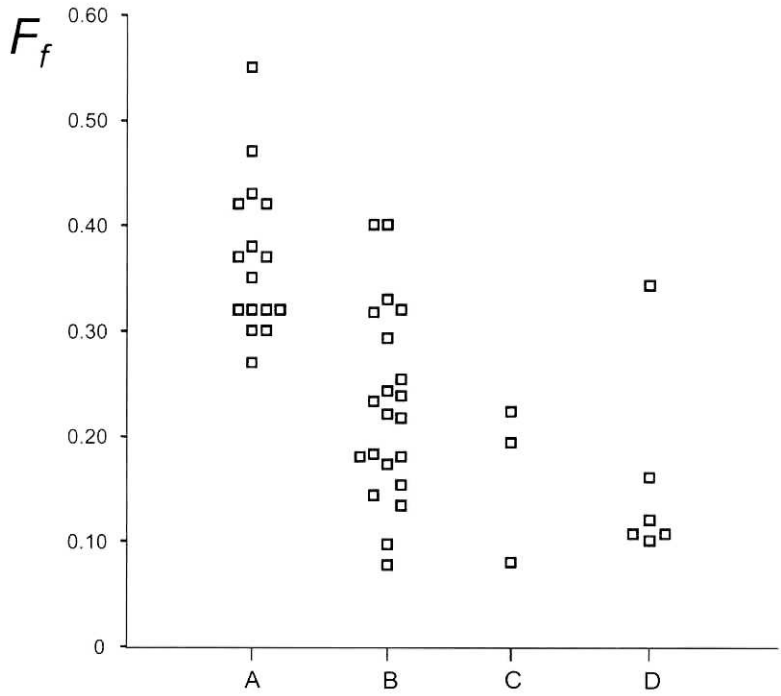

Figure 3. Plot of distribution of F_f in relation to clinical bone complications (A = healthy, B = Gaucher disease without complications, C = Gaucher disease with mild complications, D =Gaucher disease with severe complications).

This univariate logistic regression analysis showed that increase of 10% of the fat-fraction meant a decrease in the relative risk for developing bone complications by 85% ($p<0.05$). The radiological skeletal involvement measured by conventional MR imaging (in the healthy volunteers scored as zero) showed a significant inverse correlation with F_f (ρ = -0.78, $p<0.001$). Also a relation was established between the MR imaging score and the occurrence of bone complications (ρ = 0.58, $p<0.001$).

F_f in relation to other disease parameters

In general a lower F_f was found in splenectomized patients; this was nearly significant compared to the non-splenectomized group (p=0.06). The inverse relation between F_f and the volume of the liver is significant (ρ = -0.77, p<0.0001) but did not reach significance for the volume of the spleen (ρ = -0.52, p=0.79). In a univariate analysis the occurrence of bone complications was significantly associated with the presence or absence of the spleen (p=0.002) and with platelet count (p=0.01) (higher risk for bone complications in patients without a spleen and with a high platelet count). These two parameters are obviously related to each other. Pancytopenia in splenectomized patients may reflect bone marrow infiltration and is therefore possibly related to *Ff*. However, only four of nine splenectomized patients showed slightly decreased hemoglobin levels and/or platelet count. In these splenectomized patients, no relation was established between F_f and these parameters. The relation between chitotriosidase levels and F_f did not reach significance.

DISCUSSION

This is the first report that describes in an adult untreated population of Gaucher patients a close relationship between the extent of skeletal disease and a quantitative secondary parameter, that is, lumbar bone marrow fat-fraction. The presented detailed comparison of lumbar F_f and both clinical and radiological (MR imaging) skeletal disease suggests that lumbar F_f may be a sensitive predictor of ongoing skeletal disease in Gaucher disease patients. The fact that F_f correlates well with the peripheral MR imaging score, a parameter that is known to detect response to therapy [14], suggests that F_f potentially is a sensitive quantitative parameter for the evaluation of skeletal response to enzyme supplementation therapy.

This study has revealed that Dixon QCSI as assessed with MR imaging in Gaucher patients significantly relates the extent of mainly peripheral bone disease to the axial lumbar bone marrow fat-fraction F_f . Bone complications preferentially occurred in patients with an F_f less than 0.23. In a univariate logistic regression analysis, we established a further relationship between F_f and the risk for the occurrence of bone complications: when F_f decreases with 10%, the relative risk of developing

bone complications increases with 85% (p<0.05). This analysis is limited by the small sample size and the lack of longitudinal data. Nevertheless we feel that based on these data, the patients in the Gaucher disease group with a low F_f without bone complications are considered at risk. This is in concordance with an earlier observation made by Rosenthal et al. [11], when they described that marrow infiltration and replacement by Gaucher cells can remain silent for a long period of time before the appearance of clinically significant bone disease. This relation between low F_f and relative risk on bone complications is further supported by the observation made during follow-up. The two patients that suffered from bone complications during enzyme therapy had a low F_f at baseline and showed no or minor improvement in F_f during therapy [25, Hollak unpublished data]. The correlation that was suggested between low F_f and the development of bone complications but could not be proven earlier is supported in our study. Furthermore a significant difference was found in mean F_f between Gaucher disease patients and healthy volunteers.

In our data there is one patient that does not follow the trends. This patient is an outlier in fat-fraction as well as liver volume, but not in genotype (N370S/L444P). It is very difficult to find an explanation for this. The fact that he is the only patient who suffered from a bone crisis some weeks prior to the QCSI measurements may influence the local bone marrow composition and therefore the fat-fraction. However there is no literature data to support this.

Two other studies have reported on lumbar F_f in untreated type 1 Gaucher disease patients. Johnson et al. [4] performed Dixon QCSI measurements in 24 patients. Their F_f ranged from 0.006-0.32, with a mean of 0.10. Rosenthal et al. [14] studied 12 patients with type 1 Gaucher disease using Dixon QCSI; their F_f ranged from 0.006-0.26 with a mean of 0.073. Compared to these data, the present F_f 's are higher, suggesting that our patient population was less severely affected. An additional explanation for the difference may be the age difference. In the two studies mentioned, a considerable number of children and adolescents were included. The younger, healthy age groups will intrinsically show a lower Ff, because of the predominant presence of red cellular marrow in their axial skeleton [26]. During adolescence a marked conversion of red to fatty marrow occurs, resulting in a dynamic increase

in F_f values [8,25-28]. Thus in a person of younger age a measured low fat-fraction may be the sum of Gaucher disease infiltration and the presence of more red marrow. This study is the first study that compared the distribution the lumbar F_f of adult type 1 Gaucher disease patients to the distribution the lumbar F_f of adult controls with a comparable age distribution. The lumbar F_f of adult type 1 Gaucher disease patients is significantly reduced.

In two other reports Dixon QCSI data, MR imaging scores and skeletal disease manifestations are comparatively discussed [7,13]. Rodrique et al. [7] did not find the fat-fraction to be a significant determinant for the occurrence for osteonecrosis. However, correlation of lumbar F_f with less severe manifestations of skeletal disease was not evaluated in that particular study. In the study by Rosenthal et al. [14] the MR score of the peripheral skeleton and the fat-fraction measured by QCSI were analyzed as response parameter to therapy. The relationship between fat-fraction and conventional MR imaging score however was not analyzed.

There are a few limitations to consider. First one must realize that QCSI is not a standard sequence on an MR imaging machine and therefore not widely available. Thus the fat-fraction as such is not a parameter that is used worldwide. A limitation of this particular study, like in almost every paper concerning Gaucher disease, is the small number of patients that are included. In this way the statistical evaluation is hampered.

In Gaucher disease it is striking that the various parameters that monitor the possible sites of involvement such as organ volume, platelet count and history of skeletal disease show a poor correlation [4,7,14]. Although a significant correlation between F_f and liver volume was found in this study, this was not found with splenic volume. The Gaucher burden in liver and spleen does not necessarily predict the burden of Gaucher disease in bone marrow; there may be a considerable individual variation in the extent of involvement of visceral and bone marrow compartments. This could implicate that non-skeletal parameters will not adequately reflect skeletal or bone marrow involvement adequately and emphasizes the need for adequate separate quantitative assessment of bone marrow to allow overall interpretation of disease severity.

In summary, to answer the goals of our study we can conclude that fat-fraction measurements through the use of Dixon QCSI showed a close correlation with the clinical occurrence of skeletal involvement. There was a significant difference between the fat-fractions in untreated Gaucher disease patients when compared to healthy volunteers. Finally the fat-fraction may serve as a prognostic marker since univariate regression analysis showed that the decrease in fat-fraction with 10% is associated with an increased risk for occurrence of bone complications by 85%. Only a longitudinal study in patients under treatment can prove its value in clinical decision-making and outcome. In our view it is essential for optimal patient care to monitor the skeletal involvement on a regular basis and Dixon QCSI seems a valuable tool.

ACKNOWLEDGEMENT

The authors whish to thank Dr. C. van Kuijk and Dr. G. Hassan Bouber for their support in the preparation of this manuscript.

REFERENCES

1. Gaucher PCE. De l'epithelioma primitif de la rate, hypertrophie idiopathique de la rate sans leukemie. Thesis 1882; Paris.
2. Cremin BJ, Davey H and Golblatt J. Skeletal complications of Type 1 Gaucher disease: The Magnetic Resonance Features. Clin Radiol 1990; 41:244-247.
3. Miller SPF, Zirzow GC, Doppelt SH, Brady RO, Barton NW. Analysis of the lipids of normal and Gaucher bone marrow. J Lab Clin Med 1996; 127:353-358.
4. Johnson LA, Hoppel BE, Gerard EL, et al. Quantitative Chemical Shift imaging of vertebral bone marrow in patients with Gaucher disease. Radiology 1992; 182:451-455.
5. O'Keefe D, Rosenthal DI. Computed tomography and magnetic resonance imaging in Gaucher's disease. In: Bloem JL, Sartoris DJ. MRI and CT of the musculoskeletal system: a text-atlas. Baltimore: William & Wilkins, 1992; 130-138.
6. Rourke JA, Heslin DJ. Gaucher's disease; Roentgenologic bone changes over 20 year interval. AJR 1965; 94:621-630.
7. Rodrique SW, Rosenthal DI, Barton NW, Zurakowski D, Mankin HJ. Risk factors for osteonecrosis in patients with type 1 Gaucher's disease. Clin Orthop 1999 nr. 362, p 201-207.

8. Vogler III JB, Murphy WA. Bone marrow imaging. Radiology 1988; 168:679-693.
9. Rosenthal DI, Scott JA, Barranger J, et al. Evaluation of Gaucher disease using Magnetic Resonance Imaging. J Bone Joint Surg 1986; 68-A:802-808.
10. Hermann G, Shapiro RS, Fikry Abdelwahab I, Grabowski G. MR imaging in adults with Gaucher disease type 1:evaluation of marrow involvement and disease activity. Skeletal Radiology 1993; 22:247-251.
11. Rosenthal DI, Barton NW, McKusick KA, et al. Quantitative Imaging of Gaucher disease. Radiology 1992; 185:841-845.
12. Rosen BR, Fleming DM, Kushner DC, et al. Hematological Bone Marrow disorders Quantitative Chemical Shift MR Imaging. Radiology 1988; 169:799-804.
13. Mankin HJ, Rosenthal DI, Xavier R. Gaucher disease; New approaches to an Ancient Disease. Journal Bone Joint Surg Am 2001; 83:748-763.
14. Rosenthal DI, Doppelt SH, Mankin HJ, et al. Enzyme replacement therapy for Gaucher disease: skeletal responses to macrophage-targeted glucocerebrosidase. Pediatrics 1995; 96:629-637.
15. Dixon WT. Simple proton spectroscopic imaging. Radiology 1984; 153:189-194.
16. Maas M, Akkerman EM, Venema HW, Stoker J, den Heeten GJ. Dixon Quantitative Chemical Shift MR Imaging for Bone Marrow evaluation in the Lumbar Spine: an Evaluating Study in Healthy Volunteers. J Comput Assist Tomogr 2001;25:691-7.
17. Hollak CEM, Aerts JM, Goudsmit R et al. Individualized low-dose alglucerase therapy for type 1 Gaucher's disease. Lancet 1995; 345:1474-1478.
18. Maas M, Akkerman EM, Hollak CEM, Rademakers RP. Evaluation of skeletal involvement in M. Gaucher: Use of quantitative chemical shift imaging (QCSI). Eur Radiol 1997; 7: 206.
19. Sibille A, Eng CM, Kim S-J, Pastores G, Grabowski GA. Phenotype/genotype correlations in Gaucher disease Type 1: Clinical and therapeutic implications. Am J Hum Genet 1993; 52:1094-1101.
20. Sidransky E, Ginns EI. Phenotypic and genotypic heterogeneity in Gaucher disease: Implications for genetic counseling. J Genet Counsel 1994; 3:13-22.
21. Boot RG, Hollak CEM, Verhoek M, et al. Glucocerebrosidase Genotype of Gaucher Patients in the Netherlands: Limitations in Prognostic value. Hum Mutat 1997; 10:348-358.
22. Maas M, Dijkstra PF, Akkerman EM. Uniform Fat-Suppression in Hands and Feet through the use of Two Point Dixon Chemical Shift Imaging. Radiology 1999; 210:189-193.

23. Akkerman EM, Maas M. A region-growing algorithm to simultaneously remove dephasing influences and separate fat and water in two-point Dixon imaging. Proceedings of the Society of Magnetic Resonance and the European Society for Magnetic resonance in Medicine and Biology: Nice; Society of Magnetic Resonance 1995; 649.
24. Aerts JH, Hollak CEM. Plasma and metabolic abnormalities in Gaucher's disease. In Bailliere's- Clinical Haematology, A.Zimran (ed), W.B.Saunders Company Ltd, London 1997; 10(4):691-709.
25. Hollak C, Maas M, Akkerman E, den Heeten A, Aerts H. Dixon Quantitative Chemical shift imaging is a sensitive tool for the evaluation of bone marrow responses to individualized doses of enzym supplementation therapy in type 1 Gaucher disease. Blood Cells Mol Dis 2001; 27(6):1005-1012.
26. Cristy M. Active bone marrow distribution as a function of age in humans. Phys Med Biol 1981; 26(3):389-400.
27. Ishijima H, Ishizaka H, Horikoshi H, Sakurai M. Water fraction of lumbar vertebral one marrow estimated from chemical shift misregistration on MR imaging: Normal Variations with age and sex. AJR 1996; 167:355-358.
28. Rozman C, Feliu E, Berga L, Reverter JC, Climent C, Ferran MJ. Age-related variations of fat tissue fractions in normal human marrow depend both on size and number of adipocytes: a stereological study. Exp Hematol 1989; 17:34-37.

CHAPTER 5

Dixon quantitative chemical shift imaging is a sensitive tool for the evaluation of bone marrow responses to individualized doses of enzyme supplementation therapy in type 1 Gaucher disease

Carla Hollak [1], Mario Maas [2], Erik Akkerman [2], Ard den Heeten [2], Hans Aerts [3]

Dept. of Hematology[1], Radiology[2] and Biochemistry[1], Academic Medical Center, Amsterdam, The Netherlands.

Blood Cells Mol Dis 2001; 27(6):1005-1012

ABSTRACT

Type 1 Gaucher disease can be effectively treated with enzyme supplementation therapy. Bone disease is a debilitating feature of the disorder and results from infiltration of the bone marrow by Gaucher cells. The effect of treatment on bone marrow infiltration is difficult to measure, necessitating the development of sensitive techniques to allow adequate dosing. Dixon quantitative chemical shift imaging (Dixon QCSI) is a MRI technique to measure displacement of fatty marrow by Gaucher cells. Low bone marrow fat-fractions have been found in Gaucher disease. We studied the effect of individualized low doses of enzyme therapy on the fat-fractions of the lumbar spine in 12 adult Gaucher disease patients before and during treatment and in 9 untreated Gaucher controls. Fat-fractions were decreased in 9/12 patients (median 0.20, range 0.08-0.40) and equally low in the untreated Gaucher controls compared to age matched healthy volunteers (normal values 0.27-0.43, $p < 0.01$). During treatment, fat-fractions increased significantly already after 1 year in 11/12 patients (P=0.007). After 4 to 5 years, fat-fractions normalized in 11/12 patients. Fat-fractions remained low in the untreated Gaucher controls ($p = 0.5$ and 0.6 at 1 and 2 years, respectively). Six of 11 patients had a dose increase, which did not clearly affect fat-fractions.

Dixon QCSI is a sensitive tool for the measurement of the respons of bone marrow to enzyme therapy.

INTRODUCTION

Gaucher disease is the most frequently encountered lysosomal storage disorder in man. Deficiency of the lysosomal enzyme glucocerebrosidase (glucosylceramidase, EC 3.2.1.45) leads to accumulation of glucocerebroside in macrophages [1]. The clinical picture of type 1 disease encompasses hepatosplenomegaly, cytopenia, and bone involvement. Bone disease is one of the most debilitating features of type 1 Gaucher disease, including atypical bone pain, osteonecrosis, pathological fractures, and bone crises [1,2]. Enzyme supplementation therapy, using either placentally derived or recombinant glucocerebrosidase (alglucerase or imiglucerase, respectively, manufactured by Genzyme Co., MA) has proven to effectively reverse the clinical manifestations of Gaucher disease. Improvement in cytopenia and reduction of organomegaly belong to the early effects of treatment, usually being apparent after 3 to 6 months [3-5]. Monitoring of these disease manifestations is relatively easy by the application of routine blood tests and widely available modalities such as ultrasound, CT scanning or MRI, for organ volume determinations. Bone disease responds slower and is more difficult to measure. Several imaging techniques are being applied for the assessment of the severity of bone and bone marrow abnormalities. Plain radiographs and quantitative CT scanning for measurement of cortical thickness, densitometry, MRI and fat-fraction determination by Dixon quantitative chemical shift imaging (Dixon QCSI) have been used [3,6-9]. So far, changes in bone structure in respons to alglucerase treatment became apparent after years of treatment [7-9]. For the accurate application and interpretation of these different imaging techniques it is essential to divide bone disease into two different parts as has been done earlier by Rosenthal: bone structure and bone marrow infiltration. It is very likely that these two parts are related to each other: it is hypothesized that bone becomes affected because of progressive infiltration of the bone marrow with foci of Gaucher cells, possibly in combination with a toxic process around these foci [10]. This difference is increasingly important from the perspective of treatment respons assessment. Bone marrow infiltration may be rapidly reduced upon treatment, while structural changes, such as Erlenmeyer flask deformities and cortical thickness may remain unchanged for a long time. For the evaluation of the efficacy of different dosing regimens, early detection of

Gaucher cell clearance from the bone marrow is mandatory to allow dose adjustments in cases of unsatisfactory responses. Therefore, the availability of imaging techniques that focus on the extent of bone marrow infiltration are essential. Dixon QCSI is considered as a sensitive tool for measuring the degree of Gaucher cell infiltration by the decrease in fat-(triglyceride) fraction in the marrow as the result of Gaucher cell infiltration [11]. It has been shown that the triglyceride content of the bone marrow may increase during alglucerase treatment [7].
The aim of the present study is to detect early changes in the bone marrow of adult type 1 Gaucher disease patients by Dixon QCSI measurements during treatment with individualized doses of alglucerase or imiglucerase [9] in relation to overall respons.

METHODS

Patients

All patients that entered the individualized dosing study after July 1993 and completed at least 4 years of enzyme therapy were included in this study. The population consisted of 12 adult type 1 Gaucher disease patients (3 females, 9 males) of whom three were splenectomized (Table 1). A diagnosis of Gaucher disease was confirmed by decreased activity of glucocerebrosidase in leukocytes and genotyping [12,13]. Enzyme therapy was initiated according to the earlier described protocol [9]. In brief, patients are treated during the first 6 months with low doses of enzyme (alglucerase or imiglucerase 1.15 U/kg three times a week) and subsequently evaluated for treatment efficacy every 6 months thereafter. According to defined criteria based on reductions in organomegaly and improvement in cytopenia, the dose is doubled, maintained or halved to allow individualized dosing. In addition, occurrence of bone complications during treatment is an independent reason for a dose increase. Blood counts were taken every 6 months. Organ volume measurements were performed using spiral CT scanning initially every 6 months and yearly after 3 years of treatment. Dixon QCSI measurements were obtained before the initiation of enzyme supplementation therapy and every year thereafter.

Table 1. Characteristics of Gaucher disease patients before treatment with enzyme therapy (treatment group) and untreated Gaucher controls

Treatment group						Untreated Gaucher controls					
No.	sex	age (yrs)	splenic status	bone compl	SSI	No.	sex	age (yrs)	splenic status	bone compl	SSI
1	M	48	Intact	No	9	1	M	47	Intact	No	4
2	F	53	Intact	No	8	2	F	43	Intact	No	4
3	M	38	Intact	No	7	3	F	55	Intact	No	6
4	M	53	Intact	No	5	4	M	19	Intact	No	6
5	M	43	Intact	No	5	5	F	39	Intact	No	4
6	M	51	Intact	No	5	6	F	43	Intact	No	2
7	M	48	Intact	No	5	7	F	35	Intact	No	4
8	M	37	Sx	Yes	17	8	M	34	Sx	No	6
9	M	57	Sx	Yes	16	9	F	30	Sx	No	11
10	F	39	Sx	Yes	18						
11	F	38	Intact	No	4						
12	M	29	Intact	No	8						

Controls

Nine adult type 1 Gaucher disease patients that did not need or want treatment and were followed for at least 12 months served as controls (untreated Gaucher controls). This population was less severely affected than the treated patient group. Organ volumes, hematology and bone marrow fat-fractions were measured every year in these untreated patients.

Dixon-QCSI fat-fraction acquisition

In-phase and opposed-phase proton density weighted spin echo sequences were performed: TR 2500 ms, TE 22.3 ms, slice thickness 4 mm, matrix 256x256, NEX 1, FOV 350x350 mm^2, acquisition time 21 min 20 s. The paracoronal measurement acquisition slices were positioned on a mid-sagittal localizer image, passing through the middle of the posterior parts of L3, L4, and L5.

Post-processing and data analysis were performed on a Sun Sparc 20-51 workstation (Sun Microsystems, Mountain View, CA), using a previously described algorithm [14,15].
To obtain one fat-fraction value for each vertebra, we averaged the pixel values in a region of interest (ROI). The mean bone marrow fat-fraction was calculated from measurements in three separate lumbar vertebrae (L3-L5).
Standardization and reproducibility of the Dixon QCSI protocol was performed by measurements in 16 healthy volunteers (16).

Statistics
Results are given as median and range. Differences between data from patients and controls were tested by Mann-Whitney test. Differences between data obtained before and during enzyme supplementation therapy were tested by the Wilcoxon signed-rank test. A p value of <0.05 respresented a significant difference.

RESULTS

Patients
Of the 12 patients, 3 (all splenectomized) had suffered from avascular necrosis, pathological fractures and/or bone crises and 9 had not (Table 1). Patient 9 had experienced a bone crisis at the time of initial examination, located in the lumbar spine and pelvis, treated with analgesic drugs. During treatment with alglucerase, he developed a collapse of vertebral bodies L3 and L4.
No further bone complications occurred during treatment, although patient 10 experienced recurrent episodes of atypical bone pain, which led to a dose increase.
Eleven patients were initially treated with alglucerase, 1.15 U/kg three times a week and one patient (No.1) was treated with 30 U/kg every 2 weeks, because of inability to perform home treatment. Respons to treatment after 6 months according to the defined criteria was classified as moderate in 6 and insufficient in 4 (patients 4,6,10, and 12). During 4 years of treatment, doses were adjusted according to further clinical responses.

Table 2 shows the results of bone marrow fat-fraction determinations by Dixon QCSI, hemoglobin levels, platelet counts and organ volumes in relation to dose at the start of treatment and after 4 years. In patients 2 and 3 the examinations at 5 years were used, because no evaluation was performed after 4 years of treatment.

Table 2. Bone marrow fat-fractions (F), hematology, organ volumes, and dosing regimens before and after 4 to 5 years of treatment

	F (%)		Hb level (g/dl)		platelet count (x 10^9/L)		spleen volume (ml)		liver volume (ml)		dose (U/mo)	
No.	start	4 yrs	start	4 yrs	start	4 yrs	start	4 yrs	start	4 yrs	start	4 yrs
1	18	47	15.0	15.8	118	164	855	362	2269	1557	60	30
2*	22	41	10.9	11.8	48	129	1042	422	3139	2311	15	15
3*	10	18	14.6	14.6	122	156	1400	549	3695	1997	15	15
4	23	38	11.2	13.0	53	69	3118	2629	3334	2418	15	60
5	29	47	15.0	14.7	110	169	574	326	1830	1656	15	15
6	18	35	11.7	13.0	71	126	2002	823	3678	2808	15	30
7	40	50	13.8	14.4	45	145	885	438	2014	1608	15	15
8	11	28	10.1	12.2	129	320			3691	2566	15	30
9	34	42	9.3	12.5	726	457			2393	1645	15	30
10	11	30	15.8	14.4	189	286			4139	1550	15	120
11	22	48	13.1	14.6	103	246	535	256	1797	1516	15	15
12	8	28	13.4	14.9	59	58	4379	1751	3426	2445	15	40

* in pts. 2 and 3, the 5-year examination was used

Bone marrow fat-fractions

Before treatment, fat-fractions were decreased in 9/12 patients (median 0.20, range 0.08-0.40) compared to healthy volunteers with the same age and sex distribution (normal values 0.27-0.43, $p < 0.01$) [16]. The values of the initial measurements in the Gaucher patients who were going to be treated were not significantly different from the values in the untreated Gaucher controls: 5/9 had decreased fat-fractions (median 0.22, range 0.10-0.36; $p = 0.7$).

Figure 1 shows the Dixon QCSI images of the lumbar spine during treatment in patient 2, where reappearance of fatty marrow is depicted. The coloring of bone marrow in an age and sex matched healthy subject is added to the figure.

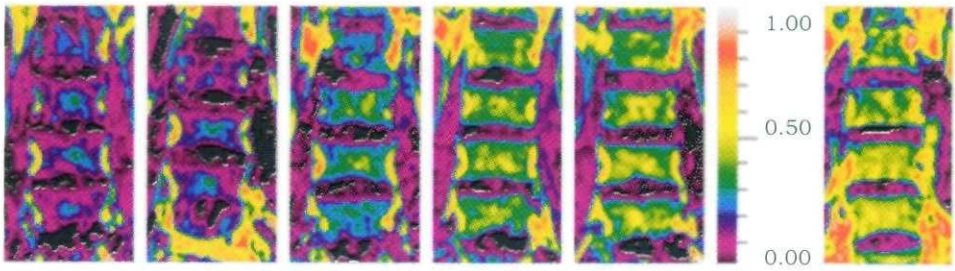

a.Aug '93 F_f = 0.22 | b.Sep '94 F_f = 0.19 | c.Oct '95 F_f = 0.34 | d.Jul '98 F_f = 0.41 | e.Jul '99 F_f = 0.45 | f. | g. F_f = 0.44

Figure 1. Increase in bone marrow fat-fraction in the lumbar spine during enzyme therapy in patient 2 (female).
a) just before therapy, at the age of 47 years.
b-e) during therapy; acquisition dates and averaged *F* values of L3-L5 are given.
f) color fat-fraction scale from black (*F* = 0.00) through yellow (0.50) to white (1.00).
g) fat-fraction image of a healthy female volunteer, aged 48.

During enzyme therapy, fat-fractions gradually increased in all patients except in patient 9 (Figure 2). A statistically significant increase in fat-fraction was already apparent after 1 year of treatment (p = 0.007). After 4 to 5 years of treatment, 11 of 12 patients had a normal bone marrow fat-fraction. One patient (patient 3) still had a low bone marrow fat-fraction of 0.18. In contrast, fat-fractions did not change in the untreated Gaucher controls during 2 years of follow-up (P=0.5 and 0.6 at 1 and 2 years, respectively; Figure 2). Patient 9, who experienced a bone crisis located in the lumbar spine, had an abnormal high fat-fraction before treatment, possibly due to fatty replacement after infarction. After 2 years of treatment, the marrow fat-disappeared as a result of collapse of his lumbar vertebrae. In the years thereafter, a gradual reappearance of fatty marrow occurred (Figure 3).

Changes in bone marrow fat-fractions in relation to overall respons

All patients showed decreases in splenic and hepatic volumes (Table 2). Platelet respons was slow in patients 4 and 12, both with large spleens. Six of 11 patients who initially received a dose of 15 U/kg per month had a dose increase as a result of insufficient respons between 6 months and 4 years of treatment (patients 4, 6, 8, 9, 10, and 12, including the most severely affected patients). The dose change is depicted in Figure 2.

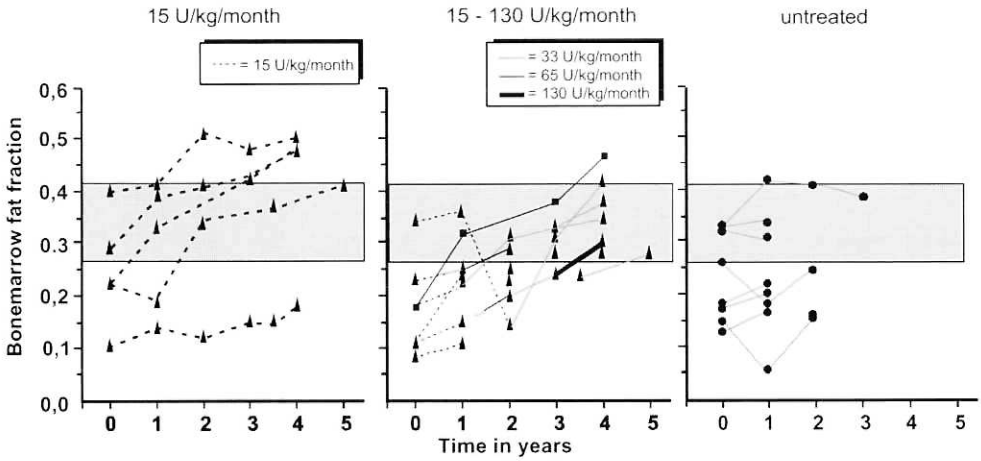

Figure 2. Bone marrow fat-fractions in treated and untreated type 1 Gaucher disease patients. Treated patients without a dose increase (left) and with a dose increase (middle) and untreated Gaucher controls (right). Stippled area, control range.

Improvement in fat-fractions were not clearly affected by a dose increase, but the number of patients is too small to draw any firm conclusions. It is clear that patient 1, who received an initial higher dose, had the most robust increase in fat-fraction. Comparison of the patients who had a dose increase with the patients on persistent low dose reveals that patients with a dose increase were generally more severely affected and also had slightly lower bone marrow fat-fractions before treatment (median 0.13 versus 0.26, p = 0.08, patient 9 excluded). The rate of improvement in fat-fractions during treatment did not differ for both groups.

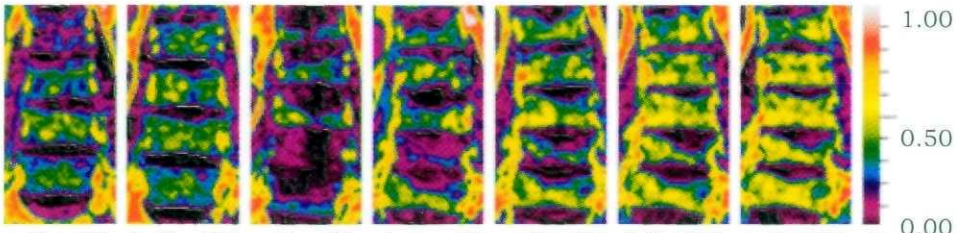

Figure 3. Change in bone marrow fat-fraction in the lumbar spine during enzyme therapy in patient 9. Very high fat-fractions were measured after bone crises in the lumbar vertebrae. After 2 years of treatment, collapse of all lumbar vertebrae occurred.
a) just before therapy.
b-g) during therapy; acquisition dates and averaged *F* values of L3-L5 are given.
h) color fat-fraction scale from black (F = 0.00) through yellow (0.50) to white (1.00).

Discussion

Bone marrow fat-fractions are decreased in the majority of adult type 1 Gaucher disease patients and normalize during treatment with enzyme supplementation. Although it is known that fat-fractions in the normal population increase slowly with age [17,18], comparison with bone marrow fat-fraction measurements in untreated Gaucher controls reveals that in the latter group of patients no significant change is apparent. It is shown that improvement in bone marrow fat-fractions upon therapy is already seen after only 1 year of treatment. An earlier study on the changes in bone and bone marrow upon enzyme therapy has reported significant improvements by different techniques after 42 months of treatment [7]. In the same study, fat-fraction determination by Dixon QCSI was also used as a tool to measure bone marrow infiltration. Significant increases in fat-fractions were observed after 42 months and normalization of bone marrow fat content was achieved in 7/11 patients. The value of these observations is, however, limited by the fact that 6/12 patients are children, in whom a natural shift from red to yellow marrow with age occurs [18,19]. No control population was included in this study to assess the fat-fractions in untreated patients. In our study only adult patients have been included and follow-up of untreated patients serve as controls to correct for changes that may occur during aging. Although the follow-up of these untreated controls is short, it is clear that most patients remained stable or had a decrease in fat-fraction which probably

reflected progressive Gaucher cell infiltration. Only 1 untreated Gaucher control, who had a normal initial fat-fraction, had an unexplained spontaneous increase, possibly related to interruption of menstrual bleeding by menopause. The lack of change in these untreated control patients compared to the significant increase in fat-fractions upon enzyme therapy after 12 months of treatment confirms the value of fat-fraction measurement for the assessment of Gaucher cell infiltration in the bone marrow and the bone marrow respons to treatment.

A pitfall in the interpretation of bone marrow fat-fractions may be the occurence of bone crises with fatty replacement of necrotic areas [10]. These abnormalities can occur in the lumbar spine and may result in high fat-fractions, despite the presence of severe bone disease. Caution must be taken in these cases. Also, in patients with already collapsed vertebrae, the interpretation of the much smaller region of interest may be difficult as depicted in Figure 3.

Earlier studies on the effect of enzyme therapy on bone disease has shown that it takes years of treatment before changes can be established [8,9]. In addition, studies on levels of exogenous administered glucocerebrosidase suggest that a smaller portion of the enzyme is taken up by the bone marrow compared to the liver [20]. Based on these observations, it has been suggested that Gaucher cells in the bone marrow are less easily cleared than storage cells in the liver and spleen and that for accurate treatment of bone marrow involvement large doses of enzyme will be needed [7]. However, the fact that skeletal abnormalities do not rapidly change does not reflect the changes in the bone marrow. A more rapid bone marrow respons is also suggested by earlier observations that low platelet counts and hemoglobin levels as a result of bone marrow failure in splenectomized patients show immediate rise after the initiation of enzyme therapy [9]. Therefore, it is more likely that the techniques applied to evaluate bone disease in type 1 Gaucher disease, such as plain X rays, dexa scans, and quantitative CT, are too insensitive to detect early changes. The present data support the fact that changes in bone marrow involvement may occur as early as 12 months after the initiation of treatment. In addition, it is shown that early and continuing marrow responses occur even with low doses of enzyme. Whether high doses of enzyme result in an even faster increase in bone marrow fat-fractions remains to be determined. The one patient on a relatively higher dose in

our study also had a very quick increase in fat-fraction. In our approach, doses have been adjusted on an individual basis, which implied that several patients (5/11) had a dose increase up to 30 to 120 U/kg per month. All patients had the same rate of improvement of bone marrow fat-fractions, but the patients that had sufficient and sustained responses to the low dose were the less severely affected patients. The question whether there is a dose dependency in the respons cannot be solved in the present study. Individualized dosing is based upon the supposition that there is indeed an effect of dose. The high interindividual variability in respons requires comparative studies in large patient populations to prove that this is indeed the case. Studies in large patient cohorts, possibly with the use of sensitive plasma markers, may eventually enlighten us regarding this issue.

Comparison of our data at 4 to 5 years with the results in the study by Rosenthal et al. [7] after 42 months shows that normalization of fat-fractions can be achieved in the majority of patients in both groups. It is, however, possible that the patients in Rosenthal's study were generally more severely affected than in our study.

Individualized dosing of enzyme supplementation therapy for Gaucher disease depends on an accurate measurement of respons to allow dose adjustments. Since bone disease may produce severe complaints and irreversible damage, it is of critical importance that bone marrow respons can be estimated early in the course of treatment. Fat-fraction determination by Dixon QCSI seems to provide an excellent tool to accomplish this, since we have found that low bone marrow fat-fractions are related to the occurrence of bone complications [16]. We have now implemented this method in our standard protocol and perform these measurements on a yearly basis. Doses of enzyme are increased when fat-fractions do not increase sufficiently or do not normalize within 3 to 4 years of treatment.

In conclusion, fat-fraction determination of the bone marrow of the lumbar spine in type 1 Gaucher disease patients reflects Gaucher cell infiltration and shows early respons to treatment. Although the technique is not (yet) widely available, it seems to be the modality of choice for the assessment of bone marrow involvement.

REFERENCES

1. Beutler E, Grabowski G. Gaucher disease. In: Scriver CR BA, Sly WS, Valle D, ed. The metabolic basis of inherited disease. New York: McGraw-Hill Publishing Company, New York, 1995; 2641-2670.
2. Stowens DW, Teitelbaum SL, Kahn AJ, Barranger JA. Skeletal complications of Gaucher disease. Medicine 1985; 64:310-322.
3. Barton NW, Brady RO, Dambrosia JM, et al. Replacement therapy for inherited enzyme deficiency - Macrophage targeted glucocerebrosidase for Gaucher's disease. N Engl J Med 1991; 324:1464-1470.
4. Figueroa ML, Rosenbloom BE, Kay AC, et al. A less costly regimen of alglucerase to treat Gaucher's disease. N Engl J Med 1992; 327:1632-1636.
5. Hollak CEM, Aerts JMFG, Goudsmit R, et al. Individualized low dose alglucerase therapy for type 1 Gaucher disease. Lancet 1995; 345:1474-1478.
6. Rosenthal DI, Scott JA, Barranger JA, et al. Evaluation of Gaucher disease using magnetic resonance imaging. J Bone Joint Surg 1986; 68A:802-808.
7. Rosenthal D, Doppelt S, Mankin H, et al. Enzyme replacement therapy for Gaucher disease: skeletal responses to macrophage-targeted glucocerebrosidase. Pediatrics 1995; 96(4):629-637.
8. Belmatoug N, Billette de Villeneur T. Skeletal response to enzyme replacement therapy for type 1 Gaucher disease: a preliminary report of the French experience. Semin Hematol 1995; 32(suppl 1):33-38.
9. Elstein D, Hadas-Halpern I, Itzchaki M, Lahad A, Abrahamov A, Zimran A. Effect of low-dose enzyme replacement therapy on bones in Gaucher disease patients with severe skeletal involvement. Blood Cells Mol Dis 1996; 22(2):104-111.
10. Stowens DW, Teitelbaum SL, Kahn AJ, Barranger JA. Skeletal complications of Gaucher disease. Medicine (Baltimore). 1985; 64(5):310-322.
11. Miller SPF, Zirzow GC, Doppelt SH, Brady RO, Barton NW. Analysis of the lipids of normal and Gaucher bone marrow. J Lab Clin Med 1996; 127:353-358.
12. Daniels LB, Glew RH. β glucosidase assays in the diagnosis of Gaucher's disease. Clin Chem 1982; 28:569-577.
13. Aerts JMFG, Donker Koopman WE, Koot M, Barranger JA, Tager JM, Schram AW. Deficient activity of glucocerebrosidase in urine from patients with type 1 Gaucher disease. Clin Chim Acta 1986; 158:155-164.
14. Maas M, Dijkstra PF, Akkerman EM. Uniform fat-suppression in hands and feet through the use of two point Dixon chemical shift imaging. Radiology 1999; 210:189-193.

15. Akkerman EM, Maas M. A region growing algorithm to simulutaneously remove dephasing influences and seperate fat and water in two point Dixon imaging. Proceedings of the Society of Magnetic Resonance and the European society for Magnetic Resonance and Biology 1995; 649.
16. Maas M, Akkerman EM, Venama HW, Stoker J, den Heeten GJ. Dixon quantitative chemical shift MRI for bone marrow evaluation in the lumbar spine: A reproducibility study in healthy volunteer. J Comp Assist Tomogr 2001; 25(5):691-697.
17. Ishijima H, Ishizaka H, Horikoshi H, Sakurai M.Water fraction of lumbar vertebral bone marrow estimated from chemical shift misregistration on MR imaging: normal variations with age and sex. Am J Roentgenol 1996; 167(2):355-358.
18. Dooms GC, Fisher MR, Hricak H, Richardson M, Crooks LE, Genant HK. Bone marrow imaging: magnetic resonance studies related to age and sex. Radiology 1985; 155:429-432.
19. Vogler JB 3rd, Murphy WA. Bone marrow imaging. Radiology 1988; 168(3):679-693.
20. Beutler E, Kuhl W, Vaughan LM. Failure of alglucerase infused into Gaucher disease patients to localize in marrow macrophages. Mol Med 1995; 1(3):320-324.

CHAPTER 6

Response of Gaucher bone disease to enzyme replacement therapy

L.W. Poll[1], M. Maas[2], M.R. Terk[3], M. Roca[4], B. Bembi[5], G. Ciana[5], N.J. Weinreb[6]

Departments of [1]Diagnostic Radiology, Heinrich Heine University, Düsseldorf, Germany;
[2]Radiology, Academic Medical Center, Amsterdam, The Netherlands;
[3]Keck School of Medicine, University of Southern California, USA;
[4]Radiology, Miguel Servet Hospital, Zaragoza, Spain;
[5]Burlo Garofolo Institute, Trieste, Italy; and
[6]University Gaucher Research Foundation Inc., University Gaucher Treatment Center, Tamarac, USA

Br J Radiology 2002; 75(Suppl. 1):A25-A36

ABSTRACT

In Gaucher disease, enzyme replacement therapy usually reduces liver and spleen volumes and improves hematological abnormalities within 1 year. In contrast, skeletal manifestations of Gaucher disease are thought to respond more slowly. For example, decreased bone marrow glycolipid infiltration and increased bone mineral density have been reported to take up to 3-4 years of treatment. In this report, we present recent studies using T1- and T2-weighted MRI and quantitative chemical shift imaging that demonstrate decreases in abnormal glucocerebroside infiltration and increases in normal fat content of bone marrow within the first year of treatment. There was no obvious relationship between age, gender, splenectomy status or genotype and the response of bone marrow to therapy. Although the dose of enzyme replacement therapy may be related to bone marrow response, no significant relationship was demonstrated in this report. Long-term enzyme replacement therapy induces continued degradation of Gaucher cell deposits, reconversion of fat marrow and increased bone mineral density. This treatment is also associated with improved or non-progressive bone symptoms and functional status in most adult patients, and it prevents the new occurrence of bone pain and bone crisis in nearly all patients. The development of more sensitive, quantitative imaging methods will help to evaluate disease severity better and to assess the response to therapy.

INTRODUCTION

Gaucher disease is classified into three types based on the presence and nature of central nervous system involvement [1]. There is substantial clinical variability within all subtypes, particularly within type 1 [2]. Disease progression in type 1 and type 3 Gaucher disease is variable but type 2 Gaucher disease progresses rapidly and is usually fatal within 2 years.

Skeletal manifestations of Gaucher disease have a greater impact on the quality of life than hematological and visceral abnormalities. Accumulation of glucocerebroside in bone marrow is associated with substandard growth in childhood and adolescence, osteopenia, lytic lesions, pathological fractures, chronic bone pain, acute episodes of excruciating bone crisis, bone infarcts, osteonecrosis, and skeletal deformities [3].

Until the advent of effective enzyme replacement therapy (ERT) with purified, macrophage-targeted, human β-glucocerebrosidase derived either from human placenta (alglucerase) or from recombinant DNA production methods (imiglucerase), treatment of skeletal manifestations was largely restricted to relief of symptoms and to *post facto* management of orthopedic complications. Improvements in hematological parameters and reductions in visceral organ volumes are observed within 6-12 months of ERT [4]. However, the skeletal response to ERT appears to take longer [5]. The severity, frequency and duration of painful bone crises may be reduced within the first year of ERT [6,7], but other measures may not improve within the first 3 years of therapy, although this may be due to the relative insensitivity of the techniques applied to detecting improvement. Long-term treatment over 3-4 years improves marrow composition and bone mass [8]. Although local disease and generalized osteopenia respond well to ERT, success in treating existent focal disease in adults is less likely because of irreversible damage such as bone death.

In this paper, we present the most recent data on the long-term effects of ERT from various centers, with a particular focus on the response of skeletal aspects.

German data

Successful ERT in adult patients results in replacement of the glucocerebroside-loaden Gaucher cells in marrow with triglyceride-rich adipocytes (yellow marrow). Thus, ERT-induced changes to bone marrow can be studied using MRI with subcutaneous fat as an internal standard [9]. At the Heinrich Heine University in Düsseldorf, Germany, a score of eight anatomical sites was used for evaluation of bone marrow abnormalities of the lower extremities. Using coronal T1- and T2-weighted spin echo MRI of the lower extremities, the response of skeletal disease to ERT in 30 patients with type 1 Gaucher disease was assessed (Table 1) [10].

Table 1. MRI protocols used in different studies

Study	Protocol details	
German data	1.0 T Gyroscan T10-NT (Philips) Body coil Femur - coronal plane 4 mm slice thickness 45 cm field of view	Matrix 256 x 192 T1-SE [TR: 615 TE:25] T2-TSE [TR: 2200 TE:120]
American data	1.5 T Signa scanner (GE) Femur - coronal plane 4 mm slice thickness 48 cm field of view	Matrix 512 x 256 T1 [TR: 650 TE: 17] T2-GRE [TR: 550 TE: 15]
Spanish data	0.5 T MR scanner (GE) Pelvis and femur - coronal plane Spine - sagittal plane 5 mm slice thickness 45 cm field of view	T1 [TR: 600 TE:20] T2 [TR: 2500 TE: 80]
Dutch data	1.5 T MR scanner (Siemens) Body coil Femur - coronal plane Lumbar spine - Sagittal plane	
	Femurs: 4 mm slice thickness 50 cm field of view NEX 2	Matrix 256 x 512 T1 [TR: 570 TE: 14] Matrix 190 x 256 Pd/T2: [TR: 3500 TE: 20-120]
	Lumbar spine: 4 mm slice thickness 29 cm field of view NEX 2	Matrix 192 x 512 T1 [TR 570 TE:14] Matrix 230 x 512 Pd/T2: [TR: 3500 TE: 20-120]

Table 2. Baseline patient and disease characteristics in the German study

Characteristic	
Male:female ratio, *n*	11:19
Median age, years [range]	48 [19-78]
Splenectomy, *n* (%)	7 (23)
Alglucerase/imiglucerase dose, *n*	
20 U/kg/2 weeks	2
30 U/kg/2 weeks	3
40 U/kg/2 weeks	7
60 U/kg/2 weeks	18
Genotype, *n*	
N370S/N370S	5
N370S/L444P	10
N370S/D409H	2
N370S/?	9
L444P/?	1
Unknown	3
Morphology, *n*	
Type A	17
Type B	13
Low SI rim lesions, *n*	
Type A	2
Type B	9[a]
Non-splenectomized	1
Splenectomized	6[b]

[a] Significant difference ($p = 0.0021$)
[b] Significant difference ($p = 0.0045$)

The baseline data for these 30 patients are shown in Table 2. The bone marrow response to ERT was analyzed by dose, by genotype and by morphology (type A morphology is homogenous and type B morphology is non-homogenous as described earlier [10]).

Non-skeletal aspects of Gaucher disease improved in all patients. After a median of 36 months of treatment (range 9-72 months), 63% of patients showed a bone marrow response, namely increased signal intensity on the follow-up MR examination owing to a partial reconversion of fat marrow (Table 3). This response was observed as early as 9 months after starting therapy (Figure 1).

The median time on ERT was similar among responders (38 months (9-66 months)) and non-responders (32 months (9-72 months)) and gender did not influence response. The median score in the responder and non-responder groups was 6.5 and 5.8, respectively (non-significant difference). An intra-individual change in this score over the longest follow-up interval was not detectable.

Table 3. German efficacy data on the effects of enzyme replacement therapy on skeletal aspects of Gaucher disease measured by magnetic resonance imaging

Population	Responders, *n* (%)		*p*
Total	19	(63)	
Splenectomized	6	(86)	
Non-splenectomized	13	(57)	0.2146 †
Morphology type A	8	(47)	
Morphology type B	11	(85)	0.0575 †
Alglucerase/imiglucerase dose			
20 U/kg/2 weeks	2	(100)	
30 U/kg/2 weeks	2	(67)	
40 U/kg/2 weeks	2	(29)	
60 U/kg/2 weeks	13	(72)	0.6531 ‡

† Two-sided Fisher's exact test
‡ Mantel-Haenszel chi-square test

In this sample, bone marrow response to ERT was not dependent on the dose of ERT, on whether patients were splenectomized or not, or on the morphology of bone disease (Table 3). However, the small number of patients makes it difficult to detect any significant differences and certain biases exist. For example, there is a trend towards a greater response in more severely affected patients with type B morphology (Table 3), but all patients with type B morphology received the highest dose of ERT, which may have biased the response data.

Focal bone lesions surrounded by a low signal intensity rim were visible on MRI in 11 patients. These lesions were most frequent in patients with

type B morphology (82%; p = 0.0021) and in splenectomized patients (86%; p = 0.0045), and did not respond to ERT, which suggests that the lesions were bone infarcts (Table 2).

In general, the skeletal response to ERT depended on the degree of bone marrow involvement, and delaying ERT may result in irreversible bone marrow changes.

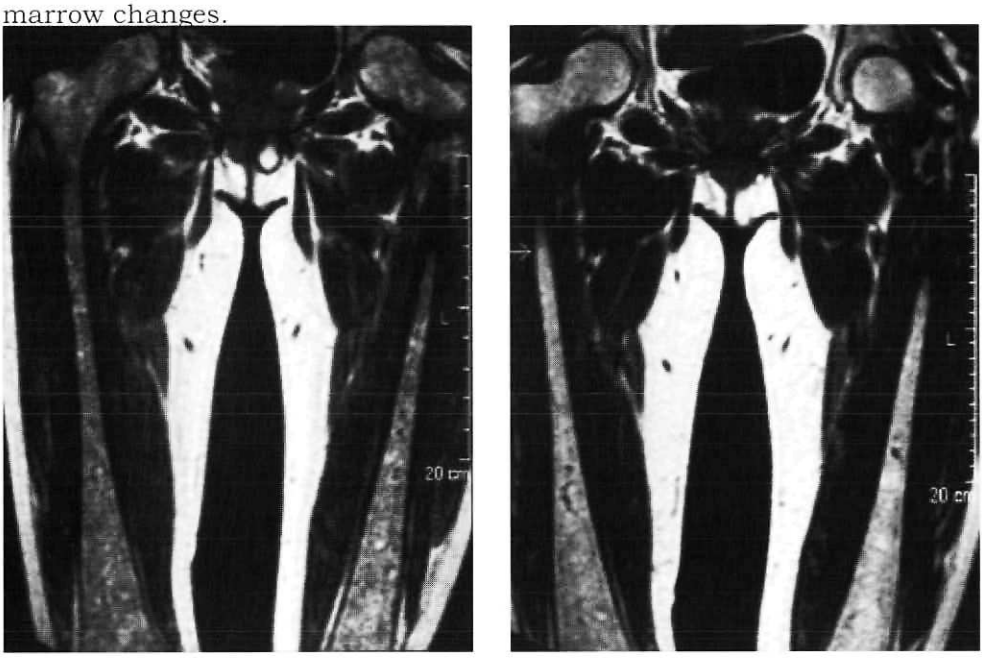

(**A**) (**B**)

Figure 1. Coronal T1-weighted magnetic resonance images of the femurs, TR/TE 615/25, of a patient with Gaucher disease from a study conducted at Heinrich Heine University, Düsseldorf: (**A**) before starting enzyme replacement therapy (ERT); (**B**) after 9 months of ERT (60 U/kg/2 weeks).

American data

Bone marrow response to ERT has also been assessed using coronal T1-weighted MRI of femurs at the Southern California School of Medicine, USA (Table 1). In addition, correlation between marrow responses and reductions in liver and spleen volumes was assessed [11]. The T1-weighted images were analyzed blindly.

Of 42 patients with Gaucher disease, 32 received ERT, of which 16 had an MRI assessment before starting ERT, and 10 patients did not receive ERT. Baseline characteristics are shown in Table 4.

Patients were treated with alglucerase or imiglucerase for a median of 34 months (range 12-56 months).

Liver volumes were reduced in 81% (26/32) of treated patients and spleen volumes were reduced in 93% (28/30) of treated, non-splenectomized patients. Overall, 44% (14/32) of patients showed a marrow response. If only patients with pretreatment MRI assessments showing abnormal marrow are included, 67% (10/15) of patients responded. Two patients had increased bone marrow signal intensity after 13 months of treatment, and it is possible that earlier MRI assessment may have detected improvement within the first year of treatment.

Table 4. Baseline patient characteristics in the American study

Characteristic	
Male:female ratio, *n*	16:26
Median age, years [range]	46 [16-78]
Splenectomy, *n* (%)	10 (24)
Alglucerase/imiglucerase dose, *n*	
None	10
7 U/kg/week	5
30 U/kg/2 weeks	12
60 U/kg/2 weeks	15

Bone marrow response was not dependent on the length of time on ERT (mean follow-up 35 months (14-38 months) and 33.6 months (13-54 months) in the non-responding and responding groups, respectively), age or gender. Analysis of the effects of ERT dosage on skeletal response was not possible because the dosage of ERT varied during the course of this study. Two (20%) of the 10 patients who had been splenectomized had a marrow response to treatment, whereas 12/22 (55%) non-splenectomized patients had a marrow response (p = 0.55; chi-square test). One untreated patient showed an apparent marrow response, the reasons for which are not clear.

A subgroup of five patients had heterogenous signal increases on T1-weighted images. In some of these patients, non-responding focal lesions were not visible on pretreatment scans and became more conspicuous after treatment. Care must be taken not to mistake these for new lesions.

Changes in T1-weighted images correlated to reductions in liver and spleen volumes. The mean spleen volume reduction was 50% in patients with a marrow response and 4% in non-responders (p = 0.00038; Students t test; Figure 2); the mean reduction in liver volume was 20% in patients with a marrow response but the volume increased by 6% in non-responders (p = 0.005).

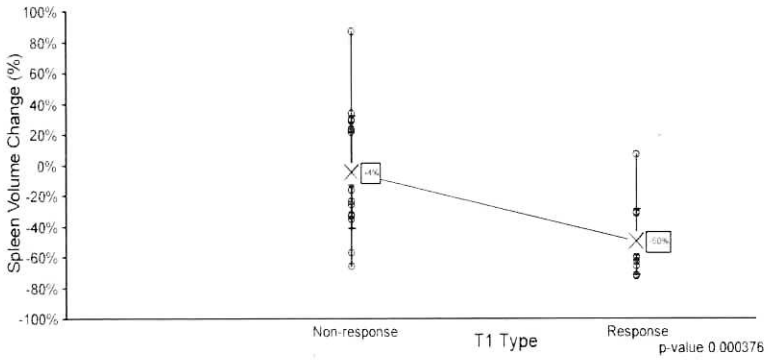

Figure 2. Plot of changes in T1-weighted marrow images against spleen volume changes for patients studied at the University of Southern California Medical School. Mean volumes are shown numerically. Reproduce from Skeletal Radiol 2000; 291:563-571 [11] with permission of the International Skeletal Society.

A quantitative method for detecting relative differences in the fat concentration in bone marrow has been tested [12]. Using bone marrow H1 spectroscopy, the ratio of the fat and water in bone marrow was determined for the metaphysis and epiphysis, and the ratio of these two values was calculated. The mean ratio in six patients with Gaucher disease significantly differed from the mean ratio in 12 normal volunteers.

Spanish data

Since 1993, all patients with Gaucher disease in Spain have been monitored in an anonymous database. By December 2000, the database included 178 patients, of whom 124 were receiving ERT. Significant improvements in hemoglobin and platelet counts and decreases in liver and spleen volume were observed in the 124 patients receiving ERT. Thirty-five patients who received ERT for at least 4 years had an improved perception of their health.

A semi-quantitative scoring system for Gaucher disease which reflects bone marrow involvement as well as other disease variables has been developed at the Miguel Servet Hospital in Zaragoza, Spain.

The spine, pelvis and femur of 18 patients with type 1 Gaucher disease were assessed by MRI (Table 1). Three distinct patterns of bone marrow involvement were defined: no infiltration (N), non-homogenous morphology pattern of infiltration (NH) and homogenous morphology pattern of infiltration (H). The NH morphology was subclassified into reticular pattern (NHR), mottled pattern (NHM) and diffuse (NHD) (Figure 3).

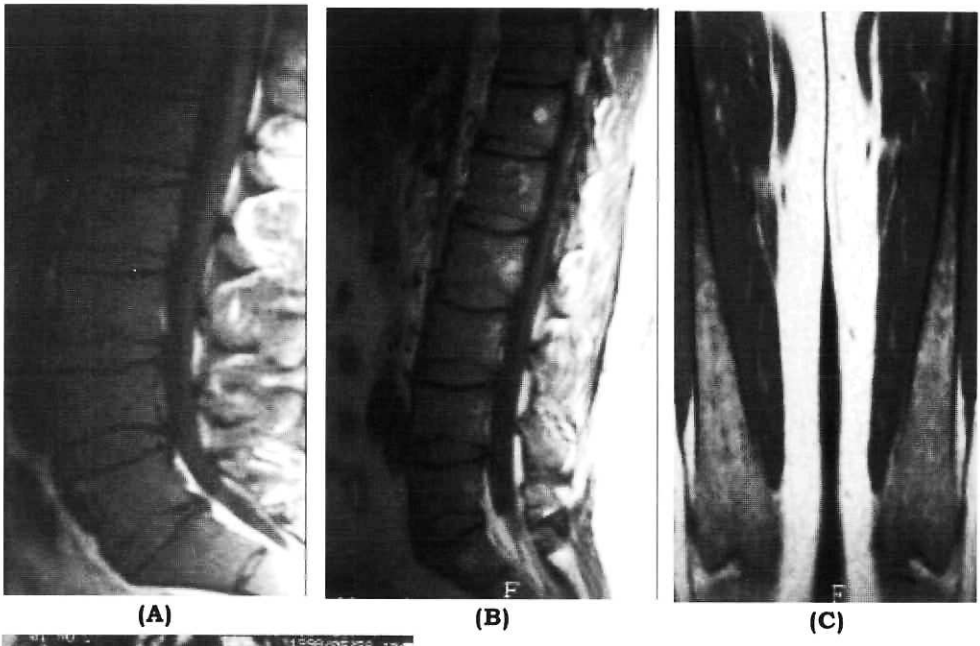

Figure 3. Patterns of bone marrow involvement on magnetic resonance images, TR/TE 600/20 from patients studied at Miguel Servet Hospital: (**A**) homogenous morphology or pattern of involvement on a sagittal T1-weighted MRI of the spine; (**B**) non-homogenous diffuse morphology on a sagittal T1-weighted MRI of the spine; (**C**) non-homogenous mottled morphology on a coronal T1-weighted MRI of the pelvis; (**D**) non-homogenous reticular morphology on a coronal T1-weighted MRI of the femurs.

The score assigned to each pattern on MRI (H = 4, NHD = 3, NHM = 2, NHR = 1, and complications = 4) was combined with the Zimran severity score index [13,14] to give a total score for disease severity. Of the 18 patients, two had mild disease (score 0-10), 14 had moderate disease (score 11-25) and two had severe disease (score 26 and above) (Table 5). Although untested for measuring response to ERT, this scoring system may be useful.

Table 5. Baseline patient and disease characteristics in the Spanish study

Characteristic	
Male:female ratio, *n*	7:11
Mean age, years [range]	40 [14-68]
Skeletal complications, *n*	
Bone infarcts	3
Osteonecrosis	6
Bone crisis	4
Vertebral collapse	2
Bone marrow imaging pattern, *n*	
Spine:	
H	7
NHD	6
NHM	2
Pelvis:	
H	11
NHD	8
NHM	4
NHR	1
Femur:	
NHD	2
NHM	4
NHR	4

H, homogenous morphology; NHD, non-homogenous diffuse morphology; NHM, non-homogenous mottled morphology; NHR, non-homogenous reticular morphology

Skeletal response to ERT (30 U/kg every 2 weeks) was measured in 6 patients using MRI. Quantification of the response was attempted by graphically representing the number of pixels on an MRI in a defined area of the lumbar spine (L3 and L4) before and after 2 years of therapy. The signal intensity increased in 3 patients, consistent with decreased bone marrow infiltration. The signal was unchanged in 2 patients. The bone marrow infiltration increased in one patient, for whom the dose of ERT was then increased to 60 U/kg every 2 weeks.
Quantitative use of MRI needs to be tested more thoroughly but may be useful in combination with other quantitative measures of bone marrow response.

Dutch data
Quantitative chemical shift imaging (QCSI), a very reproducible technique [15], can be used to measure the quantities of fat and water in bone marrow, because of the differences in the resonant frequencies of the protons in water and fat molecules [15,16]. The relative fat signal on MRI is decreased in Gaucher disease because the total mass of lipid in bone marrow is less. A correlation between QCSI and Gaucher disease severity has been demonstrated [17], and a response to ERT has been detected using QCSI [8]. QCSI is being used at the Academic Medical Center in Amsterdam, the Netherlands, to monitor the response to ERT in 58 patients with type 1 Gaucher disease. In this way the individualized dosing schemes are monitored and, if necessary, adjusted [18]. Axial bone marrow of the lumbar spine was assessed every year by QCSI and follow-up data have been collected for 24 patients (Figure 4). In 11/12 patients with follow-up data of at least two years, QCSI measured a marked elevation of the fat-fraction indicating a bone marrow response [19]; a significant increase in the fat-fraction after 1 year of treatment has already been reported [20].
Alternative quantitative MRI methods are being tested in the Netherlands because QCSI is not widely available [21,22]. One method, the vertebra-disk-ratio (VDR) is calculated from T1-weighted spin echo MRI by dividing the signal intensity of the bone marrow of the lumbar spine L3 by the signal intensity of an adjacent healthy intravertebral disc (L3/L4). The VDR of a patient can then be compared with the normal range of healthy age-matched adults [31]. In most of the patients with Gaucher disease, ERT resulted in a normalization of the VDR within 1-2 years (Figure 5). The VDR correlated well with the QCSI measurements in the same patients (Vlieger et al, submitted).

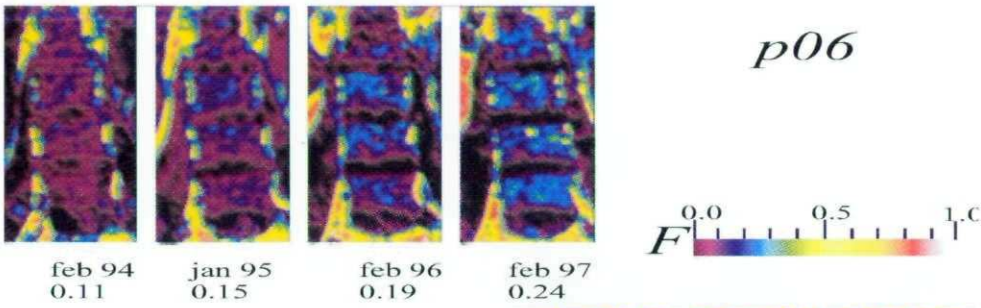

Figure 4. Colour representation of the change in the bone marrow fat fraction (as measured by QCSI every year) in the lumbar spine of a patient with Gaucher disease receiving ERT. The darker colours represent a lower fat fraction as shown on the scale.

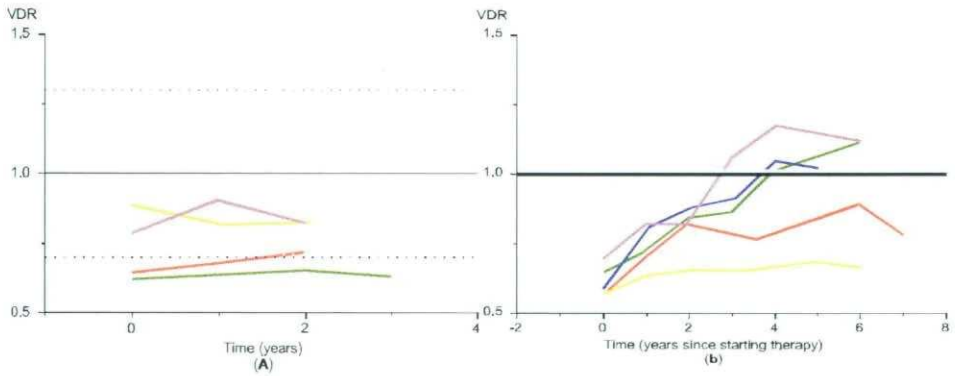

Figure 5. Change with time in VDR score in patients with Gaucher disease: (**A**) untreated patients studied at the Academic Medical Center in Amsterdam; (**B**) patients receiving enzyme replacement therapy.

The bone marrow burden score [31] may also be useful for quantifying response of bone marrow to ERT. The bone marrow burden score is based on the signal intensity of T1- and T2-weighted images of the femurs and the lumbar spine, and on the sites of infiltration. Initial data suggest that response is detected later than with QCSI, but these data are still being analyzed.

Italian data

Osteopenia in patients with Gaucher disease is associated with a significant reduction in lumbar bone mineral density (BMD) [23]. Dual-energy X-ray absorptiometry (DXA) can be used to measure BMD, and may be useful for measuring generalized osteopenia and its response to ERT in patients with Gaucher disease. DXA is being used at the Burlo Garofolo Institute in Trieste, Italy, to assess changes in lumbar BMD in patients with type 1 Gaucher disease receiving ERT.

Table 6. Baseline patient and disease characteristics in the Italian study

Characteristic	
Male:female ratio, *n*	15:9
Mean age, years [range]	34 [22-60]
Splenectomy, *n* (%)	13 (54)
Alglucerase/imiglucerase dose, range in U/kg/2 weeks	6.8-23
Skeletal symptoms, *n*	
Erlenmeyer flask deformity	14
Sclerotic changes	7
Lytic areas	12
Osteonecrosis	10
Bone crisis	5
Vertebral collapse	1
Pathological fracture	2

The baseline characteristics of 24 patients are shown in Table 6. The mean follow-up and treatment period was 5.7 years (range 4-8.1 years); only data from patients who received ERT for 4 years or longer are presented here. In most patients, there was a subjective improvement in bone pain within the first year. This improvement came in the form of relief from mechanical pain due to osteonecrosis and was observed in approximately 50% of patients. This may suggest that ERT has an effect on pain associated with Gaucher cell infiltration, which may lead to physical compression of the intramedullary blood vessels and bone marrow tissue. However, focal bone lesions, monitored with plain radiography, did not show any morphological improvement.

A worsening of femoral head deformation was evident after 6 years of treatment and two cases of progressive degenerative knee joint changes were observed owing to previous osteonecrosis of distal femur and tibial plateau, respectively. These data indicate that existing osteonecrosis and arthritic sequelae can evolve independently from treatment, and the "true bone pain" associated with such events have little chance of improving with ERT.

Table 7. Change in mean bone mineral density in 10 patients with Gaucher disease treated with enzyme replacement therapy (measured by dual-energy X-ray absorptiometry) from the Italian study

Time point	Mean bone mineral density, g/cm^2 (± SD)
Baseline	0.978 (0.094)
4-6 months	0.990 (0.103)
1 year	0.995 (0.107)
2 years	0.997 (0.967)
4.5 years	1.010 (0.110)*

* statistically significant ($p = 0.04$) change from baseline, repeated measures analysis of variance (ANOVA)

BMD measurements were taken in 10 of these patients at L1-L4 of the lumbar spine every 4-6 months for the first year then once every year. The mean BMD of these 10 patients increased within 6 months of starting ERT and continued to increase over the next 4 years (Table 7). However, the increase in the mean BMD was not significant until 4.5 years after starting ERT. The mean lumbar BMD Z score also increased significantly from -0.67 at baseline to -0.41 ($p = 0.004$; Students two sided t test) at the last DXA assessment (mean 4.5 years). Although the mean BMD Z score increased significantly, the increase in some individuals was small. In children, improvements in BMD induced by ERT may appear more rapid and consistent than in adults [32], but this probably reflects an initially lower lumbar BMD in children, who generally have more diffuse skeletal involvement. Adult patients generally present with less severe generalized osteopenia but more pronounced focal involvement. Measurement of BMD by DXA appears to be a useful indicator of the resolution of generalized osteopenia during ERT.

Gaucher Registry data

The Gaucher Registry is an international, observational, longitudinal registry initiated in 1991. Over 2000 patients have been registered [33]. Baseline data for registered patients are shown in Table 8.

Table 8. Baseline patient and disease characteristics in the Gaucher Registry

Characteristic		
Male:female ratio, % (N = 2004)	46:54	
Under 18 years old	21	
18 years old or over, % (N = 1994)	79	
Receiving ERT, % (N = 1995)	77	
Total splenectomy	28	
Partial splenectomy, % (N = 1943)	3	
Type 1 Gaucher disease, % (N = 1946)	94	
Geographic distribution, % (N = 1959)		
USA	43	
Israel	18	
UK	5	
Germany	5	
Italy	4	
France	4	
Canada	4	
The Netherlands	2	
Sweden	2	
Spain	2	
Argentina	2	
Poland	2	
Others	7	
Genotype, n (%)*	322	(29)
N370S/N370S	173	(16)
N370S/L444P	130	(12)
N370S/84GG	215	(20)
N370S/?	68	(6)
L444P/L444P	33	(3)
L444P/?	29	(3)
N370S/IVS2^{-1}	112	(10)
All others		
Unknown	15	(1)
Skeletal symptoms, n/N (%)		
Bone pain	802/1333	(60)
Bone crisis	311/1241	(25)
Radiological evidence of bone disease	1264/1415	(89)

* N = 1097

Overall, ERT reduced bone pain. Eighty-nine (52%) of 172 patients who reported a history of bone pain when they started ERT had no bone pain in the second year of treatment; most of these patients (64) had no bone pain in the first or second year of treatment. Only 8 of 116 (7%) patients who had no history of bone pain at baseline reported bone pain in the second year of ERT. For patients with a history of bone crisis, 57 of 61 (93%) had no recurrence in the second year of ERT, and only 1 of 188 (0.5%) patients with no prior history had bone crisis in the second year of therapy. Physicians providing data for the Gaucher Registry were asked to provide an overall assessment of the response of bone disease to ERT in their patients. In adults, after 3 years of treatment, 32% (12/37) were classified as improved, 57% (21/37) were classified as stable, and 11% (4/37) were classified as worse. For an additional 25 patients with data after 4 years of treatment, 20% (5/25) were classified as improved, 76% (19/25) were classified as stable, and 4% (1/25) were classified as worse.

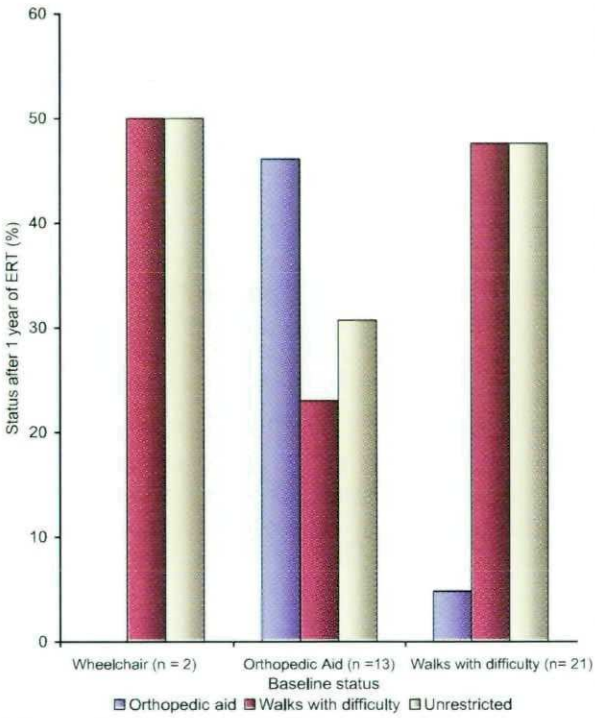

Figure 6. Change after 1 year of enzyme replacement therapy in the functional status of patients in the Gaucher Registry with restricted mobility at baseline.

Skeletal complications in Gaucher disease have a significant impact on the quality of life of patients and can severely impair the mobility of the patient. An important aim of ERT is therefore to improve the functional status of patients. Among patients on the Gaucher Registry with baseline data on mobility status, most patients with mobility problems improved or stabilized within the first year of receiving alglucerase/imiglucerase (Figure 6). 151 of 152 patients who were unrestricted at baseline remained unrestricted after 1 year of therapy; one patient had difficulty in walking.

DISCUSSION

These recent data from America and Europe demonstrate the efficacy of ERT in the treatment of Gaucher disease. Improvement in hematological parameters and reduction in visceral volumes confirm previous studies [6,24,25], and several skeletal complications improved with treatment. However, most focal skeletal complications consist of irreversible lesions that would not be expected to respond to ERT.

The most striking results were those showing a rapid response of bone marrow to ERT. In some patients, improvement in bone marrow was detected with MRI within the first year of treatment [10]. Changes were detected in the femurs of one patient after 9 months of treatment, but the findings from the Netherlands suggest that bone marrow response may be detectable, with sensitive techniques, in the lumbar spine even sooner. The observed rapid improvements in bone marrow challenge the belief that bone responses to ERT develop more slowly than visceral responses. In support of this is the observation that rapid hematological responses occur in splenectomized patients, suggesting a direct effect of ERT on the bone marrow. The evidence from these reports suggests that, even in patients with a relatively rapid bone marrow response, the bone marrow continues to improve with several years of treatment and prolonged treatment is needed to achieve normalization.

The increase in the mean BMD was evident within the first year of ERT but this did not reach significance until 4.5 years after starting ERT. Although increases were rapid in some individuals, it remains to be seen whether these increases are maintained in the longer term. Those patients who showed only minor improvements in BMD (even after several years of therapy) may be candidates for investigative trials of adjunctive agents such as bisphosphonates.

The reduction in bone pain within the first year of treatment has been demonstrated previously [6,7]. Results from the Gaucher Registry suggest that reductions in bone pain continue after the first year of therapy and that recurrence is infrequent. Bone pain in Gaucher disease takes many forms, and the causes of the different types of pain are often not well defined. The data collected so far indicate that generalized bone pain responds best to ERT whereas pain attributable to focal, irreversible lesions tends to be more resistant [10].

The faster than expected response of bone disease to ERT may be attributable to advances in imaging technology. The possibility that increased familiarity with ERT has resulted in better management of Gaucher disease should also be considered. However, no conclusions on the optimum ERT dosage can be offered on the basis of this report. The

bone marrow response did not display statistically significant dose dependence in the one study in which this was investigated, possibly because the number of patients was small and doses varied. The heterogeneity of the disease, in terms of initial presentation and disease progression, supports an individualized approach to dosing.

The findings show that bone marrow response to ERT in adults with Gaucher disease should ideally be monitored with MRI, which is the most reliable method of assessing bone marrow changes. The results appear to be consistent across the different countries (for example the German and American results are similar) [10,11]. Although these are qualitative assessments, the consistency increases our confidence in the results. Quantitative methods to measure the bone marrow response to ERT would be useful, and initial results with quantitative methods derived from MRI are promising.

QCSI is the most developed method for the quantitative assessment of bone marrow in Gaucher disease. The QCSI data presented here confirm that bone marrow fat content increases in the first year of ERT and continues to increase for at least 5-6 years. As long as this time- and resource-intensive method remains unavailable in many centers, alternative semi-quantitative methods may be useful. VDR and bone marrow burden scores appear to correlate with QCSI but these methods may be less sensitive. Pixel counts of MRIs may help to confirm the qualitative assessments of these images but the accuracy of this method remains untested. MRI scoring may be useful for assessing disease stage and response to therapy. The value of these scoring systems is unclear until they are validated, and a consensus is reached on the relevance of the locations used for measurement.

DXA is the best quantitative method for the measurement of generalized osteopenia. Changes in bone density are slow, as they are probably dependent on normalization of bone marrow. Changes in DXA scores are therefore only seen after long term treatment. DXA is insensitive to local changes, and its usefulness is limited because the natural history of osteopenia in Gaucher disease is unknown. DXA is not useful in patients with avascular necrosis of the hip, collapse of vertebrae or sclerosis, because of erroneous high values for BMD.

In general, the lack of information on the natural history of bone complications in Gaucher disease makes analysis of the response of bone pain, bone crisis and bone marrow to ERT difficult. The long-term stabilization of bone disease by ERT is considered a success, but some authors have suggested that bone disease progresses slowly or not at all in untreated adults with Gaucher disease [7,14]. In contrast, many more

reports have demonstrated progression of the skeletal aspects of Gaucher disease in most non-Jewish, untreated, adult patients [26-29]. In a recent report, one adult patient showed deterioration of bone disease on MRI within 2 years of ERT cessation [30].

Despite the success of ERT for type 1 Gaucher disease, some of the patients in the US study had no measurable bone marrow response. These patients also have relatively minor reductions in liver and spleen volumes. Inadequate dosage of ERT may explain a suboptimal response. The lack of a sensitive method for measuring bone marrow response may also explain this, and emphasizes the need for sensitive tools to assess the extent of bone marrow involvement and to direct possible dose adjustments.

In conclusion, these new data confirm the efficacy of ERT for Gaucher disease. Visceral organ volumes are reduced, hematological parameters are improved and the incidence and severity of skeletal complications are reduced. The initial response of bone marrow may be as rapid as the reductions in liver and spleen volumes in some patients, but bone marrow responses are more difficult to quantify and a maximal response usually takes a long time to achieve. Changes in the mineral phase of the skeleton are slower because they are dependent on the marrow response. However, it is imperative to emphasize that bone destruction and related pain are irreversible. T1- and T2-weighted MRI is a good method for measuring bone marrow changes and quantitative methods of measuring these changes are being studied. BMD increases can be quantified using DXA. Delaying ERT may result in irreversible changes to bone and marrow, and lead to functional disability that could otherwise be prevented.

ACKNOWLEDGMENTS

We would like to thank and acknowledge the invaluable input by P. Giraldo (Spanish Gaucher Registry), J.-A. Koch (Germany), S. vom Dahl (Germany), E.M. Akkerman (the Netherlands), J.M.F.G. Aerts (the Netherlands) and C.E.M. Hollak (the Netherlands). In addition, we are grateful for the indispensable contribution to the Gaucher Registry of the hundreds of physicians worldwide in the International Collaborative Gaucher Group.

REFERENCES

1. Brady RO. Gaucher's disease: past, present and future. Baillieres Clin Haematol 1997; 10:621-34.
2. Sidransky E, Ginns EI. Clinical heterogeneity among patients with Gaucher's disease. JAMA 1993; 269:1154-7.
3. Beutler E, Grabowski GA. Glucosylceramide lipidoses: Gaucher disease. In: Scriver CR, Beaudet AL, Sly WS, Valle D, editors. The Metabolic and Molecular Basis of Inherited Diseases, New York: McGraw-Hill, 1995; 2641-70.
4. Grabowski GA, Barton NW, Pastores G, et al. Enzyme therapy in type 1 Gaucher disease: comparative efficacy of mannose-terminated glucocerebrosidase from natural and recombinant sources. Ann Intern Med 1995; 122:33-9.
5. Grabowski GA, Leslie N, Wenstrup R. Enzyme therapy for Gaucher disease: the first 5 years. Blood Rev 1998; 12:115-33.
6. Pastores GM, Sibille AR, Grabowski GA. Enzyme therapy in Gaucher disease type 1: dosage efficacy and adverse effects in 33 patients treated for 6 to 24 months. Blood 1993; 82:408-16.
7. Beutler E, Demina A, Laubscher K, et al. The clinical course of treated and untreated Gaucher disease. A study of 45 patients. Blood Cells Mol Dis 1995; 21:86-108.
8. Rosenthal DI, Doppelt SH, Mankin HJ, Dambrosia JM, Xavier RJ, McKusick KA, et al. Enzyme replacement therapy for Gaucher disease: skeletal responses to macrophage-targeted glucocerebrosidase. Pediatrics 1995; 96:629-37.
9. Allison JW, James CA, Arnold GL, Stine KC, Becton DL, Bell JM. Reconversion of bone marrow in Gaucher disease treated with enzyme therapy documented by MR. Pediatr Radiol 1998; 28:237-40.
10. Poll LW, Koch J-A, vom Dahl S, et al. Magnetic resonance imaging of bone marrow changes in Gaucher disease during enzyme replacement therapy: first German long-term results. Skeletal Radiol 2001; 30:496-503.
11. Terk MR, Dardashti S, Liebman HA. Bone marrow response in treated patients with Gaucher disease: evaluation by T1-weighted magnetic resonance images and correlation with reduction in liver and spleen volume. Skeletal Radiol 2000; 29:563-71.
12. Tran SD, Terk MR, Colletti PM. MR spectroscopy of bone marrow: precision and reliability. American Roentgen Ray Society 100th Annual Meeting 2000; 174:60.
13. Zimran A, Sorge J, Gross E, Kubitz M, West C, Beutler E. Prediction of severity of Gaucher's disease by identification of mutations at DNA level. Lancet 1989; 2:349-52.

14. Zimran A, Kay A, Gelbart T, et al. Gaucher disease. Clinical, laboratory, radiologic, and genetic features of 53 patients. Medicine (Baltimore) 1992; 71:337-53.
15. Maas M, Akkerman EM, Venema HW, Stoker J, Den Heeten GJ. Dixon quantitative chemical shift MRI for bone marrow evaluation in the lumbar spine: a reproducibility study in healthy volunteers. J Comput Assist Tomogr 2001; 25:691-7.
16. Dixon WT. Simple proton spectroscopic imaging. Radiology 1984; 153:189-94.
17. Johnson LA, Hoppel BE, Gerard EL, et al. Quantitative chemical shift imaging of vertebral bone marrow in patients with Gaucher disease. Radiology 1992; 182:451-5.
18. Hollak CE, Aerts JM, Goudsmit R, et al. Individualised low-dose alglucerase therapy for type 1 Gaucher's disease. Lancet 1995; 345:1474-8.
19. Maas M, Akkerman EM, Hollak CEM, Aerts JFMG, den Heeten GJ. Quantitative chemical shift imaging in Gaucher disease. Eur Radiol 2000; 10:B23.
20. Hollak C, Maas M, Akkerman EM, den Heeten GJ, Aerts JFMG. Dixon quantitative chemical shift imaging is a sensitive tool for the evaluation of bone marrow responses to individualised doses of enzyme supplementation therapy in type 1 Gaucher disease. Blood Cells Mol Dis 2001; 27(6):1005-1012.
21. Maas M, Vlieger EJP, Akkerman EM, Hollak CEM, den Heeten GJ, Aerts JFMG. T1-W intensity ratio of vertebra and disc (V/D Ratio) in bone marrow evaluation: preliminary results in bone marrow. International Society for Magnetic Resonance in Medicine 1999; 1043.
22. Vlieger EJP, Maas M, Akkerman EM, Hollak CEM, Aerts JFMG, den Heeten GJ. The application of the Vertebra-Disc Ratio in a population of patients with Gaucher's disease. International Society for Magnetic Resonance in Medicine 2000; 2131.
23. Pastores G, Wallenstein S, Desnick RJ, Luckey MM. Bone density in Type 1 Gaucher disease. J Bone Min Res 1996; 11:1801-7.
24. Barton NW, Brady RO, Dambrosia JM, et al. Replacement therapy for inherited enzyme deficiency--macrophage- targeted glucocerebrosidase for Gaucher's disease. N Engl J Med 1991; 324:1464-70.
25. Beutler E, Kay A, Saven A, et al. Enzyme replacement therapy for Gaucher disease. Blood 1991; 78:1183-9.
26. Goldblatt J, Beighton P. Gaucher disease in the Afrikaner population of South Africa. S Afr Med J 1979; 55:209-10.
27. Giraldo P, Perez-Calvo JI, Giralt M, Pocovi M. Clinical characteristics of type I Gaucher's disease in Spain. Preliminary results of national survey. Spanish Group on Gaucher's Disease. Med Clin (Barc) 1997; 109:619-22.

28. Maaswinkel-Mooij P, Hollak C, van Eysden-Plaisier M, Prins M, Aerts H, Poll R. The natural course of Gaucher disease in The Netherlands: implications for monitoring of disease manifestations. J Inherit Metab Dis 2000; 23:77-82.
29. Niederau C, Birkhahn A, Ehlen C, et al. Facts and fiction of modern diagnosis of type 1 Gaucher disease: the German experience in 1996. Gauch Clin Perspec 1996; 4:5-13.
30. vom Dahl S, Poll LW, Haussinger D. Clinical monitoring after cessation of enzyme replacement therapy in M. Gaucher. Br J Haematol 2001; 113:1084-7.
31. Maas M, Poll LW, Terk MR. Imaging and quantifying skeletal imvolvement in Gaucher disease. Br J Radiol 2002: 75(Suppl. 1):A13-A24.
32. Bembi B, Ciana G, Mengel E, Terk MR, Martini C, Wenstrup RJ. Bone complications in children with Gaucher disease. Br J Radiol 2002; 75(Suppl.): in press.
33. Wenstrup RJ, Roca-Espiau M, Weinreb NJ. Skeletal aspects of Gaucher disease: a review. Br J Radiol 2002; 75(Suppl.): in press.

CHAPTER 7

The vertebra-disc ratio as a parameter for bone marrow involvement and its application in Gaucher disease

Erik-Jan P. Vlieger[1], Mario Maas[1], Erik M. Akkerman[1], Carla E.M. Hollak[2], Gerard J. den Heeten[1]

From the Departments of Radiology [1] and Hematology [2], Academic Medical Center, Amsterdam, the Netherlands

Submitted

ABSTRACT

Objective:

To establish the Vertebra Disc Ratio (VDR), the ratio of the average T1-weighted gray value of vertebral body L3 and intervertebral disc L3/L4, as a parameter for bone marrow involvement. To explore its value as alternative for bone marrow fat fraction (F_f) measured with Dixon quantitative chemical shift imaging (Dixon QCSI) in Gaucher disease.

Methods:

Age dependency and normal value for the VDR were determined in 46 controls. The VDR in untreated Gaucher disease (N=22) and long treated Gaucher disease (7.5 years, N=19) were compared to the controls. VDR as follow-up parameter was tested in treated Gaucher disease patients (N=33) and untreated Gaucher disease patients (N=8). The correlation between VDR and F_f was determined.

Results:

Age dependency was small. The normal VDR was 1.90 ± 0.30. Both untreated Gaucher disease (1.29 ± 0.31) and long treated Gaucher disease (1.70 ± 0.33) differed significantly from normal. Changes in treated Gaucher disease were significant in the first four treatment-years, in untreated Gaucher disease patients no significant changes were observed. The correlation with F_f was 0.86.

Conclusions:

The VDR is a useful parameter for evaluation of bone marrow of patients with Gaucher disease. The VDR correlates very well with F_f, so applicability is expected in diseases in which F_f has proven to be useful.

INTRODUCTION

In the radiological follow-up of infiltrating bone marrow diseases, the bone marrow fat-fraction plays an important role, as it has been shown that this quantity correlates well with disease-activity [1]. The fat-fraction can be measured using Dixon quantitative chemical shift imaging (Dixon QCSI), or with proton MR spectroscopy [2-9]. Dixon QCSI allows for the measurement of the axial bone marrow, and has good reproducibility [10]. To our best knowledge the use of Proton MR Spectroscopy to measure fat-fractions in a routine clinical setting has not been investigated.

Gaucher disease, the most prevalent lysosomal storage disorder, is caused by a deficiency of the enzyme glucocerebrosidase leading to accumulation of glycolipids in macrophages (Gaucher cells) [11]. These cells accumulate in the liver, spleen, and bone marrow. The most important clinical consequences are hepato-splenomegaly, pancytopenia, skeletal disease, and bone marrow infiltration [1,3,10-14]. Measurement of the Gaucher cell burden in the axial skeleton in untreated patients might be used as a prognostic tool for bone complications, and may indicate the need to start therapy. Since enzyme supplementation therapy for Gaucher disease [15-17] is very expensive, monitoring therapy-response is mandatory to optimize individual dosage scheme [17]. Dixon QCSI measured fat-fraction (F_f) has been advocated as the best suitable tool for this purpose [18].

Although F_f is considered the state-of-the-art modality to monitor bone marrow infiltration, a problem with this technique is that it is not widely available; special non standard MR sequences are needed, as are special post-processing tools [19,20]. In the following we propose an alternative for the bone marrow fat-fraction that is widely available and easy to use.

On plain T1-weighted images, the bone marrow of untreated patients with Gaucher disease shows a decrease in signal, because normal bone marrow fat is replaced by Gaucher cells [1] which has a low signal intensity. This reduced T1-weighted signal, however, cannot be used directly for bone marrow evaluation, since it depends on different amplification factors some of which are unknown. The inclusion of an internal reference signal leading to a ratio between these two values may solve this problem. We defined the Vertebra Disc Ratio (VDR) as the T1-weighted bone marrow signal divided by the signal of the healthy adjacent intervertebral disc, and investigated whether this could be a

valid alternative to F_f. This was done by measuring the normal range for the VDR, comparing this to the VDR in Gaucher disease, investigating whether the VDR is able to detect changes in response to therapy and calculating the correlation between the VDR and F_f.

METHODS AND MATERIALS

Patients and Controls

This investigation was carried out at a University Hospital, which serves as a national referral center for Gaucher disease [17]. Patients with Gaucher disease visited the hospital roughly every year between 1993 and 2001. Patients were retrospectively included if 1) sagittal T1- and T2-weighted images of the lumbar spine were available, 2) vertebral body L3 was intact, and 3) intervertebral disc L3/L4 was intact. Exclusion criteria were: other bone marrow disorders, malignancies, radiotherapy, recent bleeding, liver disease and renal impairment [21]. The F_f of the same patient was included in this study if the image acquisition was performed within one day of the acquisition of the T1-weighted images. We also registered whether or not a patient was under therapy.

As controls served patients undergoing MR imaging of the lumbar spine in whom no abnormalities in the vertebrae or intervertebral discs were found. Control patients were retrospectively included under the same inclusion and exclusion criteria as the Gaucher disease patients.

Data Acquisition and Processing

All conventional MR imaging was done on a 1.5T magnet (Vision, Siemens, Erlangen, Germany), using a dedicated spine coil. Routine sagittal T1-weighted and T2-weighted spin echo images were acquired. For T1-weighted imaging TE and TR ranged from 12-15 ms and 400-650 ms respectively. The VDR was calculated from the vertebral body L3 in the mid-sagittal T1-weighted spin echo image of the lumbar spine, and the intervertebral disc L3-L4 in the same image.

To exclude cortex from the measurement and to avoid partial volume averaging the edge of the above mentioned structures was excluded as follows: both vertebral body L3 and intervertebral disc L3/L4 were outlined manually using an image processing program (Photoshop 5.0, Adobe, San Jose, California, USA), see figure 1 [22]. The Regions of Interest (ROIs) thus obtained, were downsized towards the center by

15-25% using erosion, which is a morphological image processing procedure [23]. From these smaller, central ROIs the VDR was calculated as the ratio of their average gray-values.

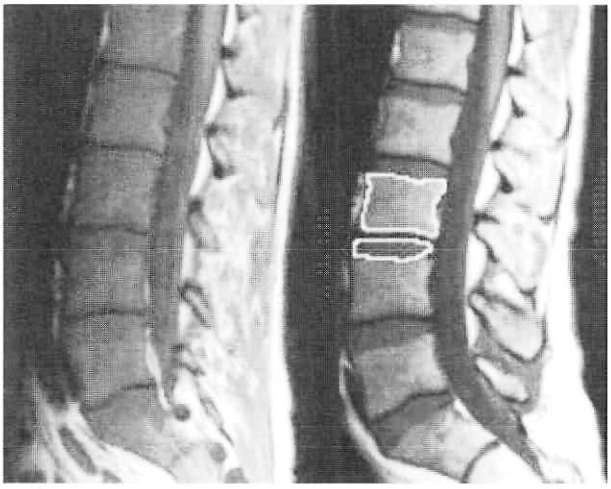

Figure 1. These images are from a Gaucher disease patient receiving treatment. The left is from 1997, the right from 2000. The VDR's were 1.20 and 1.95 respectively. In the right image the contours that were used for calculation of the VDR are shown.

For Dixon QCSI imaging, in-phase and opposed-phase proton density weighted spin echo sequences were performed with a TR of 2500 ms and a TE of 22.3 ms [19]. The measurement acquisition slices were positioned coronally. Post-processing and data analysis were performed using a previously described algorithm [20]. To obtain one fat-fraction value for L3, the pixel values were averaged over a user-defined ROI. This ROI was achieved in a similar way as described above, by outlining the cortex of L3 and then reducing the ROI's size.

Statistical analysis

All statistical analyses were performed on a Pentium PC, using Microcal Origin v. 6.0, Northampton, Massachusetts, USA. Differences between groups and differences from zero were tested with Student's t-test. Response of VDR under therapy was assessed by comparing values from two adjacent years. To establish relations between quantities (e.g.: VDR vs. age, VDR vs. F_f) we applied linear fitting (a linear fit is a way to calculate an assumed linear relationship between two quantities) and correlation coefficients where appropriate.

Statistical significance was obtained when $p<0.05$ or (equivalently) when 95% confidence interval (CI) did not overlap.

RESULTS

Patients and Controls

46 Gaucher disease patients were included (26 females, age range 19 - 71, average 42.8 years), (20 males, age range 26 - 61, average 42.2 years). 24 Patients were receiving therapy at inclusion, 13 patients started therapy during this investigation and 9 patients remained untreated.

The average number of VDR measurements per patient was 4.4, ranging from 1 to 7. These measurements spanned an average of 4.3 years, ranging from 0 (only one measurement done) to 7 years. The total number of VDR measurements was 204, the total number of simultaneously measured F_f s was 126.

46 Control patients were included, 20 males (age range 6.2 - 71.4) and 26 females (age range 2.8-71.3), with an average age of 39.9. A subgroup of 33 control patients was selected which age-matched the Gaucher disease patient group: the average age of the subgroup was 40.7, range 25.5-60.0.

VDR in controls

The average VDR of all controls (N=46) was 1.90 (standard deviation (SD) 0.30, standard error of the mean (SEM) 0.04). The average VDR of the age-matched subgroup (N=33) also was 1.90 (SD 0.30, SEM 0.05).

As the VDR is meant to serve as a longitudinal bone marrow follow-up tool and fat-fraction may increase with age [21,22], it was important to establish whether or not an age dependency existed. We assumed the following linear relationship between the VDR and the AGE of all control patients (N=46):

$$\text{VDR} = a + b * AGE\,(\text{years})$$

and the fitting procedure found the following optimal result for a (the intercept) and b (the slope, which reflects the actual age dependency), with the 95 % CI in brackets:

$$a = 1.63\ (1.52,\ 1.73)$$
$$b = 0.007\ (0.002,\ 0.011)$$

The fit is visualized in figure 2.

Since the 95% CI for the slope does not include zero, the age dependency is significant. It is, however, small: 0.007 increase in VDR per year.

Comparing this to the group standard deviation (SD 0.30, SEM 0.053) and to the changes due to therapy (0.14 in the first year, see below), we found it justified to neglect the age dependency in the further analyses, even more so since we used an age matched subgroup.

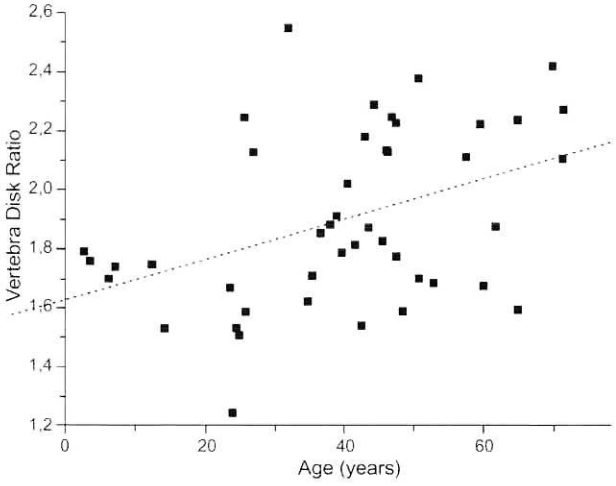

Figure 2. The linear fit (dashed line) between Vertebra Disc Ratio and Age for the controls (N=46).

VDR in Gaucher disease patients

From all the available VDR-measurements at which the patient was not receiving therapy the most recent one was selected to get one measurement per patient (N=22, average age 40.2 years, range 28.8 - 59.3 years). The average VDR in this group was 1.29 (SD 0.31, SEM 0.066). This is significantly lower ($p < 10^{-8}$) than the VDR values of the control patient group.

The date at which therapy started was defined as T=0 for each patient individually. The changes in VDR during therapy were calculated per year, using only measurements that had a time interval of 0.9 to 1.1 year. For 33 patients we had at least 2 such measurements. The yearly changes are given in Table 1, showing a significant average increase in VDR during the first four years of treatment of 0.10 to 0.14. From the fifth to the seventh year of treatment we see no significant change.

The untreated Gaucher disease-patients (N=9) did not visit as regularly as the treated patients and for these patients the method used to calculate changes in VDR, as described above, could not be used.

Table 1. Average yearly changes in Vertebra Disc Ratio (VDR) for patients receiving therapy. The change reported is the change that happened the year before, e.g. year 1 reports the change that occurred between start of therapy and one year after. The change in VDR is given with the 95% confidence interval in brackets. The change is statistically tested against the normal age related change; *p*-values marked with an asterisk are considered significant ($p<0.05$).

Treatment Duration	N	Change in VDR	*p*
1 year	11	0.14 (0.07 , 0.22)	*0.005
2 years	12	0.10 (0.04 , 0.17)	*0.01
3 years	11	0.12 (0.02 , 0.21)	*0.04
4 years	13	0.14 (0.05 , 0.23)	*0.01
5 years	12	0.09 (-0.01 , 0.18)	0.13
6 years	7	-0.04 (-0.18 , 0.11)	0.57
7 years	6	0.07 (-0.04 , 0.18)	0.32

For eight untreated patients we had more than one measurement, and we took the difference of the first and last available measurement, divided by the time (in years) between the two measurements, to estimate the average change per year. The average time between the first and last measurement was 2.6 years, ranging from 1 to 4 years. The resulting mean change in VDR per year was 0.03, with a 95% CI of (-0.08, 0.16). This is in agreement with the age dependency found in the controls.

The average VDR in treated Gaucher disease was calculated from measurements at which a Gaucher disease patient had received an average of 7.5 years of treatment (range 6-9 years); data were available for 19 individuals. The average VDR was 1.70 (SD 0.33, SEM 0.076). While this is still significantly ($p= 0.032$) lower than the VDR values of the control group (1.90), it is also significantly higher ($p=0.0002$) than the VDR in untreated Gaucher disease (1.29).

VDR versus Dixon QCSI fat-fraction

A total of 126 simultaneously measured VDRs and F_f 's were available. Assuming the following linear relationship between F_f and VDR :

$$F_f = c + d * VDR$$

the fitting algorithm found optimal values for the intercept c = -0.18 (-0.24, -0.13) and for the slope d = 0.32 (0.28, 0.35) with 95% CI in brackets, both being significantly different from zero. This is visualized in figure 3. The correlation coefficient R = 0.86 (0.72, 1.00) also was highly significantly different from zero ($p < 0.0001$).

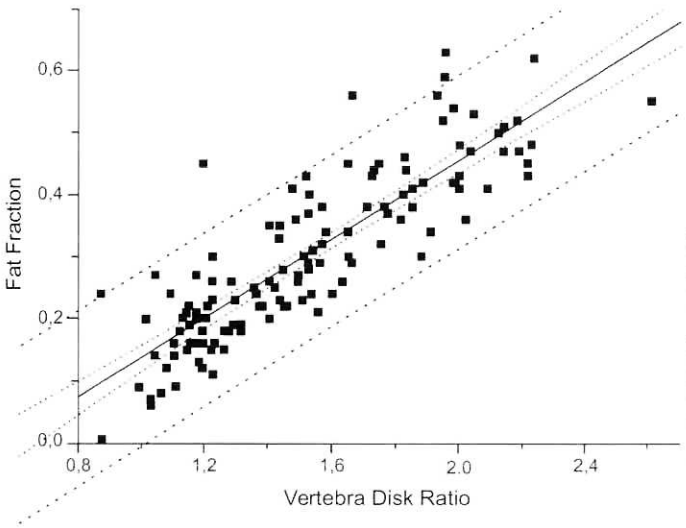

Figure 3 The linear fit (straight line) between Fat-fraction and Vertebra Disc Ratio, with confidence limits (dotted) and prediction limits (dashed).

As it was uncertain whether the relation between VDR and F_f was the same for treated and untreated patients, the fit and the correlation were repeated also for two subgroups: 1) for untreated Gaucher disease patients (1 value per patient) and for 2) treated Gaucher disease patients (2 - 4 years of treatment, preferably around 3 years of treatment, 1 value per patient).

Complete results are given in table 2. The fitting coefficients do not differ significantly between the three sets of data, which can be told from the (partly) overlapping 95% confidence intervals.

Table 2. Fit and correlation results for Vertebra Disc Ratio (VDR) and Fat-fraction (F_f). The formula of the fit is $F_f = c + d * VDR$. Coefficients c and d and the correlation R are given with their 95% confidence intervals. Results are given for patients receiving no therapy, patients having received two to four years of therapy, and all available simultaneously measured VDRs and F_f's (with multiple values per patient).

Therapy	N	c	d	Correlation	*P*
No	19	-0.08 (-0.21 , 0.06)	0.24 (0.15 , 0.34)	0.77 (0.64 , 0.91)	<0.0001
2 to 4 years	17	-0.15 (-0.31 , 0.01)	0.30 (0.20 , 0.39)	0.85 (0.69 , 1.00)	<0.0001
ALL	126	-0.18 (-0.24 ,-0.13)	0.32 (0.28 , 0.35)	0.86 (0.72 , 1.00)	<0.0001

DISCUSSION

Bone marrow infiltration is a serious clinical problem in Gaucher disease. To quantify this infiltration, the fat-fraction measured with Dixon quantitative chemical shift imaging (F_f) is state-of-the-art. However, an alternative is needed in those places where patients with Gaucher disease are treated, but F_f is not available. In this article it has been investigated whether or not the VDR is a valid alternative.

A normal range for the VDR has been established. The VDR is age dependent, though the age-dependency is very small; therefore it was ignored for the evaluation of bone marrow in Gaucher disease.

The VDR differs significantly between healthy bone marrow (controls) and bone marrow from untreated patients with Gaucher disease. The yearly VDR-changes are significant during the first four years in treated Gaucher disease patients. Although the average VDR in Gaucher disease patients is still below normal after an average therapy duration of 7.5 years, it is much higher than the average VDR in untreated Gaucher disease patients. Even though no yearly changes are significant after 4 years of treatment, this does not imply that no change occurs; it is more likely that the changes are too small to be detected with the given group

size. We will have to wait and see whether the average VDR in Gaucher disease returns to normal after an even longer therapy duration. The VDR correlates very well with F_f. This correlation is the same in treated and untreated Gaucher disease.

Limitations of this study

The normal value of the VDR has been calculated from a transverse cohort. Therefore, it is unknown what the normal longitudinal variation is. However, the use of the VDR is intended to be longitudinal. Its use in clinical practice will have to learn what normal longitudinal variations are.

The controls that were referred for MR imaging of the lumbar spine cannot be considered a healthy population, since MR of the lumbar spine was requested. The "true" normal VDR might deviate from the one published here.

In this article, the VDR has been compared to F_f. The VDR was subject to some factors which potentially increased its variance: For F_f, the imaging plane from which the data was calculated was chosen coronal to be as much parallel as possible to the coil, to reduce the effects of signal drop off caused by the surface coil. The data for the VDR were calculated from sagittal planes. TE and TR were fixed for F_f, for the VDR they varied. The F_f was calculated from the bone marrow alone; the VDR included the intervertebral disc. It is known that the water content of the disc is influenced by age [24] and can even vary within a day [25,26]. This influences the VDR, giving rise to non bone marrow related changes.

In spite of these factors the VDR shows a very good correlation with F_f, independent of the treatment status of the patient.

Conclusions

We conclude that the VDR is a very useful parameter for the radiological follow-up of bone marrow of patients with Gaucher disease. Group effects can be measured directly, for individual follow-up one has to bear in mind that the variations over time have not been measured in healthy controls.

With the VDR, a tool has been made available that allows any center with a 1.5 T MR scanner to do reliable bone marrow measurements in patients with Gaucher disease; previously this was limited to centers being able to perform Dixon QCSI. This tool opens new doors for research: if images

have been stored digitally, retrospective studies on Gaucher disease patients are possible, as most lumbar spine imaging includes T1-weighted images. It is also allowed for comparisons between different centers. Even though different centers will have different choices for TE and TR in T1-weighted images, this should not pose a problem as the VDR has not been defined with a very strict TE or TR.
For individual patient follow-up the VDR can be used as another parameter for monitoring therapy-response.

Future applications
As the correlation between F_f and VDR was very good, and independent of the treatment-status of the patient, we expect applicability in other diffuse bone marrow diseases in which F_f has proven to be useful. These include leukemia [5,27,28], aplastic anemia [5], malignant lymphoma [29], and myelofibrosis [29]. Also, the follow-up of autologous blood stem cell transplantation [30] is possible.
As proton MR spectroscopy and F_f both can be used to measure bone marrow fat-fractions, we also expect a potential use for the VDR in areas where fat-fractions measured with proton MR spectroscopy have proven their value: bone weakness and osteopenia [31,32], aplastic anemia [33], the effects of chemotherapy [34], and even bone marrow changes in anorexia nervosa [35].

REFERENCES

1. Miller SPF, Zirzow GC, Doppelt SH, et al. Analysis of the lipids of normal and Gaucher bone marrow. J Lab Clin Med 1996; 127:353-358.
2. Dixon WT. Simple proton spectroscopic imaging. Radiology 1984; 153:189-194.
3. Johnson LA, Hoppel BE, Gerard EL, et al. Quantitative Chemical Shift imaging of vertebral bone marrow in patients with Gaucher disease. Radiology 1992; 182:451-455.
4. Rosenthal DI, Barton NW, McKusick, et al. Quantitative Imaging of Gaucher disease. Radiology 1992; 185:841-845.
5. Rosen BR, Fleming DM, Kushner DC, et al. Hematological Bone Marrow disorders Quantitative Chemical Shift MR Imaging. Radiology 1988; 169:799-804.

6. Schick F, Einsele H, Weiss B, et al. Assessment of the composition of bone marrow prior to and following autologous BMT and PBSCT by magnetic resonance. Ann Hematol 1996; 72(6):361-370.
7. Schick F, Einsele H, Kost R, et al. Hematopoietic reconstitution after bone marrow transplantation: assessment with MR imaging and H-1 localized spectroscopy. J Magn Reson Imaging 1994; 4(1):71-78.
8. De Bisschop E, Luypaert R, Louis O, et al. Fat fraction of lumbar bone marrow using in vivo proton nuclear magnetic resonance spectroscopy. Bone 1993 Mar-Apr;14(2):133-136.
9. Kugel H, Jung C, Schulte O, et al. Age- and sex-specific differences in the 1H-spectrum of vertebral bone marrow. J Magn Reson Imaging 2001 Feb;13(2):263-268
10. Cremin BJ, Davey H, Golblatt J. Skeletal complications of Type 1 Gaucher disease: The Magnetic Resonance Features. Clinical Radiology 1990; 41:244-247.
11. Gaucher PCE. De l'epithelioma primitif de la rate, hypertrophie idiopathique de la rate sans leukemie. Thesis 1882; Paris.
12. O'Keefe D, Rosenthal DI. Computed tomography and magnetic resonance imaging in Gaucher's disease. In: Bloem JL, Sartoris DJ, and Eds. MRI and CT of the musculoskeletal system: a text-atlas. Baltimore: William & Wilkins, 1992; 130-138.
13. Rourke JA, Heslin DJ. Gaucher's disease; Roentgenologic bone changes over 20 year interval. AJR 1965; 94:621-630.
14. Rodrique SW, Rosenthal DI, Barton NW, et al. Risk factors for osteonecrosis in patients with type 1 Gaucher's disease. Clinical orthopedics and related research 1999; 362:201-207.
15. Barton NW, Brady RO, Dambrosia, et al. Replacement therapy for inherited enzyme deficiency - Macrophage targeted glucocerebrosidase for Gaucher's disease. New England Journal of Medicine 1991; 324:1464-1470.
16. Figueroa ML, Rosenbloom BE, Kay, et al. A less costly regimen of alglucerase to treat Gaucher's disease. New England Journal of Medicine 1992; 327:1632-1636.
17. Hollak CEM, Aerts JMFG, Goudsmit R, et al. Individualised low dose alglucerase therapy for type 1 Gaucher disease. Lancet 1995; 345:1474-1478.
18. Rosenthal DI, Doppelt S, Mankin H, et al. Enzyme replacement therapy for Gaucher disease: skeletal responses to macrophage-targeted glucocerebrosidase. Pediatrics 1995; 96(4):629-637.
19. Maas M, Dijkstra PF, Akkerman EM. Uniform Fat-Suppression in Hands and Feet through the use of Two Point Dixon Chemical Shift Imaging. Radiology 1999; 210:189-193.

20. Akkerman EM, Maas M. A region-growing algorithm to simultaneously remove dephasing influences and separate fat and water in two-point Dixon imaging. Proceedings of the Society of Magnetic Resonance and the European Society for Magnetic resonance in Medicine and Biology 1995; 649.
21. Ishijima H, Ishizaka H, Horikoshi H, et al. Water fraction of lumbar vertebral bone marrow estimated from chemical shift misregistration on MR imaging: Normal Variations with age and sex. AJR 1996; 167:355-358.
22. Maas M, Akkerman EM, Venema HW, et al. Dixon Quantitative Chemical Shift MRI for Bone Marrow Evaluation in the Lumbar Spine: A Reproducibility Study in Healthy Volunteers J Comput Assist Tomogr 2001; 25:691-697.
23. Gonzalez RC, Woods RE. Digital Image Processing. Addison Wesley, 1992; 518-524.
24. Sether LA, Yu S, Haughton VM, Fischer ME. Intervertebral disk: normal age-related changes in MR signal intensity. Radiology 1990;177(2):385-388.
25. Kingma I, van Dieën JH, Nicolay K, et al. Monitoring water content in deforming intervertebral disc tissue by finite element analysis of MRI data. Magn Reson Med 2000; 44(4):650-654.
26. Malko JA, Hutton WC, Fajman WA. An in vivo magnetic resonance imaging study of changes in the volume (and fluid content) of the lumbar intervertebral discs during a simulated diurnal load cycle. Spine 1999; 24(10):1015-1022.
27. Gerard EL, Ferry JA, Amrein PC, et al. Compositional changes in vertebral bone marrow during treatment for acute leukemia: assessment with quantitative chemical shift imaging. Radiology 1992; 183: 39-46.
28. Gückel F, Brix G, Semmler W, et al. Proton chemical shift imaging of bone marrow for monitoring therapy in leukemia. J Comput Assist Tomogr 1990; 14(6):945-959.
29. Gückel F, Brix G, Semmler W, et al. Systemic bone marrow disorders: characterisation with proton chemical shift imaging. J Comput Assist Tomogr 1990; 14(4):633-642.
30. Kauczor HU, Brix G, Dietl B, et al. Bone marrow after autologous blood stem cell transplantation and total body irradiation: magnetic resonance and chemical shift imaging. Magn Reson Imaging 1993; 11:965-975.
31. Schellinger D, Lin CS, Hatipoglu HG, Fertikh D. Potential value of vertebral proton mr spectroscopy in determining bone weakness. Am J Neuroradiol 2001; 22(8):1620-1627.
32. Wehrli FW, Hopkins JA, Hwang SN, et al. Cross-sectional study of osteopenia with quantitative MR imaging and bone densitometry. Radiology 2000; 217(2):527-538.

33. Amano Y, Kumazaki T. Proton MR imaging and spectroscopy evaluation of aplastic anemia: three bone marrow patterns. J Comput Assist Tomogr 1997; 21(2):286-292.
34. Weis J, Ciray I, Ericsson A, et al. Spectroscopic imaging of bone marrow composition in vertebral bodies. MAGMA 2001; 13(1):15-18.
35. Geiser F, Murtz P, Lutterbey G, et al. Magnetic resonance spectroscopic and relaxometric determination of bone marrow changes in anorexia nervosa. Psychosom Med 2001; 63(4):631-637.

CHAPTER 8

Quantification of bone involvement in Gaucher disease: MRI bone marrow burden score as an alternative for Dixon quantitative chemical shift imaging (Dixon QCSI)

Mario Maas[1], Cornelis van Kuijk[1], Jaap Stoker[1], Carla E.M. Hollak[2], Erik M. Akkerman[1], Gerard J. den Heeten[1]

From the Departments of Radiology[1], and Hematology[2], Academic Medical Center, Amsterdam, the Netherlands

Submitted

ABSTRACT

Purpose:

To introduce a semi-quantitative MR bone marrow burden score (BMB) with inclusion of the most dynamic axial bone marrow in Gaucher disease as an alternative for the Dixon quantitative chemical shift imaging (Dixon QCSI) technique.

Materials and Methods:

Two experienced musculoskeletal radiologists with no experience in Gaucher disease blindly analyzed MRI scans of the lumbar spine and femurs. Inter- and intra-observer variability was tested. In addition the BMB was determined as response parameter to evaluate bone marrow response to Enzyme Supplementation Therapy (EST). Finally the BMB was compared with the fat-fraction measurements obtained by Dixon QCSI.

Results:

In 30 patients (mean age 39 years (range 12-71)) the mean fat-fraction was 19.9 (range 8-40). The BMB score ranged from 3-14 points. A significant correlation was found between the two observers when using BMB (ρ= 0.91 (p<0.001)). The intra-observer variation showed a ρ= 0.99 (p< 0.0001). There was a significant correlation between BMB and QCSI ρ=-0.78 (p<0.0001)). Although BMB was less sensitive than Dixon QCSI, it showed enough sensitivity to detect bone marrow response to EST.

Conclusion:

BMB is a well reproducible semi-quantitative scoring system, which is easy to use. It combines both axial and peripheral bone marrow MRI and shows a significant correlation to QCSI. Thus, it can serve as a tool to quantify bone marrow involvement in Gaucher disease, when Dixon QCSI is not available.

INTRODUCTION

Gaucher disease is the most prevalent lysosomal storage disorder in man, leading to storage of glycocerebrosidase-loaded macrophages in bone marrow, liver and spleen [1-3]. The clinical picture of type 1 disease encompasses hepatosplenomegaly, cytopenia and bone involvement [3]. Bone disease is one of the most debilitating features of type 1 Gaucher disease, consisting of atypical bone pain, osteonecrosis, pathological fractures and bone crises [2,4]. Enzyme Supplementation Therapy (EST) for Gaucher disease has become available during the last decade [5-7]. Since this is a highly expensive therapy, adequate monitoring of response to treatment is important to facilitate dose adjustments.

Magnetic Resonance Imaging (MRI) is the modality of choice to depict bone marrow abnormalities [8-14]. It is also used to describe bone marrow invasion in a (semi-)quantitative way. At the first MRI scan of the patient the degree of bone marrow invasion is quantified, and indication for EST is considered. In order to quantitatively analyze bone marrow involvement and response to therapy, Dixon quantitative chemical shift imaging (Dixon QCSI) of the vertebral (axial) bone marrow is used [15,16]. Dixon QCSI is a modification of the Dixon technique [17] and quantifies the fat content in bone marrow by making use of the differences in the resonant frequencies of fat and water in bone marrow (3.3 ppm). The amount of fat in the bone marrow is represented in a fat-fraction F_f, which is decreased in Gaucher disease [15,17-21]. A recent study established a high reproducibility of this technique [22]. Studies using Dixon QCSI have focused on the vertebral bone marrow since it primarily contains red marrow that is very susceptible to disease arising from hematological malignancies [10,23-25]. Furthermore, the axial marrow is the first site to show bone marrow infiltration in Gaucher disease [16,21]. Therefore, measuring the axial marrow may provide the most exact status of bone marrow invasion.

Although MRI is widely available, Dixon QCSI is not included in standard packages of sequences on the MR machines and cannot be used worldwide. Therefore, several visual scoring systems are used and described in the literature [1,26-28]. As a result of these visual scoring systems a semi-quantitative approach of bone marrow invasion is established.

These bone marrow scoring systems are restricted to evaluation of the peripheral bone marrow of the lower extremity. However, none of the published semi-quantitative scoring systems has evaluated axial bone marrow nor has been compared to Dixon QCSI data.
In our opinion, an optimal scoring system should include the axial skeleton, as discussed earlier. Furthermore, there should be a good inter- and intra-observer variability and the scoring system should be reproducible and sensitive for response to therapy. So far no semi-quantitative bone marrow burden score with inclusion of the axial bone marrow has been reported.

The aims of the present study are:
To introduce a semi-quantitative bone marrow burden score with the inclusion of both axial and peripheral bone marrow in order to analyze bone marrow invasion in Gaucher disease by the use of conventional MRI.
To investigate both the inter- and intra-observer variability.
To analyze the relation between QCSI and the bone marrow burden score at baseline.
To evaluate the relation between QCSI and the bone marrow burden score during therapy.

MATERIAL & METHODS

Subjects
Our hospital serves as a national referral center for Gaucher disease [6]. Between 1993 and 1999 all untreated patients with type 1 Gaucher disease who were referred for evaluation of eligibility for enzyme treatment, were consecutively included in this study. The measurement of glucocerebrosidase activity in leukocytes and genotyping was used to confirm the diagnosis of Gaucher disease in all patients [29-31]. All patients had Dixon QCSI of the lumbar spine as part of a complete diagnostic work-up consisting of conventional T1- and T2-weighted TSE MRI sequences of the lumbar spine and femora.

Theoretical base of bone marrow burden score
In this study an alternative bone marrow burden (BMB) score is introduced, which is a combination of scoring systems of the peripheral skeleton already described and the axial bone marrow.

In the literature, the semi-quantitative scoring is based on two features consisting of signal intensity changes and sites of involvement in the peripheral skeleton [11,15,21,26,28]. In Gaucher disease, the MR characteristics of infiltrated bone marrow are predominantly low signal intensities both on T1-, T2-, and T2*-weighted sequences. Occasionally one may find an increase in signal intensity on T2-weighted sequences; this is thought to reflect active bone marrow disease, such as osteonecrosis or infarction [11,28]. Furthermore, it has been shown that Gaucher disease spreads in bone in a reproducible manner, starting in the meta-diaphysis and finally invading the epiphysis and apophysis [15,21]. The introduced bone marrow burden score (BMB) incorporates both the visual interpretation of the signal intensities and the geographic location of the disease on conventional MR images of the spine and femur. The chosen points given to the various parameters are arbitrary.

Lower extremities: (Table 1)

The marrow signal intensities on T1-weighted and T2-weighted images were graded compared to the signal intensity of subcutaneous fat, using a classification slightly modified from the one used in earlier studies [26,27].

TABLE 1. MR score of the femur (reference is subcutaneous fat)

A. Signal intensity	Score
T2 intensity hyperintense	2
T2 intensity slightly hyperintense	1
T2 intensity iso-intense	0
T2 intensity slightly hypo-intense	1
T2 intensity hypo-intense	2
T2 intensity of a mixed type	3
T1intensity (slightly) hyperintense or iso-intense	0
T1 intensity slightly hypo-intense	1
T1 intensity hypo-intense	2
B. Sites of involvement	Score
Diaphysis involved	1
Proximal epiphysis/apophysis involved	2
Distal epiphysis involved	3

The intensities were scored as hyperintense, slightly hyperintense, isointense, slightly hypo-intense and hypo-intense. Gaucher disease is expected to show hypo-intense signal intensity changes [9-11,21]. In severe cases, a mixed pattern of signal intensity is seen in the extremities with areas of high and low signal intensity especially on T2-weighted sequences. The low signal intensity is thought to be due to Gaucher cell infiltration whereas the high signal intensity is thought to reflect acute complications such as infarction or bone crisis [11,21]. The femurs were divided in 3 sites of involvement, proximal epiphysis/apophysis, (meta-)diaphysis and distal epiphysis. This is a modification of the sites of involvement score [15,21].

Lumbar spine: (Table 2)
The T1-weighted sequences were evaluated according to a non-pathological intervertebral disc as a reference for iso-intense signal intensity [13].

Table 2. MRI score of the lumbar spine (reference is intervertebral disc)

A. Signal intensity Score	score
T2 intensity hyperintense	2
T2 intensity slightly hyperintense	1
T2 intensity iso-intense	0
T2 intensity slightly hypo-intense	1
T2 intensity hypo-intense	2
T1 intensity (slightly) hyperintense	0
T1 intensity iso-intense	1
T1 intensity slightly hypo-intense	2
T1 intensity hypo-intense	3
B. Infiltration pattern	score
Patchy infiltration	1
Diffuse infiltration	2
Absence of fat in basivertebral vein region	1

The bone marrow signal intensity on T2-weighted sequences was evaluated with the presacral fat as a normal iso-intense reference.

Gaucher disease is expected to show low signal intensity on T1- and T2-weighted images [9-11,21]. In addition the infiltration pattern (patchy versus diffuse) of the disease within the vertebral bodies is graded. When MRI is used in the evaluation of hematological malignancies, a distinction is made in bone marrow infiltration patterns in the lumbar spine [13,28]. For instance, in multiple myeloma an association of the diffuse infiltration pattern with more advanced disease is hypothesized [10,12,32]. This pattern can also be recognized in Gaucher disease. The patchy infiltration pattern in Gaucher disease consists of localized areas of abnormal marrow (low signal intensity on T1- and T2-weighted images) on a background of normal bone marrow (high signal intensity and T1- and T2-weighted images). In the diffuse pattern, the bone marrow is completely replaced; on T1-weighted images bone marrow is hypo-intense or iso-intense to the intervertebral disc, and on T2-weighted images a variable decrease in signal intensity of the abnormal marrow is seen. The diffuse pattern is considered to reflect a more advanced stage of the disease. Furthermore, the absence of fat in the basivertebral vein region was noted in a binominal fashion (present/absent). Disappearance of the fat surrounding the basivertebral vein at the site where it enters the vertebral body dorsally has been described as the first sign of bone marrow invasion in malignancy [33]. Since disappearance of fat at this site had been observed in our Gaucher disease patient group, it was included as a parameter in the BMB.

BMB evaluation

Two musculoskeletal radiologists (JS,CK) who were experienced in the analysis of MR-scans, without being familiar with Gaucher disease, separately analyzed the conventional MR scans of both the femora and the lumbar spine retrospectively from hard copy. Both observers were blinded to patient characteristics and examination date. In this way the interobserver variability was tested. In order to analyze the intra-observer variability, one observer (JS) evaluated a small number of cases (N=10) twice, chosen at random, with an interval of 12 months. Both the lumbar spine and femora scores were added up leading to a total score, with a maximum of 16 (femora 8, lumbar spine 8). A higher score represented more severe bone marrow involvement (Tables 1 and 2).

To evaluate the value of the BMB as follow-up parameter one observer (JS) evaluated the MRI scans of the patients who were treated for 40 months or longer. These MRI examinations were mixed with the baseline MRI examinations, in order to make the observer unaware of the time point.
For our follow-up analysis we defined a good response to therapy as an increase of at least 3 times the precision of the measurement [34]. Since the precision of QCSI is measured as 3 points [22] we defined 2.8 x 3 points making 9 points of increase in fat-fraction a good response within 95% confidence limits [34]. The precision of BMB is discussed in the Results section. In order to analyze the separate contribution of the axial and peripheral bone marrow, we subdivided the BMB scores into the BMB lumbar spine (LS) and BMB femurs (F).

Dixon QCSI
Dixon QCSI a non-invasive, highly reproducible technique is based on the phase contrast technique described by Dixon, in which the MR signal of bone marrow is separated into the individual contributions of fat signal and water signal. In this manner, it is possible to determine fat-fractions [17,19,22,25,35]. Fat-fraction is given as a percentage of the total volume of bone marrow. As such the fat-fraction (F_f) theoretically ranges from 0 (no fat) to 1 (only fat). In a group of 16 healthy volunteers, the mean fat-fraction was measured to be 0.37 (SD 0.08) [22].

Statistics
Data were analyzed using SPSS 10-0 software (SPSS, Chicago, Illinois). Differences between groups were analyzed using the non-parametric Mann-Whitney test. A p-value of <0.05 was considered to represent significance. Correlation was calculated using the two-tailed non-parametric rank correlation (Spearman's ρ).

RESULTS

30 patients were analyzed (16 male, 14 female) with a mean age of 39.3 years (range 12-71). No patients were excluded or failed the examination. The mean fat-fraction F_f in this population was 0.20 (range 0.08-0.40). The bone marrow burden score (BMB) ranged from 3-14 points. The patient characteristics at baseline were listed in table 3.

Based on the outcome of the BMB score there was a significant correlation between the two observers with ρ= 0.91 (p<0.0001) (Figure 1). There was also a significant correlation between F_f and BMB with ρ = -0,78 (p <0.0001) (Figure 2). When the MR scans were analyzed by the same observer (JS) twice, a significant correlation was found (ρ = 0,99 (p <0.0001)).

For longitudinal follow-up the measurements of 12 patients with a follow-up interval of 40 months were analyzed for F_f and BMB (Table 4). The mean change in F_f was an increase of 0.17 (range +0.08 to +0.29).

TABLE 3. Patient characteristics

No.	sex	age (yr)	F_f	BMB	No.	sex	age (yr)	F_f	BMB
1	F	30	0.13	13	16	F	36	0.08	13
2	M	37	0.11	12	17	M	44	0.15	12
3	M	57	0.34	12	18	F	45	0.18	9
4	F	39	0.11	13	19	M	47	0.25	6
5	M	29	0.10	13	20	F	55	0.32	5
6	F	71	0.19	8	21	M	19	0.24	3
7	M	65	0.12	10	22	F	39	0.17	10
8	F	53	0.22	9	23	F	43	0.32	7
9	M	38	0.10	9	24	F	44	0.16	12
10	M	53	0.23	10	25	F	35	0.33	8
11	M	43	0.29	4	26	M	44	0.24	9
12	M	48	0.40	4	27	F	31	0.14	12
13	M	52	0.18	9	28	M	51	0.18	8
14	F	42	0.22	7	29	M	36	0.23	7
15	M	33	0.08	11	30	F	12	0.17	7

The mean change in BMB was a decrease of 3 points (range -9 to +2). According to our preset criteria 11 patients showed ≥ 9 points response to EST when F_f was considered, while 1 patient did not reach our threshold

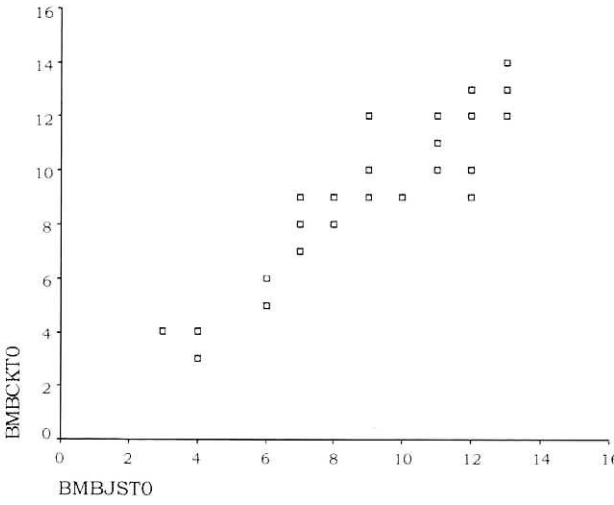

Figure 1. Correlation in BMB between two observers (ρ= 0.91 (p<0.0001)).

TABLE 4. Follow-up results in 12 patients

No.	F_f t=0	F_f t=4	BMB t=0	BMB t=4	BMB LS=0	BMB LS=4	BMB F=0	BMB F=4
1	0.11	0.28	13	10	6	3	7	7
2	0.34	0.47	12	8	4	1	8	7
3	0.11	0.38	12	7	5	0	7	7
4	0.10	0.19	13	13	6	6	7	7
5	0.22	0.41	9	4	5	1	4	3
6	0.10	0.18	9	11	4	4	5	7
7	0.23	0.42	10	1	5	1	5	0
8	0.29	0.45	4	1	1	1	3	0
9	0.18	0.47	8	1	5	1	3	0
10	0.08	0.28	11	10	6	7	5	3
11	0.18	0.35	9	10	5	6	4	4
12	0.22	0.48	7	5	4	4	3	1

t=0 prior to therapy, t=4 four years follow-up,
F_f= fat-fraction, LS = lumbar spine F= Femurs

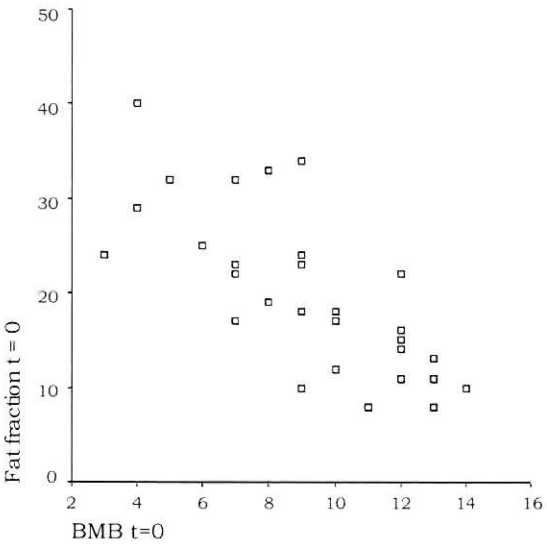

Figure 2. Relation fat-fraction and BMB in untreated patients (ρ = -0,78 (p<0.0001)).

of 9 points increase. Since the interobserver variation of BMB is low, the precision is approximately within 1 point. In this way 2.8 x 1 makes 3 points the required increase to detect response with 95% confidence. The only patient that did not reach our F_f criteria was a non-responder to treatment when the BMB was considered. Only 4 out of the 11 patients who satisfied the F_f criteria, did not satisfy our BMB criteria. In other words, there was similarity between F_f and BMB outcomes in 8 patients. When the response of the two BMB components was evaluated separately similar outcomes were obtained between the Lumbar Spine BMB and F_f in 7 patients and dissimilar outcomes in 5 patients. Further, there was agreement between the Femurs BMB and F_f in 4 patients and disagreement in 8 patients.

DISCUSSION

Dixon QCSI is thought to be the most desirable method to quantify bone marrow invasion in Gaucher disease [15,16,19-21]. However, this technique is not widely available. The need for a semi-quantitative scoring system making use of conventional, widely available MRI, in the determination of the amount of bone marrow involvement in Gaucher disease is obvious, as already indicated by several studies [11,21,26-28]. All previously described scoring systems have only been focused on the peripheral bone marrow. The most dynamic axial bone marrow, which is

thought to be the first site of invasion in Gaucher disease has not been included. This is in contrast to literature concerning hematological malignancies, in which analysis of bone marrow disease assesses axial bone marrow [8,12-14,23,24,32]. Furthermore, it is known that skeletal complications most frequently occur in the lower extremity [2,4,9,14,21,26]. These changes consisting of infarction, osteonecrosis or fractures, are almost always irreversible [28]. Therefore, a scoring system including these irreversible components would be relatively insensitive to subtle changes in bone marrow invasion as seen in Gaucher disease.

This is the first study that correlates Dixon QCSI as a bone marrow disease parameter to a semi-quantitative scoring system based on both the change in signal intensity and the sites of involvement in axial and peripheral bone marrow. The introduced bone marrow burden score shows a very good correlation with Dixon QCSI in untreated patients and is feasible with a good interobserver and intra-observer variability when used by radiologists trained in MRI analysis without having experience in Gaucher disease.

A good parameter of bone marrow invasion should also be able to detect response to treatment. This has been described as an important quality of Dixon QCSI [19,20]. Dixon QCSI shows response to therapy after 12 months [36]. In our group consisting of 12 patients response to treatment is detected by Dixon QCSI in 11 patients (92%). Our results show that BMB can also detects response in 9 patients (75%). In other words, it seems that BMB is less sensitive than Dixon QCSI. Using our preset criteria there was agreement between F_f and BMB in 8 of 12 patients. However, the studied population was small.

The scoring systems of the peripheral skeleton previously described by Terk et al. and Poll et al. also detect response to therapy [27,28]. The response rate in these studies is 67% [27] and 63% [28] respectively. The response in both of these studies was scored in a binominal fashion (responder versus non-responder). When we analyze our data in this manner we find 7 responders in the BMB Femurs group (58%) and 9 responders in the BMB overall group (75%). In our population we find more responders when a combination of visual scoring BMB of Lumbar Spine and Femurs is used. The non-responders of femur BMB in our population had irreversible changes like marrow infarction or avascular necrosis in the lower extremity. However, some of them show response in

the axial bone marrow. Therefore, one must consider that when no response is seen in the peripheral bone marrow, response may very well be present in the axial marrow. The drawback of this study is the limited number of patients in every group.

We conclude that the introduced bone marrow burden Score has a good correlation with the fat-fraction measured by Dixon QCSI. The good inter- and intra-observer correlation make it reliable and easy to use by radiologists experienced in MRI, without specific knowledge of Gaucher disease. It also seems to be able to detect response to enzyme replacement therapy, although it is less sensitive than Dixon QCSI. Further research should be performed to definitely determine the strength of BMB as a follow-up bone marrow response parameter in Gaucher disease.

ACKNOWLEDGEMENTS

The authors wish to thank Rezan Demir, MD,PhD and Mirjam R.W. Evers-van Bavel for their aid in the preparation of this manuscript.

REFERENCES

1. Lee, RE. The pathology of Gaucher disease. In: Gaucher disease: a century of deliniation and research. (eds. Desnick RJ, Gatt S, Grabowski GA). Alan R. Liss, New York 1982; 177-217.
2. Beutler, E, Grabowski, G. Gaucher disease. In: The metabolic basis of inherited disease. (eds. Scriver CR, Sly WS, Valle D). McGraw-Hill Publishing Company, New York 1995; 2641-2670.
3. Charrow J, Esplin JA, Gribble TJ, et al. Gaucher disease: recommendations on diagnosis, evaluation, and monitoring. Arch Intern Med 1998; 158:1754-60.
4. Stowens DW, Teitelbaum SL, Kahn AJ, Barranger JA. Skeletal complications of Gaucher disease. Medicine 1985; 64:310-322.
5. Barton NW, Brady RO, Dambrosia JM, et al. Dose dependent responses to macrophage-targeted glucocerebrosidase in a child with Gaucher disease. J Ped 1992; 120:277-280.
6. Hollak CE, Aerts JM, Goudsmit R, et al. Individualised low-dose alglucerase therapy for type 1 Gaucher's disease. Lancet 1995; 345:1474-1478.
7. Baker J, Niklason LT, Hill SC, and collaborators. Enzyme replacement therapy for Gaucher disease: skeletal responses to macrophage-targeted glucocerebrosidase. Pediatrics 1995; 96(4):629-637.

8. Vogler III JB, Murphy WA. Bone marrow imaging. Radiology 1988; 168:679-693.
9. Cremin BJ, Davey H, Goldblatt J. Skeletal complications of Type 1 Gaucher disease: The magnetic resonance Features. Clin Radiol 1990; 41:244-247.
10. Rosenthal DI, Scott JA, Barranger J, Mankin HJ, Saini S, Brady TJ, Osier LK, Doppelt S. Evaluation of Gaucher disease using magnetic resonance imaging. J Bone Joint Surg 1986; 68A(6).
11. Hermann G, Shapiro RS, Abdelwahab IF, Grabowski G. MR imaging in adults with Gaucher disease type I: evaluation of marrow involvement and disease activity. Skeletal Radiol 1993; 22:247-251.
12. Lecouvet FE, Vande Berg BC, Michaux L, Malghem J, Maldague BE, Jamart J, Ferrant A, Michaux JL. Stage III multiple myeloma: clinical and prognostic value of spinal bone marrow MR imaging. Radiology 1998; 209:653-660.
13. Moulopoulos LA, Dimopoulos MA. Magnetic resonance imaging of the bone marrow in hematologic malignancies. Blood 1997; 90(6):2127-2147.
14. Steiner RM, Mitchell DG, Rao VM, Schweitzer ME. Magnetic resonance imaging of diffuse bone marrow disease. Rad Clinic North America 1993; 31(2):383-409.
15. Rosenthal DI, Barton NW, McKusick KA, et al. Quantitative imaging of Gaucher disease. Radiology 1992; 185:841-845.
16. Johnson LA, Hoppel BE, Gerard EL, et al. Quantitative chemical shift imaging of vertebral bone marrow in patients with Gaucher disease. Radiology 1992; 182:451-455.
17. Dixon WT. Simple proton spectroscopic imaging. Radiology 1984; 153:189-194.
18. Miller SPF, Zirzow GC, Doppelt SH, Brady RO, Barton NW. Analysis of the lipids of normal and Gaucher bone marrow. J Lab Clin Med 1996; 127:353-358.
19. Maas M, Akkerman EM, Hollak CEM, Rademakers RP. Evaluation of skeletal involvement in M. Gaucher: Use of quantitative chemical shift imaging (QCSI). European Radiology 1997; 7(Suppl):206.
20. Rosenthal DI, Doppelt SH, Mankin HJ, et al. Enzyme replacement therapy for Gaucher disease: skeletal responses to macrophage-targeted glucocerebrosidase. Pediatrics 1995; 96:629-637.
21. O'Keeffe D, Rosenthal DI. Computed tomography and magnetic resonance imaging in Gaucher's disease. In: MRI and CT of the musculoskeletal system: a text-atlas (eds. Bloem JL, Sartoris DJ). Baltimore, William & Wilkins 1992; 130-138.

22. Maas M, Akkerman EM, Venema HW, Stoker J, Den Heeten GJ. Dixon quantitative chemical shift mri for bone marrow evaluation in the lumbar spine: a reproducibility study in healthy volunteers. J Comput Assist Tomogr 2001; 25:691-697.
23. Rosen BR, Fleming DM, Kushner DC, Zaner KS, Buxton RB, Bennet WP, Wismer GL, Brady TJ. Hematologic Bone marrow disorders: Quantitative chemical shift MR imaging. Radiology 1988; 169:799-804.
24. Gerard EL, Ferry JA, Amrein PC, Harmon DC, McKinstry RC, Hoppel BE, Rosen BR. Compositional changes in vertebral bone marrow during treatment for acute leukemia: assessment with quantitative chemical shift imaging. Radiology 1992; 183:39-46.
25. Gückel F, Brix G, Semmler W, Ho AD, Körbling, George M, van Kaick G. Proton chemical shift imaging of bone marrow for monitoring therapy in leukemia. JCAT 1990; 14(6):945-959.
26. Terk MR, Esplin J, Lee K, Magre G, Colletti PM. MR imaging of patients with Type 1 Gaucher's disease: Relationship between bone and visceral changes. AJR 1995; 165:599-604.
27. Terk MR, Dardashti S, Liebman HA. Bone marrow response in treated patients with Gaucher disease: evaluation by T1-weighted magnetic resonance images and correlation with reduction in liver and spleen volume. Skeletal Radiol 2000; 29:563-571.
28. Poll LW, Koch J-A, vom Dahl S, et al. Magnetic resonance imaging of bone marrow changes in Gaucher disease during enzyme replacement therapy: first German long-term results. Skeletal Radiol 2001; 30:496-503.
29. Sibille A, Eng CM, Kim S-J, Pastores G, Grabowski GA. Phenotype/genotype correlations in Gaucher disease Type 1: Clinical and therapeutic implications. Am J Hum Genet 1993; 52:1094-1101.
30. Sidransky E, Ginns EI. Phenotypic and genotypic heterogeneity in Gaucher disease: Implications for genetic counseling. J Genet Counsel 1994; 3:13-22.
31. Boot RG, Hollak CEM, Verhoek M, et al. Glucocerebrosidase genotype of Gaucher patients in the Netherlands: Limitations in prognostic value. Hum Mutat 1997; 10:348-358.
32. Moulopoulos LA, Varma DGK, Dimopoulos MA, Leeds NE, Kim EE, Johnston DA, Alexian R, Libshitz HI. Multiple myeloma: spinal MR imaging in patients with untreated newly diagnosed disease. Radiology 1992; 185:833-840.
33. Algra PR, Bloem JL, Valk J. Disappearance of the basivertebral vein; a new MR imaging sign of bone marrow disease. AJR 1991; 157:1129-1130.
34. Cummings SR, Black DB. Should perimenopausal women be screened for osteoporosis? Annals of Internal Medicine 1986; 104:817-823.

35. Akkerman EM, Maas M. A region-growing algorithm to simultaneously remove dephasing influences and separate fat and water in two-point Dixon imaging. Proceedings of the Society of Magnetic Resonance and the European Society for Magnetic resonance in Medicine and Biology 1995: 649.
36. Hollak C, Maas M, Akkerman EM, den Heeten A, Aerts H. Dixon Quantitative Chemical shift Imaging is a sensitive tool for the evaluation of bone marrow responses to individualized doses of enzyme supplementation therapy in type 1 Gaucher disesase. Blood Cells Mol Dis 2001; 27(6):1005-1012.

CHAPTER 9

Summary, general discussion and future research

SUMMARY

In this thesis the experiences of a University Hospital, a national referral center for Gaucher disease, in analyzing bone marrow involvement in Gaucher disease are described. After it became clear that the organomegaly and cytopenia improved upon treatment with enzyme supplementation therapy (EST), bone disease became the most important clinical issue to address. Bone disease in Gaucher disease involves two, different structures: bone structure, that is distorted and bone marrow, that is infiltrated. It is thought that the progressive infiltration of bone marrow with Gaucher macrophages eventually leads to structural bone changes. These changes may develop into areas of infarction or avascular necrosis and in the end stage into arthroplasty. For patient management this difference is important, since these structural bone changes will show a different response rate to therapy when compared to bone marrow infiltration. The apparent slow response of the osseous involvement in Gaucher disease, when measuring structural bone changes, is most likely not a good indicator for assessing bone marrow response on EST. A technique that directly evaluates the changes in bone marrow can be expected to provide more valuable information on response to therapy. Dixon quantitative chemical shift imaging (Dixon QCSI) has been described as a quantitative imaging technique of bone marrow [1-3]. This technique can be used to measure the degree of Gaucher cell infiltration in the bone marrow by detecting decrease in fat (triglyceride) fraction. The strength, limitations, value and alternatives of this DQCSI technique in Gaucher disease were explored in this thesis.

The first three chapters concern the present approaches towards imaging of skeletal disease in untreated patients with Gaucher disease, with a special focus on Dixon QCSI. Dixon QCSI is a non-standard sequence on MRI-scanners and initial research at our institution concerned implementation of the technique with evaluation of reproducibility.

In **Chapter 2** we describe a study in which the reproducibility of the Dixon QCSI technique was explored in measuring fat-fraction (F_f) in the lumbar spine (vertebrae L3, L4, and L5) in 16 adult healthy volunteers. We measured F_f in the same volunteer on different days. Furthermore, we evaluated the influence on the reproducibility of two operator-dependent

aspects, namely (re-)positioning of the measurement slice and determination of the contours from which the regions of interest (ROIs) were calculated.
The mean F_f was 0.37 (SD 0.08). The SD due to repeated measurement on different days was small, and mainly explained by slice (re-)positioning. No significant difference was found in F_f between the different levels (L3-L5). Also no differences were found in contour drawing between two operators. We concluded that the Dixon QCSI technique is a powerful non-invasive tool in evaluating bone marrow composition; when used to evaluate the same person longitudinally it had an excellent reproducibility. We therefore recommended its use in protocols concerning axial (red) bone marrow involvement or marrow characterization.

In **Chapter 3** an overview is given on the various radiological modalities that are available for imaging and quantifying skeletal involvement in Europe and the United States of America. This chapter is a reflection of a round table discussion that took place in Trieste (Italy) in April 2001. In this expert meeting a number of presentations were given concerning the various modalities that were used at various sites in the world concerning skeletal involvement in patients with Gaucher disease. There was a remarkable variation due to practical considerations such as availability and cost. However, concerning applicability it was concluded that magnetic resonance imaging (MRI) is the imaging technique of choice to evaluate bone marrow invasion as well as skeletal complications. Plain radiographs and computed tomography (CT) cannot play a significant role and therefore should not be used to assess bone marrow invasion. However, at which site of involvement the MRI should focus on remains a debate. Both the American group of Terk as well as the German group of Poll focuses on the peripheral bone marrow [4-6]. This is in contrast with the literature from the group from Boston [1-3,7-9] who focuses on the axial bone marrow being the site of involved in all known cases. The Dutch working group on Gaucher disease followed this concept, supported by the literature data on hematological malignancies that describes spread of disease through a centrifugal path of distribution [10]. The axial bone marrow is in this concept the first site of involvement. The main disadvantage of conventional MRI is the fact that it is not

quantitative. It was concluded that Dixon QCSI might be the most sensitive technique to quantify bone marrow invasion, yet an important drawback is the limited availability.

In **Chapter 4** an attempt is made to correlate the fat-fraction F_f as measured by Dixon QCSI to clinical relevant endpoints for bone disease, being the presence of chronic bone pain, bone crisis, avascular necrosis, pathological fractures and the need for surgical intervention such as joint replacement. We evaluated the F_f in 30 untreated adult patients with Gaucher disease and related this to the F_f of healthy volunteers. Furthermore, we studied the relation of F_f with presence, absence and severity of the previously mentioned bone disease parameters. The F_f in Gaucher disease patients ranged from 0.08-0.40 and was significantly lower than in the healthy population (0.27-0.55, $p<0.001$). Bone complications primarily occurred in patients with an $F_f<0.23$ and univariate logistic regression analysis indicated that for every decrease of F_f of 0.1 the risk of bone complications increased with 85%. It was concluded that the F_f of the lumbar spine measured with Dixon QCSI is associated with the occurrence of bone complications and may therefore be a clinical useful parameter. However, only a longitudinal study in patients under therapy can prove its value in clinical decision-making and outcome. Patients with Gaucher disease should be monitored for skeletal involvement on a regular basis and Dixon QCSI seems appropriate for this purpose.

The next two chapters focus on the role of imaging in evaluation of the response of bone and bone marrow disease in patients with Gaucher disease with a special attention to Dixon QCSI.
In **Chapter 5** the results of Dixon QCSI as response parameter to individualized doses of enzyme supplementation therapy (EST) in Gaucher disease are described. In 12 adult Gaucher disease patients and in 9 untreated Gaucher controls, fat-fractions (F_f) were measured prior to and during EST. During treatment F_f increased significantly already after 1 year in 11/12 patients. After 4-5 years F_f normalized in 11/12 patients, but remained low in the untreated Gaucher controls. When the fat-fractions of healthy volunteers are taken into account (**Chapter 2**), one may conclude that Dixon QCSI is a sensitive tool for measuring bone

marrow response to EST already after one year. It seems the modality of choice for the assessment of bone marrow response to EST and therefore should be included in annual follow-up of treated patients with Gaucher disease.

Chapter 6 is a reflection of a second round table discussion session held in Trieste in April 2001 on the response of Gaucher bone disease to enzyme therapy. From various centers in Europe as well as the USA data were discussed concerning the regional protocols for evaluating bone and bone marrow disease and its response to enzyme therapy. There was a wide variety of imaging protocols, with no similar protocol in any of the centers. Participants concluded that quantification is the method of choice for evaluation of the response on EST, and that every group of clinicians treating Gaucher patients has its own quantitative method of choice. Some will focus on peripheral bone marrow, others - like the Dutch working group on Gaucher disease - focus on axial bone marrow. It is thought that response of bone marrow compartment may occur as soon as the response of the visceral compartment.

Dixon QCSI is a powerful technique detecting response of bone marrow to enzyme supplementation therapy (EST) as early as after one year. However, the technique is not widely available. Therefore efforts were made to study more widespread available alternatives for Dixon QCSI, evaluating axial bone marrow. **Chapters 7 and 8** focus on potential alternatives for Dixon QCSI. In **Chapter 7** the Vertebra-Disc Ratio (VDR) is described as alternative to Dixon QCSI. The ratio of the gray value on T1-weighted images of the vertebral corpus L3 and the healthy intervertebral disc L3-L4 was determined in controls as well as treated and untreated Gaucher disease patients. The normal VDR was 1.9 ± 0.3 and differed significantly from both untreated and long treated Gaucher disease patients. The VDR is concluded a useful parameter with a good correlation with the fat-fraction. In **Chapter 8** another alternative is explored. The Bone Marrow Burden score (BMB) is the first semi-quantitative scoring system in which both the axial and peripheral bone marrow is included. In 30 Gaucher disease patients the BMB was scored by two radiologists unfamiliar to Gaucher disease. A good and significant correlation was found between the two observers, a very good intra observer variation was shown and a good and significant correlation

with Dixon QCSI was found. The detection of response to EST was present, yet less than with Dixon QCSI. Of the two components, axial lumbar spine bone marrow showed more response than peripheral femur bone marrow. BMB was concluded to be a good reproducible easy to use scoring system that can serve as alternative for Dixon QCSI, when not available.

GENERAL DISCUSSION AND FUTURE RESEARCH

The studies included in this thesis demonstrate the feasibility and clinical relevance of quantitative MR imaging with use of the Dixon QCSI technique in Gaucher patients. It showed to be a very sensitive reproducible technique that is related to clinical important features as bone complications and it detects response to therapy already after one year of treatment. In our clinical management of patients it plays an important role.

This thesis also enlightened on a limitation of the technique, namely the unavailability worldwide. Another drawback of the technique is the manual handling of the data sets. The program to acquire fat-fraction numbers from the acquired data needs a physicist's intervention. It would be beneficial when this process can be computerized in the near future.

At our institution two possible alternatives to analyze bone marrow involvement in Gaucher disease were studied; VDR and BMB. Both techniques are easy to use as standard MRI hardware and software suffices. Both techniques have been correlated with Dixon QCSI, and have been shown to detect response to EST. So which one is the best to choose? This question, though very legitimate cannot be answered by our results, since our follow-up data numbers are small. So, only a hypothetical discussion is possible. An advantage of the VDR might be the fact that a pure quantitative measurement is produced, avoiding interpretation bias produced by observers. Furthermore, this technique can be carried out on every commercially available MR machine, without the aid of a physicist. However, the inclusion of the intervertebral disc as part of a bone marrow scoring system introduces a variable that is under the influence of external factors, like age or diurnal variation [11-13]. When focusing on BMB, a strong feature of BMB might be the inclusion of both axial and peripheral bone marrow. Although our BMB results show better response detection in the lumbar spine component of BMB, in a

small number of patients a better response is detected in the peripheral femoral bone marrow. Furthermore, the fact that areas known to be at risk for developing avascular necrosis, i.e. femoral epiphysis, are included in an annual evaluation of the individual Gaucher disease patient will reassure treating clinicians. To compare the alternatives more data are necessary. For this purpose the bone marrow data throughout the world, acquired by MRI, might be assessed at a central research center. Digital MRI datasets, when stored, can be assessed for both VDR and BMB. Patients from various sites could be enrolled in a single database, from which better statistical analysis can be performed.
Another alternative for coping with the limited availability of Dixon QCSI would be to increase the availability of Dixon QCSI. Theoretically it would be possible for the pharmaceutical companies to provide the service of having a small group of physicists experienced with Dixon QCSI available for implementation and training purposes. In this way in every country a center where patients with Gaucher disease may have their annual fat-fraction measurement taken is present.

The group that is difficult to analyze with Dixon QCSI is the group of children and adolescents with Gaucher disease. In this group the amount of cellular marrow present in the axial marrow varies with age, making the measurement of fat-fractions difficult to interpret; red cellular marrow will show a low fat-fraction, which cannot be differentiated from Gaucher cell infiltration. It would be of great value to enroll children and adolescents without bone marrow disorders in a Dixon QCSI database. In this way age-matched controls are present and the evaluation of the fat-fraction obtained in young Gaucher patients (children and adolescents) could be improved. However, the practical arrangements for such a database acquisition are cumbersome.

By evaluating three lumbar spine levels with non-invasive Dixon QCSI, a large amount of axial bone marrow is analyzed. The chance of occurrence of sampling errors is minimized. Therefore, this technique is potentially powerful in the exploration and characterization of various bone marrow disorders and their response to therapy. In collaboration with the department of hematology we are planning to evaluate patients undergoing bone marrow transplants in this manner. It might be possible

to detect early response to transplantation in a non-invasive manner prior to the changes that can be found in the peripheral blood and provide us with prognostic parameters, without bone marrow sampling error [14-21]. The non-invasive capability of bone marrow characterization is a very important feature of Dixon QCSI. Especially, the use of this technique in a pediatric population of patients with bone marrow disorders is tempting. To be able to characterize bone marrow alterations due to various diseases and its response to therapy in a non-invasive manner would be of great benefit to the pediatric patient. Since in evaluating the response to therapy, the patient is its own control, the need for a data base of healthy volunteers in various age groups would not be obligatory, however desirable.

Although the value of Dixon QCSI is explored in detail in an adult population with Gaucher disease, as presented in this thesis, the possibilities for further research are present and stimulating. The exploration will continue.

REFERENCES

1. Gerard EL, Ferry JA, Amrein PC, et al. Compositional changes in vertebral bone marrow during treatment for acute leukemia: assessment with quantitative chemical shift imaging. Radiology 1992; 183:39-46.
2. Johnson LA, Hoppel BE, Gerard EL, et al. Quantitative chemical shift imaging of vertebral bone marrow in patients with Gaucher disease. Radiology 1992; 182:451-455.
3. Rosenthal DI, Barton NW, McKusick KA, et al. Quantitative imaging of Gaucher disease. Radiology 1992; 185:841-845.
4. Poll LW, Koch J-A, vom Dahl S, et al. Magnetic resonance imaging of bone marrow changes in Gaucher disease during enzyme replacement therapy: first German long-term results. Skeletal Radiol 2001; 30:496-503.
5. Terk MR, Dardashti S, Liebman HA. Bone marrow response in treated patients with Gaucher disease: evaluation by T1-weighted magnetic resonance images and correlation with reduction in liver and spleen volume. Skeletal Radiol 2000; 29:563-571.
6. Terk MR, Esplin J, Lee K, Magre G, Colletti PM. MR imaging of patients with type 1 Gaucher's disease: relationship between bone and visceral changes. AJR 1995; 165:599-604.
7. Rosenthal DI, Doppelt SH, Mankin HJ, et al. Enzyme replacement therapy for Gaucher disease: skeletal responses to macrophage-targeted glucocerebrosidase. Pediatrics 1995; 96:629-637.

8. Rosenthal DI, Scott JA, Barranger J, et al. Evaluation of Gaucher disease using magnetic resonance imaging. J Bone Joint Surg Am 1986;68:802-808.
9. Rosenthal DI, Mayo-Smith W, Goodsitt MM, Doppelt S, Mankin HJ. Bone and bone marrow changes in Gaucher disease: evaluation with quantitative CT. Radiology 1989; 170:143-6.
10. Moulopoulos LA, Dimopoulos MA. Magnetic resonance imaging of the bone marrow in hematologic malignancies. Blood 1997; 90:2127-2147.
11. Sether LA, Yu S, Haughton VM, Fischer ME. Intervertebral disk: normal age-related changes in MR signal intensity. Radiology 1990; 177(2):385-388.
12. Kingma I, van Dieën JH, Nicolay K et al. Monitoring water content in deforming intervertebral disc tissue by finite element analysis of MRI data. Magn Reson Med 2000; 44(4):650-654.
13. Malko JA, Hutton WC, Fajman WA. An in vivo magnetic resonance imaging study of changes in the volume (and fluid content) of the lumbar intervertebral discs during a simulated diurnal load cycle. Spine 1999; 24(10):1015-1022.
14. Smith SR, Williams CE, Davies JM, Edwards RHT. Bone marrow disorders: characterization with quantitative MR imaging. Radiology 1989; 172:805-810.
15. Gückel F, Brix G, Semmler W, et al. Systemic bone marrow disorders: characterisation with proton chemical shift imaging. J Comput Assist Tomogr 1990; 14:633-642.
16. Gückel F, Brix G, Semmler W, et al. Proton chemical shift imaging of bone marrow for monitoring therapy in leukemia. J Comput Assist Tomogr 1990; 14:945-959.
17. Kauczor HU, Brix G, Dietl B, Jarosch K, Knopp MV, van Kaick G. Bone marrow after autologous blood stem cell transplantation and total body irradiation: magnetic resonance and chemical shift imaging. Magn Reson Imaging 1993; 11:965-975.
18. Kauczor HU, Dietl B, Brix G, Jarosch K, Knopp MV, van Kaick G. Fatty replacement of bone marrow after radiation therapy for Hodgkin disease: unantification with chemical shift imaging. JMRI 1993; 3:575-580.
19. Lecouvet FE, Vande Berg BC, Michaux L, et al. Stage III multiple myeloma: clinical and prognostic value of spinal bone marrow MR imaging. Radiology 1998; 209:653-660.
20. Schick F, Einsele H, Weiss B, et al. Assessment of the composition of bone marrow prior to and following autologous BMT and PBSCT by magnetic resonance. Ann Hematol 1996; 72(6):361-370.
21. Schick F, Einsele H, Kost R, et al. Hematopoietic reconstitution after bone marrow transplantation: assessment with MR imaging and H-1 localized spectroscopy. J Magn Reson Imaging 1994; 4(1):71-78.

CHAPTER 10

Samenvatting

SAMENVATTING

In dit proefschrift worden de resultaten beschreven van het wetenschappelijk onderzoek met betrekking tot de beenmerg invasie bij de ziekte van Gaucher. Het beschreven onderzoek werd voornamelijk verricht in het Academisch Medisch Centrum (AMC) te Amsterdam, dat fungeert als een nationaal referentie centrum voor de ziekte van Gaucher.
Nadat duidelijk werd dat onder enzym-therapie (EST) verbetering optrad van de organomegalie en de cytopenie, werd de aandacht gericht op het skelet. De betrokkenheid van het skelet bij de ziekte van Gaucher behelst twee verschillende structuren, te weten bot en beenmerg. Aangenomen wordt dat er door progressieve infiltratie van het beenmerg met Gaucher-macrofagen uiteindelijk structurele afwijkingen van het skelet kunnen optreden. Gevolgen kunnen zijn het optreden van botinfarcten en avasculaire necrose uiteindelijk leidend tot het plaatsen van een gewrichtsprothese. Dit onderscheid tussen bot en beenmerg is van klinisch belang omdat beide structuren op een verschillende wijze zullen responderen op EST. De geobserveerde en beschreven trage respons van het skelet op EST wordt waarschijnlijk veroorzaakt door het feit dat de structurele botveranderingen zijn gekozen om respons op therapie te evalueren. Het valt echter niet te verwachten dat deze structurele veranderingen (snel) zullen en kunnen responderen.
Dixon quantitative chemical shift imaging (Dixon QCSI) is eerder beschreven als een kwantitatieve beeldvormende techniek ter evaluatie van het beenmerg [1-3]. Middels deze techniek kan de hoeveelheid vet in het beenmerg worden vastgesteld, door bepaling van de vetfractie. Evenzo kan de mate van invasie van het beenmerg met Gaucher-cellen gedetecteerd worden, omdat de vetfractie (triglyceridefractie) verlaagd is ten gevolge van de invasie. In dit proefschrift worden de ervaringen met betrekking tot de analyse van de kracht, grenzen en beperkingen van deze Dixon QCSI techniek in patiënten met Gaucher besproken. Verder worden alternatieven geëxploreerd.

In de eerste drie hoofdstukken worden de huidige technieken beschreven met betrekking tot het in kaart brengen van aantasting van het skelet bij de ziekte van Gaucher in onbehandelde patiënten. Speciale aandacht is er voor Dixon QCSI. Deze Dixon techniek is niet standaard aanwezig op MRI apparaten. Vandaar dat het eerste onderzoek zich richt op de implementatie van deze techniek.

In **hoofdstuk 2** wordt de studie beschreven waarin de reproduceerbaarheid van de Dixon QCSI techniek, waarmee de vetfractie (F_f) wordt bepaald, is geëvalueerd. In 16 gezonde volwassen proefpersonen werd de F_f in de lumbale wervelkolom (wervels L3-L5) gemeten. In dezelfde vrijwilligers werd de F_f op verschillende dagen gemeten (herhaalde meting). Daarnaast werd de invloed van verschillende *bediener-afhankelijke* variabelen onderzocht, met name het (re-)positioneren van het meetvlak en het vaststellen van de regions-of-interest (ROI's) waarin de F_f wordt berekend onderzocht. De gemiddelde F_f was 0.37 (SD 0.08). De invloed van deze parameters op de bepaling van de F_f bleek zeer gering. Er werd geen significant verschil gevonden in de F_f op verscheidene niveaus (L3-5), noch was er een significant verschil tussen twee onderzoekers in het tekenen van de contour van de ROI. Geconcludeerd werd dat Dixon QCSI een krachtige modaliteit is om op een niet invasieve, zeer reproduceerbare wijze het vetgehalte in het axiale beenmerg te kwantificeren. Wanneer dezelfde persoon in verloop van de tijd wordt gemeten, heeft de methode een zeer goede reproduceerbaarheid. Daarom wordt aanbevolen deze methode te incorporeren in protocollen met betrekking tot de evaluatie van het rode (axiale) beenmerg.

In **hoofdstuk 3** wordt een overzicht gegeven van de verschillende radiologische modaliteiten die beschikbaar zijn om de aantasting van het skelet door de ziekte van Gaucher te evalueren. Dit hoofdstuk is een weergave van een internationale ronde tafel discussie die plaats vond in Trieste (Italië) in april 2001. Hieraan werd deelgenomen door zowel Europese als Amerikaanse Gaucher onderzoekers. In de vorm van verschillende presentaties werd een overzicht verkregen van de verscheidenheid aan radiologische modaliteiten die worden gebruikt.

Hierin bleek sprake van een opmerkelijke variatie die verklaard kon worden door praktische overwegingen als beschikbaarheid en kosten. Geconcludeerd werd dat MRI de radiologische modaliteit van keuze is om zowel beenmerg invasie als aanwezigheid en uitgebreidheid van complicaties te detecteren. Zowel conventionele radiologie als CT scanning dienen hiervoor niet gebruikt te worden.
Het blijft een discussiepunt welke plek in het beenmerg middels MRI dient te worden geëvalueerd, axiaal (centraal) of perifeer. Zowel de Amerikaanse groep van Terk als de Duitse groep van Poll richtten zich op het perifere beenmerg [4-6]. Dit in schril contrast tot de literatuur van de groep uit Boston [1,3, 7-9], waarin het axiale beenmerg is gekozen. Hiervoor werd gekozen omdat het axiale beenmerg bij elke patiënt met Gaucher cellen in de Boston populatie was geïnfiltreerd. De Nederlandse onderzoeksgroep (Gaucher Instituut Nederland, GIN) evalueert vanaf het begin het axiale beenmerg conform de groep uit Boston, tevens gesteund door literatuur gegevens betreffende hematologische maligniteit. In deze literatuur wordt een centrifugale distributie beschreven, waarbij het axiale beenmerg eerder is aangedaan dan het perifere beenmerg [10]. Echter, het feit dat conventionele MRI niet kwantitatief is, werd als belangrijk nadeel beschouwd. Geconcludeerd werd dat Dixon QCSI waarschijnlijk de meest sensitieve techniek is om beenmerg invasie te kwantificeren. Echter de beperkte beschikbaarheid van deze techniek wordt beschouwd als een belangrijk nadeel.

In **hoofdstuk 4** wordt de relatie tussen de vetfractie F_f en klinisch relevante criteria voor skelet invasie, te weten het voorkomen van chronische botpijn, bot crises, avasculaire necrosis, pathologische fracturen en uiteindelijk de noodzaak tot het plaatsen van een gewrichtsprothese, beschreven. In 30 onbehandelde patiënten met de ziekte van Gaucher werd de F_f bepaald. Dit werd gerelateerd aan de F_f van gezonde vrijwilligers (uit **hoofdstuk 2**). Voorts werd de relatie tussen de aan- en afwezigheid van botcomplicaties en de F_f onderzocht. Bij patiënten met de ziekte van Gaucher bedroeg de vetfractie waarden tussen 0.08-0.40, een significant lager getal dan de vetfractie in de gezonde populatie (0.27-0.55, $p<0.001$). Bot complicaties traden op bij patiënten met een $F_f < 0.23$. Middels het verrichten van een univariate logistische regressie analyse werd berekend dat voor elke afname in F_f van

0.1 het risico van het ontwikkelen van botcomplicaties toeneemt met 85%. Geconcludeerd werd dat er een duidelijke relatie was tussen de hoogte van de F_f berekend met Dixon QCSI en de ontwikkeling van botcomplicaties; de F_f kan beschouwd worden als klinisch bruikbare en belangrijke parameter. De waarde van F_f met betrekking tot het klinisch beleid kan alleen middels een longitudinale studie worden bevestigd. Patiënten met de ziekte van Gaucher dienen regelmatig onderzocht te worden met betrekking tot beenmerg uitbreiding en Dixon QCSI is hiervoor een goede modaliteit.

De volgende twee hoofdstukken behandelen de monitoring van bot en beenmerg respons volgend op therapie. Speciale aandacht wordt besteed aan de waarde van Dixon QCSI. In **hoofdstuk 5** worden de resultaten beschreven van een studie waarin de waarde van Dixon QCSI als respons parameter voor de geïndividualiseerde enzym-therapie (EST). In 12 patiënten werd tijdens therapie de F_f bepaald. Negen patiënten zonder therapie fungeerden als controlegroep. Tijdens therapie was er een significante toename van F_f binnen één jaar in 11 van de 12 patiënten. Na 4-5 jaar was er normalisatie van de vetfractie in 11 van de 12 patiënten. Dit in tegenstelling tot de onbehandelde controle groep, waarin de vetfractie laag bleef. Geconcludeerd werd dat er al beenmerg respons te detecteren valt binnen één jaar, wanneer gebruik wordt gemaakt van Dixon QCSI. Dit lijkt daarmee de modaliteit van keuze om het beenmerg te evalueren tijdens EST. In onze optiek dient deze Dixon QCSI techniek deel uit te maken van de periodieke (jaarlijkse) follow-up van patiënten met de ziekte van Gaucher.
Het verslag van een tweede ronde tafel conferentie, in Trieste (Italië) april 2001, betreffende respons van het skelet op EST is weergegeven in **hoofdstuk 6**. Verscheidene centra in Europa en USA presenteerden hun data aangaande regionale radiologische protocollen en bijbehorende resultaten met betrekking tot respons van het skelet (bot en beenmerg) bij behandelde patiënten met de ziekte van Gaucher. Er bestond een grote variatie in radiologische protocollen. Hoewel geen enkel protocol overeenstemde, kon er wel een consensus worden bereikt over de ideale situatie. Een vorm van (semi-) kwantificatie is noodzakelijk om response op therapie te detecteren.

Verschillende groepen analyseren andere delen van het beenmerg. Sommigen analyseren het perifere beenmerg, anderen, zoals de GIN, richten zich op het axiale beenmerg. Aangenomen wordt dat het beenmerg compartiment net zo snel kan responderen op EST als het viscerale compartiment. Wel dient gebruik gemaakt te worden van een sensitieve modaliteit ten einde deze respons te detecteren.

Dixon QCSI is een sensitieve techniek die beenmerg respons op EST al binnen een jaar detecteert. Echter, deze techniek is niet standaard op MR scanners aanwezig en is daarom niet overal te gebruiken. Vanwege deze beperking is er veel aandacht gegeven aan de ontwikkeling van alternatieven, welke wereldwijd makkelijk te implementeren zijn. **Hoofdstuk 7** en **hoofdstuk 8** hebben betrekking op de ontwikkeling van potentiële alternatieven. Het eerste alternatief dat wordt besproken, in **hoofdstuk 7** is de vertebra-disc-ratio (VDR). Dit is het quotiënt van de grijswaarden van corpus L3 en gezonde discus intervertebralis L3-4, gemeten op T1-gewogen opnames. De VDR werd bepaald in 3 groepen patiënten, te weten patiënten met de ziekte van Gaucher zonder behandeling, patiënten met de ziekte van Gaucher met EST en patiënten van wie een MRI van de wervelkolom werd vervaardigd, zonder dat er sprake was van een beenmergaandoening (fungeert als controlegroep). De VDR in de controle groep was 1.9 ± 0.3, welke significant verschilde van de VDR in de twee groepen met patiënten met de ziekte van Gaucher. Verder werd er een goede correlatie met QCSI gevonden. Geconcludeerd kon worden dat VDR een bruikbaar alternatief is voor Dixon QCSI. In **hoofdstuk 8** wordt een tweede alternatief onderzocht. De bone marrow burden score (BMB) is het eerste semi-kwantitatieve scoringssysteem, waarin zowel het axiale als perifere beenmerg zijn geïncludeerd. Twee radiologen zonder ervaring met de ziekte van Gaucher beoordeelden de MRI's separaat volgens een nieuw ontwikkeld scoringssysteem (BMB). Een goede, significante correlatie werd gevonden tussen de twee beoordelaars. Verder was een zeer goede intra observer variatie en een goede significante correlatie met de vetfractie gemeten middels Dixon QCSI. Ook kon respons op therapie worden vastgesteld, echter minder snel dan met Dixon QCSI. Als opvallende bevinding werd vastgesteld dat het axiale beenmerg meer respons liet zien op therapie dan het perifere beenmerg. Geconcludeerd werd dat BMB een goed alternatief is voor Dixon QCSI.

DISCUSSIE EN TOEKOMSTIG ONDERZOEK

In dit proefschrift wordt beschreven dat kwantitatieve MRI middels Dixon QCSI een klinisch belangrijke techniek is met directe klinische consequenties. De techniek is zeer reproduceerbaar, gerelateerd aan het voorkomen van belangrijke klinische bot complicaties en in staat om de respons op EST te detecteren binnen één jaar. In de klinische follow-up van patiënten met de ziekte van Gaucher is deze techniek in het AMC uitermate belangrijk.

De belangrijkste beperking van de techniek, namelijk de beperkte beschikbaarheid wereldwijd, werd besproken. Een andere beperking is het feit dat voor het postprocessen van de geacquireerde MRI data de input van een fysicus essentieel is. Het zou van veel waarde zijn wanneer deze postprocessing volledig geautomatiseerd kan verlopen.

In het AMC werden twee alternatieven voor Dixon QCSI ontwikkeld, VDR en BMB. Beide technieken tonen een goede correlatie met de vetfractie en zijn in staat beenmerg respons op therapie vast te stellen. Voorst zijn beide technieken makkelijk te gebruiken op standaard hardware en software van de gangbare MRI apparaten. Maar welk alternatief is het beste? Hoewel deze vraag uitermate gerechtvaardigd is, kan hij op grond van onze resultaten niet expliciet beantwoord worden. Onze follow-up data zijn hiervoor te beperkt. Echter een theoretische discussie valt wel te voeren. Als voordeel van de VDR kan worden beschouwd het feit dat een pure kwantitatieve meting plaatsvindt. Verder kan deze VDR bepaling op elk standaard MRI apparaat door een getrainde radiologisch laborant geschieden. Een nadeel kan zijn dat er een nieuwe variabele is geïntroduceerd, de discus intervertebralis. Bekend is namelijk dat de samenstelling van deze discus intervertebralis beïnvloed kan worden door externe factoren, zoals leeftijd en diurnale variatie [11-13]. Een sterk punt van het tweede alternatief, de BMB, lijkt de inclusie van zowel het axiale als perifere beenmerg. Hoewel onze BMB resultaten laten zien dat er duidelijk meer respons van beenmerg op EST zichtbaar is in het axiale skelet, werd bij een klein aantal patiënten meer response gezien in het perifere beenmerg. Verder zal de inclusie in het periodieke MRI protocol van de risicogebieden voor ontwikkeling van botinfarcten of avasculaire necrosis de behandelende clinici geruststellen. Al met al zijn er meer gegevens noodzakelijk om een duidelijk wetenschappelijk gefundeerde uitspraak mogelijk te maken omtrent het te prefereren alternatief. Een

manier om op korte termijn meer data te verkrijgen is het opzetten van een internationale MRI database van patiënten met de ziekte van Gaucher over de hele wereld. Deze MRI data kunnen dan zowel qua VDR als BMB worden geëvalueerd en een adequate statistische analyse kan geschieden. Een andere manier om de beperkte beschikbaarheid op te lossen is de beschikbaarheid vergroten. Theoretisch is het voor de betrokken farmaceutische bedrijven mogelijk een of meerdere fysici met ervaring in Dixon QCSI te leveren voor implementatie- en trainingsdoeleinden. Op deze manier kan in meerdere landen waar patiënten met de ziekte van Gaucher behandeld worden ook het beenmerg adequaat worden gecontroleerd middels het vervaardigen van een jaarlijkse vetfractie.

Een groep bij wie Dixon QCSI momenteel nog niet goed genoeg is getest en daarom nog niet als klinische parameter kan worden ingezet, is de populatie van kinderen en adolescenten. Vanwege het feit dat de hoeveelheid rood cellulair beenmerg zeer variabel is in de genoemde populatie en vanwege het feit dat dit rode beenmerg omgekeerd evenredig is met de hoeveelheid vet in het beenmerg beïnvloedt het rode beenmerg direct de gemeten vetfractie. Er kan dus slecht gedifferentieerd worden tussen rood cellulair beenmerg en Gaucher cel infiltratie. Het zal zeer waardevol zijn om QCSI data te vergaren van kinderen en adolescenten zonder Gaucher. Op deze manier kan een controle groep per leeftijd worden vervaardigd. Dit zal de beenmergbeoordeling aanzienlijk vergemakkelijken. Alleen op deze manier kan dit compartiment in deze jonge populatie adequaat gecontroleerd worden. De praktische uitvoerbaarheid zal echter niet gemakkelijk zijn.

Middels Dixon QCSI kan een grote hoeveelheid axiaal beenmerg op een niet invasieve wijze worden geanalyseerd. De kans op artefacten, zoals gezien kan worden in het geval van een niet representatieve punctie is verwaarloosbaar. Daarom is deze techniek in potentie van waarde bij andere beenmergaandoeningen. In voortgaande samenwerking met de afdeling hematologie is een protocol opgesteld waarbij het aanslaan van een beenmergtransplantatie zal worden geëvalueerd middels Dixon QCSI. Detectie van aanslaan van therapie op non invasieve manier, sneller dan middels onderzoek van het perifere bloed zal prognostisch van groot belang kunnen zijn [14-21].

Het niet-invasieve karakter van Dixon QCSI is een krachtige eigenschap, waarvan met name bij de evaluatie van kinderen met beenmergafwijkingen veel voordeel te verwachten kan zijn. Om eventueel zonder beenmergpunctie de respons op therapie te detecteren bij bijvoorbeeld een maligne ziekte in het beenmerg zou een aanwinst betekenen. Aangezien in een longitudinale follow-up de patiënt zijn eigen controle zal zijn, is een database van vetfractie getallen niet noodzakelijk om respons op therapie te detecteren, echter wel wenselijk.
Hoewel de waarde van Dixon QCSI uitgebreid is onderzocht en beschreven in dit proefschrift bij volwassen patiënten met de ziekte van Gaucher, kan deze techniek voor vele indicaties waardevol zijn. Het onderzoek zal voortgaan.

REFERENCES

1. Gerard EL, Ferry JA, Amrein PC, et al. Compositional changes in vertebral bone marrow during treatment for acute leukemia: assessment with quantitative chemical shift imaging. Radiology 1992; 183:39-46.
2. Johnson LA, Hoppel BE, Gerard EL, et al. Quantitative chemical shift imaging of vertebral bone marrow in patients with Gaucher disease. Radiology 1992; 182:451-455.
3. Rosenthal DI, Barton NW, McKusick KA, et al. Quantitative imaging of Gaucher disease. Radiology 1992; 185:841-845.
4. Poll LW, Koch J-A, vom Dahl S, et al. Magnetic resonance imaging of bone marrow changes in Gaucher disease during enzyme replacement therapy: first German long-term results. Skeletal Radiol 2001; 30:496-503.
5. Terk MR, Dardashti S, Liebman HA. Bone marrow response in treated patients with Gaucher disease: evaluation by T1-weighted magnetic resonance images and correlation with reduction in liver and spleen volume. Skeletal Radiol 2000; 29:563-571.
6. Terk MR, Esplin J, Lee K, Magre G, Colletti PM. MR imaging of patients with type 1 Gaucher's disease: relationship between bone and visceral changes. AJR 1995; 165:599-604.
7. Rosenthal DI, Doppelt SH, Mankin HJ, et al. Enzyme replacement therapy for Gaucher disease: skeletal responses to macrophage-targeted glucocerebrosidase. Pediatrics 1995; 96:629-637.
8. Rosenthal DI, Scott JA, Barranger J, et al. Evaluation of Gaucher disease using magnetic resonance imaging. J Bone Joint Surg Am 1986;68:802-808.
9. Rosenthal DI, Mayo-Smith W, Goodsitt MM, Doppelt S, Mankin HJ. Bone and bone marrow changes in Gaucher disease: evaluation with quantitative CT. Radiology 1989; 170:143-6.

10. Moulopoulos LA, Dimopoulos MA. Magnetic resonance imaging of the bone marrow in hematologic malignancies. Blood 1997; 90:2127-2147.
11. Sether LA, Yu S, Haughton VM, Fischer ME. Intervertebral disk: normal age-related changes in MR signal intensity. Radiology 1990; 177(2):385-388.
12. Kingma I, van Dieën JH, Nicolay K et al. Monitoring water content in deforming intervertebral disc tissue by finite element analysis of MRI data. Magn Reson Med 2000; 44(4):650-654.
13. Malko JA, Hutton WC, Fajman WA. An in vivo magnetic resonance imaging study of changes in the volume (and fluid content) of the lumbar intervertebral discs during a simulated diurnal load cycle. Spine 1999; 24(10):1015-1022.
14. Smith SR, Williams CE, Davies JM, Edwards RHT. Bone marrow disorders: characterization with quantitative MR imaging. Radiology 1989; 172:805-810.
15. Gückel F, Brix G, Semmler W, et al. Systemic bone marrow disorders: characterisation with proton chemical shift imaging. J Comput Assist Tomogr 1990; 14:633-642.
16. Gückel F, Brix G, Semmler W, et al. Proton chemical shift imaging of bone marrow for monitoring therapy in leukemia. J Comput Assist Tomogr 1990; 14:945-959.
17. Kauczor HU, Brix G, Dietl B, Jarosch K, Knopp MV, van Kaick G. Bone marrow after autologous blood stem cell transplantation and total body irradiation: magnetic resonance and chemical shift imaging. Magn Reson Imaging 1993; 11:965-975.
18. Kauczor HU, Dietl B, Brix G, Jarosch K, Knopp MV, van Kaick G. Fatty replacement of bone marrow after radiation therapy for Hodgkin disease: unantification with chemical shift imaging. JMRI 1993; 3:575-580.
19. Lecouvet FE, Vande Berg BC, Michaux L, et al. Stage III multiple myeloma: clinical and prognostic value of spinal bone marrow MR imaging. Radiology 1998; 209:653-660.
20. Schick F, Einsele H, Weiss B, et al. Assessment of the composition of bone marrow prior to and following autologous BMT and PBSCT by magnetic resonance. Ann Hematol 1996; 72(6):361-370.
21. Schick F, Einsele H, Kost R, et al. Hematopoietic reconstitution after bone marrow transplantation: assessment with MR imaging and H-1 localized spectroscopy. J Magn Reson Imaging 1994; 4(1):71-78.

DANKWOORD

DANKWOORD

Het maken van een proefschrift wordt snel als een één-persoonsactie bestempeld. In mijn optiek is niets minder waar. Ook hier is sprake van team-effort, waarbij de promovendus als centrale-as fungeert. Mijn mede teamleden en anderen wil ik graag bedanken.

Liefste Annelies, eindelijk is het zover. Mijn boekje, toch eigenlijk ons boekje, is klaar. Bedankt voor je onvoorwaardelijke steun. Nu zal het wel rustig worden...
Bart en Rutger, ik hoop dat jullie het leuk zullen vinden tijdens de promotie. Ziet er wel raar uit hoor, papa in zo'n pinguïnpak.

Prof. dr. den Heeten, beste Ard, met jouw komst naar het AMC waren er ineens twee radiologen op één afdeling met interesse in beenmerg MRI. Jouw enthousiasme en betrokkenheid hebben het proefschrift die kant op gestuurd, waar het uiteindelijk gekomen is. De basis voor meer beenmerg MRI research is gelegd. Bedankt voor je begeleiding.
Prof. dr. Faber, beste William, veel dank ben ik je verschuldigd voor het feit dat jij toezegde het proefschrift te willen begeleiden, ten tijde van het interregnum op de afdeling radiologie. Er zullen niet veel dermatologen zijn, bij wie een radioloog zal promoveren. Jouw betrokkenheid bij het onderzoek was zeer plezierig. Wees niet bevreesd, het onderzoek naar de neuropatische voet zal voortgaan.
Dr. Akkerman, beste Erik, kompaan vanaf het eerste uur. Hoewel radiologen en fysici niet per definitie dezelfde taal spreken, hebben wij elkaar snel leren verstaan. Met de ontwikkeling van een klinisch toepasbare Dixon sequentie heb je iets heel belangrijks neergezet, iets waar je trots op kunt zijn. Veel patiënten hebben hier profijt van. Bedankt.
Dr. Stoker, beste Jaap, jouw niet aflatend vermogen om binnen een bestaande studie snel nog een volgende substudie te verzinnen, waardoor een en ander nog veel sterker zou worden, bewonder ik zeer. Dat alles daarmee wat langzamer gaat dan gepland is wat minder. Ik heb van jou geleerd waar het om gaat bij het stellen van deadlines. Bedankt voor je enthousiaste betrokkenheid en collegialiteit.

Leden van de promotiecommissie, u dank ik voor uw bereidheid in de commissie te willen plaatsnemen. Een heel divers gezelschap van verschillende disciplines en twee universiteiten. Het zwaartepunt van beenmerg MRI in Nederland ligt blijkbaar in het gebied tussen Leiden en Amsterdam.

Mijn paranimfen, Carla Hollak en Kees van Kuijk, wil ik danken voor de vriendschappelijke en uitermate plezierige samenwerking van de laatste jaren. Carla, ik hoop dat er nog veel gezamenlijk onderzoek zal geschieden. Ik zie er naar uit lange tijd met je samen te kunnen werken. Kees, dat weekend Zeeland deed het 'em. Terwijl je in het geheel niet bij het onderzoek betrokken was, gaf je veel van je vrije tijd om me te ondersteunen. Ik stel onze vriendschap zeer op prijs.

De laatste twee jaar kwam er onverwachte hulp aanlopen in de persoon van Erik Slim. Beste Erik, veel dank ben ik je verschuldigd voor je enthousiaste steun bij het lepra-onderzoek. Hoewel de biomechanische analyse is gesneuveld in ons laatste artikel, zal dit het begin van jouw (promotie-)onderzoek zijn. Voor ondersteuning kun je op me rekenen.

De oorsprong van de Dixon research ligt halverwege de jaren negentig, met een andere personele bezetting op de afdeling radiologie. Echter de mensen die aan de wieg van dit proefschrift stonden wil ik zeker niet vergeten te noemen. Piet Dijkstra, ik dank je voor mijn prima opleiding tot skeletradioloog en je plezierige hulp bij de ontwikkeling van de Dixon vet suppressie techniek. Ben Verbeeten jr. heeft in Nice, onder het genot van een Orangina, de eerste indeling van het proefschrift met mij gemaakt. Ben, bedankt voor je betrokkenheid. Ronald Rademakers dank ik voor de gestructureerde opzet van het Gaucher QCSI onderzoek. Rob Grijm dank ik voor de ruimte die ik heb gekregen ten tijde van het interregnum op de afdeling radiologie.

Zowel binnen het klinische veld van Morbus Gaucher als de neuropatische voet zijn er periodieke multidisciplinaire besprekingen. Deze besprekingen hebben mij zeer ondersteund. Ik wil alle collegae die hebben deelgenomen aan deze besprekingen bedanken voor hun bijdragen aan de discussies. Het proefschrift is er beter van geworden.

Alle collegae op de afdeling radiologie wil ik bedanken voor hun collegiale steun. Mark Romijn bedank ik speciaal vanwege het koerierschap in de eindfase van dit proefschrift, van en naar Andries.
Andries wil ik bedanken voor de fraaie lay-out van het boekje. Er kwam met de twee voorkanten iets nieuws uit Amsterdam. Uiteindelijk is het een perfect Amsterdam-Rotterdam project geworden.

Het secretariaat wil ik bedanken voor de plezierige samenwerking in vaak stressvolle tijden. Een speciaal woord van dank voor Mirjam Evers. Mirjam, jouw steun, hulp en nog veel meer gedurende het hele traject van de promotie, neen, eigenlijk al zolang we elkaar kennen, is enorm. Ik prijs me gelukkig met je vriendschap. Ik zie al uit naar ons volgend project.

Ik dank de medewerkers van de afdeling radiologie voor de plezierige samenwerking. De MRI medewerkers dank ik in het bijzonder voor het vervaardigen van de Dixon studies.

Ik dank de patiënten en proefpersonen voor hun medewerking.

Als laatste wil ik het hoofd van de afdeling radiologie, prof. dr. J.S. Laméris, bedanken. Beste Han, ik dank je voor de ruimte die ik heb gekregen om mijn onderzoek af te maken. Tijd voor een nieuwe uitdaging.

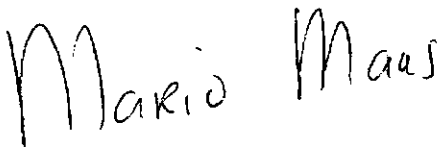

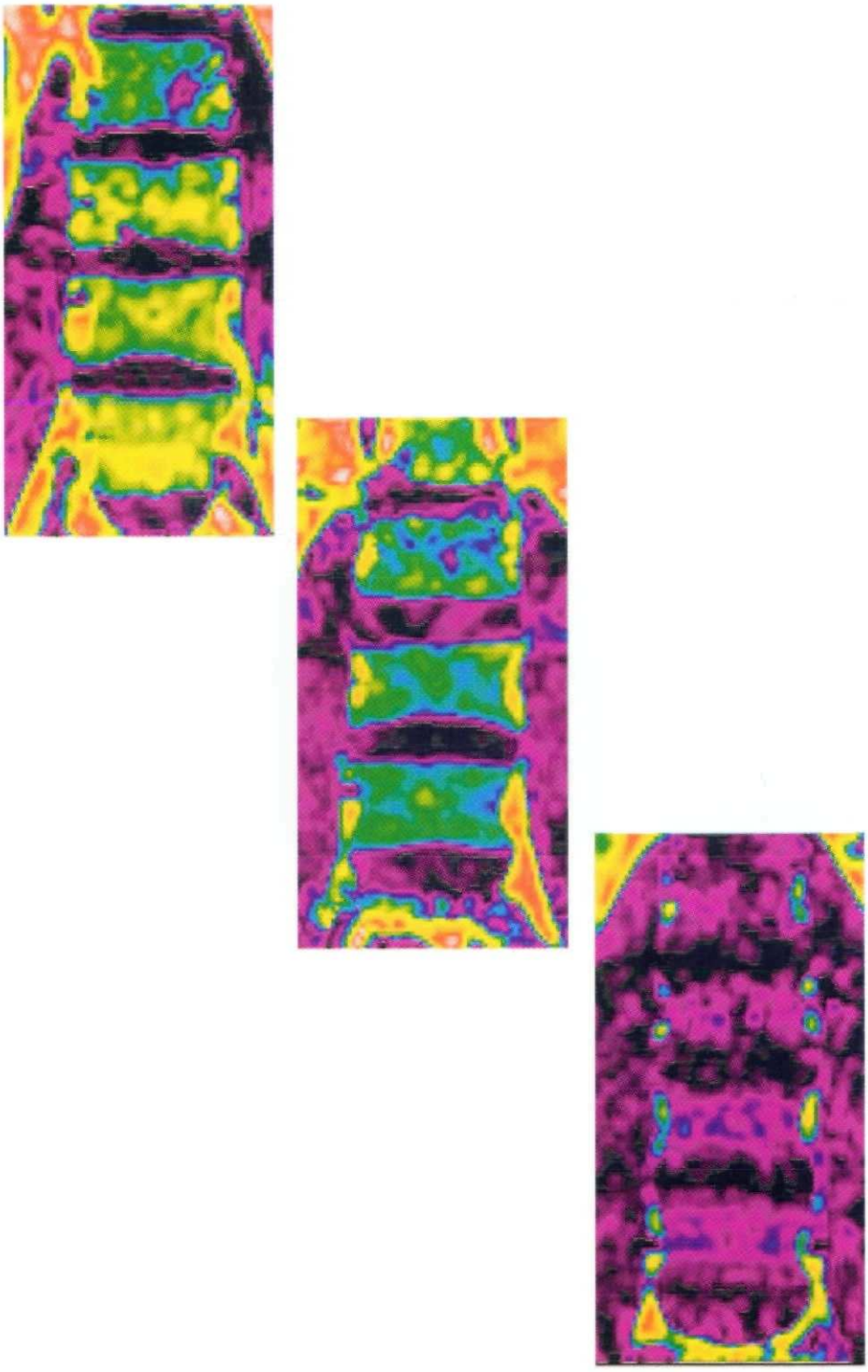

Clinical applications of Dixon chemical shift MR imaging

Morbus Hansen

Mario Maas

CLINICAL APPLICATIONS OF DIXON CHEMICAL SHIFT MR IMAGING

ACADEMISCH PROEFSCHRIFT

ter verkrijging van de graad van doctor

aan de Universiteit van Amsterdam

op gezag van de Rector Magnificus

Prof. mr. P.F. van der Heijden

ten overstaan van een door het college voor promoties ingestelde

commissie, in het openbaar te verdedigen in de Aula der Universiteit

op woensdag 19 juni 2002, te 12.00 uur

door Mario Maas

geboren te Amsterdam

Promotiecommissie

Promotores
Prof.dr. G.J. den Heeten
Prof.dr. W.R. Faber

Co-promotores
dr. E.M. Akkerman
dr. J. Stoker

Overige Leden
Prof.dr. J.S. Laméris
Prof.dr. J.L. Bloem
Prof.dr. J.M.F.G. Aerts
Prof.dr. R. Goudsmit
Prof.dr. A. Huson
dr. B. Naafs

Faculteit Geneeskunde

ISBN 90-9015888-X
© Mario Maas 2002
Printed by Ridderprint B.V. Ridderkerk

The financial support of the following companies is gratefully acknowledged:
Gaucher Stichting, Huidstichting Chanfleury van IJsselsteijn, QM Gastmann Wicher Stichting

Coloplast B.V., Genzyme Nederland B.V., Merck Sharp & Dohme B.V., Novo Nordisk Farma B.V., Oxford Glyco Sciences, Schering Nederland B.V.

Contents

Clinical applications of Dixon chemical shift MR imaging

Morbus Hansen

Chapter 1	Introduction	7
Chapter 2	Uniform fat suppression in hands and feet through the use of two-point Dixon chemical shift MR imaging *Radiology 1999; 210:189-193*	19
Chapter 3	MRI in clinically asymptomatic neuropathic leprosy feet: a baseline study *Int J Leprosy other Mycobact Dis 2001; 69: 219-224*	33
Chapter 4	MR imaging of neuropathic feet in leprosy patients with suspected osteomyelitis *submitted*	43
Chapter 5	Summary, general discussion and future research	55
Chapter 6	Samenvatting	63
	Dankwoord	73

CHAPTER 1

Introduction

* *What is Leprosy?*
* *Leprosy - Global situation*
* *Leprosy - Local situation*
* *Neuropathic foot in leprosy*
* *Imaging evaluation of osteomyelitis*
* *MRI - the Dixon technique*
* *Aim and outline of the conducted studies*

WHAT IS LEPROSY?

Leprosy is an infectious disease that is still incompletely understood and often feared. The causative micro-organism *Mycobacterium leprae (M. leprae)*, is an acid-fast obligate intracellular organism first described by Armauer Hansen in 1874 [1]. The most probable spread of the *M. leprae* is by respiratory route, and it preferably invades skin and peripheral nerves. The majority of people will not develop clinical symptoms, since an effective immune response is developed before clinical disease appears. When clinical signs occur, after an incubation period of several years, one may only have an often self-healing, single lesion (indeterminate leprosy) [2,3]. However, when self-healing does not happen, the disease can progress.

The classification of leprosy is based on the immunological response of the host towards M. leprae [4]. This is the so-called Ridley-Jopling classification with a division in tuberculoid (TT), borderline tuberculoid (BT), mid-borderline (BB), borderline lepromatous (BL) and lepromatous (LL) leprosy. The World Health Organization (WHO) nowadays classifies leprosy patients according to the number of lesions. Patients with 5 or less skin lesions are classified as paucibacillary leprosy (PB); patients with six or more skin lesions are classified as multibacillary leprosy (MB). The standard treatment for leprosy is the multidrug therapy (MTD) [5]. This MTD consists of rifampicin, dapsone and clofazimine, in which PB patients are treated with a combination of rifampicin and dapsone and MB patients are treated with a combination of rifampicin, dapsone and clofazimine. The chosen combination of drugs depends on the classification [5,6,7].

LEPROSY - GLOBAL SITUATION[8]

In 1991, WHO and its Member States committed themselves to eliminate leprosy as a public health problem by the year 2000; elimination being defined as prevalence <1 case per 10.000 people. At the end of 2000, the global prevalence of leprosy was below 1 case per 10.000. At the end of the year 2000 the latest available information indicates that there were 597.232 cases registered for treatment globally, with 719.330 cases detected during the last year of reporting. Among 122 countries considered endemic in 1985, 107 countries have reached elimination at the country level. At the end of 2000, leprosy was a public health problem in only 15 countries (prevalence rate >1 per 10.000 and population above 1 million), mainly in Africa, Asia and Latin America, of which the leading six countries are India, Brazil, Myanmar (Birma), Madagascar, Nepal and Mozambique.

LEPROSY - LOCAL SITUATION

In the Netherlands leprosy occurs as an import disease since a long time. The majority of patients nowadays are from Surinam: this is related to the colonial history. In the Academic Medical Center there is a relatively large group of patients with foot pathology due to leprosy. This group consists of patients with recent as well as longstanding neuropathic foot problems. They are treated in a multidisciplinary setting with a core of a tropical dermatologist, a surgeon, and a specialist in rehabilitation medicine (physiatrist). A specialized nurse provides regular foot and ulcer care. Registration of the complications of the feet is documented on the so-called FINU (Foot Ischemia Neuropathic Ulcer) data-form, designed by the Dutch Neuropathic Foot Society [9,10].

NEUROPATHIC FOOT IN LEPROSY

The invasion of Schwann cells by *M. leprae* with the resulting peripheral nerve damage can lead to a so-called neuropathic foot. A neuropathic foot is defined as a foot in which one or more of the neuronal functions i.e. sensory, motor function or autonomic function is disturbed (consensus Dutch Neuropathic Foot Society). In leprosy the neuropathic foot is one of the major contributors to morbidity due to peripheral nerve damage.

The total number of leprosy-patients with foot problems is estimated on 20-30% of the leprosy patients worldwide. The sensory loss means that patients may not perceive trauma, resulting in development of complications. To identify the patients that lack the preventing sensibility the Semmes Weinstein monofilament test is used [11]. The feet of patients with a sensory loss of a 10-gram force are considered neuropathic feet at risk [11].

The neuro-osteoarthropathy in leprosy is comparable to diabetes and may lead to tarsal disintegration with osteolysis, fragmentation and progressive bone resorption. In extreme cases dissolution of the mid-foot results in separation of the forefoot and the hind foot, changing all biomechanics [9,12-14]. The skeletal abnormalities are evident in 20-70 % of hospitalized patients [15]. The most important difference between leprosy and diabetes is the fact that in principle in leprosy the neurological pathology is the only pathology present ("a pure neuropathic foot"), while in diabetes there is nearly always a combination of vascular disease and neurological disease.

Ulceration and infection (cellulitis or osteomyelitis) are important complications. When a patient with a longstanding neuropathic foot presents himself with a warm foot it is a clinical challenge to discriminate neuro-osteoarthropathy from an ongoing infection. This is especially difficult in the presence of an ulcer, since an ulcer itself leads to increased local temperature [12,16]. Clinical signs are often not conclusive in discriminating between infection (cellulitis or osteomyelitis) and neuro-osteoarthropathy. The need for further evaluation with imaging is present [17].

IMAGING EVALUATION OF OSTEOMYELITIS

Osteomyelitis is a serious medical problem that is associated with significant morbidity. Osteomyelitis may result from hematogeneous spread, from adjacent soft tissue infection or direct inoculation. In neuropathic feet most often osteomyelitis is due to adjacent soft tissue infection. Accurate early diagnosis is necessary to optimize treatment strategies. Since clinical evaluation is not accurate, support from diagnostic imaging techniques is required.

Diagnosing osteomyelitis is a well-known challenge in diagnostic radiology. Various imaging modalities are investigated in the analysis of

osteomyelitis in neuropathic feet [15,18-28]. Plain radiography does not show abnormalities related to osteomyelitis until 10-20 days after the onset of symptoms. Acute osteomyelitis has a permeative pattern on conventional radiographs. Characteristic findings include osteopenia with small ill-defined lucencies in the medullar bone and cortex. A chronic osteomyelitis may show areas of sclerosis. However, the radiographic diagnosis of osteomyelitis in neuropathic feet is more difficult, the differentiation from neuro-osteoarthropathy is not easily done [15,18,25,26,29].

Radionuclide imaging can also be used [18,25,26]. Three-phase ^{99m}Technetium bone scintigraphy, ^{111}Indium white blood cells scintigraphy or ^{67}Gallium citrate scintigraphy may be used. Interpretation of three phase ^{99m}Technetium bone scintigraphy is difficult in neuropathic feet. A high false positive rate is due to the simultaneous presence of neuro-osteoarthropathy. Also, ^{67}Gallium citrate scintigraphy is generally not helpful because of the high percentage of false positive scans. Of the radionuclide modalities, ^{111}Indium white blood cells scintigraphy is thought to be the most specific for osteomyelitis and carries the highest sensitivity [18,25].

Of all available imaging modalities, Magnetic Resonance Imaging (MRI) has been described as the modality with the highest sensitivity for diagnosing osteomyelitis, and carries a high specificity for differentiating osteomyelitis from cellulitis in the neuropathic foot of diabetic patients [18-22,25,30-34]. Tissue characterisation and spatial resolution facilitate identification of associated soft tissue pathology.

Normal healthy peripheral fatty (yellow) bone marrow shows a hyperintense signal intensity (SI) both on T1-weighted spin echo (SE) images (Short Repetition Time (TR), Short Echo Time (TE)) as on dual echo Fast SE (Long TR/TE). Osteomyelitis will change the SI due to the presence of more water in the bone marrow. Since water shows high signal intensity on T2-weighted images, it is not easy to detect when using T2-weighted fast SE sequences. Fat-suppression techniques are frequently used in MR imaging of the musculoskeletal system, in order to better appreciate bone marrow abnormalities, and soft tissue pathology [23,35-37]. The suppression of the relatively high signal of fat can lead to a more efficient use of the dynamic range for the display of tissue contrast on MRI [38]. Therefore several fat-suppression techniques are used. The

most widely used technique is frequency-selective presaturation [37]. However, in areas of irregular shape and abrupt changes between soft tissue and air, such as the distal extremities (hand and foot), this technique produces uneven fat-suppression and artifacts because the required magnetic field homogeneity cannot be achieved [23,33,39]. Since much of this problem is caused by physical properties of the patient, it is largely independent of the equipment used. Another widely used technique for suppression of the fat signal is the STIR (Short Tau Inversion Recovery) sequence. STIR is based on the rapid T1 recovery of fat and is, therefore, not significantly affected by field inhomogeneities. STIR is considered the most sensitive technique for identifying subtle bone marrow pathology [23]. Unfortunately, STIR suppresses all short T1 species, including tissues that have absorbed Gadolinium (Gd). Hence, it is not possible to use STIR fat-suppression to improve the detection of contrast enhancement [35]. For the detection of osteomyelitis this is an important disadvantage, because previous studies suggested that MR imaging with both fat-suppression and Gd enhancement may be the imaging method of choice in clinically complicated situations [33,40]. For the detection of subtle bone marrow pathology, such as a low-grade chronic infection, it is mandatory to use fat-suppression sequences with the use of contrast administration in state-of-the-art musculoskeletal MRI [21,22,33]. Similarly, using fat-suppression can increase the conspicuity of enhancement after contrast administration. A homogeneous fat-suppression in the entire field of view both before and after intravenous contrast material (Gadolinium-chelate (Gd)) is necessary, to avoid misconception [23].

MRI - THE DIXON TECHNIQUE

An alternative method for fat-suppression is the phase-contrast method, first described in 1984 by Dixon, which is based on the frequency difference between fat and water [41]. It does not require a high field homogeneity in order to achieve adequate fat-suppression, thus field inhomogeneity is not a limiting factor [41,42]. This technique has been applied successfully in MR imaging of adrenal masses and bone marrow [42-46].

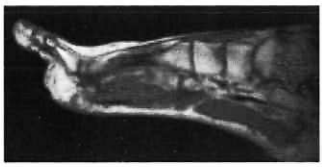

Figure 1a. In-phase (I)

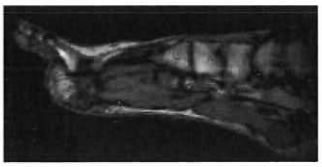

Figure 1b. Opposed-phase (O)

Figure 1c. Phase difference (ϕ)

In the original Two-Point Dixon technique, which we use, two sets of acquisitions are performed: one in which water signal (W) and fat signal (F) are "in-phase", which means that at any moment in time, the fat and water spins point in the same direction, and their signals add up in the image (Fig 1a): $I = W + F$.

In the second acquisition fat and water have opposed-phases: fat and water spins point in opposite directions, and the resulting image shows the magnitude of the difference of the fat and water signals (Fig 1b): $O = |W - F|$.

In order to separate the fat and water signals we need to know in every pixel which signal is stronger. The "phase-difference" (Fig 1c, ϕ) helps us to sort out regions with water dominant signal and regions with fat dominant signal. Borders between these regions are characterized by a 180 ° step, i.e. half way through the grey scale, e.g. from white to grey, from light grey to dark grey, or from grey to black. Borders from white to black represent 360 ° transitions, which have no physical meaning.

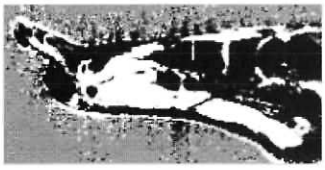

Figure 1d. Sign (S)

Figure 1e. Water image (W)

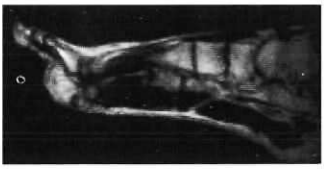

Figure 1f. Fat image (F)

With help of an algorithm, developed at our department [46] the Sign image is produced (Fig 1d, S) which shows water dominant regions (white, $S = +1$) from fat dominant regions (fat, $S = -1$).
Finally we obtain the water image (Fig 1e): $W = I + S \cdot O$,
and the fat image (Fig 1f): $F = I - S \cdot O$.

A potential problem in using this chemical shift technique is the occurrence of displacement artefacts that hamper the application of the technique [25,37]. The necessary postprocessing requires the same position with absolutely no shift of the object between the in-phase and opposed-phase sequences [46,37].

AIM AND OUTLINE OF THE CONDUCTED STUDIES

In summary MRI has been described, as an important modality to assess the neuropathic feet of diabetic patients, but has not been described in leprosy. For the detection of osteomyelitis previous studies suggest that intravenous Gadolinium administration is mandatory. Furthermore, the use of fat-suppression techniques will increase the detection of enhancement after contrast administration.

This thesis was conducted with the following research questions:
Can the Two-Point Dixon Chemical shift Imaging technique serve as a clinical feasible fat-suppression technique in the extremities?
In order to answer this question the use of Two-Point Dixon chemical shift imaging as fat-suppression technique was evaluated in 31 consecutive patients clinically suspected to have bone marrow disease. The results are reported in **Chapter 2**

What are the MRI findings of Dixon chemical shift imaging as fat-suppression technique in patients with leprosy and clinically asymptomatic neuropathic feet?
Since the technique was found a good technique for achieving uniform fat-suppression in the distal parts of the extremities, applicable in a routine clinical setting, it was used to study leprosy patients. Early detection of feet at risk may help to prevent complications. The question was raised whether changes prior to the appearance of clinical signs are present and detected by MRI. Are there MRI changes present in these patients? When changes are present, is there a role for MRI in relation to clinical management, in the early assessment of the asymptomatic neuropathic foot in leprosy patients? All available data in the literature address clinically complicated neuropathic feet. To our knowledge, no papers, concerning MRI in asymptomatic neuropathic feet, exist. The results of this study are presented in **Chapter 3**

What are the MRI findings with use of Dixon chemical shift imaging as fat-suppression technique in patients with leprosy and clinically complicated neuropathic feet, suspected for osteomyelitis?

The problem that clinicians encounter when treating leprosy patients with longstanding neuropathic feet pathology is the discrimination between neuro-osteoarthropathy and ongoing infection (cellulitis, osteomyelitis) in a patient with a warm foot, not responding to therapy. The radiological literature available on MRI and osteomyelitis in neuropathic feet nearly exclusively concerns diabetic foot pathology, being the most frequent cause of neuropathic feet in the western world. As far as we know, no papers concerning the use of MRI in neuropathic leprosy feet, clinically suspected of osteomyelitis exist. Our results are described in **Chapter 4**

In **Chapter 5** an overview of the results of the performed studies is given and the implications are discussed. Further some areas for future research are described.

REFERENCES

1. Harboe M. Armauer Hansen-The man and his work. Int J Lepr Other Mycobact Dis 1973; 41(4):417-424.
2. Noordeen SK. The epidemiology of leprosy, In: Hastings RC and Opromolla DVA (eds), Leprosy. Churchill Livingstone 1985; 15-30.
3. Jacobson RR, Krahenbuhl JL. Leprosy. Lancet 1999; 353:655-660.
4. Ridley DS, Jopling WH. Classification of leprosy according to immunity. A five-group system. Int J Lepr Other Mycobact Dis. 1966; 34(3):255-273.
5. World Health Organization. Leprosy. Fact sheet N101. 1999.
6. World Health Organization. Expert Committee on Leprosy, Sixth Report. 768. 1988. Geneva, World Health Organization. Technical Report Series.
7. World Health Organization. Action programme for the elimination of leprosy. Shortening duration of treatment of multibacillary leprosy. Weekly Epidemiological records 1997; 72:125-128.
8. World Health Organization. Weekly epidemiological record 2002; 77(1):1-8. http://www.who.int/wer.
9. Brandsma JW, Macdonald MRC, Warren AG, Cross H, Schwarz RJ, Solomon S, Kazen R, Gravem PE, Shrinivasan H. Assessment and examination of the neurologically impaired foot. Lepr Rev 2001; 72:254-262.

10. Van Egmond M, Hoeksma AF, Lankhorst GJ, Dahmen R. The inter- and intra-observer reliability of the FINU-diagram in diabetic feet. 7th European Congress of Research in Rehabilitation. Abstract. Madrid, 1-6 April 2001.
11. Anderson AM, Croft RP. Reliability of Semmes Weinstein monofilament and ballpoint sensory testing, and voluntary muscle testing in Bangladesh. Lepr Rev 1990; 70:305-313.
12. Onvlee GJ. The Charcot Foot; a critical review and observational study of a group of 60 patients. Thesis 1998.
13. Jacob S, Patil MK. Stress analyses in three-dimensional foot models of normal and diabetic neuropathy. Frontiers of Medical and Biological Engineering 1999; 1-17.
14. Jacob S, Patil MK. Three-dimensional foot modelling and analysis of stresses in normal and early stage Hansen's disease with muscle paralysis. Journal of Rehabilitation Research and Development 1999; 36:252-263.
15. Resnick D, Niwayama G. Diagnosis of bone and Joint disorders 3rd edition vol 4. Chapter 66: Osteomyelitis, septic arthritis and soft tissue infection: Organisms. WB Saunders Company Pensylvania 1995; 2486-2492.
16. Hoeksma AF, Faber WR. Assessment of skin temperature by palpation in leprosy patients: interobserver reliability and correlation with infrared thermometry. Int J Lepr 2000; 68:65-67.
17. Faber WR, Hoeksma AF, van der Kleij AJ, Maas M, Dijkstra PF. Diagnostic procedures for suspected osteomyelitis in neuropathic feet of leprosy patients. Int J Lepr 1998; 66:29A.
18. Crim JR, Seeger LI. Imaging evaluation of osteomyelitis. Crit Rev Diagn Imaging 1994; 35:201.
19. Marcus CD, Ladam-Marcus VJ, Leone J, Malgrange D, Bonnet-Grausserand FM, Mentaneau BP. MR imaging of osteomyelitis and neuropathic osteoarthropathy in the feet of diabetics. Radiographics 1996; 16:1337-1348.
20. Moore TE, Yuh, WTC, Kathol MH, El-Khoury GY, Corson JD. Abnormalities of the foot in patients with diabetes mellitus: findings on MR imaging. AJR 1991; 157:813-816.
21. Morrison WB, Ledermann HP, Schweitzer ME. MR imaging of the diabetic foot. MRI Clin North Am 2001; 9:603-613.
22. Morrison WB, Ledermann HP, Schweitzer ME. MR imaging of inflammatory conditions of the ankle and foot. MRI Clin North Am 2001; 9:615-637.
23. Peterfy CG, Linares R, Steinbach LS. Recent advances in magnetic resonance imaging of the musculoskeletal system. Rad Clin North America 1994; 32:291-311.
24. Schon LC, Easley ME, Weinfeld SB. Charcot neuroarthropathy of the foot and ankle. Clinical Orthopaedics and Related Research 1988; 349:116-131.

25. Tehranzadeh J, Wong E, Wang F, Sadighpour M. Imaging of osteomyelitis in the mature skeleton. MRI Clin North Am 2001; 39:240-250.
26. Yuh WTC, Corson JD, Baraniewski HM, et al. Osteomyelitis of the foot in diabetic patients: evaluation with plain film, 99mTc-MDP Bone scintigraphy, and MR imaging. AJR 1989; 152:795-800.
27. Yu JS. Diabetic foot and neuroarthropathy magnetic resonance imaging evaluation. Topics in Magnetic Resonance Imaging 1998; 9:295-230.
28. Tomas MB, Patel M, Marwin SE, Palestro CJ. The diabetic foot. The British Journal of Radiology 2000; 73:443-450.
29. Jones EA, Manaster BJ, May DA, Disler DG. Neuropathic osteoarhtropathy: diagnostic Dilemmas and differential diagnosis. Radiographics 2000; 20:S279-S293.
30. Craig JG, Amin MB, Wu K, Eyler WR, van Holsbeeck MT, Bouffard JA, Shirazi K. Osteomyelitis of the diabetic foot: MR imaging-pathologic correlation. Radiology 1997; 203:849-855.
31. Goodwin DW, Salonen DC, Yu JS, Broschmann J, Trudell DJ, Resnick DL. Plantar compartments of the foot: MR appearance in cadavers and diabetic patients. Radiology 1995; 196:623-630.
32. Ledermann HP, Schweitzer ME, Morrisson WB. Nonenhancing tissue on MR imaging of pedal infection: Characrterizarion of necrotic tissue and associated limitations for diagnosis of osteomyelitis and abscess. AJR 2002; 178:215-222.
33. Morrison WB, Schweitzer ME, Bock GW, Mitchell DG, Hume EL, Pathria MN, Resnick D. Diagnosis of osteomyelitis: Utility of fat-suppressed contrast-enhanced MR imaging. Radiology 1993; 189:251-257.
34. Morrison WB, Schweitzer ME, Granville Batte W, Radack DP, Russel KM. Osteomyelitis of the foot: relative importance of primary and secondary MR imaging signs. Radiology 1998; 207:625-632.
35. Rubin DA, Kneeland JB. MR imaging of the musculoskeletal system: technical considerations for enhancing image quality and diagnostic yield. AJR 1994; 163:1155-1163.
36. Mirowitz SA. Fast scanning and fat-suppression MR imaging of musculoskeletal disorders. AJR 1993; 161:1147-1157.
37. Mirowitz SA. Musculoskeletal MRI techniques: clinical magnetic resonance imaging. 2nd ed. Philadelphia, Pa: Saunders, 1996; 1797-1819.
38. Peterfy CG, Roberts T, Genant HK. Dedicated extremity MR imaging: an emerging technology. Radiol Clin North Am 1997; 35:1-20.
39. Anzai Y, Lufkin RB, Jabour BA, et al. Fat-suppression failure artifacts simulating pathology on frequency-selective fat-suppression MR images of the head and neck. AJNR 1992; 13:879-884.

40. Dangman BC, Hoffer FA, Rand FF, O'Rourke EJ. Osteomyelitis in children: gadolinium-enhanced MR imaging. Radiology 1992; 182:743-747.
41. Dixon WT. Simple proton spectroscopic imaging. Radiology 1984; 153:189-194.
42. Chan TW, Lisreud J, Kressel HY. Combined chemical-shift and phase-selective imaging for fat-suppression: theory and initial clinical experience. Radiology 1991; 181:41-47.
43. Tsushima Y, Ishizaka H, Matsumoto M. Adrenal masses: differentiation with chemical shift, fast low-angle shot MR imaging. Radiology 1993; 186:705-709.
44. Mitchell DG, Crovello M, Matteucci T, Petersen RO, Miettinen MM. Benign adrenocortical masses: diagnosis with chemical shift MR imaging. Radiology 1992; 185:345-351.
45. Dunnick NR, Korobkin M, Francis I. Adrenal radiology: distinguishing benign from malignant adrenal masses. AJR 1996; 167:861-867.
46. Akkerman EM, Maas M. A region-growing algorithm to simultaneously remove dephasing influences and separate fat and water in two-point Dixon imaging (abstr). In: Proceedings of the Society for Magnetic Resonance in Medicine and the European Society for Magnetic Resonance in Medicine and Biology 1995; 649.

CHAPTER 2

Uniform fat-suppression in hands and feet through the use of two-point Dixon chemical shift MR imaging

Mario Maas, Piet F. Dijkstra, Erik M. Akkerman

Department of Diagnostic Radiology, Academic Medical Center, Amsterdam, the Netherlands

Radiology 1999; 210:189 -193

ABSTRACT

Purpose:
To assess the potential of two-point Dixon chemical shift magnetic resonance imaging to achieve uniform fat-suppression in the distal parts of the extremities.

Materials and methods:
Two-point Dixon chemical shift imaging was performed in 31 consecutive patients clinically suspected to have bone marrow disease. In some patients, Dixon studies were performed before and after the intravenous administration of gadopentetate dimeglumine, and in some patients follow-up examinations were performed, for a total of 64 studies. Areas of interest were the hand, wrist, foot, ankle, and lower leg. There was a special interest in the neuropathic foot and osteomyelitis. The uniformity of fat-suppression in the entire field of view, the frequency of displacement artifacts, and the applicability of the technique in routine patient treatment were evaluated.

Results:
In 64 (100%) Dixon studies, uniform fat-suppression was achieved. In 59 (92%) studies, there were no displacement artifacts. In five (8%) studies, displacement artifacts occurred; however, in only one (2%) study did they severely hamper the reading. Thus, in 63 (98%) studies, adequate diagnostic quality was obtained.

Conclusion:
Two-point Dixon chemical shift imaging is a good technique for achieving uniform fat-suppression in the distal parts of the extremities. Because the frequency of displacement artifacts is low, the technique is applicable in a routine clinical setting.

INTRODUCTION

Fat-suppression techniques are frequently used in magnetic resonance (MR) imaging of the musculoskeletal system to better appreciate bone marrow abnormalities, soft-tissue disease, and cartilage [1-3]. The suppression of the relatively high signal of fat can lead to a more efficient use of the dynamic range of tissue contrast on MR images [4]. Similarly, the conspicuousness of enhancement after contrast medium administration can be increased by using fat-suppression [4,5]. The most widely used technique is frequency-selective presaturation. However, in areas of irregular shape and abrupt changes between soft tissue and air, such as the craniocervical junction and the distal extremities (hands and feet), this technique produces uneven fat-suppression and artifacts because the required magnetic field homogeneity cannot be achieved [1,6].

A good alternative technique for suppression of the fat signal is the short inversion time inversion-recovery (STIR) sequence. STIR is based on the rapid T1 recovery of fat and is, therefore, not substantially affected by field inhomogeneities. STIR is considered the most sensitive technique for identifying subtle bone marrow disease [1]. Unfortunately, STIR suppresses all short T1 species, including tissues that have absorbed gadolinium. Hence, it is not possible to use STIR fat-suppression to improve the detection of contrast medium enhancement [2]. For the detection of osteomyelitis, this is an important disadvantage, because previous studies [7,8] have suggested that MR imaging with both fat-suppression and gadolinium enhancement may be the imaging method of choice in clinically complicated situations.

An alternative method for fat-suppression is the phase-contrast method, described by Dixon in 1984 [9], that is based on the chemical shift phenomenon. This technique does not require a high field homogeneity to achieve adequate fat-suppression, thus field inhomogeneity is not a limiting factor [9]. This technique has been applied successfully in MR imaging of adrenal masses and bone marrow [10-13]. A potential problem in using this chemical shift technique is the occurrence of displacement artifacts that hamper its application [3,4]. The necessary postprocessing requires that the patient remains in the same position with absolutely no shift of the imaged structures between the in-phase and opposed-phase series [4,14].

In our hospital (Academic Medical Center, Amsterdam, the Netherlands), there is a relatively large population of patients with neuropathic foot disease, usually due to diabetes mellitus or leprosy. In this group, MR imaging is requested when infection is suspected. With our MR imager, the frequency-selective presaturation fat-suppression of the distal extremities is inhomogeneous. Because much of this problem is caused by physical properties of the patient, it is largely independent of the equipment used [1,6], so we looked for an alternative technique. In a pilot study, we found the two-point Dixon chemical shift MR imaging technique in combination with the administration of gadopentetate dimeglumine promising [15]. Subsequently, the present study was conducted to answer the following questions: **a**) Is two-point Dixon chemical shift imaging useful in obtaining uniform fat-suppression in the hands and feet? **b**) Is this technique applicable in a clinical setting for the evaluation of bone marrow disease in the extremities? **c**) At what frequency do displacement artifacts occur?

MATERIAL & METHODS

Patients

Between November 1994 and January 1996, 31 consecutive patients (13 male, 18 female; mean age, 55 years; age range, 13-85 years) clinically suspected of having bone marrow disease were referred for MR imaging. The location of the suspected disease was the foot and ankle (n=23), lower legs (n=5), or hand and wrist (n=3). Indications were mainly infection and posttraumatic changes. In this group, there were 14 patients with neuropathic foot disease with possible osteomyelitis.

Two-point Dixon chemical shift imaging was performed as an extension of the routine clinical MR imaging examination. In four patients, follow-up two-point Dixon chemical shift imaging examinations were performed. In a previous study [15], the image quality of two-point Dixon chemical shift imaging was tested in four healthy volunteers.

Two-Point Dixon Chemical Shift Imaging Technique

All MR examinations were performed at our institution (Academic Medical Center, Amsterdam, the Netherlands) on a 1.5 T Magnetom 63SP/4000 imager (Siemens, Erlangen, Germany). The hand or foot of interest was placed inside the circularly polarized head coil.

This coil was used because it provided the best signal-to-noise ratio; the quality of our dedicated extremity coil at that time was inferior to the quality of the head coil. The technique we used is based on the chemical shift technique described by Dixon [9]. A Dixon study consists of two spin-echo series. The first one is a conventional spin-echo series. The second series is identical to the first one, except that the 180 ° inverting radio-frequency pulse is shifted by a time τ, such that in the center of the readout gradient ($k_x = 0$) the signals of water and fat have opposed-phases [9,16]. The value of τ depends on the field strength (1.5 T) and on the frequency difference between fat ($-CH_2-$) and water (H_2O), which is approximately 3.4 ppm. Because of the presence of other resonances in the fat molecules, the optimal value for τ varies a little with the chemical composition of the lipids [17]. For the extremities, we use an optimal τ of 1.17 msec.

In the conventional spin-echo series, the water and fat signals are in-phase, yielding images in which water and fat signal intensities add up. The opposed-phase series yields images in which the water and fat signal intensities are subtracted. By combining the two sets of images with a proper postprocessing procedure, the water and fat signals are separated, which leads to images in which there is only a water signal, so-called water-only images, and therefore fat-suppression, and images in which there is only a fat signal, so called fat-only images. The postprocessing was performed on a workstation (SPARC 20-51; Sun Microsystems, Mountain View, Calif) by using a region-growing algorithm developed in our department [14].

In the present examinations, we used T1-weighted Dixon studies (570-620/17 [repetition time msec/echo time msec]; section thickness, 3 mm; number of signals acquired, two to three; matrix 256 x 256; field of view, 150-240 mm). The acquisition time was 5-7 minutes for one spin-echo series and therefore was 10-14 minutes for a Dixon study. The series were performed in succession, because it was not possible to image the in-phase and opposed-phase series interleaved.

Administration of Gadopentetate Dimeglumine

As mentioned in the introduction, the use of gadopentetate dimeglumine with STIR is not appropriate. Gadolinium produces a shortening of the T1 in water, and because STIR suppresses all short T1 species, it suppresses

fat and gadolinium-containing water alike. The Dixon technique, on the other hand, like the conventional fat-saturation method, is based on the frequency difference between fat and water. So, T1-weighted Dixon water-only images will show gadolinium enhancement just as conventional T1-weighted images do.
Gadopentetate dimeglumine (0.1 millimole per kilogram of body weight; Magnevist; Schering, Berlin, Germany) was administered intravenously when desirable, mainly for the demarcation of abscesses or the detection of osteomyelitis. We routinely performed one Dixon study before and one after the administration of gadopentetate dimeglumine.

Analysis
In retrospect, two musculoskeletal radiologists (M.M., P.F.D.) analyzed the consecutive Dixon studies by consensus and considered the following parameters: **a**) Uniformity was defined as overall uniform fat-suppression in the entire field of view. For this purpose, water-only images were evaluated. Uniformity was scored as "Yes" or "No". **b**) Displacement artifacts were scored by interpreting the water-only images as showing **I**) "no displacement" or good image quality, **II**) "little displacement" or acceptable, still diagnostic image quality; or **III**)"much displacement" or unacceptable, nondiagnostic image quality. The fat-only images were not used for diagnostic purposes.

RESULTS

Dixon studies
Of the 31 patients, one patient with neuropathic foot disease could not refrain from moving during MR imaging, which led to motion artifacts on the conventional MR image; so, no Dixon postprocessing was performed. In the remaining 30 patients (12 male, 18 female; mean age 54.5 years; age range, 13-85 years), 64 Dixon studies were performed (Table 1).
In seven patients (eight Dixon studies; one patient underwent two Dixon studies) there was no need for the administration of gadopentetate dimeglumine. Sixteen patients (32 Dixon studies; 16 studies before and 16 studies after contrast medium administration) underwent a single examination with the administration of gadopentetate dimeglumine. Two patients underwent an examination before and after the administration of gadopentetate dimeglumine and the same in a follow-up study

(eight Dixon studies), and two patients underwent an examination before and after the administration of gadopentetate dimeglumine and the same in two follow-up studies (12 Dixon studies). In three patients, Dixon studies were performed only after the administration of gadopentetate dimeglumine because there were logistic problems. This resulted in four Dixon studies, because one patient underwent two Dixon studies.

Table 1. Distribution of patients and Dixon Studies

Examinations	No. of Patients (n = 30)	Neuropathic Feet (n = 13)	No. of Dixon Studies (n = 64)
One examination: Dixon studies without Gadolinium enhancement	7	1	8
One examination: Dixon studies after Gadolinium enhancement	3	3	4
One examination: Dixon studies before and after Gadolinium enhancement	16	7	32
Two examinations (one follow-up): Dixon studies before and after Gadolinium enhancement	2	1	8
Three examinations (two follow-up): Dixon studies before and after Gadolinium enhancement	2	1	12

Analysis

Uniformity.- In 64 (100%) Dixon studies, uniform fat-suppression in the entire field of view was attained. This was evident to both radiologists. There were no artifacts in the fat-water separation. The water-only images showed no areas of persistent fat signal intensity (Fig. 1). Also, in the phalanges, there was complete fat-suppression.

Figure 1. Sagittal, water-only, non-contrast medium-enhanced, MR image (620/17) of the foot. There is homogeneous fat-suppression in both the bone marrow and the subcutaneous fat. No displacement artifacts are seen.

Displacement-artifacts. - In 59 (92%) Dixon studies, there was no sign of displacement. in four (6%) Dixon studies, we found little displacement (Fig. 2a).

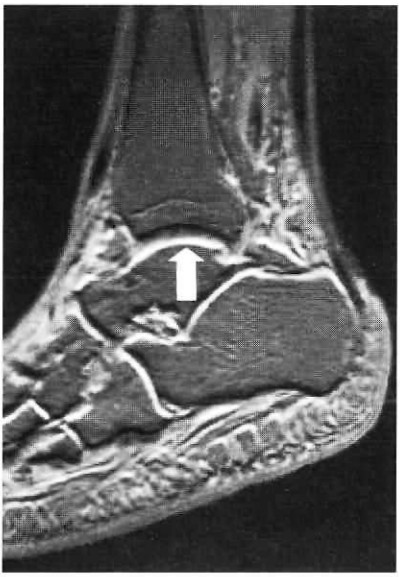

a.

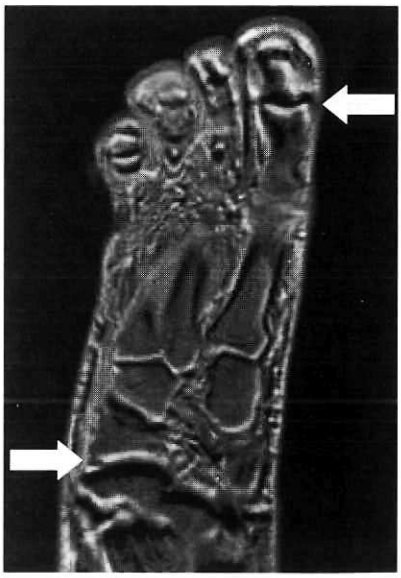

b.

Figure 2. (a) Sagittal, water-only, unenhanced, MR image (620/17) of the foot shows minor displacement artifacts (arrow) best appreciated at the margins of the bones. (b) Axial water-only MR image (620/17) of the foot shows severe displacement artifacts (arrows), which hampered interpretation.

However, in this group of patients, the interpretation of the studies was not a problem, as an adequate evaluation was possible. In only one (2%) Dixon study was the displacement severe; in this patient, the in-phase and opposed-phase images were of good quality, but the patient had moved between the two series. Therefore, the postprocessed images were not of diagnostic quality (Fig. 2b). Consensus between the two radiologists about the degree of displacement artifact was readily achieved in all cases. Thus, in 63 (98%) Dixon studies, the MR image was of diagnostic quality, and interpretation was not hampered by displacement artifacts.

Discussion

For the detection of subtle bone marrow disease, use of fat-suppression sequences in state-of-the-art musculoskeletal MR imaging is mandatory [1]. The appreciation of subtle bone marrow changes is easier when the high signal of the fatty bone marrow is suppressed. The STIR sequence and the frequency-selective presaturation sequence, both of which are routine sequences on the modern MR imager, can fulfill this need adequately for most parts of the human body. In clinically complex situations, there is an additional value in using intravenously administered gadopentetate dimeglumine [7]. Because, from a diagnostic point of view, STIR is incompatible with this use of gadolinium (as gadolinium shortens T1), the use of frequency-selective presaturation is necessary. However, the high field homogeneity that is essential for this technique cannot be attained in hands and feet, which causes inhomogeneous fat-suppression. Inhomogeneous fat-suppression leads to problems in the investigation of neuropathic foot disease and osteomyelitis; this is a problem recognized in the literature [15,18].

Because chemical shift imaging, as described by Dixon [9], in combination with an appropriate postprocessing technique, such as that developed in our department [14,15], is a potentially good alternative for obtaining fat-suppressed images, we examined its use in a clinical setting on a routine basis.

We were able to obtain uniform fat-suppression in the entire field of view in every study. However, we did not perform another fat-suppression technique at the same time, which renders a comparative study of several techniques impossible.

A potential weakness of the Dixon technique is the shift of position between the in-phase and opposed-phase series, which leads to displacement artifacts [1,3]. Because the amount of displacement perpendicular to the imaging plane cannot be estimated from the image data, and because nonuniform displacement (eg, the bending of a toe) is even harder to quantify, we chose a qualitative analysis of this phenomenon. Displacement artifacts were encountered in only five (8%) Dixon studies. Only one (2%) Dixon study was inconclusive because of too much displacement between in-phase and opposed-phase images. To prevent displacement artifacts, we seek to develop a sequence in which both the in-phase and opposed-phase series can be acquired interleaved in one sequence. Thus, our clinical results with this Dixon technique are both applicable and promising.

Diagnosing osteomyelitis is a well-known challenge in diagnostic radiology [19,20]. In neuropathic foot disease, the discrimination between neuropathic osteoarthropathy and osteomyelitis is an additional problem. Because of inhomogeneous suppression of the high marrow signal on both T1-weighted spin-echo and fast T2-weighted spin-echo images, some parts of the foot cannot be judged adequately and are prone to misconception [1]. Therefore, homogeneous fat-suppression in the entire field of view both before and after the intravenous administration of gadopentetate dimeglumine is mandatory. The results of the present study indicate that our two-point Dixon chemical shift imaging technique leads to good uniform fat-suppression. Its potential to help obtain images both before and after the intravenous administration of gadopentetate dimeglumine is an important development and may be of benefit in diagnosing osteomyelitis in complex situations and in the distal parts of the extremities, such as the neuropathic foot (Fig. 3). Further studies in this field are necessary and will be performed.

With respect to the research questions posed in the introduction, we can conclude the following: **a**) Two-point Dixon chemical shift imaging can be used to obtain uniform fat-suppression in the hands and feet. **b**) Two-point Dixon chemical shift imaging is applicable in a clinical setting on a routine basis.

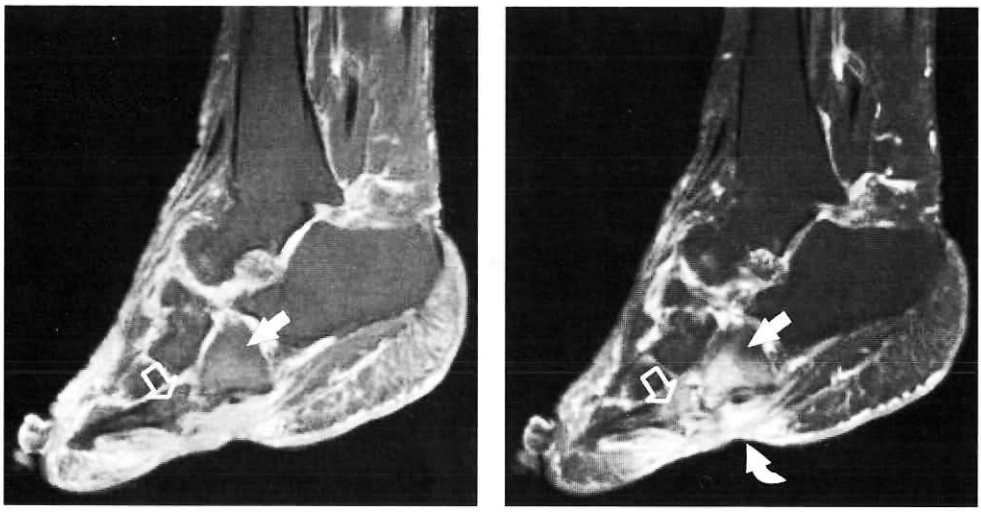

a. **b.**

Figure 3. Sagittal water-only MR images (620/17) (a) before and (b) after the intravenous administration of gadopentetate dimeglumine in a patient with neuropathic foot disease and an arthrodesis in the tibiotalar joint. a shows slight hyperintensity in the cuboid bone (solid arrow) and the base of the fourth metatarsal bone (open arrow). b shows marked focal enhancement in the cuboid bone (solid straight arrow) and the base of the fourth metatarsal bone (open arrow), which supports the clinical diagnosis of osteomyelitis. Also, note the plantar ulcer with cellulitis (solid curved arrow).

Because of its potential to help obtain fat-suppressed images both before and after the administration of gadopentetate dimeglumine, the technique can be used in evaluating bone marrow disease in the hands and feet, where the magnetic field is less homogeneous. Therefore, this technique is of potential benefit in the diagnosis of osteomyelitis, especially in complex situations, such as those involving neuropathic foot disease. Further study is necessary to explore this. (**c**) Displacement artifacts occur in a minority of studies.

ACKNOWLEDGMENTS

The authors thank Feikje M. Gubler, MD, PhD, Edwin J.R van Beek, MD, PhD, William R. Faber, MD, PhD, and Mirjam R.W. Evers-van Bavel for their aid in the preparation of this manuscript and Gerard J. den Heeten, MD, PhD, Jaap Stoker, MD, PhD, and Henk W. Venema, PhD, for their valuable suggestions during the revision process.

REFERENCES

1. Peterfy CG, Linares R, Steinbach LS. Recent advances in magnetic resonance imaging of the musculoskeletal system. Radiol Clin North Am 1994; 32:291-311.
2. Rubin DA, Kneeland JB. MR imaging of the musculoskeletal system: technical considerations for enhancing image quality and diagnostic yield. AJR 1994; 163:1155-1163.
3. Mirowitz SA. Fast scanning and fat-suppression MR imaging of musculoskeletal disorders. AJR 1993; 161:1147-1157.
4. Mirowitz SA. Musculoskeletal MRI techniques: clinical magnetic resonance imaging. 2nd ed. Philadelphia, Pa: Saunders, 1996; 1797-1819.
5. Peterfy CG, Roberts T, Genant HK. Dedicated extremity MR imaging: an emerging technology. Radiol Clin North Am 1997; 35:1-20.
6. Anzai Y, Lufkin RB, Jabour BA, et al. Fat-suppression failure artifacts simulating pathology on frequency-selective fat-suppression MR images of the head and neck. AJNR 1992; 13:879-884.
7. Morrison WB, Schweitzer ME, Bock GW, et al. Diagnosis of osteomyelitis: utility of fat-suppressed contrast-enhanced MR imaging. Radiology 1993; 189:251-257.
8. Dangman BC, Hoffer FA, Rand FF, O'Rourke EJ. Osteomyelitis in children: gadolinium-enhanced MR imaging. Radiology 1992; 182:743-747.
9. Dixon WT. Simple proton spectroscopic imaging. Radiology 1984; 153:189-194.
10. Chan TW, Lisreud J, Kressel HY. Combined chemical-shift and phase-selective imaging for fat suppression: theory and initial clinical experience. Radiology 1991; 181:41-47.
11. Tsushima Y, Ishizaka H, Matsumoto M. Adrenal masses: differentiation with chemical shift, fast low-angle shot MR imaging. Radiology 1993; 186:705-709.
12. Mitchell DG, Crovello M, Matteucci T, Petersen RO, Miettinen MM. Benign adrenocortical masses: diagnosis with chemical shift MR imaging. Radiology 1992; 185:345-351.
13. Dunnick NR, Korobkin M, Francis I. Adrenal radiology: distinguishing benign from malignant adrenal masses. AJR 1996; 167:861-867.
14. Akkerman EM, Maas M. A region-growing algorithm to simultaneously remove dephasing influences and separate fat and water in two-point Dixon imaging (abstr). In: Proceedings of the Society for Magnetic Resonance in Medicine and the European Society for Magnetic Resonance in Medicine and Biology 1995; 649.

15. Maas M, Akkerman EM, Dijkstra PF, Verbeeten B Jr. Fat-suppression imaging of hands and feet using a two-point Dixon technique (abstr). In: Proceedings of the Society for Magnetic Resonance in Medicine and the European Society for Magnetic Resonance in Medicine and Biology 1995; 1518.
16. Lee JKT, Dixon WT, Ling D, Levitt RG, Murphy WA Jr. Fatty infiltration of the liver: demonstration by proton spectroscopic imaging. Radiology 1984; 153:195-201.
17. Brix G, Heiland S, Bellemann ME, Koch T, Lorenz WJ. MR imaging of fat-containing tissues: valuation of two quantitative imaging techniques in comparison with localized proton spectroscopy. Magn Reson Imaging 1993; 11:977-991.
18. Peterfy CG, Garvin GJ, Tirman PFJ, Majumdar S, Wendland M, Genant HK. Incomplete fat-suppression with spectral presaturation on MR images of the foot and ankle: clinical implications and practical solutions (abstr). In: Proceedings of the Society for Magnetic Resonance in Medicine and the European Society for Magnetic Resonance in Medicine and Biology 1995; 1516.
19. Moore TE, Yuh WTC, Kathol MH, El-Khoury GY, Corson JD. Abnormalities of the foot in patients with diabetes mellitus: findings on MR imaging. AJR 1991; 157:813-816.
20. Marcus CD, Ladam-Marcus VJ, Leone J, Malgrange D, Bonnet-Gausserand FM, Menanteau BP. MR imaging of osteomyelitis and neuropathic osteoarthropathy in the feet of diabetics. RadioGraphics 1996; 16:1337-1348.

CHAPTER 3

MRI in clinically asymptomatic neuropathic leprosy feet: A baseline study

Mario Maas[1], Erik J. Slim[1], Erik M. Akkerman[1], William R. Faber[2]

[1]Department of Radiology, [2]Department of Dermatology, Academic Medical Center, Amsterdam, the Netherlands

Int J Leprosy other Mycobact Dis 2001; 69: 219-224

INTRODUCTION

Leprosy is an infectious disease caused by *Mycobacterium leprae*, that affects 2-10 million patients worldwide. It preferably invades skin and peripheral nerves.

In leprosy the neuropathic foot is one of the major contributors to morbidity due to peripheral nerve damage. Repeated injury subsequently may lead to considerable osseous and articular destruction secondary to sensory loss. The skeletal abnormalities may be severe and are evident in 20 % - 70 % of hospitalized patients [15]. The neuro-osteoarthropathy (Charcot deformity) in leprosy is comparable to that in diabetes and may lead to tarsal disintegration with osteolysis, fragmentation and progressive bone resorption. In extreme cases, dissolution of the midfoot results in separation of the forefoot and the hind foot, changing all biomechanics and weight bearing areas.

Diagnostic problems begin when a patient develops a neuropathic foot with clinical signs of inflammation, for example, ulceration, cellulitis, osteomyelitis and neuro-osteoarthropathy (Charcot foot). Clinical signs often are not conclusive in discriminating between infection (cellulitis or osteomyelitis) and neuro-osteoarthropathy [6]. Early detection of feet at risk is preferable to help prevent these complications.

Diagnosing osteomyelitis is a well known challenge in diagnostic radiology [9,10]. Magnetic Resonance Imaging (MRI) has been described as an important modality to assess the neuropathic feet of diabetic patients [2,5,18]. For the detection of subtle bone marrow pathology it is mandatory to use fat-suppression sequences in state-of-the-art musculoskeletal MRI [14]. A homogeneous fat-suppression in the entire field of view, both before and after intravenous contrast material (Gadolinium-chelate (Gd)) is necessary to avoid confusion [14]. This can adequately be achieved by the use of two-point Dixon chemical shift imaging (TPDCSI) [8].

The question was raised whether changes prior to the appearance of clinical signs are present and detected by early MRI. Since it is likely that early changes may occur, this lack of information may hamper the adequate reading of the MRI studies of symptomatic patients. All data available in the literature address clinically complicated neuropathic feet. To our knowledge, no papers concerning MRI in asymptomatic neuropathic feet exist.

In this study our goal was to answer the following questions: **a)** What is the MRI appearance of the asymptomatic neuropathic foot in leprosy patients? Are there MRI changes present in these patients? **b)** When changes are present, is there a role for MRI in relation to clinical management in the early assessment of the asymptomatic neuropathic foot in leprosy patients?

MATERIAL & METHODS

Patients

From the database of the outpatient clinic of the Department of Dermatology, Academic Medical Center, Amsterdam, The Netherlands, 10 adult patients (5 male, 5 female, mean age 54 years (31-70 years) with leprosy were selected. Inclusion criteria for entering this study were neuropathic feet with a normal or nearly normal foot, i.e., no Charcot deformity, no ulcer, and no signs of inflammation at the time of the study. The dermatologist in charge of the leprosy clinic (WRF) screened patients for inclusion. None of the feet had a history of osteomyelitis. The skin temperature was measured by palpation [7]. No active ulcers and/or signs of inflammation were found. All patients entering the study signed an informed consent. The Medical Ethics Committee of our hospital approved the study.

A neuropathic foot was defined as a foot in which one or more of the neuronal functions, i.e., sensory, motor function or autonomic functions, were disturbed (consensus of the Dutch Neuropathic Foot Society). Sensory loss was tested using the Semmes-Weinstein monofilament test [1]. Patients were included when the sensory loss was a 10-gram force.

MRI procedure

An MRI examination was performed using a 1.5 Tesla Vision (Siemens, Erlangen, Germany). The foot of interest was placed inside the circularly polarized head coil. This coil was used because it provided the best signal to noise ratio. The MRI protocol consisted of: Sagittal Turbo-STIR (short tau inversion recovery) (3mm), T1-weighted Dixon sequence [8], sagittal and coronal dual echo T2-weighted FSE (fast spin echo) (3mm); after the administration of Gd intravenously T1-weighted Dixon sequence and a coronal fat-suppression T1-weighted sequence. The MRI-examinations were evaluated by a musculoskeletal radiologist blinded to the clinical findings (MM).

Table 1. Clinical demographics of the patients at the intake at the outpatient clinic .

No	Sex	Age	Type	Clinical history	Foot	Footform	Ulcer	Callus	Sensibility	Paresis	Skin
1	F	66	BL	negative	right	clawtoes	no	no	impaired	no	normal
2	M	69	LL	negative	left	clawtoes	no	no	impaired	no	hyper-keratosis
3	M	44	BL	negative	right	normal	no	MTP1	impaired	peroneal nerve	dry skin
4	F	48	LL	negative	right	normal	no	MTP1	impaired	peroneal nerve	normal
5	M	53	BL	negative	right	normal	no	MTP5	impaired	no	dry skin
6	M	70	BT	negative	left	normal	no	no	impaired	no	hyperpig-mentation
7	F	41	BT	negative	left	normal	no	no	impaired	next digitorum	normal
8	F	47	L	Ulcer distal phalanx digit 1	right	clawtoes	no	no	impaired	no	fissures
9	M	32	BL	negative	right	normal	no	no	impaired	no	dry skin
10	F	46	L	negative	right	shortened dig IV, V	no	no	impaired	no	normal

BL=borderline lepromatous, LL=lepromatous leprosy , BT= borderline tuberculoid,
L =Lepromatous (Lepromatous side of the spectrum)

RESULTS

Clinical findings (Table 1)

The right foot was examined in eight patients and the left foot in two patients. The shape of the foot was completely normal in six patients. Claw toes were present in two patients, and two patients showed minor deformities due to earlier disease. No ulcers were present. Callus was present in three patients, twice located beneath the first metatarsophalangeal (MTP) joint and once beneath the fifth MTP joint.

Sensory function was impaired in all patients. Motor function was normal in seven patients. Three patients showed a paresis. The autonomic function, as demonstrated by dry skin and fissures, was impaired in five patients.

MRI findings (Table 2)

Bone marrow: In 9 of the 10 patients there was a normal MR signal in the bone marrow; no bone marrow edema was found. There was no bone marrow enhancement seen after administration of contrast material. No bone destruction was found.

Table 2. MRI results of all patients.

No.	Bone marrow edema	Effusion	Subcutaneous fat	Enhancement	Fistula/ ulceration	Midfoot changes
1	no	MTP1	infiltr. MTP1,2,3,4	no	no	early osteoarthritis
2	no	MTP1	infiltr. MTP1	MTP1	MTP1	
3	MTP1	MTP1	infiltr. MTP1	MTP1	no	
4	no	MTP1	intact	no	no	early osteoarthritis
5	no	MTP1	infiltr. MTP1	no	no	
6	no	no	infiltr. MTP1	no	no	
7	no	no	infiltr. MTP1	MTP1	no	early osteoarthritis
8	no	no	intact	no	no	
9	no	MTP1	intact	no	no	
10	no	MTP1	intact	no	no	

Joints: Joint effusion was seen in seven patients, and in all of these patients located in the first MTP joint. Local contrast enhancement in the first MTP joint was present in three patients.

Soft tissue: Infiltration of the subcutaneous fat was depicted in six patients, and in all of these patients was located plantar to the first MTP joint.

The skin was intact on the surface of the foot in 9 of the 10 patients. An unexpected fistula was found in one patient, located at the first MTP joint.

Midfoot: In two patients, early osteoarthritic changes were found in the midfoot. No disintegration of the tarsus was found.

DISCUSSION

MRI is the most valuable imaging technique in the evaluation of complications of the diabetic neuropathic foot [9,12,17]. The use of homogeneous fat-suppression in combination with contrast administration is found to be a very sensitive tool in evaluating neuropathic feet [9,11]. All data are from diabetic patients, being by far the most common cause of neuropathic feet in the Western world.

This study is new because it includes leprosy patients who represent another important cause of neuropathic foot pathology. We investigated clinically asymptomatic feet in order to acquire a baseline MRI for leprosy patients. Since it can be expected that in future MRI will be part of imaging protocols for leprosy patients with complications of a neuropathic foot, it is to be expected that MRI results will gain influence on clinical decision-making. This necessitates a study in clinical asymptomatic patients in order to acquire a baseline database of MRI findings. This may be the only way to adequately detect the changes that represent osteomyelitis in the complicated patient group.

The results that we found are remarkable. All of our patients had no clinical symptoms at the time of MRI, yet MRI abnormalities were found in almost all patients. The most striking findings were the changes located in the region of the first MTP joint in the majority of patients (90%) (Figure 1 and 2).

These abnormalities ranged from degradation and interruption of the subcutaneous fat, plantar fascia, and a small fistula to effusion/synovitis in the first MTP joint.

The soft tissue damage in the foot, plantar to the first metatarsal bone, has been described in diabetic feet with a significant difference between neuropathic and non-neuropathic feet [3]. It was hypothesized that the subcutaneous lesions may consist of fibrosis [3] or hemorrhage [4]. Moreover, it was suggested that the presence of this fatpad degradation might precede plantar ulceration.

Figure 1. Sagittal T1 out of phase Dixon image of the foot of patient 1. Note the normal plantar subcutaneous fat (with a bright signal). The interruption of the subcutaneous fat plantar to the metatarsophalangeal joint is illustrated with an arrow.

Figure 2. Detailed sagittal Dixon fat sat water image of the first metatarsophalangeal joint of patient 7. Note the enhancement of the head of the first metatarsal bone (one arrow) and the joint effusion/synovitis (two arrows).

The same suggestion can be made in the leprosy population. Stress analysis studies in three-dimensional foot models of leprosy patients show that the musculoskeletal stresses during walking are higher in leprosy patients than in healthy controls, being 24%-65% higher in early stage leprosy patients [13]. Patil *et al.* [13] conclude that the highest soft tissue stresses and shear stresses occur in the push off phase in scar tissue. The difference in shear stresses between the sole of the foot and the adjacent soft tissue layer in the scar tissue is about three times the normal value [13]. Since the push-off phase of the walking cycle takes place under the metatarsals, this may be related to the changes we found in our group of patients. Our findings support the conclusion that this may precede the development of plantar ulcers in these patients.

Our study reveals significant MRI findings in asymptomatic neuropathic feet in patients with leprosy. The changes we found with fat-suppressed contrast-enhanced MRI are possibly related to the future development of ulcerations. It is conceivable that these changes can be detected when more thorough physical examination is performed. A consequence of this study could be that more attention is paid to the clinical examination of asymptomatic neuropathic feet.

Further research is necessary to investigate the potential role of MRI in the early detection of complications and its role in the clinical management of leprosy patients with neuropathic feet. Also, because of the recent introduction of less-expensive, dedicated extremity MRI, the implementation of MRI in the workup of leprosy patients may soon be possible outside the Western world.

SUMMARY

This study was undertaken to analyze the magnetic resonance imaging (MRI) findings in the clinically asymptomatic neuropathic feet of leprosy patients. Since in the literature no MRI data are available concerning the asymptomatic neuropathic foot in leprosy, the interpretation of MRI examinations in clinical suspected neuropathic feet in leprosy is difficult.

We examined 10 adult leprosy patients with clinically asymptomatic neuropathic feet. Inclusion criteria were a normal or near normal neuropathic foot, without signs of inflammation. All patients underwent an MRI protocol with the inclusion of two-point Dixon chemical shift imaging as fat-suppression sequence. We found MRI changes in almost all patients. The most striking were the changes located in the region of the first metatarsophalangeal (MTP) joint. These changes ranged from degradation and interruption of the subcutaneous fat to effusion/synovitis in the first MTP joint.

This study reveals significant MRI changes in clinically asymptomatic neuropathic feet in patients with leprosy. These changes may relate to the development of ulcerations. MRI may play an important role in detecting feet at risk and may influence clinical decision making.

ACKNOWLEDGEMENT

The Q. M. Gastman-Wichers Foundation financially supported this study.

The authors wish to thank Dr. Gemila Hassan Bouber and Mrs. M.R.W. Evers-van Bavel for their support in the preparation of this manuscript. Prof dr. A. Huson is acknowledged for his critical review of the manuscript.

REFERENCES

1. Anderson AM, Croft RP. Reliability of Semmes Weinstein monofilament and ballpoint sensory testing, and voluntary muscle testing in Bangladesh. Leprosy Review 1990; 70:305-313.
2. Beltran J, Campanini DS, Knight C, McCalla M. The diabetic foot: magnetic resonance evaluation. Skeletal Radiology 1990; 19:37-41.
3. Brash PD, Foster JE, Anthony P, Tooke JE. Magnetic resonance imaging techniques demonstrate soft tissue damage in the diabetic foot. Diabet Med 1999; 16:55-61.
4. Brash PD, Foster JE, Vennart W, Daw J, Tooke JE. Magnetic resonance imaging reveals Micro-haemorrhage in the feet of diabetic patients with a history of Ulceration. Diabet Med 1996; 13:973-978.
5. Craig JG, Amin MB, Wu K, Eyler WR, van Holsbeeck MT, Bouffard JA, Shirazi K. Osteomyelitis of the diabetic foot: MR imaging-pathologic correlation. Radiology 1997; 203:849-855.
6. Faber WR, Hoeksma AF, van der Kleij AJ, Maas M, Dijkstra PF. Diagnostic procedures for suspected osteomyelitis in neuropathic feet of leprosy patients. Int J Lepr 1998; 66:29A.
7. Hoeksma AF, Faber WR. Assessment of skin temperature by palpation in leprosy patients: interobserver reliability and correlation with infrared thermometry. Int J Lepr 2000 ; 68 :65-67.
8. Maas M, Dijkstra PF, Akkerman EM. Uniform fat suppression in hands and feet through the use of two-point Dixon chemical shift MR imaging. Radiology 1999; 210:189-193.
9. Marcus CD, Ladam-Marcus VJ, Leone J, Malgrange D, Bonnet-Grausserand FM, Mentaneau BP. MR imaging of osteomyelitis and neuropathic osteoarthropathy in the feet of diabetics. Radiographics 1996; 16:1337-1348.
10. Moore TE, Yuh WTC, Kathol MH, El-Khoury GY, Corson JD. Abnormalities of the foot in patients with diabetes mellitus: findings on MR imaging. AJR 1991; 157:813-816.
11. Morrison WB, Schweitzer ME, Bock GW, Mitchell DG, Hume EL, Pathria MN, Resnick D. Diagnosis of osteomyelitis: Utility of fat-suppressed contrast-enhanced MR imaging. Radiology 1993; 189:251-257.
12. Morrison WB, Schweitzer ME, Wapner KL, Hecht PJ, Gannon FH, Behm WR. Osteomyelitis in feet of diabetics: Clinical accuracy, surgical utility, and cost-effectiveness of MR imaging. Radiology 1995; 196:557-564.
13. Patil KM, Jacob S. Mechanics of tarsal disintegration and plantar ulcers in leprosy by stress analysis in three-dimensional foot models. Indian J Leprosy 2000; 72:69-86.

14. Peterfy CG, Linares R, Steinbach LS. Recent advances in magnetic resonance imaging of the musculoskeletal system. Rad Clin North America 1994; 32:291-311.
15. Resnick D, Niwayama G. Diagnosis of bone and Joint disorders 3rd edition vol 4. Chapter 66: Osteomyelitis, septic arthritis and soft tissue infection: Organisms. WB Saunders Company Pensylvania 1995; 2486-2492.
16. Schon LC, Easley ME, Weinfeld SB. Charcot neuroarthropathy of the foot and ankle. Clinical Orthopaedics and Related Research 1998; 349:116-131.
17. Tomas MB, Patel M, Marwin SE, Palestro CJ. The diabetic foot. The British Journal of Radiology 2000; 73:443-450.
18. Yuh JS. Diabetic foot and neuroarthropathy magnetic resonance imaging evaluation. Topics in Magnetic Resonance Imaging 1998; 9:295-230.

CHAPTER 4

MR Imaging of neuropathic feet in leprosy patients with suspected osteomyelitis

Mario Maas [1], Erik J. Slim [1,4], Agnes F. Hoeksma [4], Ad J. van der Kleij [3], Erik M. Akkerman [1], Gerard J. den Heeten [1], William R. Faber [2]

Department of Radiology [1], Dermatology [2] and Surgery [3], Academic Medical Center and the department of Rehabilitation, Jan van Breemen Institute [4], Amsterdam, the Netherlands

Submitted

INTRODUCTION

The invasion by *Mycobacterium leprae* of Schwann cells with the resulting peripheral nerve damage can lead to a so-called neuropathic foot. Ulceration and infection (cellulitis or osteomyelitis) are important complications. Repeated injury secondary to the neuropathy may lead to tarsal disintegration with osteolysis, fragmentation and progressive bone resorption. In extreme cases dissolution of the mid-foot results in separation of the forefoot and the hindfoot, changing all biomechanics and weight bearing areas [1,11,12,22]. The neuro-osteoarthropathy in the foot is a cause of considerable morbidity in leprosy [9,12,22,26]. Therefore, when a patient with a neuropathic foot presents himself with a warm foot, it is a clinical challenge to discriminate between neuro-osteoarthropathy and an ongoing osteomyelitis. Especially, this is difficult in the presence of an ulcer, because an ulcer itself leads to increased local temperature [10,22].

Various diagnostic modalities have been investigated in the analysis of osteomyelitis in neuropathic feet [5,13,24,28]. Magnetic Resonance Imaging (MRI) has been described as an important modality to assess osteomyelitis in the neuropathic foot of diabetic patients [16,18-20,27]. Tissue characterisation and spatial resolution facilitate identification of associated soft tissue pathology [2-4,16,30]. To detect subtle bone marrow pathology, such as a low-grade chronic infection, it is mandatory to use fat-suppression sequences with the use of contrast administration [19-21]. A homogeneous fat-suppression in the entire field of view both before and after intravenous contrast material (Gadolinium-chelate (Gd)) is required, to avoid artefacts and misreading [23]. This can adequately be achieved by the use of two-point Dixon chemical shift imaging (TPDCSI) [14,19].

The radiological literature available on MRI and osteomyelitis in neuropathic feet nearly exclusively concerns diabetic foot pathology, being the most frequent cause of neuropathic feet in the western world. However, leprosy is an important cause of neuropathic feet worldwide. According to the latest World Health Organization (WHO) information at the end of the year 2000 597.232 cases are on treatment, and 719.330 new cases are reported [29].

Literature concerning MRI and leprosy is scarce. Recently, an MRI study of neuropathic leprosy feet without clinical signs of inflammation was published [15]. As far as we know, no papers concerning the use of MRI in neuropathic leprosy feet, clinically suspected of osteomyelitis exist. In this paper we present our results with MRI in leprosy patients with neuropathic feet clinically suspected for osteomyelitis. The purpose of this study was to analyze the value of MRI in diagnosing osteomyelitis as a single diagnostic procedure. The MRI findings are compared to the signs described in literature for evaluating osteomyelitis. These MRI results were compared to the gold standard (bone biopsy or bone culture) or when no gold standard was available the MRI results were compared to the clinical outcome after six months.

MATERIAL & METHODS

Patients

We retrospectively evaluated all consecutive MRI studies, following the Dixon protocol (see later) of the foot in leprosy patients performed in the period 1994-2000. All patients had longstanding neuropathic foot pathology and were clinically suspected for inflammation; they had a neuropathic warm swollen foot that did not respond to conservative weight reduction therapy. A neuropathic foot was defined as a foot in which one or more of the neuronal functions i.e. sensory, motor function or autonomic function was disturbed (consensus of the Dutch Neuropathic Foot Society) [7]. Furthermore, the clinical follow-up had to cover a period of six months.

Clinical criteria

Patient charts were reviewed for clinical information concerning leprosy classification [25], presence and location of an ulcer and clinical signs of inflammation. Twelve patients with neuropathic feet clinically suspected for osteomyelitis were investigated, in which 18 MRI studies were performed. The patients were classified as borderline lepromatous (n=3), borderline tuberculoid (n=1), and at the lepromatous side of the spectrum (n=8).

The gold standard for the diagnosis of osteomyelitis was a positive culture and/or histopathology taken from bone material.

Clinical outcome after 6 months follow-up was retrospectively evaluated in cases where histopathology or culture was not available or not conclusive. A combination of clinical criteria was evaluated in a consensus reading by a dermatologist (WRF), a physiatrist (AFH) and a surgeon (AJvdK). The clinical criteria that were evaluated were response on antibiotic treatment, nature of surgical treatment when performed, persistent signs of inflammation, status of the ulcer, change in deformity.

Diagnostic criteria (MRI)

A total number of 24 MR studies in 12 adult leprosy patients (9 male, 3 female; mean age 63 years; age range 45-81 years) were included for evaluation. Of these 24 MR studies 18 were performed because of clinical suspicion of osteomyelitis. Follow-up MRI was performed in 6 patients (6 MRI studies).

MRI

MRI examination was performed using a 1.5 Tesla Vision (Siemens, Erlangen, Germany). All MRI studies were performed following the Dixon protocol [6,14,15]. This protocol consisted of: sagittal turbo-STIR (short tau inversion recovery) (3mm), T1-weighted Dixon sequence with in- and opposed-phase images, sagittal dual echo T2-weighted FSE (Fast Spin Echo) (3mm); after the intravenous administration of Gadolinium chelate (0.1 millimol per kilogram of body weight) T1-weighted Dixon sequence with in- and opposed phase images [6,14,15].

To evaluate the MRI studies signs were used as described in literature concerning diabetic neuropathic feet [16,19,20,27]. Typical, primary MRI signs are decreased marrow signal intensity on T1-weighted images, increased signal intensity on fat suppressed T2-weighted and/or fast STIR images, and focal marrow enhancement after Gadolinium-enhanced fat-suppressed T1-weighted images [14,17,20,21,28]. Secondary MRI signs are: the presence of a cutaneous ulcer, cellulitis, a soft tissue mass, a soft tissue abscess, a sinus tract, and cortical interruption [21,30]. One musculoskeletal radiologist (MM) retrospectively evaluated the images blinded to all clinical information except the knowledge of clinical suspicion for osteomyelitis. The signal intensity of the bone marrow on T1-weighted in and out of phase Dixon images, fast STIR images and Gadolinium enhanced T1-weighted in and out of phase Dixon images (primary signs) was classified as normal or abnormal on a data

collecting form. The secondary signs were classified as present or absent. Furthermore, the site of involvement was noted (medial arch, central compartment or lateral arch) [8,12].

RESULTS

Clinical findings

In 8 patients there was one event of suspected osteomyelitis. In 4 patients there were multiple events of suspected osteomyelitis; in 3 patients there were 2 events of suspected osteomyelitis, and in 1 patient there were 4 events of suspected osteomyelitis. The foot of involvement was 6 times right and 12 times left. The location of the ulcer was 2 times at the medial side, 14 times at the lateral side, and 2 times an ulcer was present at the medial and lateral side.

The results of the gold standard are listed in table 1. When evaluating results from bone biopsy or bone culture and/or preset clinical criteria, without detailed knowledge of the MRI results, the diagnosis osteomyelitis was made in 16 of 18 events (88.9%).

Table 1. Results of clinical follow-up in diagnosing osteomyelitis

Event	Gold standard	Clinical outcome	Event	Gold standard	Clinical outcome
1		Pos	10		Pos
2		Pos	11	Pos	
3	Pos		12	Pos	
4	Pos		13		Neg
5	Pos		14		Pos
6		Pos	15		Neg
7		Pos	16	Pos	
8		Pos	17	Pos	
9	Pos		18		Pos

Diagnostic findings (MRI)

In a total number of 18 events of suspected osteomyelitis we encountered 17 MRI examinations positive for primary MR signs for osteomyelitis (94.4%). Decreased signal on T1 in and out of phase on 16 MRI (88.9%), increased signal on T2 on 13 MRI (72.2%), fast SE STIR on 13 MRI (72.2%), and focally marrow enhancement after gadolinium-enhanced fat suppressed T1 on 17 MRI (94.4%) (Table 2).

Table 2. Primary MRI signs: number of positive findings on various MRI sequences

Positive primary sign	T1	T2	STIR	Contrast
Number of MRI (%)	16 (88.9%)	13 (72.2%)	13 (72.2%)	17 (94.4%)

The secondary signs were positive in all MRI examinations (100%). Cellulitis was present in all cases (100%). A cutaneous ulcer in the region of the suspected osteomyelitis was also present in all cases (100%). Cortical interruption was found in 16 investigations (88.9%). A sinus tract was present in 5 cases (27.7%). A soft tissue abscess was present in 3 cases (16.6%). A soft tissue mass was found on two occasions (11.1%) (Table 3).

Table 3. Presence of positive secondary MRI signs

Positive secondary sign	Cellulitis	Ulcer	Cortical interruption	Sinus tract	Soft tissue abscess	Soft tissue mass
Number of MRI (%)	18 (100%)	18 (100%)	17 (88.9%)	5 (27.7%)	3 (16.6%)	2 (11.1%)

An example of positive primary signs and secondary signs at the lateral side of the foot is shown in figure 1.

Figure 1a. Two-point Dixon fat suppression image of the right foot of a 79-year-old female patient. Note the degradation of the plantar fat with the presence of soft tissue edema (interrupted arrow) and the high signal intensity in the partly destroyed cuboid bone (non-interrupted arrow).

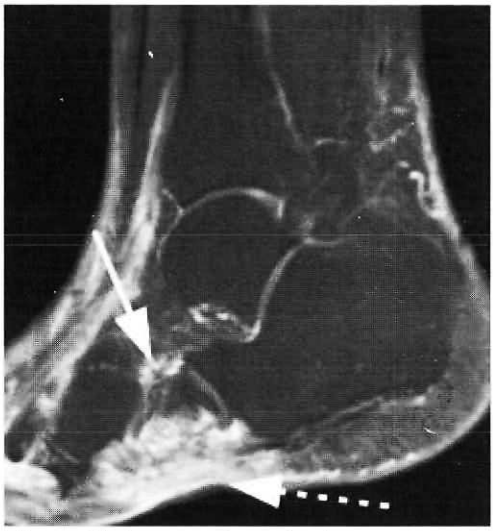

Figure 1b. Same patient after intravenous gadolinium chelate administration. Note the marked enhancement at the lateral side of the foot both in the soft tissue (cellulitis) (interrupted arrow) and in the cuboid bone (osteomyelitis) (non-interrupted arrow).

The sites of involvement (MRI)

The sites of involvement: medial-central-lateral, on MRI were analysed. The areas of osteomyelitis were located at the medial site (MTP1 joint, os metatarsal 1, cuneiform 1, navicular bone) in 3 events, medial/central in 2 events, central (MTP 2-3, os metatarsal 2-4) in 3 events, lateral (MTP 4-5 joint, os metatarsal 4-5, cuboid, calcaneus) in 9 events. In 1 patient all three areas were involved.

Follow-up (MRI)

Six follow-up MRI were made after antibiotic treatment. Mean time of follow-up was 5 months. A complete healing of the ulcer occurred in two patients with a normal follow-up MRI.

Two patients had an improved but still abnormal MRI; the MRI changes that were seen were a reduction but still present zone of enhancement of the bone marrow. Both patients eventually showed a complete clinical remission. The foot of the patient that showed an unchanged follow-up MRI despite continued antibiotics eventually was amputated.

Discussion

Osteomyelitis is a well-known complication in patients with neuropathic foot pathology [4,13,16,19,20,24,26,28,30]. These patients may develop ulcers that persist over a long period of time. In this way spread of infection *per continuitatem* can cause an infection of the osseous structures in the foot. Clinical examination lacks specificity in this patient group, since by clinical examination alone it is difficult to differentiate between cellulitis, osteomyelitis and neuro-osteoarthropathy [22,26]. MR imaging is potential powerful in the evaluation of the neuropathic foot; it is useful for the evaluation of presence and extent of osteomyelitis, as well as for the identification of the presence and extent of associated soft tissue abnormalities that may have clinical importance, such as cellulitis, abscess, and sinus tract [4,16,18-21,27,30]. Nearly all data available on MRI and neuropathic feet concern patients suffering from diabetes. As far as we know this is the first report on the use of MRI as a diagnostic procedure in neuropathic leprosy feet suspected for osteomyelitis.

When analyzing the primary MRI signs for osteomyelitis we found in our population that in 17 out of 18 events (94.4%) primary MRI signs were positive. Decreased signal intensity on in and out of phase T1-weighted images and the marrow enhancement after gadolinium administration on fat-suppressed T1 were the most frequent encountered abnormalities. In our retrospective analysis (gold standard and/or clinical outcome) 16 out of 18 events were diagnosed as positive for osteomyelitis. Comparing this evaluation with the primary MRI signs there was agreement in 17 out of 18 events. The disagreement found in one patient was caused by the primary MRI sign focal marrow enhancement after contrast administration. Therefore, we conclude that these primary signs, used in evaluating MRI examinations in diabetics can adequately be used to analyze MRI examinations in leprosy patients with longstanding complicated neuropathic feet.

Of the secondary MR signs ulcer and cellulitis were present in all cases. The areas on MRI suspected of osteomyelitis were in continuity with the ulcer. The relation between ulcer and osteomyelitis has also been described in diabetes [5]. In contrast to diabetic feet only a minority of examinations revealed a sinus tract or soft tissue abscess in our population [21]; it seems that these latter secondary signs are infrequently found in leprosy. However, the presence of an ulcer and cellulitis is common in leprosy patients with longstanding neuropathic feet suspected for osteomyelitis. Contrary to diabetic foot literature the secondary MRI signs seem of no additional value in diagnosing osteomyelitis in a population of leprosy patients with longstanding neuropathic foot disease. However, the value of these findings in a patient population of leprosy patients with neuropathy and clinical suspicion of inflammation, without longstanding disease was not evaluated in this study. For this purpose a study is currently conducted.

The present study demonstrates in 9 events MRI changes suspected for osteomyelitis at the lateral side only (50%). In a minority of events these changes were found at the medial side only (16.7%). This is in contrast to the results found in a recent study of asymptomatic neuropathic feet in leprosy patients in which 90 percent of the MRI changes were located at the medial site of the foot [15]. Most likely the biomechanics in the two patient groups (clinically unsuspected versus clinically suspected in longstanding neuropathic foot disease) are different. Biomechanical analysis in early tarsal disintegration shows the highest stress to occur during the push off phase in the bones of the lateral foot arch [12]. Perhaps this is caused by inversion due to paralysis of the lateral musculature. An analysis of the walking cycle in two groups of leprosy patients with neuropathic feet with and without clinical abnormalities may be of additional value in order to analyse the stress distribution.

When a leprosy patient with longstanding neuropathic foot disease is suspected of osteomyelitis clinical examination lacks specificity. Contrast enhanced MRI with the use of two-point Dixon chemical shift imaging, as fat-suppression technique is a valuable technique to detect osteomyelitis. The primary MR signs known from literature, concerning diabetic neuropathic foot can adequately be assessed. MRI can serve as a one step diagnostic strategy to diagnose osteomyelitis in leprosy patients with a longstanding neuropathic foot problem.

SUMMARY

This study was undertaken to analyze the MRI findings in leprosy patients with neuropathic feet, suspected for osteomyelitis. As far as we know, no papers concerning osteomyelitis and MRI in neuropathic leprosy feet are present.

We included MRI examination of 18 events of suspected osteomyelitis in 12 leprosy patients. All patients with longstanding neuropathic foot problems were clinically suspected for osteomyelitis. All patients underwent the MRI protocol with the inclusion of two-point Dixon chemical shift imaging as fat-suppression sequence.

For the MRI evaluation we used signs that are described in literature for detecting osteomyelitis in diabetic feet. The primary MRI signs were positive in 17 of 18 patients. The secondary MRI signs were positive in 100% of patients.

Our results show that MRI with the use of two-point Dixon chemical shift imaging is a promising diagnostic modality to detect osteomyelitis in the presence of neuro-osteoarthropathic changes in patients with leprosy. Whenever available MRI could play an important role in detecting osteomyelitis in leprosy patients with longstanding neuropathic feet, suspected for osteomyelitis.

REFERENCES

1. Brandsma JW, Macdonald MRC, Warren AG, Cross H, Schwartz RJ, Solomon S, Kazen R, Gravem PE, Shrinivasan H. Assessment and examination of the neurologically impaired foot. Leprosy Review 2001; 72:263-275.
2. Brash PD, Foster JE, Anthony P, Tooke JE. Magnetic resonance imaging techniques demonstrates soft tissue damage in the diabetic foot. Diabet Med 1999; 16:55-61.
3. Brash PD, Foster JE, Vennart W, Daw J, Tooke JE. Magnetic resonance imaging reveals Micro-haemorrhage in the feet of diabetic patients with a history of Ulceration. Diabet Med 1996; 13:973-978.
4. Craig JG, Amin MB, Wu K, Eyler WR, van Holsbeeck MT, Bouffard JA, Shirazi K. Osteomyelitis of the diabetic foot: MR imaging-pathologic correlation. Radiology 1997; 203:849-855.
5. Crim JR, Seeger LI. Imaging evaluation of osteomyelitis. Crit Rev Diagn Imaging 1994; 35:201.
6. Dixon WT. Simple proton spectroscopic imaging. Radiology 1984; 153:189-194.

7. Faber WR, Hoeksma AF, van der Kleij AJ, Maas M, Dijkstra PF. Diagnostic procedures for suspected osteomyelitis in neuropathic feet of leprosy patients. Int J Lepr 1998; 66:29A.
8. Goodwin DW, Salonen DC, Yu JS, Broschmann J, Trudell DJ, Resnick DL. Plantar compartments of the foot: MR appearance in cadavers and diabetic patients. Radiology 1995; 196:623-630.
9. Guocheng Z, Wenzhong L, Liangbin Y, Zhongmin Y, Xiangsheng C, Tisheng Z, Ganyun Y. An epidemiological survey of deformities and disabilities amomg 14,257 cases of leprosy in 11 countries. Leprosy review 1993; 64:143-149.
10. Hoeksma AF, Faber WR. Assessment of skin temperature via palpation of the neuropathic foot. 1st world congress of ISPRM 2001.
11. Jacob S, Patil MK. Stress analyses in three-dimensional foot models of normal and diabetic neuropathy. Frontiers of Medical and Biological Engineering 1999; 1-17.
12. Jacob S, Patil MK. Three-dimensional foot modelling and analysis of stresses in normal and early stage Hansen's disease with muscle paralysis. Journal of Rehabilitation Research and Development 1999; 36:252-263.
13. Lipman BT, Collier BD, Carrera GF, et al. Detection of osteomyelitis in the neuropathic foot: nuclear medicine, MRI and conventional radiography. Clin Nuclear Med 1998; 23:77-82.
14. Maas M, Dijkstra PF, Akkerman EM. Uniform fat suppression in hands and feet through the use of two-point Dixon chemical shift MR imaging. Radiology 1999; 210:189-193.
15. Maas M, Slim FJ, Akkerman EM, Faber WR. MRI in clinically asymptomatic neuropathic leprosy feet: a baseline study. Int J Leprosy and Other Mycobact Dis 2001; 69:219-224.
16. Marcus CD, Ladam-Marcus VJ, Leone J, Malgrange D, Bonnet-Grausserand FM, Mentaneau BP. MR imaging of osteomyelitis and neuropathic osteoarthropathy in the feet of diabetics. Radiographics 1996; 16:1337-1348.
17. Moore TE, Yuh WTC, Kathol MH, El-Khoury GY, Corson JD. Abnormalities of the foot in patients with diabetes mellitus: findings on MR imaging. AJR 1991; 157:813-816.
18. Morrison WB, Ledermann HP, Schweitzer ME. MR imaging of the diabetic foot. MRI Clin North Am 2001; 9:603-613.
19. Morrison WB, Ledermann HP, Schweitzer ME. MR imaging of inflammatory conditions of the ankle and foot. MRI Clin North Am 2001; 9:615-637.
20. Morrison WB, Schweitzer ME, Bock GW, Mitchell DG, Hume EL, Pathria MN, Resnick D. Diagnosis of osteomyelitis: Utility of fat-suppressed contrast-enhanced MR imaging. Radiology 1993; 189:251-257.

21. Morrison WB, Schweitzer ME, Granville Batte W, Radack DP, Russel KM. Osteomyelitis of the foot: relative importance of primary and secondary MR imaging signs. Radiology 1998; 207:625-632.
22. Onvlee GJ. The Charcot Foot; a critical review and observational study of a group of 60 patients, Thesis 1998.
23. Peterfy CG, Linares R, Steinbach LS. Recent advances in magnetic resonance imaging of the musculoskeletal system. Rad Clin North America 1994; 32:291-311.
24. Resnick D, Niwayama G. Diagnosis of bone and Joint disorders 3rd edition vol 4. Chapter 66: Osteomyelitis, septic arthritis and soft tissue infection: Organisms. WB Saunders Company Pensylvania 1995; 2486-2492.
25. Ridley DS, Jopling WH. Classification of Leprosy according to immunity. A five-group system. International Journal of Leprosy and Other Mycobaterial Diseases 1996; 34(3):255-273.
26. Schon LC, Easley ME, Weinfeld SB. Charcot neuroarthropathy of the foot and ankle. Clinical Orthopaedics and Related Research 1998; 349:116-131.
27. Tehranzadeh J, Wong E, Wang F, Sadighpour M. Imaging of osteomyelitis in the mature skeleton. MRI Clin North Am 2001; 39:240-250.
28. Tomas MB, Patel M, Marwin SE, Palestro CJ. The diabetic foot. The British Journal of Radiology 2000; 73:443-450.
29. World Health Organization. Weekly epidemiological record, 2002; 77(1):1-8. http://www.who.int/wer
30. Yu JS. Diabetic foot and neuroarthropathy magnetic resonance imaging evaluation. Topics in Magnetic Resonance Imaging 1998; 9:295-230.

CHAPTER 5

Summary, general discussion and future research

SUMMARY

In this thesis a new application based on an earlier described MRI technique is introduced. W.T. Dixon has described the basics of this technique, two-point chemical shift imaging, in 1984; a spectroscopic technique that can be used for imaging purposes (simple spectroscopic imaging) [1]. Two-point Dixon chemical shift imaging (Dixon technique) is based on the phase difference between water and fat when performing MRI. Conventional qualitative MR images are based on the sum of the signals of water and fat, while with the Dixon technique the relative contribution of water and fat to the overall MR signal are separated.

In our hospital there is a relatively large population of patients with neuropathic foot disease, usually caused by diabetes mellitus or leprosy. MRI as a diagnostic procedure is regularly performed in our institution for suspicion of osteomyelitis in in this population. A reliable homogeneous fat-suppression technique is necessary in particular in MRI investigations in case of suspected osteomyelitis [2-4]. With our MR imager, the frequency-selective presaturation fat-suppression did not provide a homogeneous fat-suppression in the distal extremities, a problem known from literature [5,6]. Since this is mainly caused by physical properties of the patient, it is largely independent of the equipment used.

In **Chapter 2** a study concerning the clinical use of two-point Dixon chemical shift imaging as fat-suppression technique is described. In this study 31 consecutive patients clinically suspected of having bone marrow disease in distal parts of the extremities were evaluated with the Dixon technique. Since this technique consists of two MRI sequences, in-phase and opposed-phase series, a potential problem is displacement of the patients' hand or foot between these two series. The uniformity of fat-suppression, the frequency of occurring displacement artifacts and the applicability in routine clinical setting were investigated. A uniform fat-suppression was achieved in all 64 studies (100%). Displacement artifacts that severely hampered MRI reading were only present in one examination (2%). Two-point Dixon chemical shift imaging was concluded to be a reliable, excellent technique for achieving uniform fat-suppression in distal parts of the extremities and applicable in routine clinical setting. Our group of patients with neuropathy and suspected osteomyelitis consist of patients suffering from diabetes mellitus or leprosy. Although there is extensive literature on MRI in patients with diabetes mellitus

suspected for osteomyelitis, no literature at all is present concerning MRI in patients with leprosy suspected for osteomyelitis [2-4, 7-13].

Chapter 3 is, as far as we know, the first MRI paper on neuropathic feet in leprosy. We studied 10 leprosy patients with neuropathic feet, without complications, clinically not suspected of infection. The purpose was to obtain a baseline of the MRI changes, with the Dixon technique as fat-suppression technique, which could be present in leprosy. Almost all patients showed MRI changes, of which 90% were located in the region of the first metatarsophalangeal joint. An important finding was the degradation and interruption of the subcutaneous fat pad at the plantar side of the medial foot. From literature on MRI in patients with diabetes mellitus it is known that these changes may consist of hemorrhage and/or fibrosis [7,14]. It is hypothesized that these changes may precede the development of plantar ulcers in leprosy, as is suggested in diabetes mellitus. MRI could play an important role in detecting (areas of) neuropathic feet that are at risk for developing ulcers; this may influence clinical decision-making.

In **Chapter 4** the clinical problem, which initiated this research, is described. Leprosy patients with longstanding complicated neuropathy with a persistent warm foot in the presence of a non-healing ulcer, clinically suspected for osteomyelitis are described. Clinical examination lacks specificity in this patient group. A total number of 18 MRI investigations in 12 leprosy patients were analyzed. The accepted primary MRI criteria for osteomyelitis (low signal intensity on T1-weighted images, high signal intensity on T2 and (t)STIR or fat-suppression images and enhancement after intravenous contrast administration) [2-4,7-13] were positive in 17 of 18 MRI examinations. Of the secondary MRI signs earlier described for neuropathic feet of patients suffering from diabetes mellitus (ulcer, cellulitis, cortical interruption, sinus tract and abscess), an ulcer and cellulitis were present in all patients [2]. When compared to the gold standard for the diagnosis osteomyelitis (positive culture and/or histopathology taken from bone material) or clinical outcome after 6 months follow-up (when the gold standard was not available or not conclusive) there was agreement in 17 of 18 events. This study indicates that the primary MRI criteria established for diabetes can adequately be used in a population of patients with leprosy and longstanding neuropathic foot disease, for the detection of osteomyelitis.

Contrary to diabetes literature the secondary MRI signs seem of no additional value in diagnosing osteomyelitis in these leprosy patients.

GENERAL DISCUSSION AND FUTURE RESEARCH

The studies included in this thesis demonstrate the feasibility and clinical relevance of a new fat-suppression technique used in evaluating neuropathic feet in leprosy. This concerns patients in which MRI examinations, to our knowledge, have not yet been performed. Fat-suppression through the use of two-point Dixon chemical shift imaging provides homogeneous fat-suppression in the entire field of view. It is used in daily practice in particular when feet are imaged and fat-suppression after intravenous contrast administration is necessary. A limitation of the technique is that it is not a standard sequence on the MR machine and that post-processing is required.

Besides providing good qualitative imaging results by separating fat from water, this Dixon technique has the potential of providing quantitative data of fat and water. This is discussed in detail in the other part of this thesis, for another clinical application (Gaucher disease). This intrinsic possibility of the technique may proof to be of value in patients with neuropathic feet. The development of claw toes, a clinical problem in neuropathic feet, is thought to be caused by decrease in function of the intrinsic muscles of the forefoot. This has been analyzed by measuring the volume of these muscles with the use of MRI, hypothesizing that a decrease in volume of these muscles is related with the presence of claw toes [15]. On MRI this presents as a decrease in volume of muscle fibers, and an increase in intramuscular fat. By using the Dixon technique, the fractions of water and fat in these muscles can be analyzed. An earlier detection of loss of water might be found and feet at risk for developing claw toes might be identified. This clinical problem and the possible role for Dixon MRI is currently under investigation in a collaboration between the departments of radiology and internal medicine of our hospital.
Another intrinsic feature of the Dixon technique is the acquired out of phase (opposed-phase) sequence. In a regular in-phase MR image both fat and water contribute to the signal. In an opposed-phase signal fat and water are contributing in opposite direction to the MR signal. This means that areas in which water and fat are present in approximately equal

amount, the MRI signal is approaching zero. Therefore, areas of low signal intensity on the opposed-phase T1-weighted images in bone marrow represent areas with an equal percentage of fat and water. A sharp demarcation of areas with much water is seen. After intravenous contrast administration enhancement may be seen in these areas. The clinical relevance of these findings should be explored in another study, in which various sequences such as (t)STIR, Dixon fat-suppression, fat saturation T2-weighted TSE and Dixon opposed-phase images are compared.

Data are presented of MRI examinations in the neuropathic foot of leprosy patients in the Netherlands. We investigated neuropathic feet of patients without complications or complaints. We hypothesize that changes in the plantar fat pad at the first MTP joint in these patients may precede ulceration [7,14]. When, by intensifying physical examination these MR findings can be detected, this may lead to improvement in preventing the ulcer development. The second group of patients consisted of patients with a complicated foot with longstanding neuropathy and suspicion of osteomyelitis. MRI abnormalities compatible with osteomyelitis were detected at the medial side of the foot as well as (more frequently) at the lateral side of the foot. Patients with neuropathic feet, without longstanding disease, that have an ulcer or cellulitis, without clinical suspicion of osteomyelitis, are a group of interest. What are the MRI findings in these patients? What are the sites of involvement? It would be of interest to evaluate these patients. In this way a more complete overview of MR abnormalities in leprosy is obtained. In order to approach this target we currently work together with the Institute Oswaldo Cruz, Fiocruz, Rio de Janeiro, Brazil.

The study described in **Chapter 3** revealed surprising results. In this chapter patients with leprosy and neuropathic feet without complications and clinically unsuspected of infection were studied. In these patients degradation of plantar fat pad at the medial side of the foot, in the region of the MTP 1 joint, was found. This new finding led us into a brief exploration of the biomechanics of the neuropathic foot in leprosy. Literature on this topic is sparse. Only a few authors published on the biomechanics in neuropathic feet, in a small number of patients [16-19].

It is stated that the alteration of biomechanics in neuropathic feet may influence the disturbance of plantar fat pad leading to hemorrhage and fibrosis and to fat pad degradation, which might precede ulcer development. These MRI detected findings were located primarily on the medial side of the foot, plantar to the first MTP joint. In order to conclude that in this particular patient population the medial side of the foot is at risk for developing ulceration and that this is due to changes in the biomechanics in this population needs confirmation in a larger patient population. The findings in the patients population of longstanding complicated neuropathic foot disease, described in **chapter 4**, differed from the previous ones since abnormalities were found in half of the patients on the lateral side of the foot. It seems that from a biomechanical point of view there is a difference between the two patient groups. There is little literature on the biomechanics in complicated neuropathic leprosy feet. Brandsma et al. hypothesized that the function of the ankle joint might be of importance in changing biomechanics from medial to lateral side of the foot in walking [20]. This might be a cause for the different distribution of MRI changes in the two groups. It would be of interest to analyze the walking cycle in different groups of leprosy patients with neuropathic feet. In this way more information is gained on the stress distribution in the foot. These findings should be correlated with the function of the ankle joint and with the MRI findings. In this way more information on the feet at risk, more precise the areas in the foot that are at risk will be obtained, thereby increasing the possibilities for prevention. In the western world neuropathic feet are far more commonly seen in patients suffering from diabetes mellitus. This most often is a combination of neural and vascular pathology; thereby differing from leprosy patients, who have, in essence a pure neuropathic foot. In our hospital there are outpatient clinics for patients with diabetes mellitus as well as leprosy. This combination is not often found. It would be of interest to start a comparative study between the two groups, focussing on the nature and the distribution of MRI changes. These findings should be correlated with biomechanical analysis and should be performed in patients with complicated longstanding neuropathic foot disease as well as patients with non-complicated neuropathic foot.

MRI examinations in leprosy patients with neuropathic feet are valuable. In non-complicated neuropathic feet, abnormalities are encountered that are hypothesized to represent areas at risk for developing ulcerations. In complicated feet suspected for osteomyelitis the extent of infection, both in soft tissue as well as bone marrow is visualized. Two-point Dixon chemical shift imaging is a good qualitative technique, producing a uniform fat-suppression in the entire field of view. The potential value of the other specific qualities of this technique, i.e. the out of phase sequence and the quantitative fat/water fraction measurement are promising and can be part of future research.

REFERENCES

1. Dixon WT. Simple proton spectroscopic imaging. Radiology 1984; 153:189-194.
2. Morrison WB, Schweitzer ME, Granville Batte W, Radack DP, Russel KM. Osteomyelitis of the foot: relative importance of primary and secondary MR imaging signs. Radiology 1998; 207:625-632.
3. Morrison WB, Ledermann HP, Schweitzer ME. MR imaging of inflammatory conditions of the ankle and foot. MRI Clin North Am 2001; 9:615-637.
4. Tehranzadeh J, Wong E, Wang F, Sadighpour M. Imaging of osteomyelitis in the mature skeleton. MRI Clin North Am 2001; 39:240-250.
5. Peterfy CG, Garvin GJ, Tirman PFJ, Majumdar S, Wendland M, Genant HK. Incomplete fat-suppression with spectral presaturation on MR images of the foot and ankle: clinical implications and practical solutions (abstr). In: Proceedings of the Society for Magnetic Resonance in Medicine and the European Society for Magnetic Resonance in Medicine and Biology 1995; 1516.
6. Anzai Y, Lufkin RB, Jabour BA, et al. Fat-suppression failure artifacts simulating pathology on frequency-selective fat-suppression MR images of the head and neck. AJNR 1992; 13:879-884.
7. Craig JG, Amin MB, Wu K, Eyler WR, van Holsbeeck MT, Bouffard JA, Shirazi K. Osteomyelitis of the diabetic foot: MR imaging-pathologic correlation. Radiology 1997; 203:849-855.
8. Crim JR, Seeger LI. Imaging evaluation of osteomyelitis. Crit Rev Diagn Imaging 1994; 35:201.
9. Marcus CD, Ladam-Marcus VJ, Leone J, Malgrange D, Bonnet-Grausserand FM, Mentaneau BP. MR imaging of osteomyelitis and neuropathic osteoarthropathy in the feet of diabetics. Radiographics 1996; 16:1337-1348.

10. Moore TE, Yuh WTC, Kathol MH, El-Khoury GY, Corson JD. Abnormalities of the foot in patients with diabetes mellitus: findings on MR imaging. AJR 1991; 157:813-816.
11. Morrison WB, Ledermann HP, Schweitzer ME. MR imaging of the diabetic foot. MRI Clin North Am 2001; 9:603-613.
12. Morrison WB, Schweitzer ME, Bock GW, Mitchell DG, Hume EL, Pathria MN, Resnick D. Diagnosis of osteomyelitis: Utility of fat-suppressed contrast-enhanced MR imaging. Radiology 1993; 189:251-257.
13. Morrison WB, Schweitzer ME, Wapner KL, Hecht PJ, Gannon FH, Behm WR. Osteomyelitis in feet of diabetics: Clinical accuracy, surgical utility, and cost-effectiveness of MR imaging. Radiology 1995; 196:557-564.
14. Brash PD, Foster JE, Vennart W, Daw J, Tooke JE. Magnetic resonance imaging reveals micro-haemorrhage in the feet of diabetic patients with a history of ulceration. Diabet Med 1996; 13:973-978.
15. Bus SA, Yang QX, Wang JH, Smith MB, Wunderlich R, Cavanagh PR. Intrinsic muscle atrophy and toe deformity in the diabetic neuropathic foot: an MRI study. Submitted.
16. Jacob S, Patil MK. Stress analyses in three-dimensional foot models of normal and diabetic neuropathy. Frontiers of Medical and Biological Engineering 1999; 1-17.
17. Jacob S, Patil MK. Three-dimensional foot modelling and analysis of stresses in normal and early stage Hansen's disease with muscle paralysis. Journal of Rehabilitation Research and Development 1999; 36:252-263.
18. Patil KM, Jacob S. Mechanics of tarsal disintegration and plantar ulcers in leprosy by stress analysis in three-dimensional foot models. Indian J Leprosy 2000; 72:69-86.
19. Patil KM, Braak LH, Huson A. Analyzis of stresses in two-dimensional models of normal and neuropathic feet. Med & Biol Eng & Comput 1996; 34:280-284.
20. Brandsma JW, Macdonald MRC, Warren AG, Cross H, Schwarz RJ, Solomon S, Kazen R, Gravem PE, Shrinivasan H. Assessment and examination of the neurologically impaired foot. Lepr Rev 2001; 72:254-262.

CHAPTER 6

Samenvatting

SAMENVATTING

In dit proefschrift wordt het onderzoek beschreven van een nieuwe applicatie van een al langer bestaande MRI techniek. W.T. Dixon heeft de basis van de techniek, two-point chemical shift imaging, al beschreven in 1984 als een op spectroscopie gebaseerde beeldvormende techniek (simpel spectroscopie imaging) [1]. Deze Dixon techniek is gebaseerd op het fase-verschil tussen water en vet. Conventionele kwalitatieve MRI plaatjes zijn samengesteld uit de som van het signaal van water en vet, terwijl middels de Dixon techniek de individuele bijdrage van water en vet aan het MRI signaal kan worden gescheiden.

In het Academisch Medisch Centrum (AMC) is een speciale aandacht voor het ziektebeeld "de neuropatische voet". Hoewel de belangrijkste oorzaak hiervan wereldwijd de ziekte diabetes mellitus is, is in het AMC lepra, M. Hansen, eveneens een belangrijke veroorzaker van neuropatische voet pathologie. Wanneer er sprake is van een gecompliceerde neuropatische voet, klinisch verdacht voor ontsteking, wordt er regelmatig MRI onderzoek verricht. Tijdens dit MRI onderzoek dienen in ieder geval sequenties vervaardigd te worden met goede onderdrukking van het vet signaal (vetsuppressie) na intraveneuze contrasttoediening Op deze manier dient een laaggradige chronische osteomyelitis te worden uitgesloten [2-4]. Vanuit de literatuur is bekend dat een goede, homogene onderdrukking van het vet signaal lastig is, met name in de periferie van de extremiteiten (handen en voeten) [5,6].

In **hoofdstuk 2** wordt een studie beschreven betreffende het gebruik van two-point Dixon chemical shift imaging als vetsuppressie techniek. Er werden 31 opeenvolgende patiënten, verdacht voor beenmergpathologie in de extremiteiten, met deze techniek geëvalueerd. De techniek bestaat uit twee MRI series, T1 in-fase en uit-fase. Een potentieel probleem is het bewegen van de patiënt tussen de twee series, met als gevolg falen van de techniek. Tijdens de studie werd vooral gelet op de frequentie van voorkomen van deze bewegingsartefacten, de homogeniteit van de vetsuppressie en de mogelijkheid deze techniek in het standaard MRI protocol op te nemen. Er werd een homogene uniforme vetsuppressie gevonden in alle 64 studies (100%). Slechts in één studie (2%) was sprake van beweging tussen de twee series, zodanig dat er geen goede evaluatie kon plaatsvinden. Geconcludeerd werd dat de two-point Dixon chemical shift imaging techniek een betrouwbare, gemakkelijk klinisch te

gebruiken vetsuppressie techniek is met prima vetsuppressie in handen en voeten.

De patiënten in het AMC met neuropatische voeten en hieraan gerelateerde complicaties bestaan voor een belangrijk deel uit patiënten met lepra. De MRI literatuur over gecompliceerde neuropatische voeten met verdenking op osteomyelitis beschrijft voornamelijk patiënten met diabetes mellitus; er bestaat nauwelijks literatuur over MRI bij lepra patiënten met een gecompliceerde neuropatische voet [2-4,7-13].
Hoofdstuk 3 is voor zover bekend het eerste MRI onderzoek over de neuropatische lepravoet. Bij tien patiënten met een neuropatische lepravoet, zonder complicaties, klinisch onverdacht, werd een MRI vervaardigd met de Dixon-techniek als vetsuppressie techniek. Op deze manier werd een uitgangssituatie verkregen van afwijkingen die aanwezig kunnen zijn bij de ongecompliceerde neuropatische lepravoet. Bij de meerderheid van de patiënten werden MRI afwijkingen gevonden, voor 90% gelokaliseerd in of rondom de grote teen (MTP 1). Een opvallende bevinding was de aantasting of onderbreking van het subcutane vet plantair van het kopje van os metatarsale 1. Vanuit de diabetes literatuur is bekend dat deze veranderingen van het subcutane vet kunnen bestaan uit bloeding en/of fibrose [14,15]. Vanuit de diabetes literatuur wordt verondersteld dat deze veranderingen het voorstadium zijn van de ontwikkeling van een ulcus. Deze gedachte lijkt ook aannemelijk in de leprapopulatie. Middels MRI kunnen wellicht risicogebieden voor het ontstaan van ulcera worden gedefinieerd bij patiënten die klinisch onverdacht zijn. Dit kan klinisch handelen beïnvloeden, bijvoorbeeld in het kader van preventie.

In **Hoofdstuk 4** wordt het klinische probleem, dat de aanleiding is geweest voor het ontstaan van dit onderzoek, beschreven. Een warme voet bij een lepra patiënt met een lang bestaande neuropathie is klinisch verdacht voor infectie. Osteomyelitis dient te worden uitgesloten. Het lichamelijk onderzoek is hiervoor niet specifiek genoeg.
Bij 12 patiënten met lepra, klinisch verdacht voor osteomyelitis in een gecompliceerde neuropatische voet zijn in totaal 18 MRI's gemaakt. De algemeen geldende primaire MRI criteria om osteomyelitis te diagnosticeren (laag signaal op T1-gewogen plaatjes, hoog signaal op

T2-gewogen en (T)STIR of vetsuppressie plaatjes en aankleuring na intraveneuze contrast toediening) [2-4,7-13] waren aanwezig in 17 van de 18 MRI onderzoeken. De secundaire MRI criteria, eerder beschreven bij patiënten met diabetes, bestaan uit de aanwezigheid van een ulcus, cellulitis, onderbreking van de cortex van het bot, een fistelkanaal of een abces. Deze criteria waren 100% aanwezig in de onderzochte populatie. Deze MRI bevindingen zijn vergeleken met de gouden standaard, te weten een positieve botkweek en/of histopathologie. Indien de gouden standaard niet aanwezig of niet conclusief was, werd de klinische uitkomst na 6 maanden follow-up als gouden standaard beschouwd. Hiermee vergeleken was er overeenstemming met de MRI gegevens in 17 van de 18 MRI's. Geconcludeerd werd dat de bekende primaire MRI criteria, zoals bekend van diabetes, adequaat gebruikt kunnen worden bij de evaluatie van lepra MRI's ter detectie van osteomyelitis. De secundaire criteria lijken bij lepra niet van aanvullende waarde.

DISCUSSIE EN TOEKOMSTIG ONDERZOEK

In dit proefschrift zijn verschillende MRI studies besproken welke vervaardigd zijn in neuropatische voeten van leprapatiënten. In deze populatie zijn er naar onze mening geen eerdere MRI onderzoeken gepubliceerd. De geëxploreerde vetsuppressie techniek, two-point Dixon chemical shift imaging, zorgt voor een homogene vetsuppressie in het gehele beeld. Het wordt in het standaard MRI protocol voor neuropatische voeten gebruikt, wanneer intraveneus contrast wordt gegeven en homogene vetsuppressie essentieel is. Een beperking van de techniek is het feit dat het geen standaard sequentie is en dat postprocessing noodzakelijk is.

Naast het separeren van vet en water voor kwalitatieve doeleinden heeft de Dixon techniek de mogelijkheid om kwantitatieve vet en water informatie te verschaffen. Deze eigenschap is uitgebreid beschreven in het andere deel van dit proefschrift, betreffende M. Gaucher, echter kan ook van waarde zijn bij patiënten met neuropatische voeten. Een belangrijk klinisch probleem in deze populatie is de ontwikkeling van klauwtenen. Deze deformatie wordt waarschijnlijk veroorzaakt door functieverlies van de intrinsieke spieren in de voorvoet. Dit is geanalyseerd middels het meten van het volume van de intrinsieke musculatuur gebruikmakend van MRI beelden. Gedacht wordt dat het volumeverlies van de spier, met

vettige degeneratie gerelateerd is aan het ontstaan van klauwtenen [16]. Wanneer nu de Dixon techniek de vet- en waterfractie van deze spieren kan leveren, kunnen spieren, die macroscopisch kwalitatief intact lijken, kwantitatief worden geëvalueerd en kan eventueel verlaging van de waterfractie worden vastgesteld. Wellicht dat dit het voorstadium is van functieverlies, met later het ontstaan van vettige degeneratie. Op deze manier zouden voeten die het risico lopen klauwtenen te ontwikkelen eerder kunnen worden opgespoord. De analyse van de klauwtenen en de mogelijke rol hierin voor de Dixon techniek wordt momenteel onderzocht in een samenwerkingsverband tussen de afdelingen Interne Geneeskunde en Radiologie van het AMC.
Een andere eigenschap van de Dixon techniek is de verkregen uit-fase T1-gewogen serie. In een regulier (in-fase) T1-gewogen MRI beeld dragen vet en water beiden bij aan het MRI signaal. In de uit-fase series dragen vet en water in tegengestelde richting bij aan het MRI signaal. Dat wil zeggen dat in die gebieden waar evenveel water als vet aanwezig is, het signaal zal uitdoven. Daarom representeren laag signaal gebieden in het beenmerg in deze T1 uit-fase beelden zones waarin evenveel vet als water aanwezig zal zijn. Vaak wordt er een scherpe demarcatie gezien tussen deze gebieden en de gezonde, hoog signaal beenmerg gebieden. Na toediening van intraveneus contrast kan er in deze zones aan kleuring plaatsvinden. Deze observaties zijn in het verleden gedaan, echter de klinische relevantie ervan is nog niet onderzocht. Een vergelijkende studie waarin de verschillende MRI sequenties, (T)STIR, Dixon vet-suppressie, T2-gewogen vet-suppressie en Dixon uit-fase, met elkaar worden vergeleken kan hier een antwoord op geven.

Dit proefschrift beschrijft Nederlandse data van leprapatiënten met neuropatische voeten zonder complicaties en zonder klachten. Geponeerd werd dat de middels MRI waargenomen veranderingen in het plantaire vet, juist onder het MTP 1 gewricht, een voorstadium kunnen zijn van de ontwikkeling van ulceraties [14,15]. Indien het lichamelijk onderzoek wordt geïntensiveerd kunnen de op MRI afwijkende gebieden wellicht ook op de polikliniek of in het veld worden gedetecteerd.
De tweede groep die geanalyseerd is, betreft Nederlandse leprapatiënten met lang bestaande gecompliceerde neuropatische voeten met klinische verdenking op osteomyelitis.

Hierin zijn MRI afwijkingen gevonden die wijzen op osteomyelitis zowel aan de mediale zijde van de voet als (meer frequent) aan de laterale zijde van de voet. Er is dus een duidelijk verschil: MRI afwijkingen mediaal (MAP 1) bij de ongecompliceerde neuropatische voet, versus vooral lateraal bij de gecompliceerde neuropatische voet. De populatie die nog niet is beschreven, betreft leprapatiënten met lang bestaande neuropatische voet, met thans een ulcus of cellulitis, zonder klinische verdenking op osteomyelitis. Wat zijn de MRI afwijkingen bij deze patiënten? Welke delen van de voet, mediaal of lateraal, zijn in meerderheid betrokken? Indien ook deze populatie middels MRI kan worden geëvalueerd, zal er een nagenoeg volledig beeld verkregen zijn van de afwijkingen die aanwezig kunnen zijn bij neuropatische lepra voeten. Om dit te bewerkstelligen werken we momenteel samen met het Institute Oswaldo Cruz, Fiocruz, Rio de Janeiro, Brazilië.

De studie van de ongecompliceerde neuropatische voet, beschreven in **hoofdstuk 3**, leverde opvallende onverwachte resultaten. De aantasting van het plantaire subcutane vet, en dan vooral de plaats, mediaal, was een nieuwe bevinding. Dit gaf aanleiding tot een nadere evaluatie van de biomechanica van neuropatische voeten bij patiënten met lepra. Er is hierover nauwelijks literatuur te vinden. Slechts een paar auteurs hebben hierover geschreven [17-20]. Zij concludeerden dat de veranderde biomechanica van de neuropatische voet van invloed kan zijn op de status van het plantaire vet, met als gevolg het ontstaan van bloedingen en fibrose subcutaan. Een en ander zou als voorstadium voor ulceratie kunnen worden beschouwd. Voordat geconcludeerd kan worden dat de MRI afwijkingen welke door ons beschreven zijn, een risico dan wel voorstadium zijn voor het ontstaan van ulceraties, dient een grotere populatie onderzocht te worden. De gevonden afwijkingen in de populatie met langer bestaande neuropatische voet, met name de betrokkenheid van de laterale voet in de helft van de patiënten, suggereert een (ver)ander(d)e biomechanica in de twee groepen. Er is echter ook zeer weinig literatuur over de biomechanica in gecompliceerde neuropatische lepra voeten. Volgens Brandsma zou de functie van het enkel gewricht van invloed zijn op de verandering van de biomechanica tijdens het lopen [21].

Dit kan een reden zijn voor de verschillen in distributie van MRI afwijkingen in de beschreven twee groepen. Het is interessant om de analyse van "het lopen" in de verschillende groepen te verrichten. Op deze manier kan er meer informatie verkregen worden over de verdeling van de belasting in de voet tijdens het lopen. Wanneer deze informatie gekoppeld wordt aan de functie van het enkel gewricht en de bevindingen van vervaardigd MRI onderzoek, kan de biomechanica van de verschillende groepen wellicht beter begrepen worden. Waarschijnlijk wordt op deze manier meer informatie verkregen over gebieden van hogere belasting, waar een ulcus zich zou kunnen ontwikkelen. Eventueel kan dit leiden tot een betere preventie.
In de westerse wereld wordt het ziektebeeld van de neuropatische voet vooral gezien bij patiënten met diabetes mellitus. Bij diabetes is vaak sprake van een combinatie van neuropathie en (micro-)angiopathie, terwijl bij lepra bijna altijd sprake is van een "pure" neuropatische voet. In het AMC worden beide populaties gezien, een zeldzame combinatie. Het is van belang een vergelijkende MRI studie te verrichten tussen de twee groepen, gericht op de aard en de verdeling van de MRI afwijkingen. Deze studie dient dan gekoppeld te worden aan een biomechanische analyse en dient te worden verricht in ongecompliceerde en gecompliceerde neuropatische voeten.

MRI bij leprapatiënten met neuropatische voeten is waardevol. Bij patiënten met een niet gecompliceerde neuropatische voet zijn middels MRI afwijkingen gevonden, waarvan gedacht wordt dat deze het voorstadium zijn van een ulcus. In gecompliceerde neuropatische voeten verdacht voor osteomyelitis werd de aanwezigheid en uitbreiding van de infectie zowel in het beenmerg als in de weke delen gedemonstreerd. Middels de two-point Dixon chemical shift imaging techniek kan een homogene vetsuppressie verkregen worden in het gehele veld. De potentiële waarde van de kwaliteiten van de techniek, met name de uit-fase sequentie en de kwantitatieve vet-water meting lijken veelbelovend en zullen deel uitmaken van verder wetenschappelijk onderzoek.

REFERENCES

1. Dixon WT. Simple proton spectroscopic imaging. Radiology 1984; 153:189-194.
2. Morrison WB, Schweitzer ME, Granville Batte W, Radack DP, Russel KM. Osteomyelitis of the foot: relative importance of primary and secondary MR imaging signs. Radiology 1998; 207:625-632.
3. Morrison WB, Ledermann HP, Schweitzer ME. MR imaging of inflammatory conditions of the ankle and foot. MRI Clin North Am 2001; 9:615-637.
4. Tehranzadeh J, Wong E, Wang F, Sadighpour M. Imaging of osteomyelitis in the mature skeleton. MRI Clin North Am 2001; 39:240-250.
5. Peterfy CG, Garvin GJ, Tirman PFJ, Majumdar S, Wendland M, Genant HK. Incomplete fat-suppression with spectral presaturation on MR images of the foot and ankle: clinical implications and practical solutions (abstr). In: Proceedings of the Society for Magnetic Resonance in Medicine and the European Society for Magnetic Resonance in Medicine and Biology 1995; 1516.
6. Anzai Y, Lufkin RB, Jabour BA, et al. Fat-suppression failure artifacts simulating pathology on frequency-selective fat-suppression MR images of the head and neck. AJNR 1992; 13:879-884.
7. Craig JG, Amin MB, Wu K, Eyler WR, van Holsbeeck MT, Bouffard JA, Shirazi K. Osteomyelitis of the diabetic foot: MR imaging-pathologic correlation. Radiology 1997; 203:849-855.
8. Crim JR, Seeger LI. Imaging evaluation of osteomyelitis. Crit Rev Diagn Imaging 1994; 35:201.
9. Marcus CD, Ladam-Marcus VJ, Leone J, Malgrange D, Bonnet-Grausserand FM, Mentaneau BP. MR imaging of osteomyelitis and neuropathic osteoarthropathy in the feet of diabetics. Radiographics 1996; 16:1337-1348.
10. Moore TE, Yuh WTC, Kathol MH, El-Khoury GY, Corson JD. Abnormalities of the foot in patients with diabetes mellitus: findings on MR imaging. AJR 1991; 157:813-816.
11. Morrison WB, Ledermann HP, Schweitzer ME. MR imaging of the diabetic foot. MRI Clin North Am 2001; 9:603-613.
12. Morrison WB, Schweitzer ME, Bock GW, Mitchell DG, Hume EL, Pathria MN, Resnick D. Diagnosis of osteomyelitis: Utility of fat-suppressed contrast-enhanced MR imaging. Radiology 1993; 189:251-257.
13. Morrison WB, Schweitzer ME, Wapner KL, Hecht PJ, Gannon FH, Behm WR. Osteomyelitis in feet of diabetics: Clinical accuracy, surgical utility, and cost-effectiveness of MR imaging. Radiology 1995; 196:557-564.

14. Brash PD, Foster JE, Vennart W, Daw J, Tooke JE. Magnetic resonance imaging reveals micro-haemorrhage in the feet of diabetic patients with a history of ulceration. Diabet Med 1996; 13:973-978.
15. Bus SA, Yang QX, Wang JH, Smith MB, Wunderlich R, Cavanagh PR. Intrinsic muscle atrophy and toe deformity in the diabetic neuropathic foot: an MRI study. Submitted.
16. Jacob S, Patil MK. Stress analyses in three-dimensional foot models of normal and diabetic neuropathy. Frontiers of Medical and Biological Engineering 1999; 1-17.
17. Jacob S, Patil MK. Three-dimensional foot modelling and analysis of stresses in normal and early stage Hansen's disease with muscle paralysis. Journal of Rehabilitation Research and Development 1999; 36:252-263.
18. Patil KM, Jacob S. Mechanics of tarsal disintegration and plantar ulcers in leprosy by stress analysis in three-dimensional foot models. Indian J Leprosy 2000; 72:69-86.
19. Patil KM, Braak LH, Huson A. Analyzis of stresses in two-dimensional models of normal and neuropathic feet. Med & Biol Eng & Comput 1996; 34:280-284.
20. Brandsma JW, Macdonald MRC, Warren AG, Cross H, Schwarz RJ, Solomon S, Kazen R, Gravem PE, Shrinivasan H. Assessment and examination of the neurologically impaired foot. Lepr Rev 2001; 72:254-262.

DANKWOORD

DANKWOORD

Het maken van een proefschrift wordt snel als een één-persoonsactie bestempeld. In mijn optiek is niets minder waar. Ook hier is sprake van team-effort, waarbij de promovendus als centrale-as fungeert. Mijn mede teamleden en anderen wil ik graag bedanken.

Liefste Annelies, eindelijk is het zover. Mijn boekje, toch eigenlijk ons boekje, is klaar. Bedankt voor je onvoorwaardelijke steun. Nu zal het wel rustig worden...
Bart en Rutger, ik hoop dat jullie het leuk zullen vinden tijdens de promotie. Ziet er wel raar uit hoor, papa in zo'n pinguïnpak.

Prof. dr. den Heeten, beste Ard, met jouw komst naar het AMC waren er ineens twee radiologen op één afdeling met interesse in beenmerg MRI. Jouw enthousiasme en betrokkenheid hebben het proefschrift die kant op gestuurd, waar het uiteindelijk gekomen is. De basis voor meer beenmerg MRI research is gelegd. Bedankt voor je begeleiding.
Prof. dr. Faber, beste William, veel dank ben ik je verschuldigd voor het feit dat jij toezegde het proefschrift te willen begeleiden, ten tijde van het interregnum op de afdeling radiologie. Er zullen niet veel dermatologen zijn, bij wie een radioloog zal promoveren. Jouw betrokkenheid bij het onderzoek was zeer plezierig. Wees niet bevreesd, het onderzoek naar de neuropatische voet zal voortgaan.
Dr. Akkerman, beste Erik, kompaan vanaf het eerste uur. Hoewel radiologen en fysici niet per definitie dezelfde taal spreken, hebben wij elkaar snel leren verstaan. Met de ontwikkeling van een klinisch toepasbare Dixon sequentie heb je iets heel belangrijks neergezet, iets waar je trots op kunt zijn. Veel patiënten hebben hier profijt van. Bedankt.
Dr. Stoker, beste Jaap, jouw niet aflatend vermogen om binnen een bestaande studie snel nog een volgende substudie te verzinnen, waardoor een en ander nog veel sterker zou worden, bewonder ik zeer. Dat alles daarmee wat langzamer gaat dan gepland is wat minder. Ik heb van jou geleerd waar het om gaat bij het stellen van deadlines. Bedankt voor je enthousiaste betrokkenheid en collegialiteit.

Leden van de promotiecommissie, u dank ik voor uw bereidheid in de commissie te willen plaatsnemen. Een heel divers gezelschap van verschillende disciplines en twee universiteiten. Het zwaartepunt van beenmerg MRI in Nederland ligt blijkbaar in het gebied tussen Leiden en Amsterdam.

Mijn paranimfen, Carla Hollak en Kees van Kuijk, wil ik danken voor de vriendschappelijke en uitermate plezierige samenwerking van de laatste jaren. Carla, ik hoop dat er nog veel gezamenlijk onderzoek zal geschieden. Ik zie er naar uit lange tijd met je samen te kunnen werken. Kees, dat weekend Zeeland deed het 'em. Terwijl je in het geheel niet bij het onderzoek betrokken was, gaf je veel van je vrije tijd om me te ondersteunen. Ik stel onze vriendschap zeer op prijs.

De laatste twee jaar kwam er onverwachte hulp aanlopen in de persoon van Erik Slim. Beste Erik, veel dank ben ik je verschuldigd voor je enthousiaste steun bij het lepra-onderzoek. Hoewel de biomechanische analyse is gesneuveld in ons laatste artikel, zal dit het begin van jouw (promotie-)onderzoek zijn. Voor ondersteuning kun je op me rekenen.

De oorsprong van de Dixon research ligt halverwege de jaren negentig, met een andere personele bezetting op de afdeling radiologie. Echter de mensen die aan de wieg van dit proefschrift stonden wil ik zeker niet vergeten te noemen. Piet Dijkstra, ik dank je voor mijn prima opleiding tot skeletradioloog en je plezierige hulp bij de ontwikkeling van de Dixon vet suppressie techniek. Ben Verbeeten jr. heeft in Nice, onder het genot van een Orangina, de eerste indeling van het proefschrift met mij gemaakt. Ben, bedankt voor je betrokkenheid. Ronald Rademakers dank ik voor de gestructureerde opzet van het Gaucher QCSI onderzoek. Rob Grijm dank ik voor de ruimte die ik heb gekregen ten tijde van het interregnum op de afdeling radiologie.

Zowel binnen het klinische veld van Morbus Gaucher als de neuropatische voet zijn er periodieke multidisciplinaire besprekingen. Deze besprekingen hebben mij zeer ondersteund. Ik wil alle collegae die hebben deelgenomen aan deze besprekingen bedanken voor hun bijdragen aan de discussies. Het proefschrift is er beter van geworden.

Dankwoord

Alle collegae op de afdeling radiologie wil ik bedanken voor hun collegiale steun. Mark Romijn bedank ik speciaal vanwege het koerierschap in de eindfase van dit proefschrift, van en naar Andries.
Andries wil ik bedanken voor de fraaie lay-out van het boekje. Er kwam met de twee voorkanten iets nieuws uit Amsterdam. Uiteindelijk is het een perfect Amsterdam-Rotterdam project geworden.

Het secretariaat wil ik bedanken voor de plezierige samenwerking in vaak stressvolle tijden. Een speciaal woord van dank voor Mirjam Evers. Mirjam, jouw steun, hulp en nog veel meer gedurende het hele traject van de promotie, neen, eigenlijk al zolang we elkaar kennen, is enorm. Ik prijs me gelukkig met je vriendschap. Ik zie al uit naar ons volgend project.

Ik dank de medewerkers van de afdeling radiologie voor de plezierige samenwerking. De MRI medewerkers dank ik in het bijzonder voor het vervaardigen van de Dixon studies.

Ik dank de patiënten en proefpersonen voor hun medewerking.

Als laatste wil ik het hoofd van de afdeling radiologie, prof. dr. J.S. Laméris, bedanken. Beste Han, ik dank je voor de ruimte die ik heb gekregen om mijn onderzoek af te maken. Tijd voor een nieuwe uitdaging.

Mario Maas

CLINICAL APPLICATIONS OF DIXON CHEMICAL SHIFT MR IMAGING

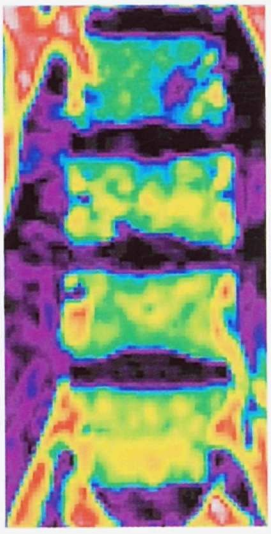

Morbus Gaucher

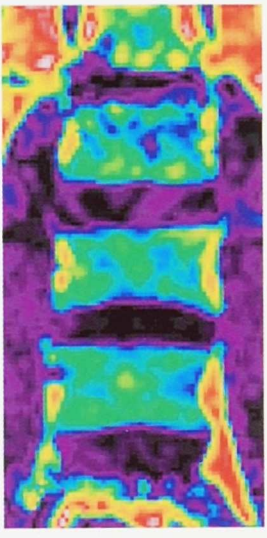

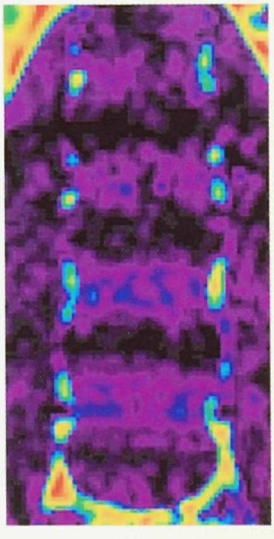

Mario Maas